

ON THE ELECTRONIC STRUCTURE OF
FREE AND PROTEIN-BOUND ISOALLOXAZINES

CENTRALE LANDBOUWCATALOGUS



0000 0086 6331

Promotor : dr. F. Müller
hoogleraar in de biochemie

Co-promotor: dr. C. Veeger
, hoogleraar in de biochemie ,

NN08201,925

AN KEES EWEG

ON THE ELECTRONIC STRUCTURE OF FREE AND
PROTEIN-BOUND ISOALLOXAZINES

roefschrift

er verkrijging van de graad van
octor in de landbouwwetenschappen,
p gezag van de rector magnificus,
r. C.C. Oosterlee,
ogleraar in de veeteeltwetenschap,
n het openbaar te verdedigen
p woensdag 22 december 1982
es namiddags te vier uur in de aula
an de Landbouwhogeschool te Wageningen.

LANDBOUWHOGESCHOOL
WAGENINGEN

ISBN = 194685-03

Cover Photograph: Laser-excitation of isoalloxazines using the equipment for time-resolved fluorescence spectroscopy described in chapter 2.

STELLINGEN

1. De door Yamaguchi *et al.* voorgestelde ladingsherverdeling in de aangeslagen singuletoestanden van 5-deazaflavine is op niets gebaseerd.

H. Yamaguchi, A. Koshiro, Y. Harima, K. Mori en F. Yoneda, *Spectrochim. Acta* 37A (1981) 51.
2. De door Ahmad en Tollin voorgestelde verandering van het reactiemechanisme voor het verval van triplet-flavine in flavine semichinon bij zekere waarde der dielectrische constante van het oplosmiddel, is in strijd met hun experimentele uitkomsten.

I. Ahmad en G. Tollin, *Biochemistry* 20 (1981) 5925.
3. Fragata heeft gelijk in zijn stelling dat Schmidt's experimenten met amphiflavines geen bewijs leveren voor de hypothese dat amphifiele chromoforen dieper in het hydrofobe gedeelte van membranen zinken bij de faseovergang gel \rightarrow vloeibaar kristal. In de hieruit voortvloeiende polemiek voeren beide onderzoekers evenwel onjuiste argumenten aan.

W. Schmidt, *J. Membrane Biol.* 47 (1979) 1; M. Fragata, *ibid.* 60 (1981) 163; W. Schmidt, *ibid.* 60 (1981) 164.
4. Jung en Tollin's experimentele resultaten geven geen rechtvaardiging voor hun hypothese dat de 7,8-dimethylbenzeenring in flavine bepalend zou zijn voor de redox eigenschappen.

J. Jung en G. Tollin, *Biochemistry* 20 (1981) 5124.
5. Ondanks het feit dat het tegenovergestelde wordt gesuggereerd, bepalen Johansson *et al.* geen absolute richtingen van de overgangsdipoolmomenten in flavine.

L.B.Å. Johansson, Å. Davidsson, G. Lindblom en K. Razi Naqvi, *Biochemistry* 18 (1979) 4249.
6. De fijnstructuur rond 10.1 eV in het UV fotoelectronspectrum van uracil wordt door Palmer *et al.* ten onrechte toegekend aan het voorkomen van tautomeren in de damp van uracil.

M.H. Palmer, I. Simpson en R.J. Platenkamp, *J. Mol. Struct.* 66 (1980) 243; G. Lauer, W. Schäfer en A. Schweig, *Tetrahedron Letters* 45 (1975) 3939.

7. Als gevolg van een onjuiste interpretatie van de gemeten diffusiesnelheid van 1-hexeen in zeoliet ZSM-5 betwijfelen Haag *et al.* ten onrechte de geldigheid van het klassieke diffusiemodel volgens Knudsen.

W.O. Haag, R.M. Lago en P.B. Weisz, Faraday Discuss. Chem. Soc. 72 (1982) 317 (Publ. 1981).

8. Gezien het feit dat zich tussen de chemisch-kinetische en quantummechanische benadering van het begrip "transition state" een gapende kloof blijkt te bevinden, speciaal in het geval van enzymatische reacties, dienen (bio)chemici, fysici en biologen zich niet te beperken tot hun eigen specialisatie maar wezenlijk multidisciplinair te denken.

E.K. Thornton en E.R. Thornton, in: Transition States of Biochemical Processes, eds. R.D. Gandour en R.L. Schowen (Plenum Press, New York, 1978); G.M. Maggiora en R.E. Christoffersen, *ibid.*

9. Zelfs het uitvoeren van een MINDO/3-SCF-LCAO-MO berekening op LSD werkt hallucinerend.

M.J.S. Dewar, Science 187 (1975) 1037.

10. Hoe alledaags de problemen en frustraties verbonden aan het bedrijven van theoretische chemie zijn bewijst de "editorial note" betreffende het matrixelement $\langle \sigma | \mathbf{H} | \sigma \rangle$ in een van Hoffmann's artikelen.

Note 20 in: R. Hoffmann, Acc. Chem. Res. 4 (1971) 1.

11. De onder vele musici levende gedachte dat de "toonkwaliteit" van een blaasinstrument, zo deze al objectief meetbaar is, zou toenemen naarmate men het instrument uit "edeler" (hout - zilverlegering - goudlegering) materiaal vervaardigt, is in flagrante tegenspraak met de fysische wetten die het functioneren van het instrument bepalen. De gedachte ligt derhalve verankerd in de psychologie van betreffende musici.

S.E. Parker, J. Acoust. Soc. Amer. 19 (1947) 415; A.H. Benade, *ibid.* 31 (1959) 137.

12. Indien de voorgestelde toekomstige vakgroep wetenschapsdynamica in haar doelstellingen slaagt, zal dit tot een afname van de dynamiek in de wetenschap aanleiding geven.

Commentaar op de RAWB nota, Chemisch Weekblad, 78e jaargang, no. 29/30, 22 juli 1982.

J.K. Eweg

On the electronic structure of free
and protein-bound isoalloxazines
22 december 1982, Wageningen.



.....?

(Citaat zonder woorden)

Je kunt aan één molecuul een leven lang meten,
Zonder de levensduur dáárvan te weten.

(De "Kerstklaas" alias "Sinterman" op
bezoek bij de afdeling Biochemie te
Wageningen als "Visiting Professor",
december 1977)

Aan Marja,
Aan mijn Ouders.

CONTENTS

CHAPTER 1	GENERAL INTRODUCTION	1
	References and notes	6
CHAPTER 2	EXPERIMENTAL TECHNIQUES AND CALCULATION PROCEDURES	8
	2.1. Preparative chemistry and purification procedures	8
	2.2. Vacuum system	8
	2.3. Spectroscopic equipment	8
	2.4. Photoelectron spectrometer	13
	2.5. Molecular orbital calculations	13
	2.5.1. SCF-Formalism	13
	2.5.2. Methods employing the Neglect of Differential Overlap	16
	2.5.3. Spectroscopic Data	19
	References	20
CHAPTER 3	LUMINESCENCE OF SOME ISOALLOXAZINES IN APOLAR SOLVENTS	22
	3.1. Introduction	22
	3.2. Materials and methods	22
	3.2.1. Purification of solvents	22
	3.2.2. Synthesis of new isoalloxazine derivatives	23
	3.2.3. Preparation of samples	23
	3.2.4. Measurement of the dielectric constant	24
	3.2.5. Equipment	24
	3.3. Results	24
	3.3.1. Luminescence in 2-MTHF	26
	3.3.2. Luminescence in 3-MP	30
	3.4. Discussion	32
	References and notes	35
CHAPTER 4	SPECTRAL PROPERTIES OF (ISO)ALLOXAZINES IN THE VAPOUR PHASE	37
	4.1. Introduction	37
	4.2. Materials and methods	38
	4.2.1. Synthesis of isoalloxazine derivatives	38
	4.2.2. Preparation of the samples	38
	4.2.3. Equipment	38
	4.3. Results	39
	4.4. Discussion	47
	References and note	50
CHAPTER 5	HE(I) AND HE(II) PHOTOELECTRON SPECTRA OF ALLOXAZINES AND ISOALLOXAZINES	52
	5.1. Introduction	52
	5.2. Experimental	53
	5.3. Calculation procedures	53
	5.4. Experimental results and spectral assignments	54
	5.4.1. Isoalloxazine derivatives in the oxidized form	54
	5.4.2. 1,3-dimethyl-alloxazine	60
	5.4.3. 1,3,7,8,10-pentamethyl-1,5-dihydro-isoalloxazine	65

5.5. Calculated results	66
5.5.1. <i>The influence of substitution</i>	69
5.5.2. <i>The influence of reduction</i>	69
5.6. Discussion	76
References and notes	80

CHAPTER 6	ANOMALOUS INTRAMOLECULAR HYDROGEN BOND IN 10-HYDROXYALKYL ISO-ALLOXAZINES AS REVEALED BY PHOTOELECTRON SPECTROSCOPY, AND THE IMPLICATIONS FOR OPTICAL SPECTRA	83
-----------	---	----

6.1. Introduction	83
6.2. Experimental and theoretical section	84
6.3. Results	85
6.3.1. <i>Photoelectron spectra and orbital structure</i>	85
6.3.2. <i>The isoalloxazine optical spectrum</i>	95
6.4. Discussion	101
References and notes	104

CHAPTER 7	ON THE ENIGMA OF OLD YELLOW ENZYME'S SPECTRAL PROPERTIES	106
-----------	--	-----

7.1. Introduction	106
7.2. Materials and methods	108
7.3. Results and discussion	109
7.3.1. <i>Absorption and CD spectra</i>	109
7.3.2. <i>Luminescence spectra</i>	114
7.3.3. <i>Theoretical data</i>	122
7.3.4. <i>Electron paramagnetic resonance (ESR) spectra</i>	129
7.4. Conclusions	130
References and notes	132

CHAPTER 8	ON THE ELECTRONIC STRUCTURE OF FREE AND PROTEIN-BOUND ISO-ALLOXAZINES, A POSTSCRIPT	135
-----------	---	-----

APPENDIX 1	CONFIGURATION INTERACTION DATA ON OXIDIZED ISOALLOXAZINE DERIVATIVES	142
------------	--	-----

SUMMARY	157
---------	-----

SAMENVATTING	161
--------------	-----

LIST OF ABBREVIATIONS

A	Absorbance (Optical Density)
calc.	calculated
CARS	Coherent Anti-Stokes Raman Scattering
CD	Circular Dichroism
CI	Configuration Interaction
CNDO/S	Complete Neglect of Differential Overlap, S = Spectroscopic
corr.	corrected
CT	Charge Transfer
CW	Continuous Wave
D	Debye (10^{-18} esu.cm = 3.3356×10^{-30} Coul.m): Unit of dipole moment
EC	Enzyme Commission (number)
ESCA	Electron Spectrometer for Chemical Analysis (cf. XPS)
ESR	Electron Spin Resonance (Spectroscopy)
FAD	Flavin Adenine Dinucleotide
FMN	Flavin Mononucleotide (Riboflavin-5'-phosphate)
FWHM	Full Width at Half Maximum
He(I)	Helium-I radiation (21.21 eV = 584 Å)
He(II)	Helium-II radiation (40.81 eV = 304 Å)
4-HNBBA	4-Hydroxy-N-n-butylbenzamide
HOMO	Highest Occupied Molecular Orbital
INDO/S	Intermediate Neglect of Differential Overlap, S = Spectroscopic
IR	Infrared
ISC	Intersystem crossing
k_{ISC}	Intersystem crossing rate constant
LASER	Light Amplification by Stimulated Emission of Radiation
LCAO	Linear Combination of Atomic Orbitals
LNDO/S	Local Neglect of Differential Overlap, S = Spectroscopic
LUMO	Lowest Unoccupied Molecular Orbital
4-MBA	4-Methoxy-benzaldehyde
MINDO	Modified Intermediate Neglect of Differential Overlap
MO	Molecular Orbital
3-MP	3-Methyl-pentane
2-MTHF	2-Methyl-tetrahydrofuran
NADH	Nicotinamide Adenine Dinucleotide, reduced form
NAD ⁺	Nicotinamide Adenine Dinucleotide, oxidized form
NADPH	Nicotinamide Adenine Dinucleotide Phosphate, reduced form
NADP ⁺	Nicotinamide Adenine Dinucleotide Phosphate, oxidized form
NDDO	Neglect of Diatomic Differential Overlap
NMR	Nuclear Magnetic Resonance
ODMR	Optical Detection of Magnetic Resonance
ORD	Optical Rotatory Dispersion
OYE	Old Yellow Enzyme
PPP	Pariser-Parr-Pople (computational method)
PRDDO	Partial Retention of Diatomic Differential Overlap
RR	Resonance Raman (Spectroscopy)
SCF	Self Consistent Field
SHG	Second Harmonic Generation
Tris	Tris(hydroxymethyl)-aminomethane
uncorr.	uncorrected
UPS	Ultraviolet Photoelectron Spectroscopy
UV	Ultraviolet

LIST OF ABBREVIATIONS (CONTD.)

XPS	X-ray Photoelectron Spectroscopy
ZDO	Zero Differential Overlap
ϕ_f	Quantum yield of fluorescence
ϕ_p	Quantum yield of phosphorescence
ν_{ex}	Excitation wavenumber (in cm^{-1})
$\Delta\bar{\nu}_{ex}$	Excitation bandwidth (in cm^{-1})
$\bar{\nu}_{em}$	Emission wavenumber or wavenumber of detection (in cm^{-1})
$\Delta\bar{\nu}_{em}$	Detection bandwidth (in cm^{-1})
τ_0	Radiative lifetime
τ_f	Actual (fluorescence) lifetime
τ_p	Phosphorescence lifetime

VOORWOORD

Bij het gereedkomen van mijn proefschrift, waarvan het schrijven zelf te beschouwen is als de spreekwoordelijke top van de ijsberg gezien het feit dat de oorspronkelijke vraagstelling noodzakelijkerwijs moest leiden tot enerzijds ontwikkelingswerk aan laboratorium instrumentatie en infrastructuur en anderzijds tot vergaande samenwerking met en veelvuldig reizen naar andere instituten in Nederland, wil ik gaarne diegenen bedanken die in belangrijke mate hebben bijgedragen tot het welslagen van een en ander. Primair is dat mijn hooggeschatte promotor Prof. Dr. F. Müller. Beste Franz, het is niet overdreven te stellen dat zonder jouw ondersteuning vanuit een enorme flavine-chemische vakkennis en ervaring en zonder jouw bescherming tegen oneerlijke concurrentie, het onderzoek zou zijn vastgelopen. Jouw steun in het, met zekere koppigheid vasthouden aan het streven oorspronkelijk overeengekomen doelstellingen te verwezenlijken ondanks tegenslagen van technische aard, heb ik hogelijk gewaardeerd. Mijn hooggeschatte co-promotor Prof. Dr. Cees Veeger dank ik voor de kritische begeleiding en de zorg dat het onderzoek niet ontaardde in een "l'art pour l'art" bedrijven van fysische chemie maar gericht bleef op biochemische relevantie.

Hiernaast gaat mijn dank uit naar vele LH collega's. Dr. Ton Visser en Dr. Hans Grande dank ik voor de wijze waarop zij mij op de vakgroep biochemie hebben ingewerkt. De laatste dank ik ook voor zijn hulp bij de ESR metingen aan Old Yellow Enzyme. Belangrijke bijdragen aan het onderzoek van dit enzym werden ook geleverd door Willem van Berkel. Arie van Hoek dank ik voor zijn assistentie in de luminescentie metingen met de CR-18 laser, Ir. Peter Kampmeijer vervaardigde het computerprogramma om gecorrigeerde spectra in fraaie plaatjes weer te geven en Jillert Santema verzorgde mijn om- c.q. bijscholing die mij als leek op biochemisch terrein in staat stelde het Ka-practicum biochemie te geven en te beoordelen welke student het "vliegbriefje" waardig was. Bery Sachteleben en Martin Boumans dank ik voor hun schitterende tekenwerk en Jenny Toppenberg-Fang en Lenny Weldring voor het verzorgen van een aantal manuscripten van tijdschrift-artikelen.

Woorden van dank ook aan een aantal medewerkers van de Universiteit van Amsterdam. Ten eerste aan Prof. Dr. Joop van Voorst bij wie ik het "vak" als doctoraal student en vooral dankzij het continueren van de samenwerking na mijn vertrek naar Wageningen, mocht leren. Ik heb zijn belangrijke bijdragen aan het onderzoek, mede door het beschikbaar stellen van vele dagen meettijd op het

voortreffelijke instrumentarium van de vakgroep Fysische Chemie, zeer gewaardeerd. Voorts wil ik in deze vakgroep bedanken de collega's Dick Beelaar voor zijn hulp bij de laser-experimenten en zijn vele technische adviezen, vooral op het gebied van photomultipliers; Jan van Tiel, Bas Rooswijk en Sijb Oostenga voor hun adviezen op vacuum-technisch gebied en Ab van den Bergh en Gerard IJsselstein voor hun hulp om tot het vervaardigen van fluorescentie-vrije kwartscellen te komen. Bij de vakgroep Anorganische Chemie werden de allereerste fotoelectron spectra van flavines verkregen. Deze doorbraak was mogelijk dankzij de uitstekende samenwerking met Prof. Dr. Ad Oskam, Dr. Henk van Dam en Andries Terpstra en de vakkundig, door Jan Ernsting geregistreerde thermogrammen, die het inzicht verschaften hoe ver men te ver kon gaan bij het verhitten van de flavines. Drs. Jaap Louwen maakte mij wegwijs in het huidige operating system van de CDC Cyber. Gaarne dank ik ook Dr. Steef de Bruijn (vakgroep Theoretische Chemie), Prof. Dr. Jan Verhoeven (vakgroep Organische Chemie) en Cor Worrell (vakgroep Algemene en Anorganische Chemie, Rijksuniversiteit Utrecht) voor hun vele waardevolle suggesties en ideeën.

I wish to express my sincere gratitude to Prof. Dr. Hans H. Jaffé (University of Cincinnati, Cincinnati, Ohio, USA) for encouraging and stimulating discussion and for supplying the results of his calculations on isoalloxazine. His results finally convinced me that my own CI-programs did not contain trivial errors.

Met genoegen denk ik ook terug aan mijn werkzaamheden op het Centraal Rekeninstituut van de Rijksuniversiteit Leiden, wellicht Nederlands meest "gebruikersvriendelijke" computercentrum, dankzij een uitstekende afdeling voorlichting. Mijn dank geldt hier Drs. Ben Hesper voor alle programmeer-adviezen, het beschikbaar stellen van eigen routines en een niet aflatende belangstelling voor voortgang en resultaten van het onderzoek. Rinco van der Baan en zijn opvolger Cees Drop (voorheen IBM- 370/158-Amdahl operator) beheerden de PDP 11/70 op zodanig voortreffelijke wijze dat zelfs headcrashes geen kopzorgen voor de gebruiker betekenden. In Cees bedank ik ook alle overige, mij niet bij name bekende, IBM - Amdahl operators die zelfs om tien uur 's avonds nog bereid bleken een tape op te spannen of waar nodig BIWAØØØØ een "zetje te geven". Dankzij Drs. Peter van Rossum was het CRI zelfs met een gebroken been bereikbaar.

In Wageningen ondervond ik technische ondersteuning van de Technisch-Fysische Dienst voor de Landbouw (TFDL). Hier dank ik met name de instrumentmakers M. van Ginkel en M.W. Hoogstede voor hun uitstekende werk. Mijn goede bennekomse burens Joke en Dick Veenendaal dank ik voor al hun goede zorgen voor huis en haard gedurende mijn veelvuldige omzwervingen door het land.

Mijn ouders dank ik, niet alleen voor het feit dat zij mij in staat stelden mijn opleiding te volgen, maar ook voor hun hulp bij mijn vestiging in Bennekom

onder wat moeilijke privé omstandigheden. Bovendien dank ik mijn vader voor de wijze waarop hij uit een paar schetsjes op een kladje een voortreffelijke werktekening maakte van de "Ware and Cunningham two-level furnace" t.b.v. de wageningsse TFDL. Tenslotte, last but not least dank ik mijn echtgenote, Drs. Marja MacLaine Pont. Zij verzorgde al het typewerk voor dit boekje, assisteerde vele malen bij experimenten in het weekend en was zelfs bereid, tegen haar principes in, achter zoiets engs als een computer terminal te kruipen. Ik zal haar bijdragen niet licht vergeten.

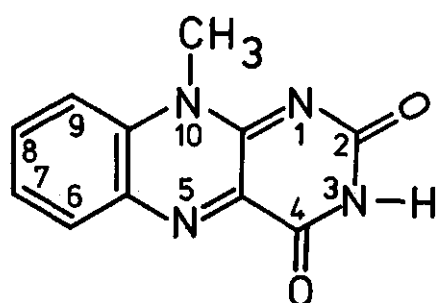
Chapters 3 - 7 have been published separately.

- Chapter 3: J.K. Eweg, F. Müller, A.J.W.G. Visser, C. Veeger, D. Bebelaar and J.D.W. van Voorst, Photochem. Photobiol. 30 (1979) 463.
Chapter 4: J.K. Eweg, F. Müller, D. Bebelaar and J.D.W. van Voorst, Photochem. Photobiol. 31 (1980) 435.
Chapter 5: J.K. Eweg, F. Müller, H. van Dam, A. Terpstra and A. Oskam, J. Amer. Chem. Soc. 102 (1980) 51.
Chapter 6: J.K. Eweg, F. Müller, H. van Dam, A. Terpstra and A. Oskam, J. Phys. Chem. 86 (1982) 1642.
Chapter 7: J.K. Eweg, F. Müller and W.J.H. van Berkel, Eur. J. Biochem. (1982), in the press.

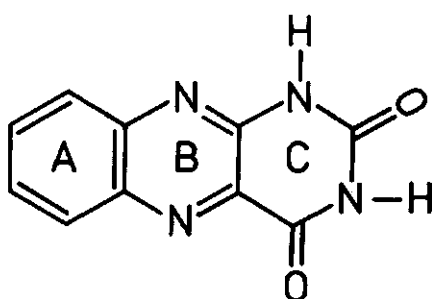
The work described in this thesis was supported by the Netherlands Foundation for Chemical Research (S.O.N.) with financial aid from the Netherlands Organization for the Advancement of Pure Research (Z.W.O.).

1 GENERAL INTRODUCTION

Isoalloxazine chemistry was born in 1932. In that year Warburg and Christian^{1,2} isolated an enzyme from yeast which, after appropriate purification, was found to contain a characteristic yellow dye. In the following years the nature of this dye was the subject of extensive studies¹⁻⁷. By synthesis⁸ its molecular structure was finally confirmed to be that of the compound which is nowadays called riboflavin-5'-phosphate or flavin-mono-nucleotide (FMN), a derivative of isoalloxazine. Theorell⁹ was the first to show that the constituents of the enzyme (the dye and a carrier protein) could be dissociated and recombined again, demonstrating that the dye was non-covalently bound to the, so-called, apoprotein. This experiment was also the first reversible dissociation of a holoenzyme into its prosthetic group and an apoenzyme. Ironically, the physiological role of this "Old Yellow Enzyme" is still entirely unknown, even after almost fifty years of research. However, in those fifty years science revealed the ubiquity of flavins in nature as the prosthetic group of many enzymes. These enzymes constitute a large group within the main class of oxido-reductases and electron carriers. They will be referred to as flavoproteins hereafter. The physiological function of the most important flavoproteins is described, for example, in Lehninger's textbook on biochemistry¹⁰.



iso-alloxazine

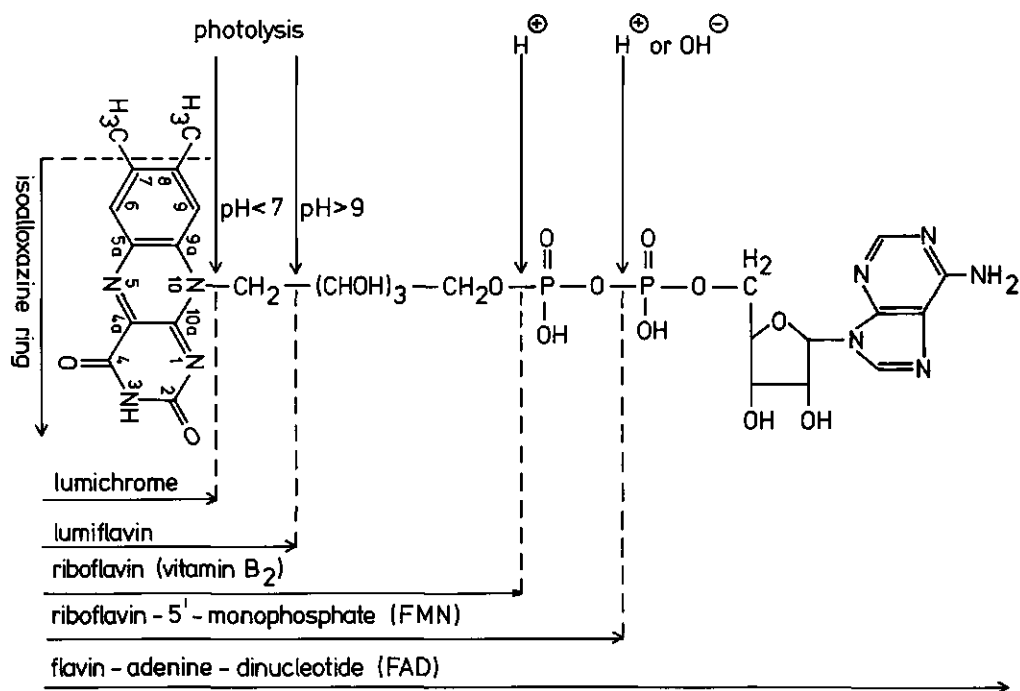


alloxazine

Scheme 1.1. Molecular structure of the simplest stable alloxazine and isoalloxazine.

Flavin is the commonly used name for all 7,8-dimethyl-isoalloxazine derivatives. Isoalloxazine itself, whose index name according to CA¹¹ is benzo[g]pteridine-2,4 (3H,10H)-dione, can formally be regarded as the tautomeric form of alloxazine. The molecular structures of both compounds in their simplest form are given in Scheme 1.1. Isoalloxazine can exist only when the system carries a carbon substituent at position 10. When the ring system carries no other substituents than hydrogen atoms it only occurs in the alloxazine tautomeric form. Recently, the alloxazine \leftrightarrow isoalloxazine tautomerism, both in the electronic ground and excited states, has become the subject of scientific investigation¹²⁻¹⁸.

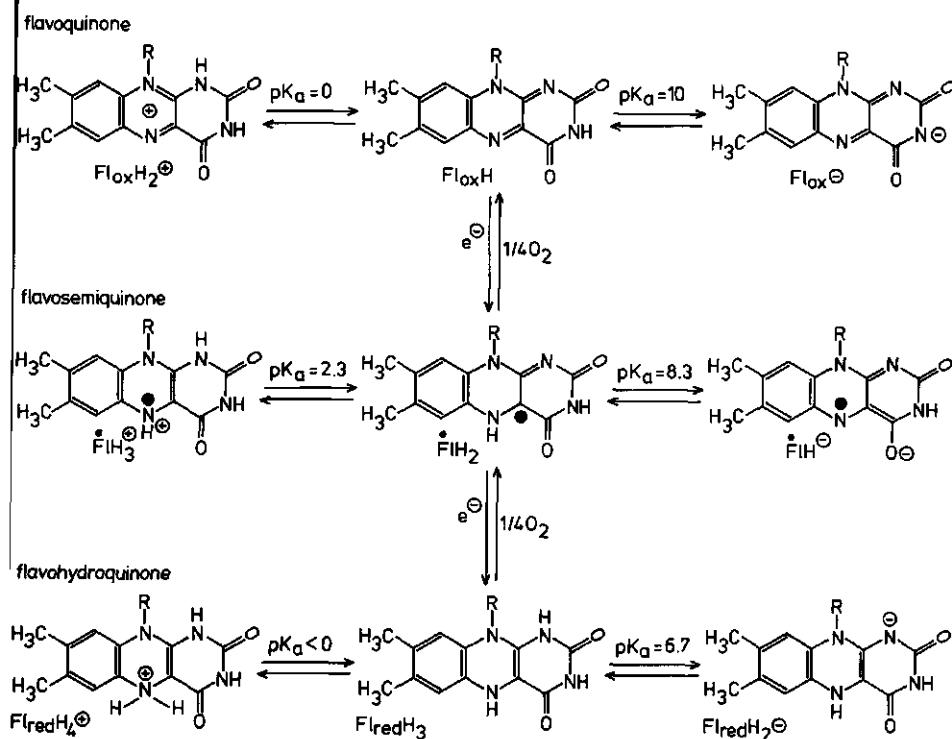
The molecular structures of isoalloxazine derivatives, which are important in physiological processes, are pictured in Scheme 1.2. In biochemical catalysis,



Scheme 1.2. Molecular structures of naturally occurring isoalloxazines and their decomposition by hydrolysis and photolysis.

the flavoproteins owe their unique properties to the existence of three possible oxidation states of isoalloxazine, *viz.* the oxidized (quinone), half reduced

semiquinone) and fully reduced (hydroquinone) forms. Each form can occur at least in three different states of protonation as is shown in Scheme 1.3.



Scheme 1.3. The various redox states of isoalloxazine.

The research of all these states, both free and protein-bound, constitutes an impressive scientific endeavour. The "state of the art" of isoalloxazine (physiological) chemistry and molecular biology at the time the results contained in Chapters 1 to 5 were published as separate papers (cf. page opposite to p. 1), was adequately described in the proceedings of six international symposia¹⁹⁻²⁴, a discussion meeting²⁵ and general review articles²⁶⁻³⁰. More specialistic review articles were devoted to 1) The binding of flavins to flavoproteins³¹; 2) Electron transferring properties³²; 3) Flavin fluorescence^{26,33}; 4) The interaction of flavins with aromatic amino acids³⁴; 5) The differences between flavins and 5-deaza-flavin derivatives with respect to redox properties, both free and protein-bound³⁵; 6) The flavin molecular geometry as determined by X-ray crystallography^{36,37} and 7) Flavin photochemistry³⁸.

Like in Old Yellow Enzyme, the isoalloxazine prosthetic group in other enzymes is generally non-covalently bound to the apoprotein. Exceptions, for

example, are succinate dehydrogenase¹⁰, monoamine oxidase³⁹ and D-gluconolactone dehydrogenase⁴⁰, which contain a covalently bound isoalloxazine prosthetic group. The latter ones will not be considered here. The *general* property of flavoproteins has given strong impetus to spectroscopic studies on isoalloxazines, in protein-bound and free occurrence. For the benefit of these studies, also a large variety of derivatives which do not naturally occur, was synthesized^{27,28,41}. The main aim of these studies invariably is to reveal both the intrinsic properties of the (iso)alloxazine electronic system and the way such properties depend on the molecular environment of the chromophore. It is clear that all kinds of environmental interactions are possible, ranging from simple solute-solvent dipolar interaction to specific interactions like H-bond formation and the complexation of the isoalloxazine nucleus with amino acid residues in an apoprotein³⁴. The complexation of protein-bound isoalloxazine with a substrate molecule prior to the chemical conversion of the latter by virtue of the catalytic activity of the prosthetic group is, of course, of particular importance.

A large variety of spectroscopic techniques (UV absorption and emission, CD, ORD, IR, NMR, ESR, ODMR, Resonance Raman and CARS) was applied in isoalloxazine research. In view of the contributions to this research from Wageningen, The Netherlands^{42,43} it was desirable to undertake a more detailed study than was done before, on the *photophysics of isoalloxazines*, with special attention to the *photophysical properties of the isolated molecule*. As long as such properties are not entirely known, it is hazardous to draw far reaching conclusions from optical spectra which are characterized by their lack of information rather than their information content. Moreover, how can one distinguish between the intrinsic properties of such a complex molecule as isoalloxazine and properties which arise from its interaction with "the outside world", as long as the former properties are not established unambiguously? In this respect it should also be realized that almost every biochemist intuitively agrees with the common statement, that the large variety of properties which has been discovered for flavoproteins thus far, must arise from a large variety of intermolecular interactions of isoalloxazine with its molecular environment. Otherwise it is hard to explain such a variety of properties of enzymes which all owe their catalytic activity to one and the same molecule.

This thesis will be confined to an investigation of the (iso)alloxazine chromophore by means of optical spectroscopy in a wide wavelength-range (30.4 nm - 900 nm). To be more specific, the problems existing at the time this investigation was started (cf. literature cited on p. 3), can be summarized as follows:

- 1: The published continuous wave (CW) optical spectra of (iso)alloxazines (absorption, emission, excitation) were very diffuse. This is caused by the absence of molecular symmetry (no symmetry-forbidden electronic transitions) and the fact that most (iso)alloxazine derivatives are only soluble in very polar solvents. Therefore, a resolved vibrational structure was rarely observed in these spectra, which made it difficult to determine even ordinary photophysical properties such as the relative intensities of vibronic transitions corresponding to one particular electronic transition, the location of 0-0 bands in optical spectra with an accuracy of a few hundred cm^{-1} and the Stokes-loss. Investigators who succeeded in obtaining a reasonable spectral resolution of vibrational spacings^{14,33,44-46} did not pay more attention to it than common statements. Only Koziol and Koziolowa¹⁵ and Miller *et al.*⁴⁷ treated the subject of vibrational structure more explicitly. Some isoalloxazine vibrational frequencies were determined from CARS experiments⁴⁸ but, up till now, their assignment is still subject to discussion⁴⁹ (cf. Chapter 8, p. 135). Two-photon excitation⁵⁰ also provided no new insights.
- 2: Various techniques in the field of time-resolved optical spectroscopy yielded a large variety of data on fluorescence lifetimes^{13,51-55}, phosphorescence lifetimes⁵⁵⁻⁵⁹ and intersystem-crossing rate constants^{55,58,59}. The results revealed an extreme sensitivity of the excited state kinetics of (iso)alloxazines towards external perturbations. Again the discrimination between intramolecular and intermolecular aspects was very difficult. Experiments carried out under circumstances where nice spectral resolution could be obtained lacked the determination of fluorescence lifetimes.
- 3: A large number of quantum mechanical calculations was performed on (iso)alloxazines. These are discussed in detail in Chapters 5 and 6 (pp. 52 and 83). Here it is sufficient to emphasize that, apart from the shortcomings of such calculations, additional difficulties emerge in the verification of the theory by comparison with optical spectra which are seriously broadened (*vide supra*). So, especially better experimental results were required to check the validity of the theory.
- 4: As long as problems 1 to 3 cannot be brought closer to a solution, the interpretation of CW and time-resolved optical spectra will suffer from uncertainties.

In the study of these problems it was attempted to approach the conditions under which (iso)alloxazines can exist as isolated molecules as closely as possible.

In this respect, the spectroscopy on (iso)alloxazines in the vapour phase not

only proved to be feasible, but it also yielded a wealth of information. Successively, it was tried to use this information in the interpretation of more complex phenomena observed from Old Yellow Enzyme.

REFERENCES AND NOTES

- 1 O. Warburg and W. Christian, *Naturwiss.* 20 (1932) 688; *ibid.* 20 (1932) 980.
- 2 O. Warburg and W. Christian, *Biochem. Z.* 254 (1932) 438; *ibid.* 257 (1933) 492; *ibid.* 258 (1933) 496; *ibid.* 263 (1933) 228; *ibid.* 266 (1933) 377.
- 3 Ph. Ellinger and W. Koschara, *Chem. Ber.* 66 (1933) 315.
- 4 R. Kuhn, P. György and T. Wagner-Jauregg, *Chem. Ber.* 66 (1933) 317.
- 5 R. Kuhn, K. Reinmund, H. Kaltschmitt, R. Ströbele and H. Trischman, *Naturwiss.* 23 (1935) 260.
- 6 P. Karrer, K. Schöpp and F. Benz, *Helv. Chim. Acta* 18 (1935) 426.
- 7 H. Theorell, *Biochem. Z.* 275 (1935) 344.
- 8 R. Kuhn, H. Rudy and F. Weygand, *Chem. Ber.* 69 (1936) 1543.
- 9 H. Theorell, *Naturwiss.* 22 (1934) 289; *ibid.*, *Biochem. Z.* 272 (1934) 155.
- 10 A.L. Lehninger, *Biochemistry* (Worth, New York, 2nd. ed., 1975).
- 11 Chemical Abstracts, Vol. 76, Index Guide, Columbus, Ohio, 1972.
- 12 P.S. Song, M. Sun, A. Koziolowa and J. Koziol, *J. Amer. Chem. Soc.* 96 (1974) 4319.
- 13 R.D. Fugate and P.S. Song, *Photochem. Photobiol.* 24 (1976) 479.
- 14 J. Koziol and A. Koziolowa, in: *Flavins and Flavoproteins, Physicochemical Properties and Function*, Proc. Int. Meeting, ed. W. Ostrowsky (Polish Scientific Publishers, Warsaw and Cracow, 1977).
- 15 J. Koziol and A. Koziolowa, in: *Flavins and Flavoproteins*, Proc. 6th. Int. Conf., eds. K. Yagi and T. Yamano (Japanese Scientific Soc. Press, Tokyo, 1980).
- 16 P.S. Song, Q. Chae and M. Sun, in: *Excited States of Biological Molecules*, Proc. Int. Conf., ed. J.B. Birks (Wiley, Chichester, 1976).
- 17 N. Lasser and J. Feitelson, *Photochem. Photobiol.* 25 (1977) 451.
- 18 S. Bergström and B. Holmström, Proc. 7th IUPAC. Symp. *Photochem.* (1978) 40.
- 19 E.C. Slater (ed.): *Flavins and Flavoproteins*, Proc. 1st. Int. Conf., B.B.A. Library, Vol. 8 (Elsevier, Amsterdam, 1966).
- 20 K. Yagi (ed.): *Flavins and Flavoproteins*, Proc. 2nd. Int. Conf. (University Park Press, Baltimore, 1968).
- 21 H. Kamin (ed.): *Flavins and Flavoproteins*, Proc. 3rd. Int. Conf. (University Park Press, Baltimore, 1971).
- 22 There are no official proceedings of the 4th. meeting. Main contributions in *Z. Naturf.* 27b (1972) 1011-1122.
- 23 T.P. Singer (ed.): *Flavins and Flavoproteins*, Proc. 5th. Int. Conf. (Elsevier, Amsterdam, 1976).
- 24 K. Yagi and T. Yamano (eds.): *Flavins and Flavoproteins*, Proc. 6th. Int. Conf. (Japanese Scientific Soc. Press, Tokyo, 1980).
- 25 W. Ostrowsky (ed.): *Flavins and Flavoproteins, Physicochemical Properties and Function*, Proc. Int. Meeting (Polish Scientific Publishers, Warsaw and Cracow, 1977).
- 26 G.R. Penzer and G.K. Radda, *Quart. Rev. Biophys.* 21 (1967) 43.
- 27 P. Hemmerich, *Fortschr. Chem. Org. Naturst.* 33 (1976) 451.
- 28 J. Yoshimura, in: *Method. Chim.*, eds. F. Korte and M. Goto (Academic Press, New York, 1977).
- 29 D.B. McCormick, in: *Nutr.*, 4th. ed. (Nutr. Found., Washington D.C., 1976).
- 30 P. Hemmerich, G.N. Nagelschneider and C. Veeger, *FEBS Letters* 8 (1970) 69.

- 31 W.R. Weimar and A.H. Neims, in: Riboflavin, ed. R. Rivlin (Plenum, New York, 1975).
- 32 P. Hemmerich, Adv. Chem. Ser. 162 (1977) 312.
- 33 K. Yagi, in: Biochemical Fluorescence Concepts, eds. R.F. Chen and H. Edelhoch, Vol. 2 (Dekker, New York, 1976).
- 34 D.B. McCormick, Photochem. Photobiol. 26 (1977) 169; *ibid.*, Jerusalem Symp. Quantum Chem. Biochem. 10 (1977) 233.
- 35 P. Hemmerich, V. Massey and H. Fenner, FEBS Letters 84 (1977) 5.
- 36 M. von Glehn, Thesis, University of Stockholm, Sweden, Chem. Commun. XI (1971).
- 37 M. Leijonmarck, Thesis, University of Stockholm, Sweden, Chem. Commun. VIII (1977).
- 38 S. Ohishi, Vitamin 53 (1979) 35.
- 39 P. Hemmerich, A. Ehrenberg, W.H. Walker, L.G.E. Eriksson, J. Salach, P. Bader and T.P. Singer, FEBS Letters 3 (1969) 37.
- 40 M. Shimizu, S. Murakawa and T. Takahashi, Agric. Biol. Chem. 41 (1977) 2107.
- 41 Cf. Chapter 3 and refs. therein; Chapter 4 and refs. therein.
- 42 Several theses embody the research on flavins and flavoproteins carried out at the Agricultural University, Department of Biochemistry, Wageningen, The Netherlands: A.J.W.G. Visser (1975); T.W. Bresters (1975); J. Krul (1975); H.J. Grande (1976); R.A. de Abreu (1978) and C.G. van Schagen (in preparation).
- 43 R.K. Wierenga, Thesis, University of Groningen, Groningen, The Netherlands (1978).
- 44 Cf. Chapter 3, references 13-15 and 35.
- 45 P.S. Song, T.A. Moore, W.H. Gordon, M. Sun and C.N. Ou, in: Organic Scintillators and Liquid Scintillation Counting (Academic Press, New York, 1971).
- 46 S. Ghisla, V. Massey, J.M. Lhoste and S.G. Mayhew, Biochemistry 13 (1974) 589.
- 47 F. Müller, S.G. Mayhew and V. Massey, Biochemistry 12 (1973) 4654.
- 48 P.K. Dutta, J.R. Nestor and T.G. Spiro, Proc. Natl. Acad. Sci. USA. 74 (1977) 4146; *ibid.*, Biochem. Biophys. Res. Commun. 83 (1978) 209.
- 49 J. Lee, Personal Communication.
- 50 N.Y.C. Chu and K. Weiss, Chem. Phys. Letters 27 (1974) 567.
- 51 Ph. Wahl, J.C. Auchet, A.J.W.G. Visser and F. Müller, FEBS Letters 44 (1974) 23.
- 52 A.J.W.G. Visser, H.J. Grande, F. Müller and C. Veeger, Eur. J. Biochem. 45 (1974) 99.
- 53 Ph. Wahl, J.C. Auchet, A.J.W.G. Visser and C. Veeger, Eur. J. Biochem. 50 (1975) 413.
- 54 Cf. Chapter 3, references 24 and 31.
- 55 M.S. Grodowski, B. Veyret and K. Weiss, Photochem. Photobiol. 26 (1977) 341.
- 56 G.R. Brunk, K.A. Martin and A. Nishimura, Biophys. J. 16 (1976) 1373.
- 57 W.M. Moore, J.C. McDaniels and J.A. Hen, Photochem. Photobiol. 25 (1977) 505.
- 58 Cf. Chapter 3, references 36 and 37.
- 59 D.E. Edmondson, F. Rizzuto and G. Tollin, Photochem. Photobiol. 24 (1977) 445.

2 EXPERIMENTAL TECHNIQUES AND CALCULATION PROCEDURES

2.1. PREPARATIVE CHEMISTRY AND PURIFICATION PROCEDURES

Since a large variety of compounds was studied by several experimental techniques, their synthesis or isolation and subsequent purification will be described in the individual following chapters. Often the decision to synthesize new derivatives was initiated by previous experimental experience.

2.2. VACUUM SYSTEM

A pyrex vacuum-line with a liquid nitrogen cooled cold trap was used in the preparation of the sample cells. The line was connected to a two-stage pumping system consisting of a rotary pump (Edwards type ED 150) and an oil diffusion pump (Edwards type E01) charged with 11 ml silicone oil (Corning MS 704). The connection consisted of a baffle valve with a two-inch pyrex-to-stainless-steel seal (Hositrad) on top. Provision was made to allow for the connection of several types of standard glassware to the vacuum line. The variable concentration cells (cf. Chapter 3) and sample cuvettes for vapour phase spectrometry (cf. Chapter 4) were sealed to the vacuum line. Utmost care was taken in the design of the system, to make the distance from the sealed cuvette *via* the cold trap to the baffle valve as short as possible. The pressure was measured with a Penning- 8 model ionization gauge (Edwards). Optimum performance in a thoroughly cleaned system yielded a pressure of 1.1 μ Torr (0.15 mPa).

2.3. SPECTROSCOPIC EQUIPMENT

The equipment used for the measurements of the continuous wave (CW) spectra and phosphorescence lifetimes is described in detail by Langelaar *et al.*¹. In case of extremely weak phosphorescence signals, an argon ion laser was used to replace the conventional Xe-arc excitation source. Further details are described in Chapter 3.

The fluorescence lifetimes were measured by the method of single photon counting². This method determines the fluorescence decay curve from the statistical probability to detect a single photon of fluorescence a certain time after

the fluorescent sample has been excited with a light pulse, which preferably is infinitely short compared to the characteristic decay time of the fluorescence. The quoted probability decays with the same lifetime as that of the fluorescence, provided a single photon is detected per excitation pulse. The decay curve of the fluorescence intensity with time, therefore, is easily obtained from a plot of the number of photons detected in a time-interval of width Δt at a time t after the pulse, versus t . Originally, conventional flash lamps were used to produce the excitation pulse³⁻⁷, i.e. thyatron triggered low-pressure gas discharges and free running relaxation oscillator high-pressure gas discharges, both operating at high voltage. This brings the time-resolution of the experiment in the nano-second time domain. Some authors attempted to penetrate into the sub-nanosecond time domain by deconvolution techniques⁴⁻⁸, but this gives marginal improvement only and it has the disadvantage of additional computational labour.

Significant improvement of the time resolution, however, can be achieved by the application of an actively mode-locked laser as excitation source. Locking of the longitudinal cavity modes of a laser is accomplished by modulating them in amplitude. Amplitude modulation of an electro-magnetic wave produces side-bands at frequencies which are the sum and the difference of the carrier wave frequency (the mode frequency) and the modulation frequency. If the modulation frequency is chosen such that the side-bands produced by the modulation of one particular mode are coincident with the adjacent modes, the oscillations of these modes become correlated, i.e. they become synchronized in phase and amplitude. Since the mode-spacing of a laser in the frequency domain equals $c/2\ell$ (where c is the velocity of light and ℓ the laser-mirror separation), the modes will all be "locked" if the modulation frequency is set equal to $c/2\ell$. The laser output then will be the coherent superposition of a large number of modes with a constant frequency-difference of $c/2\ell$. Except for a very short time-interval occurring once per cycle of duration $2\ell/c$, these modes will interfere destructively or, mathematically, the laser output in the time domain will be the Fourier transform of its mode spectrum in the frequency domain. Thus the output is a train of short pulses (~ 200 ps FWHM for a noble gas ion laser) with a repetition rate of $c/2\ell$.

The modulation element is generally an acousto-optic loss modulator⁹⁻¹², (mode-locker) which is mounted in the laser cavity in close proximity to one of the mirrors, usually the 100% reflecting back mirror. The principle of its operation is the diffraction of light from the laser optical axis by a standing acoustic wave in the mode-locker crystal, i.e. the crystal acts as a phase grating. Consequently, the modulation frequency is twice the rf. frequency at which

the mode-locker is driven. The acoustic resonances of the mode-locker should not be too narrow because that will cause the laser to go out of lock too easily by small thermal fluctuations. Technical details of this very elegant technique can be found in the literature⁹⁻¹¹, especially for the mode-locking of the argon ion¹² and krypton ion¹³ lasers, respectively.

In the experiments described in this thesis, either a mode-locked CR - 5 or a mode-locked CR-18 model argon ion laser was employed. Data concerning the optimum performance obtained are summarized in Table 2.1.

TABLE 2.1.
OPTIMUM PERFORMANCE OF THE ARGON LASER USED IN FLUORESCENCE DECAY MEASUREMENTS.

Wavelength (nm)		Tube current (A)			Average mode- locked power (mW)			Pulse width (FWHM) (ps)	
		a)	b)	c)	a)	b)	c)	a);b)	c)
363.8	(CR-18)	-	-	50	-	-	100	-	300
465.8	(CR-5)	34	-	-	80	-	-	150	-
472.7	(CR-5)	32	-	-	70	-	-	220	-
476.5	(CR-5)	16	17	26	50	65	150	200	240
488.0	(CR-5)	10	13	-	40	75	-	180	-

Various partially transmitting output-mirrors: a) 5% T; b) 12% T; c) 30% T (CR-5) and 2.5% T (CR-18).

The extension to other wavelengths than the argon emission lines was accomplished by a CR - 490 model jet-stream dye laser. The dye laser was forced to mode-lock by the method of synchronous pumping¹⁴⁻¹⁶. In this method, the optical length of the dye laser cavity is adjusted to a submultiple or to the same as that of the mode-locked laser used to pump it. (The CR - 5 model in the present work). In this way, the mode-spacing in the dye laser becomes equal to or an integral multiple of that of the pumping laser. Thus the modulated output of the latter forces mode-locking in the dye laser automatically. We used equal cavity lengths for both lasers to obtain the same repetition frequency for both systems. Transform limited pulses were obtained from the dye laser. Typical values using Rhodamine 6G as dye were 4.5 ps FWHM using a 2-elements Lyot-filter as tuning element and 7.5 ps FWHM using a 3-elements Lyot-filter¹⁷. These values were measured with interferometry and SHG generation¹⁷. A detailed description of the system and its performance was given by De Vries *et al.*¹⁷.

The pulse repetition frequency ($c/2\ell = 94.576$ MHz for the CR - 5 system) was reduced by demodulation using a Coherent Associates model 22 electro-optical modulator for the wavelengths in the visible region. It was driven at a frequency obtained by dividing the mode-locker drive frequency by 1024, so the reduced

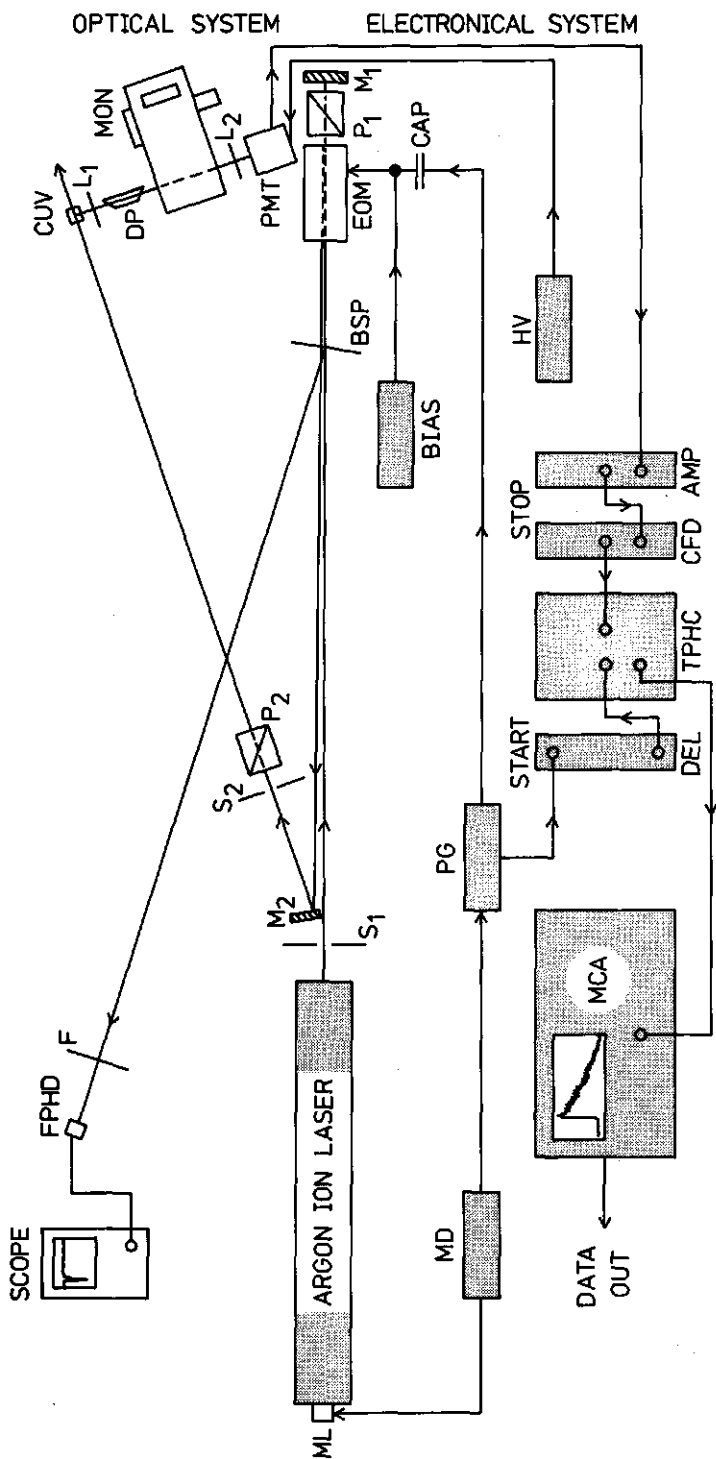


Figure 2.1. Equipment for time-resolved fluorescence spectroscopy. SCOPE = Tektronix Sampling Oscilloscope (S-6 Sampling Head, 7S11 and 7T11 plug-in units); FPHD = Fast Photodiode (~ 80 ps FWHM); F = Density Filter; CUV = Cuvette; L₁ and L₂ = lenses; DP = Dove Prism (rotates the image over 90° around the optical axis); MON = Zeiss MM12Q Monochromator; PMT = Photomultiplier; M₁ and S₂ = Stops; BSP = Beam Splitter; EOM = Model 22 Electro-optical Modulator (Coherent Associates); P₁ and P₂ = Polarizers; M₁ and M₂ = Mirrors; MD = Mode-locked Driver; PG = Pulse Generator (in 47.288 MHz, out 46.180 kHz); BIAS = Bias voltage supply for adjustment of the modulator transmittance contrast ratio; CAP = Separation Capacitor; HV = High Voltage Power Supply for PMT; DEL = Variable Delay; TPHC = Ortec Model 457 Biased Time to Pulse Height Converter; CFD = Ortec Model 463 Constant Fraction Discriminator; AMP = Ortec Model 454 Amplifier; MCA = Ortec Model 6220 Multi Channel Analyzer.

repetition frequency was 46.180 kHz. The laser beam was passed twice through the modulator, giving a contrast ratio of 40,000 between the transmitted and the suppressed pulses. The 46 kHz signal was also used to start the Ortec Model 457 biased time to pulse-height converter, the central device of the single photon counting system. For optimum adjustment of the whole system, a model 580 E.G. & G Radiometer with Narrow Beam Adapter proved to be indispensable. A schematic drawing of the entire system is given in Fig. 2.1.

In this experimental setup, the time resolution is determined by the photomultiplier¹⁸. Transit time fluctuations of the photoelectrons in the photocathode - first dynode space constitute a serious "bottle neck" for its time-resolving power^{18,19}. Therefore, the time resolution of the detection system was optimized using either the fundamental or frequency-doubled pulses from the dye laser. For this purpose, the sample cuvette (cf. Fig. 2.1) was replaced by a MgO diffusor. In order to obtain maximum time resolution, it was absolutely necessary to focus the light emerging from the exit slit of the detection monochromator on the photocathode of the photomultiplier. This was done by means of the lens L_2 indicated in Fig. 2.1. When the full half field angle on the entrance side of the monochromator was illuminated, the spot on the photocathode had a size of 3×8 mm. Additionally, the lens L_2 (cf. Fig. 2.1) was used to displace the image of the exit slit over the photocathode surface. Scanning the cathode in this way provided the optimum configuration of the detection system, i.e. the best possible time resolution. By this procedure, the speed of the photomultiplier was found to depend considerably on the particular place where the photocathode was illuminated. Scanning in a direction parallel to the axis of curvature of the dynodes yielded a speed which was virtually independent of the location of the slit-image, whereas scanning in a direction perpendicular to the dynode curvature axis yielded a large variation in speed. Typical values of the pulse width after detection ranged from 395 to 335 ps FWHM for a Philips XP 2020 photomultiplier operated according to the manufacturers recommendations and illuminated with 590 nm light-pulses from the dye laser. Increase of the potential applied to the first and second dynodes by a factor of 1.2 and 1.1 with respect to the previous situation, respectively, increased the range of the pulse width to 520 - 280 ps FWHM. When the position of the lens L_2 (cf. Fig. 2.1) is taken such that the speed of the photomultiplier is independent of the potential applied to the dynodes 1 and 2 over a rather wide range, a pulse of 350 ps FWHM was observed. In this configuration the wavelength-dependence of the pulse width was measured for the two types of photomultipliers which we had at our disposal

(the Philips XP 2020 and 56 DUVP/03). The latter type was used frequently in flash lamp excitation single photon counting measurements³⁻⁷. The results are given in Fig. 2.2. From these data it was immediately clear that further exper-

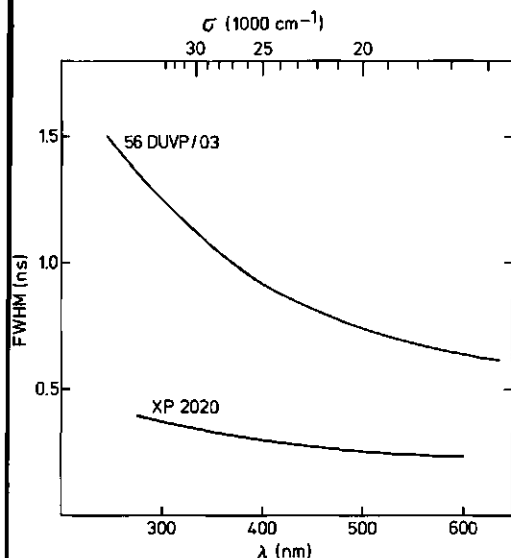


Figure 2.2. Wavelength-dependence of the speed of two photomultipliers used for single photon counting. Irradiation was performed with ~ 10 ps pulses from a synchronously pumped dye laser (cf. text for explanation). High voltage: 2.2 kV for the 56 DUVP/03 and 2.6 kV for the XP 2020. Data by courtesy of D. Bebelaar¹⁸.

iments should be done with the XP 2020. Detailed data on the speed of several types of photomultipliers will be published in the near future¹⁸.

2.4. PHOTOELECTRON SPECTROMETER

Photoelectron spectra were measured on a Perkin-Elmer PS 18 photoelectron spectrometer modified with a Helectros He(I) - He(II) source. A detailed description of this instrument is given by Rabalais²⁰. This instrument was found to be the only one on which (iso)alloxazine spectra could be measured due to the very short distance from the probe to the target chamber. When this distance is too long, no sufficient vapour pressure can be obtained in the target chamber from a compound with such a low volatility as (iso)alloxazine.

2.5. MOLECULAR ORBITAL CALCULATIONS

2.5.1. SCF-Formalism

The aim of all quantum chemical methods is the evaluation of electronic

properties of molecules from a solution of the time-independent molecular Schrödinger equation²¹

$$H\Psi = E\Psi \quad (2.1)$$

This eigenvalue problem can only be solved by a number of approximations. First the Born-Oppenheimer approximation²² is adopted in which the nuclei of the molecule are taken to be fixed in the calculation of the eigenfunction Ψ which, consequently, contains the nuclear configuration only as a parameter. This reduces the Hamilton operator H to:

$$H = - \sum_{p=1}^n \frac{1}{2} \nabla_p^2 - \sum_{A=1}^N \sum_{p=1}^n Z_A r_{Ap}^{-1} + \sum_{p<q}^n r_{pq}^{-1} + \text{constant} \quad (2.2)$$

in which the first term represents the total electronic kinetic energy, the second term represents the potential energy of the n electrons due to the presence of N nuclei of charge Z_A and the third term represents the potential energy arising from the mutual repulsion of the electrons. The distances between the particles are indicated by r_{Ap} (nucleus-electron) and r_{pq} (electron-electron). The sum of the first two terms is usually called the *Core Hamiltonian* H^C . Eq. (2.2) is expressed in atomic units, a system employing the Bohr radius as unit of length, the protonic charge as unit of charge and the electronic mass as unit of mass. Conversion factors can be found in the literature²¹.

The eigenfunction Ψ is approximated by the *orbital approximation*, i.e. it is written as a determinantal function of one-electron wavefunctions χ_i , giving in normalized form for a closed-shell electronic system of $2n$ electrons:

$$\Psi = \{(2n)!\}^{-\frac{1}{2}} \sum_P (-1)^P \mathbf{P} \{\chi_1(1) \cdot \chi_2(2) \dots \chi_{2n}(2n)\} \quad (2.3)$$

The operator \mathbf{P} permutes the coordinates of the electrons to produce the determinant, $(-1)^P$ being +1 or -1 for even or odd permutations, respectively. Eq. (2.3) treats the electrons as indistinguishable particles and it satisfies the Pauli exclusion principle²¹. Further approximation is made by assigning electrons in pairs to the same spatial orbitals ψ_i , i.e. all χ_j in eq. (2.3) are replaced by pairs $\psi_i(p)\alpha(p)$ and $\psi_i(q)\beta(q)$ for electrons of α -spin and β -spin, respectively. In the so-called unrestricted SCF-procedures this approximation is relaxed²¹. The total electronic energy is given by the expectation value:

$$E = \langle \Psi | H | \Psi \rangle = \int \Psi^* H \Psi \, d\tau \quad (2.4)$$

which yields after straightforward calculation²¹:

$$E = 2 \sum_{i=1}^n H_{ii}^C + \sum_{i=1}^n \sum_{j=1}^n (2J_{ij} - K_{ij}) \quad (2.5^a)$$

or, alternatively,

$$E = 2 \sum_{i=1}^n \epsilon_i - \sum_{i=1}^n \sum_{j=1}^n (2J_{ij} - K_{ij}) \quad (2.5^b)$$

The terms appearing in eq. (2.5) are given by:

⁰ Matrix element of the core hamiltonian:

$$H_{ii}^C = \langle \psi_i(1) | H^C | \psi_i(1) \rangle \quad (2.6)$$

⁰ Coulomb integral:

$$J_{ij} \equiv (ii|jj) = \langle \psi_i(1)\psi_j(2) | r_{12}^{-1} | \psi_i(1)\psi_j(2) \rangle \quad (2.7)$$

⁰ Exchange integral:

$$K_{ij} \equiv (ij|ij) = \langle \psi_i(1)\psi_j(2) | r_{12}^{-1} | \psi_j(1)\psi_i(2) \rangle \quad (2.8)$$

⁰ One-electron orbital energy:

$$\epsilon_i = H_{ii}^C + \sum_{j=1}^n (2J_{ij} - K_{ij}) \quad (2.9)$$

Normally one proceeds by expressing the one-electron wavefunctions as *linear combination of atomic orbitals*, the *LCAO-Approximation*

$$\psi_i = \sum_{\mu} c_{\mu i} \phi_{\mu} \quad (2.10)$$

The *LCAO-SCF method* (SCF = Self Consistent Field) consists of the substitution of (2.10) into (2.5) to (2.8) and a subsequent variational treatment in which the total energy is minimized subject to the boundary condition of orthonormality of the orbitals, i.e.

$$S_{ij} = \langle \psi_i(1) | \psi_j(1) \rangle = \sum_{\mu, \nu} c_{\mu i}^* c_{\nu j} S_{\mu\nu} = \delta_{ij} \quad (2.11)$$

In (2.11) the overlap between the AO's ϕ_{μ} and ϕ_{ν} is indicated by $S_{\mu\nu}$ and δ_{ij} is the Kronecker symbol ($\delta_{ij} = 1$ for $i=j$ and $\delta_{ij} = 0$ for $i \neq j$). The variational treatment uses the Lagrange method of undetermined multipliers, which finally transform into the orbital energies ϵ_i . The ϵ_i are found to satisfy the well-known *Roothaan equations*^{21,23}:

$$\sum_{\nu} (F_{\mu\nu} - \epsilon_i S_{\mu\nu}) c_{\nu i} = 0 \quad (2.12)$$

In which $F_{\mu\nu}$ is the matrix element of the *Fock Operator*.

$$F_{\mu\nu} = H_{\mu\nu}^c + \sum_{\lambda\sigma} P_{\lambda\sigma} \{(\mu\nu|\lambda\sigma) - \frac{1}{2}(\mu\lambda|\nu\sigma)\} \quad (2.13)$$

and $P_{\lambda\sigma}$ is the element of the *Density Matrix*

$$P_{\lambda\sigma} = 2 \sum_{i=1}^{\text{occ}} c_{\lambda i}^* c_{\sigma i} \quad (2.14)$$

In eq. (2.14) the summation runs over the occupied orbitals only. The notation of the two-electron integrals is analogous to that defined in (2.7) and (2.8). Details of the mathematics can be found in the literature²¹. Equation (2.12) is most conveniently written in matrix form.

$$\mathbf{FC} = \mathbf{SCE} \quad (2.15)$$

in which \mathbf{E} represents the diagonal matrix of the ϵ_i . By applying the well-known Löwdin transformation:

$$\mathbf{F}' = \mathbf{S}^{-\frac{1}{2}} \mathbf{F} \mathbf{S}^{-\frac{1}{2}} \quad ; \quad \mathbf{C}' = \mathbf{S}^{\frac{1}{2}} \mathbf{C} \quad (2.16)$$

in which $\mathbf{S}^{-\frac{1}{2}}$ has the property that

$$\mathbf{S}^{-\frac{1}{2}} \mathbf{S} \mathbf{S}^{-\frac{1}{2}} = \mathbf{I} \quad (2.17)$$

\mathbf{I} being the unit matrix, the problem is further reduced to a standard eigenvalue problem

$$\mathbf{F}' \mathbf{C}' = \mathbf{C}' \mathbf{E} \quad (2.18)$$

Equation (2.18) is solved by iteration: calculate \mathbf{F} (depending on \mathbf{C} through the density matrix \mathbf{P}) using a trial set of orbitals, solve eq. (2.18) to obtain a new \mathbf{C} matrix, recalculate \mathbf{F} , solve (2.18) again and repeat until \mathbf{C} does not change further within a given tolerance. This is a suitable task for an electronic computer.

2.5.2. Methods employing the Neglect of Differential Overlap

Having expressed the MO eigenvalue problem in the SCF form, the next task is to evaluate the elements of the Fock matrix (eq. 2.13) numerically.

In the CNDO method, i.e. the *Complete Neglect of Differential Overlap approximation*^{21,24}, only valence electrons are treated explicitly. The inner shells are considered as part of the (rigid) core and enter parametrically into ². The basic approximation is the application of the *Zero Differential Overlap approximation*²¹ to all products of valence AO's, giving:

$$(\mu\nu|\lambda\sigma) = \delta_{\mu\nu}\delta_{\lambda\sigma} (\mu\mu|\lambda\lambda) \quad (2.19)$$

In order to preserve rotational invariance²¹, the surviving integrals in eq. (2.19) are taken to be only dependent on the nature of the atoms A and B to which μ and ν belong and not on the actual type of orbital (s, p, d), hence

$$(\mu\mu|\lambda\lambda) = \gamma_{AB} \text{ (all } \mu \text{ on A; all } \lambda \text{ on B)} \quad (2.20)$$

The evaluation of the matrix elements $H_{\mu\nu}^C$ in eq. (2.13) proceeds by separating them into two types, one for which μ and ν belong to the same atom and another for which μ and ν belong to different atoms. The approximations are²¹:

$$\begin{aligned} H_{\mu\nu}^C &= \delta_{\mu\nu} U_{\mu\mu} - \sum_{B \neq A} \delta_{\mu\nu} V_{AB} \quad (\mu; \nu \text{ on A}) \\ H_{\mu\nu}^C &\equiv \beta_{\mu\nu} = \frac{1}{2}(\beta_A^O + \beta_B^O) S_{\mu\nu} \quad (\mu \text{ on A; } \nu \text{ on B}) \end{aligned} \quad (2.21)$$

$U_{\mu\mu}$ is the energy of ϕ_μ in the bare field of the core of its own atom, V_{AB} is the interaction of ϕ_μ on A with the cores of the other atoms B, $\beta_{\mu\nu}$ is the *resonance integral* describing the lowering of the energy of an electron being in the field of two cores simultaneously and β_A^O and β_B^O are semi-empirical parameters, characteristic for the atoms A and B, respectively. The resonance integrals lead to chemical bonding. $U_{\mu\mu}$ is essentially an atomic parameter which is approximated in the CNDO/2 version^{21,25} by:

$$U_{\mu\mu} = -\frac{1}{2}(I_\mu + A_\mu) - (Z_A - \frac{1}{2})\gamma_{AA} \quad (2.22)$$

whereas V_{AB} is approximated in this version by the neglect of penetration integrals^{21,25} leading to:

$$V_{AB} = Z_B \gamma_{AB} \quad (2.23)$$

Z_A and Z_B represent the net charge on the core atoms A and B, respectively. Adding the density matrix elements on one atom A, giving P_{AA} , the total valence-electron density on A, we finally obtain upon substitution of (2.19) to (2.23) into (2.13) and arranging terms^{21,25}:

$$F_{\mu\mu} = -\frac{1}{2}(I_{\mu} + A_{\mu}) + \{(P_{AA} - Z_A) - \frac{1}{2}(P_{\mu\mu} - 1)\}\gamma_{AA} + \sum_{B \neq A} (P_{BB} - Z_B)\gamma_{AB} \quad (2.24)$$

$$F_{\mu\nu} = \frac{1}{2}(\beta_A^0 + \beta_B^0)S_{\mu\nu} - \frac{1}{2}P_{\mu\nu}\gamma_{AB}$$

For the calculation of spectral properties the CNDO/2 method was refined by Del Bene and Jaffé²⁶. This *CNDO/S Method* (S = Spectroscopic) was shown to be capable of predicting a large variety of spectral data very satisfactorily²⁶⁻³⁵. The refinement consists of a discrimination between σ and π overlap in the calculation of $\beta_{\mu\nu}$

$$\beta_{\mu\nu} = \frac{1}{2}\kappa(\beta_A^0 + \beta_B^0)S_{\mu\nu} \quad (2.25)$$

in which $\kappa = 1$ for σ -overlap and $\kappa = 0.585$ for p_{π} -overlap. Additionally, the whole CNDO/2 parameterization was changed. The parameterization used in this thesis was the most recent one³⁰ and is given in Table 2.2. The two-center two-

TABLE 2.2.
CNDO/S PARAMETERS (eV)

atom	β_A^0	γ_{AA}	$I_s + A_s$	$I_p + A_p$
H	-12.0	12.85	14.35	-
C	-17.5	10.93	29.92	11.61
N	-26.0	13.10	40.97	16.96
O	-45.0	15.27	54.51	21.93
F	-50.0	17.36	56.96	24.36

electron integrals were approximated using the Nishimoto-Mataga formula³⁶ giving in atomic units:

$$\gamma_{AB} = \{R_{AB} + 2/(\gamma_{AA} + \gamma_{BB})\}^{-1} \quad (2.26)$$

Dividing R_{AB} by 14.40 turns the units into eV for the γ and into Å for R_{AB} ($1\text{Å} = 0.1 \text{ nm}$).

Further refinements of the all-valence electron calculation methods are: 1) the Intermediate Neglect of Differential Overlap^{21,37} (INDO); 2) the Modified INDO method or MINDO method of which the 3rd. version (MINDO/3) is applied frequently^{38,39}; 3) the Neglect of Diatomic Differential Overlap²⁴ (NDDO) and 4) the LINDO/S method⁴⁰, the latter method (Local Neglect of Differential Overlap) being developed recently and hitherto only applied to hydrocarbons.

It was shown by Roothaan²³ that the orbital energies obtained from a LCAO-MO-SCF calculation equal the negative of the experimentally observed

ionization potentials, provided the electron correlation and reorganization can be neglected²⁰. This constitutes the well-known *Koopmans theorem*⁴¹. The accuracy of theoretical methods, therefore, can be tested in a rather direct way by photoelectron spectroscopy²⁰ (cf. Chapter 5).

5.3. Spectroscopic Data

Spectroscopic properties were calculated by the method of *Configuration Interaction (CI)*. This method, set forth by Pople⁴² and Pariser⁴³, describes the excited state as a linear combination of determinantal wavefunctions (cf. eq. 2.3) in which electrons are excited from an occupied orbital to an unoccupied one, i.e. as a *linear combination of excited configurations*. The general formulas for the interaction matrix elements between configurations are given in Table 2.3. When the orbitals ψ_i , ψ_j , ψ_k and ψ_l are determined by an SCF procedure, obviously the matrix **F** is diagonal, so $F_{ki} = \epsilon_i \delta_{ki}$. This causes all interaction matrix elements between the ground state Ψ_0 and the excited configurations $\Psi_{i \rightarrow k}$ to vanish, a property which is known as *Brillouin's Theorem*. The CI procedure involves the diagonalisation of a matrix with elements $H_{mn} - E \delta_{mn}$ in which H_{mn} and E are given in Table 2.3. Further mathematical details and formulas for transition moments

TABLE 2.3.
ELEMENTS OF THE CI MATRIX^{a)}

	Ψ_0	$\Psi_{i \rightarrow k}$	$\Psi_{i \rightarrow l}$	$\Psi_{j \rightarrow k}$	$\Psi_{j \rightarrow l}$
0	E				
$i \rightarrow k$	$2\frac{1}{2}F_{ki}$	$E - \epsilon_i + \epsilon_k - (J_{ik} - K_{ik}) \pm K_{ik}$ ^{b)}	$F_{kl} - (ii kl)$	$-F_{ji} - (ij kk)$	$-(ij kl)$
$i \rightarrow l$	$2\frac{1}{2}F_{li}$	$F_{kl} + 2(ik il) - (ii kl)$			
$j \rightarrow k$	$2\frac{1}{2}F_{kj}$	$-F_{ji} + 2(ik jk) - (ij kk)$			
$j \rightarrow l$	$2\frac{1}{2}F_{lj}$	$2(ik jl) - (ij kl)$			

^{a)} Only one type of element given; upper half: triplets, lower half: singlets;
^{b)} + \rightarrow singlet; - \rightarrow triplet. ($i \neq j \neq k \neq l$).

can be found in the original papers^{42,43}.

Photoionization cross-sections, necessary for the interpretation of photoelectron spectra (cf. Chapter 5), were derived according to the method of Allison⁴⁴. In the calculation an electron is assumed to be excited into a continuum to give a spin singlet. The final state wavefunction Ψ_{i+j} thus is a configuration in the sense discussed above, except that the one-electron wavefunction

describing the free electron is an unbound state and not a molecular orbital. It is conveniently approximated by a normalized plane wavefunction in a cubic box of edge length L with wave-vector \mathbf{k}

$$|PW(\mathbf{k})\rangle = (k^3 L^3 / 6\pi^2)^{1/2} \exp i(\mathbf{k} \cdot \mathbf{r}) \quad (2.27)$$

The transition probability to such a configuration is calculated with time-dependent perturbation theory^{20,44} (Fermi's Golden Rule), yielding the differential cross-section of producing photoelectrons in an element of solid angle $d\Omega$ with radiation of unit polarization vector \mathbf{u}

$$\frac{d\sigma}{d\Omega} = \frac{e^2 k L^3}{2\pi m c \hbar^2 \omega} |\mathbf{u} \cdot \mathbf{P}_{oj}|^2 \quad (2.28)$$

in which \mathbf{P}_{oj} is the complex quantity

$$\mathbf{P}_{oj} = 2^{1/2} \hbar \left[\mathbf{k} \langle \psi_j | PW(\mathbf{k}) \rangle + i \sum_{\ell=1}^{\text{occ}} \langle \psi_j | \nabla | \psi_{\ell} \rangle \langle \psi_{\ell} | PW(\mathbf{k}) \rangle \right] \quad (2.29)$$

In these expressions, e and m denote the electronic charge and the electronic mass, respectively, \hbar is Planck's constant divided by 2π , ω is the radiation frequency and ∇ is the conventional gradient operator which is also employed in the calculation of transition moments. The evaluation of (2.27) to (2.29) is treated extensively in the literature^{20,42}.

REFERENCES

- 1 J. Langelaar, G.A. de Vries and D. Bebelaar, J. Sci. Instr. 46 (1969) 149.
- 2 L.M. Bollinger and G.E. Thomas, Rev. Sci. Instr. 32 (1961) 1044.
- 3 W.R. Ware, in: Creation and Detection of the Excited State, Vol. 1, ed. A.A. Lamola (Marcel Dekker, New York, 1971).
- 4 A.E.W. Knight and B.K. Selinger, Aust. J. Chem. 26 (1973) 1.
- 5 C. Lewis, W.R. Ware, L.J. Doemeny and T.L. Nemzek, Rev. Sci. Instr. 44 (1973) 107.
- 6 Ph. Wahl and J.C. Auchet, Biochim. Biophys. Acta 285 (1972) 99.
- 7 Ph. Wahl, J.C. Auchet and B. Donzel, Rev. Sci. Instr. 45 (1974) 28.
- 8 B. Valeur and J. Moirez, J. Chim. Phys. 70 (1973) 500.
- 9 L.E. Hargrove, R.L. Fork and M.A. Pollack, Appl. Phys. Letters 5 (1964) 4.
- 10 S.E. Harris and O.P. McDuff, IEEE J. Quantum Electron. QE-1 (1965) 245.
- 11 O.P. McDuff and S.E. Harris, IEEE J. Quantum Electron. QE-3 (1967) 101.
- 12 S.J. Heising, S.M. Jarrett and D.J. Kuizenga, Appl. Phys. Letters 18 (1971) 516.
- 13 S.J. Heising, S.M. Jarrett and D.J. Kuizenga, IEEE J. Quantum Electron. QE-7 (1971) 205.
- 14 B.B. Snively, in: Organic Molecular Photophysics, Vol. 1, ed. J.B. Birks (Wiley, London, 1973).
- 15 C.K. Chan and O. Sari, Appl. Phys. Letters 25 (1974) 7.
- 16 J.M. Harris, R.W. Chrisman and F.E. Lytle, Appl. Phys. Letters 26 (1975) 1.

- 7 J. de Vries, D. Bebelaar and J. Langelaar, *Opt. Commun.* 18 (1976) 24.
- 8 D. Bebelaar, Personal Communication.
- 9 B. Sipp, J.A. Miehe and R. Lopez-Delgado, *Opt. Commun.* 16 (1976) 202.
- 10 J.W. Rabalais: *Principles of Ultraviolet Photoelectron Spectroscopy* (Wiley, London, 1977).
- 11 J.A. Pople and D.L. Beveridge: *Approximate Molecular Orbital Theory* (McGraw-Hill, New York, 1970).
- 12 M. Born and J.R. Oppenheimer, *Ann. Physik* 84 (1927) 457.
- 13 C.C.J. Roothaan, *Rev. Mod. Phys.* 23 (1951) 69.
- 14 J.A. Pople, D.P. Santry and G.A. Segal, *J. Chem. Phys.* 43 (1965) S129.
- 15 J.A. Pople and G.A. Segal, *J. Chem. Phys.* 44 (1966) 3289.
- 16 J. Del Bene and H.H. Jaffé, *J. Chem. Phys.* 48 (1968) 1807, *ibid.* 48 (1968) 4050, *ibid.* 49 (1968) 1221, *ibid.* 50 (1969) 1126.
- 17 R.L. Ellis, R. Squire and H.H. Jaffé, *J. Chem. Phys.* 55 (1971) 3499.
- 18 R.L. Ellis, G. Kuehnlenz and H.H. Jaffé, *Theoret. Chim. Acta* (Berlin) 26 (1972) 131.
- 19 G. Kuehnlenz, C.A. Masmanidis and H.H. Jaffé, *J. Mol. Struct.* 15 (1973) 445.
- 20 G. Kuehnlenz and H.H. Jaffé, *J. Chem. Phys.* 58 (1973) 2238.
- 21 H.M. Chang and H.H. Jaffé, *Chem. Phys. Letters* 23 (1973) 146.
- 22 R.L. Ellis and H.H. Jaffé, *J. Mol. Spectr.* 50 (1974) 474.
- 23 H.H. Jaffé, C.A. Masmanidis and H.M. Chang, *J. Comput. Phys. (USA)* 14 (1974) 180.
- 24 R.L. Ellis, H.H. Jaffé and C.A. Masmanidis, *J. Amer. Chem. Soc.* 96 (1974) 2623.
- 25 H.M. Chang, H.H. Jaffé and C.A. Masmanidis, *J. Chem. Phys.* 79 (1975) 1109, *ibid.* 79 (1975) 1118.
- 26 K. Nishimoto and N. Mataga, *Z. Phys. Chem. (Frankfurt am Main)* 12 (1957) 335.
- 27 J.A. Pople, D.L. Beveridge and P.A. Dobosh, *J. Chem. Phys.* 47 (1967) 2026.
- 28 M.J.S. Dewar, *Science* 187 (1975) 1037.
- 29 R. Bingham, M.J.S. Dewar and D. Lo, *J. Amer. Chem. Soc.* 97 (1975) 1285.
- 30 G. Lauer, K.W. Schulte and A. Schweig, *J. Amer. Chem. Soc.* 100 (1978) 4925.
- 31 T. Koopmans, *Physica (Utrecht)* 1 (1934) 104.
- 32 J. Pople, *Proc. Phys. Soc. (London)* A68 (1955) 81.
- 33 R. Pariser, *J. Chem. Phys.* 24 (1956) 250.
- 34 F.O. Ellison, *J. Chem. Phys.* 61 (1974) 507.

3 LUMINESCENCE OF SOME ISOALLOXAZINES IN APOLAR SOLVENTS

3.1. INTRODUCTION

Flavins in their ground and excited electronic states participate in many biological reactions¹. Therefore, the luminescent properties of isoalloxazines have been the subject of several investigations. An excellent review of the literature up till 1967 was written by Penzer and Radda². During the last decade, a large number of additional data, including quantum mechanical calculations, have been published. The calculations cover the entire region of commonly used methods including Hückel^{3,4}, Extended Hückel^{5,6}, SCF-PPP⁷⁻¹⁰, CNDO^{6,9} and MINDO/3¹¹. However, experimental results and especially nuclear magnetic resonance data are not completely in agreement with these calculations¹², so to test the theoretical model more thoroughly, we have undertaken a more detailed study of the properties of the electronically excited states of some isoalloxazines.

Since it is known that the resolution of the electronic absorption spectrum is better in less polar solvents¹³⁻¹⁸, which facilitates the comparison with known theoretical data, we attempted to increase the solubility of some isoalloxazines in highly apolar organic solvents by substitution of the N₃ and N₁₀ positions of the isoalloxazine ring with long aliphatic side chains. This enabled us to use 2-methyl-tetrahydrofuran (2-MTHF) and 3-methyl-pentane (3-MP) as solvent, giving sufficient concentrations of these isoalloxazine derivatives in fluid as well as glassy solution at 77 K. In order to characterize the optical properties of isoalloxazines in more detail, a wide range of temperature was employed.

3.2. MATERIALS AND METHODS

3.2.1. Purification of solvents

3-MP, purum, (from Fluka) was dried on molecular sieves, refluxed for 6 hr with sodium in nitrogen-atmosphere and distilled subsequently over freshly added sodium wire. The flask containing the main fraction was attached to a vacuum system and the solvent was degassed by distillation at 10 μ Torr (1.3 mPa) into a storage vessel containing molecular sieves. Solvent removed from the storage vessel by distillation in vacuum showed 100% transmission for $\lambda > 240$ nm; 63% at

220 nm; 56% at 215 nm and 40% at 210 nm (measured in a 1 cm cuvette). 2-MTHF, purum, (from Merck) was dried on molecular sieves followed by removal of the stabilizer on an Al_2O_3 -column. Subsequently, the solvent was dried¹⁹ with CaH_2 , refluxed for 10 hr with freshly added CaH_2 in nitrogen atmosphere until H_2 -generation had ceased, followed by immediate distillation. The main fraction was collected on LiBH_4 and distilled at 10 μTorr (1.3 mPa) over two sodium-mirrors prepared by vacuum sublimation of the metal onto the wall of a round-bottom flask. The solvent was stored on CaH_2 . Solvent removed from the storage vessel by distillation in vacuum showed 100% transmission for $\lambda > 270$ nm; 87% at 260 nm; 74% at 250 nm and 25% at 240 nm (1 cm cuvette).

Vacuum distillations were performed by cooling the collection vessel. All solvents were free from emission under irradiation with a 1600 W Xe-arc source.

3.2.2. Synthesis of new isoalloxazine derivatives

7,8-Dimethyl-10-*n*-octadecyl-isoalloxazine and 7,8-dimethyl-10-isopropyl-isoalloxazine were obtained by condensation of 1,2-dinitro-4,5-dimethyl-benzene with the corresponding amine according to the procedure of Leonard and Lambert²⁰. To improve solubility in apolar solvents, the compounds were methylated at N_3 as described by Hemmerich²¹. 7,8,10-Trimethyl-3-*n*-undecyl-isoalloxazine was obtained by treatment of 7,8,10-trimethyl-isoalloxazine¹² in dimethylformamide with undecylbromide (Fluka) in the presence of K_2CO_3 at room temperature for 24 hr. All compounds were purified to homogeneity by a procedure described previously¹². The melting points given below are uncorrected.

Elemental analysis:

3,7,8-Trimethyl-10-*n*-octadecyl-isoalloxazine (m.p. 428-430 K):

$\text{C}_{31}\text{H}_{48}\text{N}_4\text{O}_2 \cdot 0.2\text{H}_2\text{O}$	calc.	C 72.65	H 9.53	N 10.94%
(512.02)	found	C 72.5	H 9.2	N 11.6 %

3,7,8-Trimethyl-10-isopropyl-isoalloxazine (m.p. 563-564 K):

$\text{C}_{16}\text{H}_{18}\text{N}_4\text{O}_2 \cdot \frac{1}{2}\text{H}_2\text{O}$	calc.	C 62.50	H 6.24	N 18.24%
(307.19)	found	C 62.9	H 6.1	N 18.2 %

7,8,10-Trimethyl-3-*n*-undecyl-isoalloxazine (m.p. 478-480 K):

$\text{C}_{24}\text{H}_{34}\text{N}_4\text{O}_2$	calc.	C 70.21	H 8.35	N 13.65%
(410.54)	found	C 69.9	H 8.4	N 13.8 %

It should be noted that the elemental analyses of compounds I and III indicate that the crystalline materials contain some residual solvent in non-stoichiometric amounts. The synthesis of the other compounds has been described elsewhere (Grande *et al.*¹² and references therein).

3.2.3. Preparation of samples

Solutions were prepared in a variable concentration cell, consisting of a $1 \times 1 \times 3$ cm suprasil quartz cuvette with a pyramidal shaped bottom, connected to a side-arm with a storage-bulb by means of a quartz-to-pyrex seal. The cell was sealed to the vacuum system, degassed by heating at a pressure below 10 μTorr (1.3 mPa), refilled with oxygenfree nitrogen to enable introduction of the solute into the storage-bulb followed by sealing-off the opening. Solvent was subsequently distilled into the storage-bulb in vacuum, the solution was degassed by freeze-thaw techniques and the cell was sealed-off at a pressure of 2 to 4 μTorr (0.27-0.53 mPa). Due to photolability of the isoalloxazines, only illumination by sodium lamps was used.

3.2.4. Measurement of the dielectric constant

The dielectric constant of 2-MTHF was measured by inserting the solvent in a capacitor. Calibration was made by using solvents with known dielectric constants (purissimum grade) and correction for geometry changes upon cooling to 77 K were applied. All values were extrapolated to zero-frequency to obtain the static dielectric constant.

3.2.5. Equipment

Absorption spectra were recorded on a Cary-14 spectrophotometer. Continuous Wave (CW) emission and excitation spectra were recorded on the spectrofluorometer described by Langelaar *et al.*²². The instrument was equipped with a 1600 W Xe-arc source, a Zeiss MM12Q excitation monochromator and a Zeiss M20 detection monochromator fitted with an EMI 9558 QA photomultiplier (S-20 spectral response photocathode). Both phase sensitive amplification and photon counting could be used. For the correction of the excitation spectra, the power output spectrum of the excitation source was measured with a model 580 E.G. & G. Radiometer with narrow beam adaptor. By using the same equipment, the detection system was calibrated by comparison of the detector output upon irradiation with a standard light source with the radiometer output under the same conditions. Phosphorescence lifetimes were determined by a similar detection system as mentioned above, after excitation with the 476.5 nm emission line of an argon ion laser. The exciting light was modulated by an electro-mechanical shutter, triggering a multichannel analyzer in multichannel-scaling-mode. Fluorescence lifetimes were measured by the method of single photon counting²³, after excitation with a mode-locked CR-5 model argon ion laser also operated at 476.5 nm ($20,987\text{ cm}^{-1}$) with 50 mW average mode locked power. The 94.576 MHz pulse repetition frequency was extracavity demodulated to 46.180 kHz by passing the laser beam twice through a Coherent Associates model 22 electro-optical modulator giving a contrast ratio of 40,000 between the transmitted and suppressed pulses. The laser pulse was 300 ps full width at half maximum (FWHM), broadened to 365 ps after detection by a Zeiss MM12Q monochromator equipped with a Philips XP 2020 photomultiplier. The spectral bandwidth could always be kept below 400 cm^{-1} on the Zeiss monochromators and was actually set to $25\text{--}75\text{ cm}^{-1}$ in the majority of the measurements.

Data handling was performed by feeding the spectra and calibration curves into a PDP-11/45 computer by means of a Tektronix Graphic Tablet. Correction and averaging was done on a IBM 370/158 system to which the PDP was connected. The spectra were integrated for the determination of radiative lifetimes. The actual fluorescence lifetimes were so long compared to the excitation pulse width, that awkward deconvolution procedures could be avoided.

3.3. RESULTS

All compounds investigated generally display the same overall spectral characteristics. The continuous wave absorption, emission and excitation spectra are almost equally shaped when compared in one particular solvent, e.g. 2-MTHF, but they are considerably influenced by the solvent polarity. Formal introduction of alkyl substituents into positions N_3 , N_{10} , C_7 , and C_8 , which was shown to

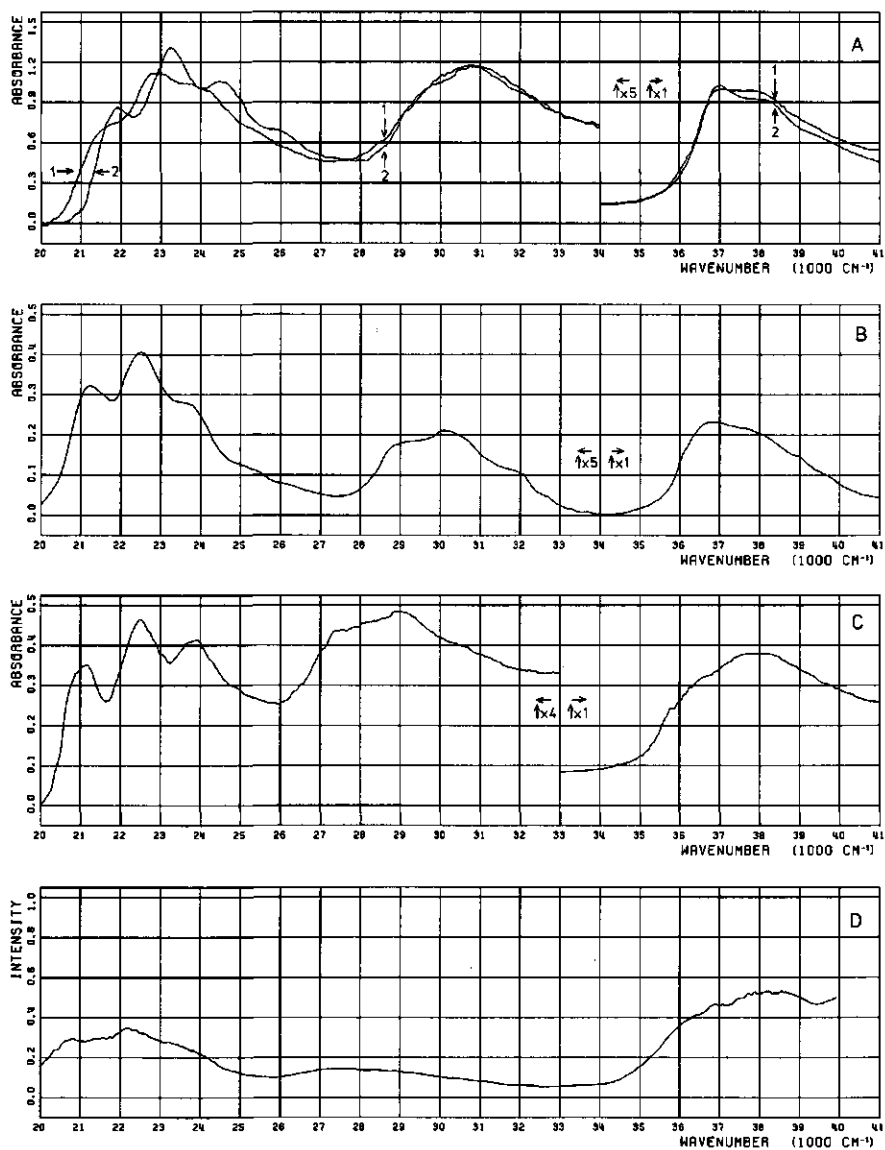


Figure 3.1. Absorption and excitation spectra of various isoalloxazines. (A) Absorption spectrum of 3,10-dimethylisoalloxazine (V) in 2-methyltetrahydrofuran; curve 1: 300 K, 24 μM ; curve 2: 77 K, 29 μM . (B) Absorption spectrum of 3,7,8-trimethyl-10-n-octadecylisoalloxazine (I) in 3-methylpentane, 300 K, 6.6 μM . (C) as (B) but at 77 K. (D) Excitation spectrum of 3,7,8-trimethyl-10-n-octadecylisoalloxazine (I) in 3-methylpentane at 77 K, detected at $17,600\text{ cm}^{-1}$, $\Delta\bar{\nu}_{\text{em}} = 300\text{ cm}^{-1}$, $\Delta\bar{\nu}_{\text{ex}} = 100\text{ cm}^{-1}$ ($c = 6.6\text{ }\mu\text{M}$). The absorbance scale is expanded in the long wavelength regions ($20,000 - 34,000\text{ cm}^{-1}$ in A and B; $20,000 - 33,000\text{ cm}^{-1}$ in C).

affect charge densities in the molecule¹², only shifts the continuous wave spectra by 500 cm^{-1} , which value is never exceeded (Table 3.1). The decay constants, however, are more sensitive to the nature of the substituents in the various positions of the isoalloxazine ring, in agreement with earlier observations²⁴.

3.3.1. Luminescence in 2-MTHF

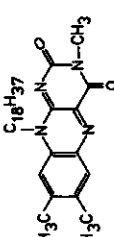
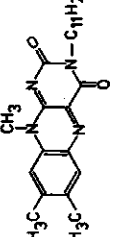
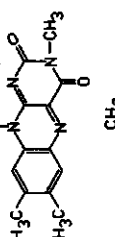
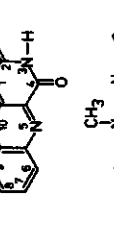
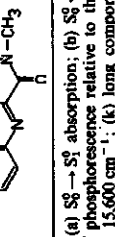
The continuous wave spectra of compounds I to V in 2-MTHF are very similar. Representative spectra obtained at 300 and 77 K, respectively, are given in Figs 3.1A and 3.2A. In all cases, the corrected excitation spectra both of fluorescence and phosphorescence were found to match the absorption spectrum completely.

Going from fluid to solid solution, the usual decrease of the inhomogeneous broadening due to different solute-solvent interactions is observable, revealing a distinct vibrational structure in the absorption, emission and excitation spectra. The vibrational mode giving the observed progression has a frequency of 1250 cm^{-1} . A similar value was obtained from temperature difference spectra²⁵. It is well known from the spectroscopy on aromatic hydrocarbons that only totally symmetric vibrational modes give rise to distinct progressions²⁶. Thus, comparing the observed 1250 cm^{-1} vibrational frequency of the isoalloxazine molecule with the commonly observed 1400 cm^{-1} C - C stretching mode in aromatic hydrocarbons and taking into account the presence of nitrogen and oxygen atoms in isoalloxazine, it seems likely that the former frequency can also be assigned to a skeleton stretching mode.

Because of the absence of molecular symmetry in the isoalloxazine ring, there will be no symmetry-forbidden electronic transitions. Therefore, we can use the 1250 cm^{-1} vibrational progression to establish the band origins in the spectra, yielding the wavenumbers of the 0-0 electronic transitions (cf. Table 3.1). Freezing of the solutions to 77 K causes a blue shift of both the $S_0 \rightarrow S_1$ absorption and the $S_0 \rightarrow S_1$ emission bands, the shift being the larger for the fluorescence. Consequently, the Stokes-loss as determined from the $S_0^0 \rightarrow S_1^0$ absorption and the $S_0^0 \rightarrow S_1^0$ emission transitions, decreases slightly. In case of isoalloxazine solutions in 3-MP (*vide infra*), the blue shift in absorption is not observed indicating a substantially smaller solute-solvent interaction in this case.

Despite careful degassing procedures, we could not observe $S_0 \rightarrow T_1$ phosphorescence when the temperature was raised above $\sim 103\text{ K}$, probably due to softening of the 2-MTHF-glass. In the small temperature range from 77 K to 103 K, how-

TABLE 3.1.
SPECTRAL DATA OF VARIOUS ISOALLOXAZINES

Compound	No.	Solvent	Temp. (K)	Solubilities (M)	$\bar{\nu}_c$ (cm ⁻¹) ^a	$\bar{\nu}_{N-H}$ (cm ⁻¹) ^b	Stokes-loss (cm ⁻¹)	τ_0 (ns) ^d	τ_i/τ_0	ϕ_i^f	$\phi_p \times 10^{10}$	τ_p (ms) ^g
	I	2-MTHF 2-MTHF 3-MIP 3-MIP	300 77 300 77	$\sim 10^{-3}$ $\sim 10^{-3}$ 5.5×10^{-6} 5.5×10^{-6}	21,280 21,550 21,300 21,200	20,100 20,500 20,450 $\sim 18,300$	1180 1050 850 $\sim 15,000$	12.3 12.0 13.5 $\sim 15,000$	6.50 9.18 9.45 j	0.53 0.77 0.70 j	0.54 0.76 0.54	10.2 341 40; 13 ^k
	II	2-MTHF 2-MTHF 3-MIP 3-MIP	300 77 300 77	$\sim 10^{-3}$ $\sim 10^{-3}$ 9.5×10^{-6} 9.5×10^{-6}	21,250 21,500 21,280 21,150	20,100 20,450 20,450 $\sim 18,300$	1150 1050 830 $\sim 15,000$	12.4 12.4 13.4 $\sim 15,000$	6.65 9.15 9.21 i	0.54 0.74 0.69 i	0.49 0.67 0.53	333 50; 13 ^m
	III	2-MTHF 2-MTHF	300 77	$\sim 10^{-3}$ $\sim 10^{-3}$	21,280 21,550	20,100 20,450	1180 1100	12.4 12.4	7.32 8.96	0.59 0.72	0.56 0.69	304
	IV	2-MTHF 2-MTHF	300 77	$\sim 10^{-3}$ $\sim 10^{-3}$	21,750 21,930	20,450 20,900	1300 1030	14.9 15.4	4.38 10.40	0.29 0.68	0.30 0.70	134
	V	2-MTHF 2-MTHF	300 77	$\sim 10^{-4}$ $\sim 10^{-4}$	21,750 21,930	20,400 20,800	1350 1130	14.9 15.3	3.74 10.12	0.25 0.66	0.22 0.62	168

(a) $S_0^0 \rightarrow S_0^0$ absorption; (b) $S_0^0 \rightarrow S_0^0$ fluorescence; (c) $S_0^0 \rightarrow T_1^0$ phosphorescence; (d) radiative lifetime; (e) actual lifetime; (f) fluorescence quantum yield; (g) quantum yield of phosphorescence relative to that of fluorescence; (h) phosphorescence lifetime; (i) inhomogeneous, component 1; 5.6 ns, component 2; 14.0 ns at 19,000 cm⁻¹ and 20.0 ns at 15,600 cm⁻¹; (j) long component at 15,000 cm⁻¹, short component at 17,500 cm⁻¹; (k) inhomogeneous, component 1; 5.2 ns, component 2; 11.3 ns at 19,000 cm⁻¹ and 14.3 ns at 15,600 cm⁻¹; (m) long component at 15,000 cm⁻¹, short component at 17,500 cm⁻¹.

ever, the phosphorescence was found to shift in the same direction as the $S_0 \leftarrow S_1$ fluorescence, leaving the $S_1 - T_1$ energy difference unaltered. The failure to observe phosphorescence at room temperature with a fluorometer which in principle is capable of determining quantum yields as low as 10^{-6} , seems to agree with the short triplet lifetimes of isoalloxazines at room temperature, as determined recently by Grodowsky *et al.*²⁷.

More pronounced is the influence of substituents and temperature on the relative intensities of the various vibronic transitions in the $S_0 \rightarrow S_1$ absorption and $S_0 \leftarrow S_1$ emission bands. Methylation of the molecule in positions 7 and 8 causes a slight increase ($\sim 20\%$) of the intensity of the $S_0 \rightarrow S_1$ 0-0 transition relative to that of the $S_0 \rightarrow S_1$ 0-1 transition, consistent with light absorption data obtained by other authors¹³⁻¹⁸. The apparent Franck-Condon maximum for the $S_0 \rightarrow S_1$ absorption is found to coincide with the 0-1 band in all absorption spectra. The Franck-Condon maximum observed in the fluorescence spectrum, however, is found to shift from the 0-1 band in fluid solution to the 0-0 band in solid solution, the effect being more pronounced for the smaller molecules (compounds IV and V) than for the larger ones. Parallel to this, a drastic increase of the fluorescence quantum yield is observed upon solidification of 2-MTHF.

Without exception, we measured a single exponential decay both of fluorescence and phosphorescence in 2-MTHF. A typical semilogarithmic plot of the fluorescence decay is given in Fig. 3.3. The actual lifetimes (τ_f) were found to be constant over the whole fluorescence spectrum and are collected in Table 3.1, together with the radiative lifetimes (τ_0) obtained from the integrated absorption and emission spectra using the Birks-Dyson formula²⁶ and the molar extinction coefficients, determined as described previously²⁴. The optical densities were corrected for contraction of the solvent upon cooling the samples. The quantum yields were determined using fluorescein in 0.1 N NaOH as a standard²⁸, which was shown to have a quantum yield of 0.92. The quantum yields were found to agree quite well with the ratio τ_f/τ_0 (Table 3.1), hence the actual lifetime of the isoalloxazine fluorescence can be used reliably to estimate the quantum yield of fluorescence, confirming previous observations²⁴.

Because internal conversion to the first excited singlet state is a very rapid process²⁷, we clearly observe only emission from the first excited singlet and triplet states. This is confirmed by: 1) The independence of the lifetimes upon the emission and excitation wavelength and 2) the constant degree of polarization ($p = 0.42$, error $\lesssim 5\%$) over the entire fluorescence spectrum after excitation of the $S_0^0 \rightarrow S_1^0$ transition. Furthermore, we measured the polarized

excitation spectrum of compound V at 77 K exhibiting (error $\lesssim 5\%$) a wavenumber-independent degree of polarization within the region of one absorption band, contrary to earlier results^{14,15}. The values obtained are $p = 0.42$ for the $S_0 \rightarrow S_1$ band, $p = 0.25$ for the $S_0 \rightarrow S_2$ band and $p = 0.20$ for the $S_0 \rightarrow S_3$ band, measured and corrected in the same way as was done previously¹⁴. These data show no evidence for possible vibronic interactions or the presence of two electronic transitions in the region from $21,000\text{ cm}^{-1}$ to $27,000\text{ cm}^{-1}$ as proposed previous-

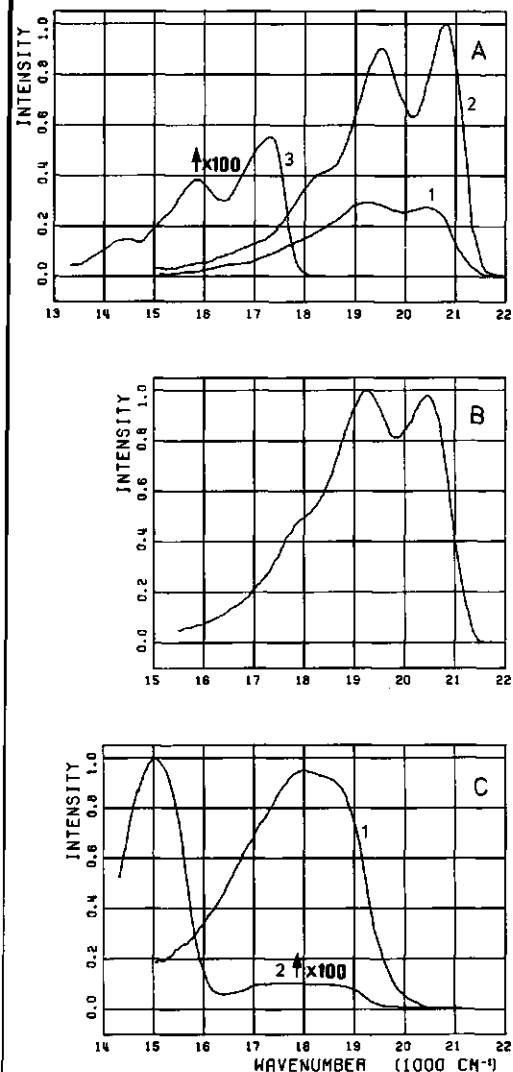


Figure 3.2. Emission spectra of various isoalloxazines. (A) 3,10-Dimethylisoalloxazine (V) in 2-methyl-tetrahydrofuran; curve 1: fluorescence at 300 K; curve 2: fluorescence of the same sample at 77 K; curve 3: phosphorescence (intensity multiplied by 100 prior to plotting) of the same sample at 77 K. Excitation wavenumber $21,500\text{ cm}^{-1}$, $\Delta\bar{\nu}_{\text{ex}} = 26\text{ cm}^{-1}$, $\Delta\bar{\nu}_{\text{em}} = 50\text{ cm}^{-1}$, $c = 31\text{ }\mu\text{M}$. (B) Emission of 3,7,8-trimethyl-10-(n-octadecyl)-isoalloxazine (I) in 3-methylpentane at 300 K. Excitation at $21,300\text{ cm}^{-1}$, $\Delta\bar{\nu}_{\text{ex}} = 40\text{ cm}^{-1}$, $\Delta\bar{\nu}_{\text{em}} = 50\text{ cm}^{-1}$, $c = 6.6\text{ }\mu\text{M}$. (C) Prompt (curve 1) and delayed (curve 2) emission of 3,7,8-trimethyl-10-(n-octadecyl)isoalloxazine at 77 K under the same optical conditions as (B), $c = 6.6\text{ }\mu\text{M}$. Intensity of the delayed emission (curve 2) multiplied by 100 prior to plotting.

ly^{14,15}. The lifetimes of phosphorescence (τ_p) and the quantum yields of phosphorescence relative to that of fluorescence, were determined at 77 K only (Table 3.1). Both quantities are very sensitive to temperature, probably due to softening of the 2-MTHF glass which is reported to occur above 98 K²⁹. The values given in Table 3.1 are, therefore, the maximum values obtained under our experimental conditions.

3.3.2. Luminescence in 3-MP

Only two compounds could be dissolved in 3-MP. They show nice spectral resolution already at room temperature (Figs. 3.1B and 3.2B). Again the corrected excitation spectra match the absorption spectra completely. The same characteristic vibrational frequency of 1250 cm⁻¹ as observed in 2-MTHF is also observed here. At room temperature, the fluorescence decay is a single exponential. The long lifetime of ~ 9 ns exceeds all previously reported values of isoalloxazines in fluid solution at room temperature. The relative intensities of the vibrational bands in the spectra are not very different from those observed in 2-MTHF at room temperature.

When the solutions in 3-MP are frozen, however, the spectra change very drastically (Figs. 3.1C and 3.2C). A broad, structureless prompt emission (Fig. 3.2C curve 1) with a lifetime in the nanosecond time domain and a delayed emission (Fig. 3.2C, curve 2) with a lifetime in the millisecond time domain are now observed. The delayed emission consists of two spectral bands, centered at $\sim 18,000$ cm⁻¹ (coincident with the prompt emission) and at $\sim 15,000$ cm⁻¹. The excitation spectra of all these strongly red-shifted emission bands all have the same shape but differ considerably from the absorption spectrum under the same conditions (cf. Fig. 3.1D and 3.1C). The decay of the prompt emission becomes bi-exponential with a short component of ~ 5 ns which is independent of the detection wavenumber and a long component which ranges from 10 to 20 ns depending on the detection wavenumber (cf. Table 3.1 and Fig. 3.3). These values are obtained after subtraction of the background due to the delayed emission from the decay curves. The delayed emission has a single exponential decay on the red ($\bar{\nu} < 15,000$ cm⁻¹) and blue ($\bar{\nu} > 18,000$ cm⁻¹) edges of the spectrum but is bi-exponential in between. Analysis of the decay curves shows that the shortest lifetime (13 ms) is associated with the emission band at 18,000 cm⁻¹ and the longest lifetime (40-50 ms) is associated with the emission band at 15,000 cm⁻¹. In the region where the two bands overlap, the relative intensities of the two components as

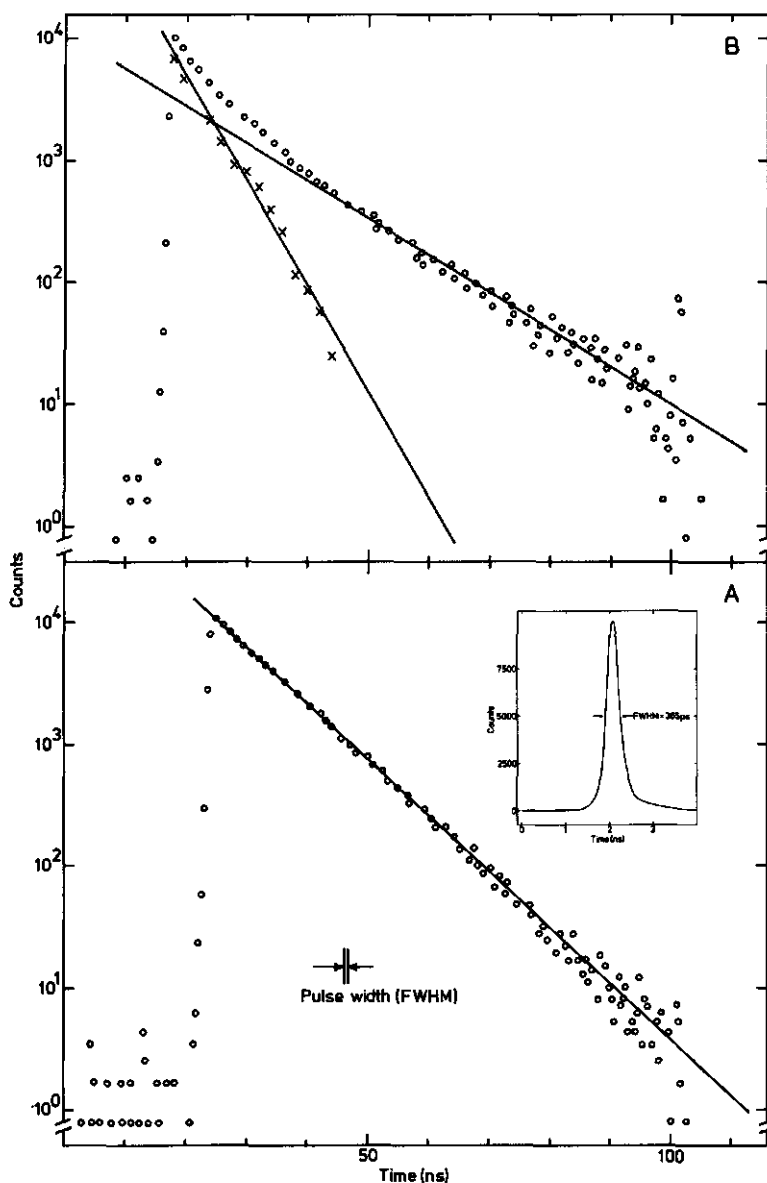


Figure 3.3. Fluorescence decay of 3-*n*-undecyl-7,8,10-trimethylisoalloxazine (II) under various conditions after laser excitation. (A) In 2-methyltetrahydrofuran, 77 K, detection at $20,450\text{ cm}^{-1}$, $\Delta\bar{\nu}_{\text{em}} = 28\text{ cm}^{-1}$ ($c = 9.8\text{ }\mu\text{M}$). (B) Prompt emission observed in 3-methylpentane at 77 K; detection at $15,500\text{ cm}^{-1}$, $\Delta\bar{\nu}_{\text{em}} = 400\text{ cm}^{-1}$ ($c = 9.6\text{ }\mu\text{M}$). The background due to the delayed emission has been subtracted from the curve. Insert: Excitation pulse from the argon ion laser used in the measurements of (A) and (B), observed after replacement of the sample compartment by a magnesium-oxide diffusor. (For details see Materials and Methods).

determined from the decay curves, agree quite well with an estimate made by extrapolation of the two bands observed in the continuous wave spectrum of the delayed emission (Fig. 3.2C, curve 2). Apparently, both transitions observed in the delayed emission decay single-exponentially but with different lifetimes in the millisecond time domain. When the temperature is raised to 300 K, the spectra in Figs. 3.1B and 3.2B reappear, the fluorescence decay becomes single-exponential again and no delayed emission can be observed. It should be noted that the relative intensities of the emission spectra in fluid as compared to rigid solution show poor reproducibility but, in every experiment, the total emission intensity drops at least one order of magnitude in rigid solution.

3.4. DISCUSSION

The improved resolution of the isoalloxazine spectrum obtained in apolar solvents enabled us to establish the energy of the electronically excited states more accurately than was possible in polar solvents where, due to broadening and overlap of the individual vibronic bands, no vibrational structure can be observed. Regarding the fact that the $S_0 \rightarrow S_1$ 0-1 vibronic transition is the most intense one in the long-wavelength band in the absorption spectrum, it is clear that the maximum of the $S_0 \rightarrow S_1$ band observed in polar solvents is not coincident with the 0-0 transition. The origin of the $S_0 \rightarrow S_1$ band in polar solvents is thus at lower energy ($\sim 1200 \text{ cm}^{-1}$) than is suggested by the maximum of the absorption band. This finding agrees well with recent conclusions drawn by Dutta *et al.* from resonant coherent anti-Stokes Raman scattering spectra (CARS) obtained from isoalloxazine derivatives and some flavoproteins³⁰. The experimentally observed 0-0 transition energies are compared with calculated data in Table 3.2.

The improvement of the spectral resolution also shows that the shape of the $S_0 \leftarrow S_1$ emission band is determined mainly by the solvent influence on the Franck-Condon factors of the individual vibronic transitions. This influence is much more pronounced in the emission than in the absorption spectra of isoalloxazines. For this reason, care should be taken in interpreting the structureless optical spectra which are frequently observed from isoalloxazines in polar solvents of protic character or from flavoproteins. Regarding the results obtained in non-protic solvents, it becomes clear that spectral shifts observed in protic solvents do not necessarily imply a change of the $S_0^0 \rightarrow S_1^0$ or $S_0^0 \leftarrow S_1^0$ electronic transition energies. This is illustrated by the fluorescence properties of

TABLE 3.2.

COMPARISON OF OBSERVED ELECTRONIC TRANSITIONS OF ISOALLOXAZINES WITH CALCULATED DATA (IN CM^{-1})

Compound	Transitions	Experimental	SCF-PPP-CI ^{a)}	CNDO ^{b)}	MINDO/3 ^{c)}
II, III	$S_0 \rightarrow S_1$	21,300-21,500	23,700	-	21,700
	$S_0 \rightarrow S_2$	28,500-29,000	27,600; 30,900	-	28,700
	$S_0 \rightarrow S_3$	36,800-36,900	36,900	-	d)
	$S_0 \rightarrow S_4$	45,100	45,900	-	d)
IV, V	$S_0 \rightarrow S_1$	21,600-21,900	-	-	21,500
	$S_0 \rightarrow S_2$	29,700-29,900	-	-	29,100
	$S_0 \rightarrow S_3$	37,000-37,100	-	-	e)
II, III	$T_1 \rightarrow S_0$	16,700	13,700; 16,100 ^{b)}	28,600	16,600; 17,200
	$T_1 \rightarrow S_0$	17,200	-	-	17,300

a) from ref. 9; b) from ref. 6; c) from ref. 11 (without configuration interaction); d) 8 different transitions ranging from 31,100 to 42,000; e) 3 different transitions ranging from 31,100 to 35,800.

transhydrogenase³¹, where a distinct blue shift of the isoalloxazine fluorescence can be observed when potassium phosphate and NADP^+ are added to a solution of this enzyme in Tris-HCl buffer at pH 7.6. This effect is easily explained by conformational changes of the isoalloxazine prosthetic group in the enzyme, affecting the Franck-Condon envelope of the emission spectrum.

From the observed 0-0 transitions, we also obtained more precise values for the Stokes-loss than previously available²⁴. Considering the theories of solvent influence on absorption and emission spectra^{26,32}, it can be seen that a simple semiquantitative description can be given in terms of the Onsager theory of dielectrics provided there are no specific solute-solvent interactions like H-bond formation. For this reason, carefully purified non-protic solvents and alkylated isoalloxazine derivatives were used. The difference between the $S_0 \rightarrow S_1$ absorption ($\bar{\nu}_a$) and $S_0 \rightarrow S_1$ emission transition ($\bar{\nu}_e$) for a molecule embedded in a spherical cavity of radius a , in a solvent with static dielectric constant ϵ and index of refraction n , obeys the equation:

$$\Delta\bar{\nu} = \bar{\nu}_a - \bar{\nu}_e = \frac{2(\mu_e - \mu_g)^2}{hca^3} P; \text{ where } P = \left[\frac{\epsilon - 1}{2\epsilon + 1} - \frac{n^2 - 1}{2n^2 + 1} \right] \quad (3.1)$$

the dipole moments of the solute molecule in its ground and first electronically excited state are given by μ_e and μ_g , respectively, h is Planck's constant and c is the velocity of light in vacuum.

The values of ϵ and n are known for 3-MP³³, i.e. $\epsilon = 1.907$ and $n = 1.381$ at 293 K and 486 nm. Our measurement of ϵ for 2-MTHF yielded 6.25 at 293 K and 1.52 at 77 K. The value of ϵ is made up by two contributions originating from the electric dipole moments of the solvent molecules and their electronic polariz-

ability. Clearly, dipolar contribution to ϵ will vanish upon freezing the solvent to a low-temperature glass, so the observed reduction is easily explained. The high frequency limit of the dielectric constant³³ equals n^2 , so this quantity, often referred to as dynamical dielectric constant, is only dependent on the electronic polarizability. Therefore, we assume no drastic change of n^2 upon freezing 2-MTHF and take the tabulated value³³ $n = 1.406$ (293 K, 589 nm) for all temperatures. Substitution of these values in eq. (3.1) yields an increasing factor P in the order: $P = 0.000$ for 3-MP at 293 K; $P = 0.055$ for 2-MTHF at 77 K and $P = 0.192$ for 2-MTHF at 293 K. Equation (3.1), therefore, predicts an increasing Stokes-loss with increasing P , a tendency which agrees qualitatively with the experimental values (cf. Table 3.1). However, irrespective of the value of μ_e and μ_g , the theory predicts the Stokes-loss to be zero in 3-MP at 293 K whereas a value of 850 cm^{-1} is observed. This indicates an intramolecular contribution to $\Delta\bar{\nu}$ for which eq. (3.1) does not account. It is, therefore, very probable that the isoalloxazine molecule possesses different molecular conformations in its ground and first electronically excited singlet and triplet states. This is supported by the absence of a mirror-symmetry relationship between the absorption and emission spectra and the solvent influence on the Franck-Condon envelopes. So, electronic excitation causes changes in molecular conformation which in turn are dependent on molecular environment.

The possibility that Franck-Condon factors may change considerably is also supported by the theory described by Henry and Siebrand³⁴. These authors have shown that anharmonicity of molecular vibrations, when taken into account, may displace the maximum of the Franck-Condon envelope from the 0-0 transition, so small external perturbations may affect the spectral properties of molecules in this sense considerably.

Solvent-interaction and substituents both influence the non-radiative decay of the molecule considerably without affecting the radiative lifetimes much (cf. Table 3.1), in confirmation of the earlier results of Koziol¹³ and the proposals made by Song³⁵. Unfortunately, we could not determine intersystem-crossing quantum yields but, using the values of the actual lifetimes and quantum yields of fluorescence, we can estimate limiting values for k_{isc} , assuming no $S_1 \rightarrow S_0$ internal conversion. From the data in Table 3.1 we obtain values ranging from $2.6 \times 10^7 \text{ s}^{-1}$ to $2.0 \times 10^8 \text{ s}^{-1}$ depending on solvent and substituent. These values are smaller than those obtained in aqueous and alcoholic solution^{27,36,37}.

The enormous red shift of 3000 cm^{-1} and complete loss of vibrational structure in the emission spectra of isoalloxazine in 3-MP at 77 K certainly cannot

explained in terms of simple solvent interactions. The difference between the excitation spectrum of the shifted emission and the absorption spectrum indicates that the emitting species is no longer a simple monomer isoalloxazine molecule. This is supported by the long component observed in the decay of the prompt emission with a longer actual lifetime than the radiative lifetime of the first excited singlet state of isoalloxazine in polar solvents. The variation of the long component with wavelength may be due to the presence of a variety of solute clusters with different fluorescence lifetimes. In the delayed emission, where the shortest lifetime is associated with the short wavelength band and the longest lifetime with the long wavelength band, we interpret the former as being due to delayed fluorescence and the latter as phosphorescence emission, respectively. The energy difference of the two bands is 3300 cm^{-1} giving a Boltzmann factor of $\sim 10^{-25}$ at 77 K so, the delayed fluorescence will not be due to thermal activation of a single triplet to the first excited singlet state but, due to triplet-triplet annihilation of triplet excitons because the phenomenon is observed in solid solution only. Freezing a solution of isoalloxazine in 3-MP to 77 K clearly causes association of the solute molecules. A similar behaviour was reported for riboflavin-tetrabutyrates¹⁵. The experimental difficulties in obtaining reproducible emission characteristics, even from very dilute 3-MP matrices, obstruct a more precise determination of the composition of the emitting species.

REFERENCES AND NOTES

- 1 Cf. Chapter 1 and references therein.
- 2 G.R. Penzer and G.K. Radda, *Quart. Rev. Biophys.* 21 (1967) 43.
- 3 B. Pullman and A. Pullman, *Proc. Natl. Acad. Sci. USA.* 45 (1959) 136.
- 4 G. Karreman, *Bull. Math. Biophys.* 23 (1961) 55.
- 5 R. Norrestam, P. Kierkegaard, B. Stensland and L. Torbjörnsson, *Chem. Comm.* (1969) 1250.
- 6 P.S. Song, *J. Phys. Chem.* 72 (1969) 536.
- 7 B. Grabe, *Biopolym. Symp.* 1 (1964) 283.
- 8 J.L. Fox, K. Nishimoto and L.S. Forster, *Biochim. Biophys. Acta* 109 (1965) 626, *ibid.* 136 (1967) 544.
- 9 B. Grabe, *Acta Chem. Scand.* 26 (1972) 4084, *ibid.* A28 (1974) 363.
- 10 P.S. Song, *Int. J. Quantum Chem.* 3 (1969) 303.
- 11 M.F. Teitell, S.-H. Suck and J.L. Fox, *Theoret. Chim. Acta* (Berlin) 60 (1981) 127, J.L. Fox, Personal Communication.
- 12 H.J. Grande, C.G. van Schagen, T. Jarbandhan and F. Müller, *Helv. Chim. Acta* 60 (1977) 348.
- 13 J. Koziol, *Photochem. Photobiol.* 5 (1966) 41, *ibid.* 5 (1966) 55, *ibid.* 9 (1969) 45.
- 14 M. Sun, T.A. Moore and P.S. Song, *J. Amer. Chem. Soc.* 94 (1972) 1730.
- 15 P.S. Song, T.A. Moore and W.E. Kurtin, *Z. für Naturf.* 27b (1972) 1011.
- 16 A. Bowd, P. Byrom, J.B. Hudson and J. Turnbull, *Photochem. Photobiol.* 8 (1968) 1.

- 17 J.M. Lhoste, Proc. 1st. Eur. Biophys. Congress 4 (1971) 221.
- 18 K. Yagi, in: Biochemical Fluorescence Concepts, Vol. 2, ed. R.F. Chen and H. Edelhoch (Dekker, New York, 1976).
- 19 L.F. Fieser and M. Fieser: Reagents for Organic Synthesis (Wiley, London, 1967).
- 20 N.J. Leonard and R.F. Lambert, J. Org. Chem. 34 (1969) 3240.
- 21 P. Hemmerich, Helv. Chim. Acta 47 (1964) 464.
- 22 J. Langelaar, G.A. de Vries and D. Bebelaar, J. Sci. Instr. 46 (1969) 149.
- 23 Cf. Chapter 2, section 2.3.
- 24 A.J.W.G. Visser and F. Müller, Helv. Chim. Acta 62 (1969) 593.
- 25 F. Müller, S.G. Mayhew and V. Massey, Biochemistry 12 (1973) 4654.
- 26 J.B. Birks: Photophysics of Aromatic Molecules (Wiley, London, 1970).
- 27 M.S. Grodowski, B. Veyret and K. Weiss, Photochem. Photobiol. 26 (1977) 341.
- 28 W.R. Dawson and M.W. Windsor, J. Phys. Chem. 72 (1968) 3251.
- 29 J.D.W. van Voorst and G.J. Hoijsink, J. Chem. Phys. 42 (1965) 3995.
- 30 P.K. Dutta, J.R. Nestor and T.G. Spiro, Proc. Natl. Acad. Sci. USA. 74 (1977) 4146.
- 31 C. Veeger, A.J.W.G. Visser, J. Krul, H.J. Grande, R.A. de Abreu and A. de Kok in: Flavins and Flavoproteins, Proc. 5th. Int. Conf., ed. T.P. Singer (Elsevier, Amsterdam, 1976).
- 32 J.B. Birks, in: Organic Molecular Photophysics, Vol. 2, ed. J.B. Birks (Wiley London, 1975).
- 33 Landolt-Börnstein: Eigenschaften der Materie in ihren Aggregatzuständen, Vol. 6, Elektrische Eigenschaften I (Springer, Berlin, 1959).
- 34 B.R. Henry and W. Siebrand, in: Organic Molecular Photophysics, Vol. 1, ed. J.B. Birks (Wiley, London, 1973).
- 35 P.S. Song, in: Flavins and Flavoproteins, Proc. 3rd. Int. Conf., ed. H. Kamin (University Park Press, Baltimore, 1971).
- 36 A.J.W.G. Visser, G.J. van Ommen, G. van Ark, F. Müller and J.D.W. van Voorst, Photochem. Photobiol. 20 (1974) 227.
- 37 A.J.W.G. Visser, F. Müller and J.D.W. van Voorst, Bioch. Biophys. Res. Comm. 77 (1977) 1135.

SPECTRAL PROPERTIES OF (ISO)ALLOXAZINES IN THE VAPOUR PHASE

1. INTRODUCTION

In context with our work on the luminescent properties of isoalloxazines in fluid and solid solution¹ and in order to determine precisely to what extent the photophysical properties of the isoalloxazine molecule depend on the molecular environment, it was desirable to study the molecule in the *isolated state*. This requires a spectroscopic study of the molecule in the vapour phase at very low pressures, such that the average time interval between two molecular collisions is much longer than the fluorescence lifetime of about 10 ns¹. Two observations encouraged us to perform such experiments. First, mass spectra can be obtained from the isoalloxazines used in previous work^{1,2} and, secondly, Knappe³ observed that 3,7,8-trimethyl-10-(β -hydroxyethyl)-isoalloxazine and 3,7,8-triethyl-10-(γ -hydroxypropyl)-isoalloxazine can be sublimed at atmospheric pressure, suggesting that other isoalloxazine derivatives could be sublimed at lower pressures.

It is not to be expected that a vibrational structure will be observable in the vapour phase spectrum of an isoalloxazine compound at the relatively high temperature needed to obtain a reasonable concentration of the compound in the vapour phase. Classically, the excess vibrational energy of the molecule at a temperature T equals $\frac{1}{2}kT$ per vibrational degree of freedom, giving for 3,10-dimethyl-isoalloxazine at 450 K: $\frac{1}{2}(3N-6)kT = 12,196 \text{ cm}^{-1}$ ($N = 28$). So, at temperatures of 400 - 500 K ($kT = 278 - 347 \text{ cm}^{-1}$) there will be a considerable thermal population of vibrationally excited states corresponding to the electronic ground state. This will intensify higher sequence bands of the $S_0 \rightarrow S_n$ transitions relative to spectra measured at lower temperature. When a large part of the Boltzmann distribution is transferred to the S_1 -state upon electronic excitation, the vibrational structure in both absorption (or excitation) and emission spectra will thus be blurred out completely by sequence congestion^{4,5}.

Therefore, the main purpose of this Chapter is to describe the non-radiative behaviour of the isoalloxazine chromophore, determined under conditions where one can reasonably be expecting to observe isolated molecules.

4.2. MATERIALS AND METHODS

4.2.1. Synthesis of isoalloxazine derivatives

3,10-Dimethyl-7-fluoro-isoalloxazine: 4-Fluoro-2-nitro-aniline (Aldrich; 2.0 g) was methylated in a mixture of conc. H_2SO_4 and formaldehyde as described previously². Recrystallization of the product thus obtained from ethanol gave 1.8 g (83%) of N-methyl-4-fluoro-2-nitro-aniline of m.p. 343-345 K.

$\text{C}_7\text{H}_7\text{FN}_2\text{O}_2$	calc.	C 49.42	H 4.15	F 11.17	N 16.47%
(170.14)	found	C 49.6	H 4.2	F 11.1	N 16.6 %

Catalytic reduction of N-methyl-4-fluoro-2-nitro-aniline (2.5 g) and condensation with alloxan-hydrate² gave 3.1 g (80%) of 10-methyl-7-fluoro-isoalloxazine. Methylation at N_3 and purification by column chromatography² gave analytically pure 3,10-dimethyl-7-fluoro-isoalloxazine:

$\text{C}_{12}\text{H}_9\text{FN}_4\text{O}_2 \cdot \text{H}_2\text{O}$	calc.	C 51.76	H 3.95	F 6.83	N 20.13%
(278.23)	found	C 51.8	H 3.9	F 6.8	N 20.0 %

The other compounds used in this investigation were synthesized as described previously^{1,2}.

4.2.2. Preparation of the samples

Sample cells consisted of a 1 cm suprasil quartz cuvette, connected to a pyrex tube with side arm by means of a quartz-to-pyrex seal. There was a constriction between this seal and the side arm. After closing the side arm by a rubber stopper, the cell was sealed to the vacuum system, degassed by heating at a pressure of ~ 10 μTorr (1.33 mPa) and refilled with oxygen-free nitrogen. Subsequently, solid isoalloxazine was introduced through the side arm onto the bottom of the cuvette, the side arm sealed-off and the solid moved upwards by sublimation (2 μTorr = 0.27 mPa, ~ 500 K) until it had precipitated between the constriction and the top of the cuvette. Then the cuvette was sealed-off at the constriction.

At the beginning of the sublimation process, some vapour was released due to the enclosed solvent molecules in the isoalloxazine crystals from the recrystallization process. Sublimation in vacuum, therefore, can be used successfully to purify isoalloxazines. During the sublimation process only illumination by sodium lamps was used to prevent possible photochemical decomposition of the compounds.

4.2.3. Equipment

Spectroscopic equipment and data handling were identical to the methods applied previously¹. Time resolved fluorescence spectroscopy, however, was now extended to other excitation wavenumbers, made possible by technical improvement. Apart from the 476.5 nm (20,987 cm^{-1}) emission line of the CR-5 model argon ion laser, also the lines at 472.7 nm (21,155 cm^{-1}) and 465.8 nm (21,468 cm^{-1}) could be mode-locked. A mode-locked CR-18 model argon ion laser was used in the ultra-violet (363.8 nm = 27,488 cm^{-1}) region. In the latter case, the pulse repetition frequency could not be reduced by demodulation, limiting the time-window for observation to 13 ns. For this reason, ultraviolet excitation was only applied

for compounds with short fluorescence lifetimes. The laser beam was focussed sharply into the sample cuvette in order to produce a very narrow fluorescent filament in the isoalloxazine vapour. Utmost care was taken to obtain a proper optical image of this filament on the entrance slit of the Zeiss MM12Q detection monochromator. This was achieved by rotating the image of the horizontal filament by means of a Dove prism to match the vertically positioned slit. Lenses were chosen such as to match the half field angle of the monochromator. The beam emerging from the exit slit was focussed on the photocathode of the XP 2020 photomultiplier to obtain the maximum possible time resolution (pulse width was 350 ps full width at half maximum after detection). For further details cf. Chapter 2, Section 2.3.

Sample cuvettes were heated using a two-level furnace as described by Ware and Cunningham⁶ and Werkhoven⁷. Its dimensions were adapted to our spectroscopic equipment. The lower level of the furnace consisted of an oil bath in which the pyrex tube attached to the cuvette was immersed. The upper level, equipped with suprasil quartz windows, held the cuvette. The cuvette was in thermal contact with a copper block to stabilize its temperature. The temperatures of both levels were controlled independently by two Ether "mini" temperature controllers and Ni/Cr thermocouples. The temperature of the cuvette was maintained 20 K above that of the lower level to prevent precipitation of isoalloxazine on the cuvette walls. The vapour pressure was thus governed by the temperature of the lower level of the furnace.

4.3. RESULTS

The structures of the compounds under investigation are given in Scheme 1.1 (p.1). A preliminary selection of derivatives, apparently suitable for spectroscopic examination in the vapour phase, was made on the basis of their melting points observed at atmospheric pressure. Derivatives with low melting points, however (compounds IV and VI, cf. Table 4.1), were found either to melt or to decompose, even when the pressure was reduced to 2 μ Torr (0.27 mPa), whereas the other compounds showed rapid sublimation. Because cuvettes with an optical path length longer than 1 cm did not fit into the two-level furnace, it was not possible to measure vapour phase absorption spectra for compounds I to V due to their extremely low vapour pressures (Table 4.1). Thus compound VI was the only *iso*-alloxazine derivative that could be used for absorption spectrometry in the vapour phase (Fig. 4.1A). On the other hand, the alloxazines (compounds VII and VIII) have easily measurable absorption spectra and no detectable decomposition occurred during the experiments as could be judged from examination of different parts within one absorption spectrum. All the spectral bands observed show a proportional increase in intensity relative to each other when the temperature is raised. As an example, the temperature-dependence of the absorption spectrum of compound VIII is given in Fig. 4.1B. The optical density measured at 523 K was 0.25 at $26,600\text{ cm}^{-1}$ (376 nm).

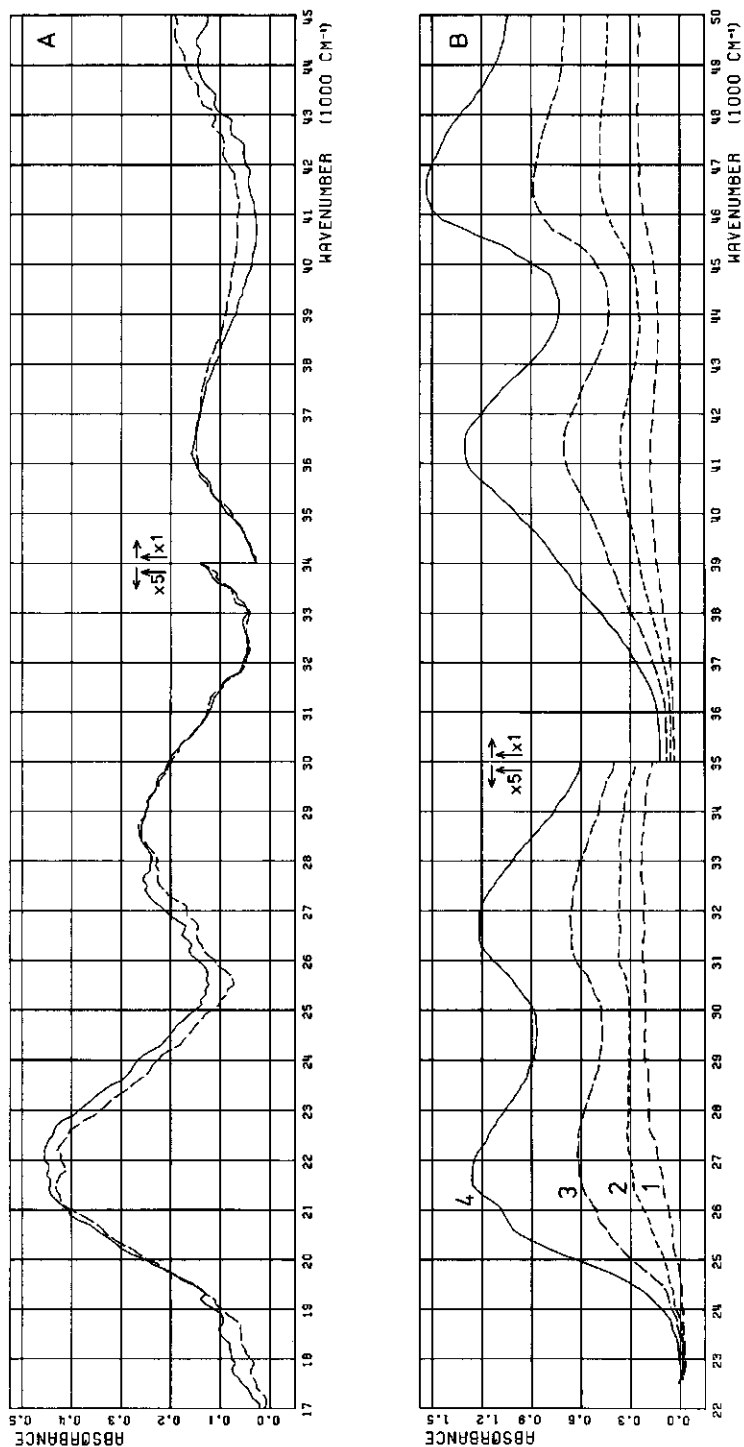


Figure 4.1. Absorption spectra of (iso)alloxazines in the vapour phase at various temperatures (1 cm light path). A) Riboflavin-tetra-acetate (VI) at 450 K. Solid line: Spectrum taken immediately after stabilization of the temperature; dotted line: Spectrum taken after 15 min. (indicating some decomposition). B) 1,3,7,8-tetramethylalloxazine (VIII) at various temperatures; curve 1: 473 K; curve 2: 493 K; curve 3: 508 K and curve 4: 523 K.

When the vapour pressure is calculated from the absorbance, assuming an extinction coefficient of $5600 \text{ M}^{-1} \text{ cm}^{-1}$ ($S_0 \rightarrow S_1$ transition) as determined in solution^{8,9} (*vide infra*), the heat of evaporation (Δ) can be calculated according to the Clausius-Clapeyron relationship¹⁰. When $\ln p$ was plotted against $1/T$, a linear curve was obtained. From this, values of $\Delta = 79.5 \text{ kJ mole}^{-1}$ and $\Delta = 81.6 \text{ kJ mole}^{-1}$ were calculated for the compounds VII and VIII, respectively, using linear regression analysis ($r^2 \geq 0.98$).

The absorption spectra of compounds VI to VIII enable us to check if the molecules can be regarded as isolated during the lifetime of their electronically first excited singlet state. From simple classical kinetic gas theory¹⁰, the collision frequency Z for one vapour molecule can be derived as:

$$Z = 2^{\frac{1}{2}} \pi N d^2 \left[\frac{8kT}{\pi m} \right]^{\frac{1}{2}} \quad (4.1)$$

where N is the number of molecules with diameter d per unit volume, $(8kT/\pi m)^{\frac{1}{2}}$ is the average molecular velocity of the molecules with mass m at an absolute temperature T , and k denotes Boltzmann's constant. Assuming the vapour behaves as an ideal gas, the concentration of molecules in the vapour phase is

$$C = N/L = n/V = p/RT \quad (4.2)$$

in which L denotes Avogadro's number, R the gas constant and n the number of moles in the vapour. Because the molar mass $M = mL$, we finally obtain

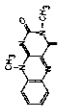
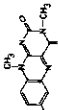
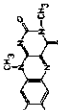
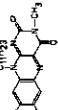
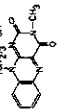
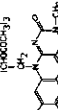
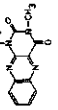
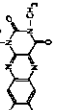
$$Z = 4\pi^{\frac{1}{2}} L p d^2 (RTM)^{-\frac{1}{2}} = 6.24 \times 10^7 \sigma^2 p (TM)^{-\frac{1}{2}} \quad (4.3)$$

where σ is the molecular diameter in Å and p is the vapour pressure in Torr (1 Torr = 133.3 Pa). Substituting $M = 270$ (compound VIII), $T = 523 \text{ K}$ and $\sigma \approx 10 \text{ Å}$ (the molecular size as estimated from crystallographic data^{11,12}) one obtains $Z = 2.42 \times 10^7 \text{ s}^{-1}$ ($p = 1.46 \text{ Torr} = 194 \text{ Pa}$) for compound VIII. Similarly we obtain $Z = 2.6 \times 10^6 \text{ s}^{-1}$ ($p = 0.21 \text{ Torr} = 27.6 \text{ Pa}$) for compound VI at 450 K, as derived from the optical density of 0.09 for the $S_0 \rightarrow S_1$ transition ($22,000 \text{ cm}^{-1} = 455 \text{ nm}$), assuming $\epsilon = 12,000 \text{ M}^{-1} \text{ cm}^{-1}$. So, the condition of isolated excited singlet vapour molecules is amply satisfied in our experiments since the time interval between two molecular collisions (Z^{-1}) is larger than the actual fluorescence lifetime by several orders of magnitude (cf. Table 4.1).

Throughout the calculations, we assumed ϵ to be the same in solution and in the vapour phase because the (iso)alloxazine electronic transitions are strongly electric dipole-allowed. A small deviation from this assumption, however, cannot

TABLE 4.1.

SPECTRAL DATA OF VARIOUS ISOALLOXAZINES AND ALLOXAZINES IN THE VAPOUR PHASE.

Compound	No.	mp (K), a)	sp (K), b)	$\bar{\nu}_a$ (cm ⁻¹), c)	$\bar{\nu}_f$ (cm ⁻¹), d)	τ_f (ns), e)	τ_o (ns), f)
	I	576-582 (subl., decomp.)	475	23,200 (ex) 30,600 (ex) —	20,100	1.7	22.1
	II	549-551 (decomp.)	430	22,900 (ex) 30,400 (ex) —	19,900	1.4 and 4.6	22.0
	III	579-582	475	22,900 (ex) 30,400 (ex) —	19,600	3.4	22.3
	IV	425-427	425 (melts)	22,800 (ex) 31,000 (ex) —	19,800	2.9	18.6
	V	521-523	490	23,200 (ex) 29,000 (ex) —	20,000	6.1 and 15.0	22.0
	VI	456-457 (decomp.)	485	22,000 (abs) 28,000 (abs) 36,200 (abs) 44,100 (abs)	—	—	—
	VII	521-523	435	25,900 (sh, abs, ex) 26,600 (abs, ex) 31,900 (abs, ex) 41,300 (abs) 46,600 (abs)	23,900	< 0.5	31.6
	VIII	526-528	440	25,700 (sh, abs, ex) 26,500 (abs, ex) 31,000 (abs, ex) 41,300 (abs) 46,500 (abs)	23,800	< 0.5	30.0

a) Melting point under atmospheric pressure; b) Sublimation temperature at 2 μ orr (0.27 mPascal); c) Position of absorption maxima determined from absorption spectra (abs) or excitation spectra (ex, sh = shoulder) at 523 K; d) Position of fluorescence maximum at 523 K; e) Actual lifetime of fluorescence at 493 K; f) Estimated radiative lifetime. (subl. = sublimation; decomp. = decomposition).

alter the foregoing conclusion.

Compound VI reached its maximum vapour pressure at 450 K. Further increase of the temperature did not cause an increase of the absorbance, apparently due to its thermal instability. Among the substances investigated, this compound is also the only one from which no fluorescence could be observed in the vapour phase. This observation suggested the possibility of radical formation upon thermal decomposition. Such radicals could easily be formed by homolytic thermal cleavage of the ester bonds of riboflavin-tetraacetate and subsequent reactions of the radicals might yield alloxazine as product. This was verified by analysis of the products formed during the sublimation procedure and the spectroscopic measurements. Besides a tarlike residue, needleshaped, pale yellow crystals were formed and upon opening of the cell acetic acid could easily be detected (odour). Mass spectral analysis of the crystals revealed an intense molecular peak with $m/e = 256$. The accompanying fragmentation pattern displayed peaks at $m/e = 227$, $m/e = 199$, $m/e = 171$ and $m/e = 156$, indicating expulsion of the fragments CH_3N , CH_3NCO , $\text{CH}_3\text{N}(\text{CO})_2$ and $\text{CH}_3\text{N}(\text{CO})_2\text{NH}$, respectively. This shows the decomposi-

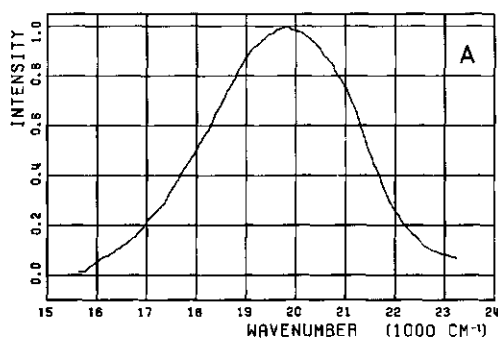
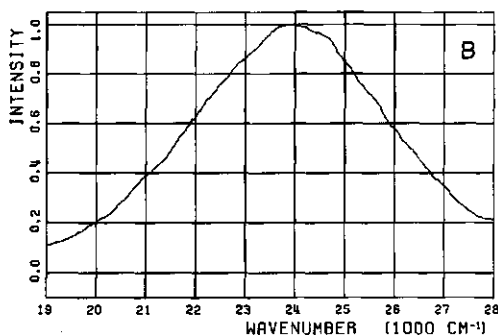


Figure 4.2. Fluorescence emission spectra of (iso)alloxazines in the vapour phase. (A) 3,7,8,10-tetramethyl-isoalloxazine (III) at 490 K. Excitation at $25,000\text{ cm}^{-1}$; $\Delta\bar{\nu}_{\text{ex}} = 700\text{ cm}^{-1}$; $\Delta\bar{\nu}_{\text{em}} = 300\text{ cm}^{-1}$. (B) 1,3,7,8-tetramethyl-alloxazine (VIII) at 470 K. Excitation at $29,000\text{ cm}^{-1}$; $\Delta\bar{\nu}_{\text{ex}} = 315\text{ cm}^{-1}$; $\Delta\bar{\nu}_{\text{em}} = 255\text{ cm}^{-1}$.



tion product of compound VI to be 3,7,8-trimethyl-alloxazine which was easily confirmed by a mass spectrum of this compound. Our mass spectra were also in perfect agreement with those obtained from alloxazines by various other authors¹³⁻¹⁵. Furthermore, solutions of the pale crystals exhibited the characteristic absorption spectrum of alloxazines.

From all compounds except VI, broad structureless vapour phase emission and excitation spectra were observed. Within the separate groups of alloxazines and isoalloxazines, these spectra show differences of only a few hundred cm^{-1} in the location of the band maxima (cf. Table 4.1). Representative emission spectra for

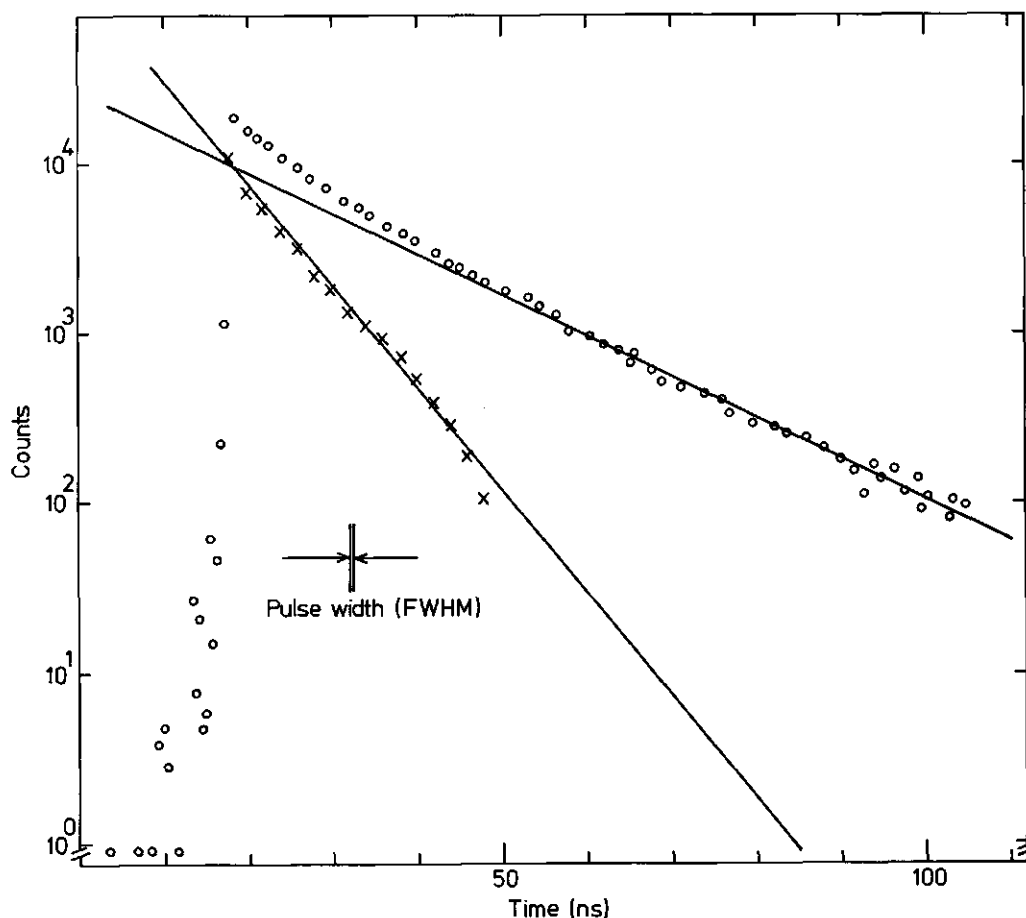


Figure 4.3. Fluorescence decay of 3-methyl-10-(γ -hydroxypropyl)-isoalloxazine (V) at 423 K. Excitation with the 476.5 nm ($20,987 \text{ cm}^{-1}$) emission line of an argon ion laser. Detection at $19,000 \text{ cm}^{-1}$ (526 nm); $\Delta\bar{\nu}_{\text{em}} = 970 \text{ cm}^{-1}$. Excitation pulse 350 ps FWHM.

an alloxazine and an isalloxazine derivative in the vapour phase are given in Fig. 4.2. Phosphorescence emission was not detectable. Due to the low vapour pressure and instrumental limitations, we could only measure the excitation spectra of the fluorescence at wavenumbers below $35,000\text{ cm}^{-1}$. All compounds show some deviation in their vapour phase excitation spectra as compared to those in solution with respect to the relative intensities of the $S_0 \rightarrow S_1$ band and the $S_0 \rightarrow S_2$ band. The relative intensity of the $S_0 \rightarrow S_2$ band appears to decrease in the vapour phase. However, the absorption spectra do not show this phenomenon. For this reason, the wavenumbers for the $S_0 \rightarrow S_2$ transition given in Table 4.1 must be taken with care. Furthermore, during the spectroscopic measurements a very slow but still measurable conversion of isalloxazine into alloxazine was observed. This could be monitored by the disappearance of the isalloxazine emission spectrum and concomitant appearance of the alloxazine emission spectrum. The reaction was faster for those compounds carrying large substituents at N_{10} . Quantification of the reaction was very difficult because the process also occurs in the dark at high temperature and low pressure. It was, therefore, not possible to obtain unambiguous results after excitation into the *second* electronically excited singlet state of isalloxazines. For this reason, excitation was limited to the $S_0 \rightarrow S_1$ electronic transition in the lifetime measurements.

The fluorescence decay of (iso)alloxazines in the vapour phase is substantially different from the decay observed in solution^{1,16}. Firstly, the average lifetimes are substantially shorter at high temperatures in the vapour phase and, secondly, the *is*alloxazines do not show a single exponential decay (Fig. 4.3). The deviation from a single exponent indicates the presence of a thermal distribution over vibrationally excited states corresponding to the S_1 state. This causes a variety of hot molecules which differ with respect to their actual lifetimes, so the decay possibly is multi-exponential. On the other hand, an analysis of the decay curves in more than two time constants is not feasible. Therefore, the decay curves were analyzed in terms of one or two components in such a way that at least a difference of about one order of magnitude was maintained between the characteristic decay time of the pulse ($\sim 220\text{ ps}$) and the lifetime of the short component. In the case where the short component approaches the decay time of the pulse, only average lifetimes are given. The results obtained at 493 K are summarized in Table 4.1 for excitation at $20,987\text{ cm}^{-1}$ (476.5 nm) and detection in the band maxima of the continuous wave emission spectra (spectral band width of detection $\Delta\tilde{\nu} \approx 1000\text{ cm}^{-1}$).

The alloxazine derivatives show a fluorescence decay curve which is almost

identical with that of the excitation pulse. Only a slight broadening (~ 80 ps) is observed, so the fluorescence lifetime of alloxazine in the vapour phase certainly will be shorter than 500 ps.

Compounds I, III and IV did not show any measurable differences in their decay curves when the fluorescence decay was measured at different excitation and detection wavenumbers, but the short lifetimes make the analysis difficult. Compounds II and V, which have longer fluorescence lifetimes, gave decay curves which were easier to analyze. When the detection wavenumber was changed, the two lifetimes (from the analysis) were not affected, but their relative contribution changed. The short component is predominantly present at high emission wavenumbers whereas its relative contribution decreases with decreasing wavenumber. Typical values for the relative contribution of the short component to the total emission intensity of compound V in the vapour phase at 493 K range from 0.72 at $19,000\text{ cm}^{-1}$ to 0.47 at $16,000\text{ cm}^{-1}$. When the excitation wavenumber is changed, the relative contribution of the two components to the total emission at any single detection wavenumber remains constant. However, both lifetimes show a slight increase ($\sim 5\%$) on changing the exciting light from the $20,987\text{ cm}^{-1}$ (476.5 nm) line to the $21,468\text{ cm}^{-1}$ (465.8 nm) line of the argon laser.

Only for compound II and V we could measure the temperature dependence of the fluorescence decay over a rather wide range. The results are given in Table 4.2. The reciprocals of the lifetimes were analyzed in an Arrhenius plot. Plots of $\ln \tau^{-1}$ versus $1/T$ are linear, except for the short component observed from compound II, which suffers from large experimental errors due to its small value. From linear regression analysis ($r^2 \geq 0.95$), activation energies can be calculated yielding values of 550 cm^{-1} (τ_1 of compound II), 407 cm^{-1} (τ_1 of compound V) and 599 cm^{-1} (τ_2 of compound V). Compound II decomposed rapidly during the single photon counting experiments at 523 K. The decomposition could be seen as a drastic decrease of the total count rate in the course of the measurements. The reciprocal of the fluorescence lifetime observed at 523 K, however, fits perfectly into the Arrhenius plot, so apparently this lifetime is not influenced by decomposition.

Finally, the radiative lifetimes (Table 4.1) were estimated using the band areas obtained from the continuous wave emission and excitation spectra and, where possible, absorption spectra. The radiative lifetime was calculated according to the Birks-Dyson formula¹⁷.

TABLE 4.2.
TEMPERATURE DEPENDENCE OF THE FLUORESCENCE DECAY OF TWO ISOALLOXAZINE DERIVATIVES
IN THE VAPOUR PHASE (a).

) compound II (cf. Table 4.1)

(K)	kT (cm ⁻¹)	τ_1 (ns)	τ_2 (ns)	α_1	α_2
413	287	6.57	1.62	0.38	0.62
443	308	5.17	1.38	0.37	0.63
473	329	4.90	1.66	0.32	0.68
493	343	4.61	1.36	0.33	0.67
513	357	4.32	1.42	0.26	0.74
523	363	4.27	1.36	0.23	0.77

) compound V (cf. Table 4.1)

(K)	kT (cm ⁻¹)	τ_1 (ns)	τ_2 (ns)	α_1	α_2
423	294	18.07	7.19	0.50	0.50
443	308	17.15	6.50	0.40	0.60
463	322	16.56	5.97	0.33	0.67
483	336	15.37	5.57	0.32	0.68
493	343	14.77	5.37	0.28	0.72

) Excitation with the 20,987 cm⁻¹ (476.5 nm) emission line of an argon ion laser; detection at 19,000 cm⁻¹ (526 nm), $\Delta\bar{\nu} = 1000$ cm⁻¹. Decay curves were analyzed according to:

$$I(t)/I(0) = \alpha_1 \exp(-t/\tau_1) + \alpha_2 \exp(-t/\tau_2)$$

4. DISCUSSION

Although the continuous wave vapour phase spectra of (iso)alloxazines suffer from serious broadening due to sequence congestion, they can be interpreted by comparison with the spectra obtained in solution, where, under appropriate experimental conditions, a vibrational structure can be observed¹. Using this vibrational structure, it was established that for isalloxazines in fluid solution at 400 K the maxima of the $S_0 \rightarrow S_1$ absorption and the $S_0 \leftarrow S_1$ emission transitions are not coincident with the pure electronic transitions, but with the 0-1 vibronic transitions. Similar results were obtained on alloxazines^{8,9}. Based on Stokes-loss considerations, we conclude that the vapour phase absorption and emission spectra have a similar property. If the band maxima in these spectra were coincident with the pure electronic transitions, the Stokes-loss would be of the order of 2700 cm⁻¹ for alloxazines and 3000 cm⁻¹ for isalloxazines in the vapour phase (cf. Table 4.1). From the 0-0 transitions observed in fluid and glassy solution, the Stokes-loss was found to range from 850 to 1300 cm⁻¹, a value which previously was already regarded to be anomalously high¹. Following the same considerations as before¹, the Stokes-loss is predicted to be zero

in the vapour phase spectra, because the index of refraction and the dielectric constant of the "medium" now both will be unity. This is confirmed by the elaborate study on solvent effects by Bakhshiev¹⁸. Additionally, the absorption spectrum of alloxazine vapour even shows a shoulder on the low wavenumber edge of the $S_0 \rightarrow S_1$ band which apparently is of vibrational origin. The slight red shift observed in this spectrum on raising the temperature, can be ascribed to thermal population of vibrationally excited states corresponding to the electronic ground state. The same phenomenon is also responsible for sequence congestion.

Consequently, subtraction of two vibrational quanta¹ of 1250 cm^{-1} from the wavenumber-difference between the band maxima of the $S_0 \rightarrow S_1$ absorption and $S_0 \leftarrow S_1$ emission bands, yields an approximate value for the Stokes-loss under the present experimental conditions. Values ranging from $\sim 500\text{ cm}^{-1}$ for isoalloxazines to 200 cm^{-1} for alloxazines are obtained in this way. Because we are dealing with *isolated molecules* in their electronically first excited singlet state, these non-zero values are due to an intramolecular process. This supports our earlier conclusion that the isoalloxazine molecule changes its molecular conformation upon electronic excitation¹.

The actual fluorescence lifetimes of isoalloxazines were found to be shorter in the vapour phase than in solution. The opposite was observed for the radiative lifetimes which, however, may suffer from an uncertainty in the value of the molar extinction coefficient $\epsilon(\bar{\nu})$, as applied in the Birks-Dyson formula¹⁷. According to this formula, the radiative lifetime τ_0 of a singlet \rightarrow singlet transition is given by:

$$1/\tau_0 = 2.88 \times 10^{-9} \cdot (n_f^3/n_a) \cdot \langle \bar{\nu}_f^{-3} \rangle_{\text{Av}}^{-1} \cdot \int \epsilon(\bar{\nu}) \cdot d\ln \bar{\nu} \quad (4.4)$$

in which the factor $\langle \bar{\nu}_f^{-3} \rangle_{\text{Av}}^{-1}$ is related to the fluorescence spectrum $F(\bar{\nu})$ by

$$\langle \bar{\nu}_f^{-3} \rangle_{\text{Av}}^{-1} = \{ \int F(\bar{\nu}) \cdot d\bar{\nu} \} / \{ \int F(\bar{\nu}) \cdot \bar{\nu}^{-3} \cdot d\bar{\nu} \} \quad (4.5)$$

The constant is taken such that the wavenumber $\bar{\nu}$ is expressed in cm^{-1} . For experiments done in dilute solution in a transparent solvent of negligible optical dispersion, the indices of refraction at the absorption (n_a) and emission (n_f) wavenumbers are assumed to be equal. Statistical analysis of the factors $\langle \bar{\nu}_f^{-3} \rangle$ and $\int \epsilon(\bar{\nu}) \cdot d\ln \bar{\nu}$ as calculated from the spectral band areas shows no significant differences between the results in the vapour phase and those obtained previously in solid or liquid solution¹.

In this analysis we assumed again that the value of $\epsilon(\bar{\nu})$ (i.e. the value of

the quantum mechanical transition moment) is the same in solution and in the vapour phase. Thus, to a good degree of approximation, τ_0 only depends on n . By setting $n = n_a = n_f$ in eq.(4.4), τ_0 becomes inversely proportional to n^2 , which is supported by a study of Olmsted¹⁹. For commonly applied organic solvents, $n \approx 1.4$ so, in the vapour phase where $n = 1$, τ_0 has increased roughly by a factor of 2, which can be seen by comparison of the present results (cf. Table 4.1) with those obtained before¹.

As a consequence of the increase of the radiative lifetime and the decrease of the actual fluorescence lifetime of (iso)alloxazines in the vapour phase (cf. Table 4.1) as compared to solution^{1,16}, the quantum yield of fluorescence must be substantially smaller in the vapour phase. Hence, the non-radiative decay of the S_1 state is enhanced in the vapour phase due to very efficient *intra*-molecular dark-processes in the isolated molecule. Possibly a conformational change which likely occurs upon electronic excitation as discussed above, may play an important role therein. We do not expect that direct photodissociation in the S_1 state generally will contribute considerably to the observed decay. When a molecule is excited into a dissociative electronic state, i.e. the potential energy surface for the nuclear motion in that state is repulsive for all values of the coordinates of certain nuclei, the lifetime of such a state will be of the order of the period of a molecular vibration, i.e. ~ 0.1 ps. This would exclude fluorescence on a nanosecond time scale. Only for compound VI such a process may be important. For the other compounds the S_1 state apparently decays through ordinary channels like internal conversion and intersystem crossing into other vibronic states, in which the molecule, of course, may undergo subsequent dissociation. In this respect, it should be noted that the decomposition of compound II at 523 K did not affect its fluorescence lifetime and that, in spite of all efforts, we could not establish an experimental difference in the decomposition rates occurring in the dark and during illumination. Moreover, alloxazines which were stable in our experiments, behave similarly as isoalloxazines regarding their lifetimes.

From this point of view the concept of photochemical reactions occurring in the S_1 state of isoalloxazines as proposed by Song and Metzler²⁰ and Song²¹, needs reconsideration. These investigators reported that the major photoproduct of isoalloxazine is alloxazine. Conversely, we observe a slow thermally activated formation of alloxazine which seems to be unaffected by irradiation. However, under our experimental conditions solid isoalloxazine exists in thermal equilibrium with its vapour and, for that reason, ground state surface reactions in the solid phase cannot be excluded.

Additionally, Song proposed intramolecular complexing of N₁ of isoalloxazine with its ribityl side chain^{20,21} in order to explain its excited singlet photochemistry. The existence of such a complex in the electronic ground state is supported by recent ¹⁵N-NMR experiments²². Remarkably, the fluorescence lifetime of compound V largely exceeds that of all other isoalloxazine derivatives studied (cf. Tables 4.1 and 4.2). This compound is also the only one which can form an intramolecular complex due to the presence of the hydroxyl group in its N₁₀ side-chain. We do not consider this to be just a coincidence. According to the fundamental theory on radiationless processes^{23,24}, a molecule of the size of isoalloxazine will exhibit a non-radiative decay according to the statistical limit. So, in terms of density of states, one of the factors governing the non-radiative decay of the S₁ state, the fluorescence lifetime of compound V cannot exceed that of compound I. Nevertheless, the observed lifetime of compound V exceeds that of compound I by almost one order of magnitude under identical conditions. This suggests that some intramolecular process must affect vibronic coupling considerably. This process may be intramolecular complexation, which is not accompanied by a photochemical process regarding the fact that the observed lifetime is lengthened. In condensed media, the solvation apparently prevails due to which this phenomenon is not observed.

REFERENCES AND NOTE

- 1 Cf. Chapter 3 or: J.K. Eweg, F. Müller, A.J.W.G. Visser, C. Veeger, D. Bebeelaar and J.D.W. van Voorst, *Photochem. Photobiol.* 30 (1979) 463.
- 2 H.J. Grande, C.G. van Schagen, T. Jarbandhan and F. Müller, *Helv. Chim. Acta* 60 (1977) 348.
- 3 W.R. Knappe, *Chem. Ber.* 108 (1975) 2422.
- 4 M. Stockburger, in: *Organic Molecular Photophysics*, Vol. 1, ed. J.B. Birks (Wiley, London, 1973).
- 5 J.P. Byrne and I.G. Ross, *Aust. J. Chem.* 24 (1971) 1107.
- 6 W.R. Ware and P.T. Cunningham, *J. Chem. Phys.* 43 (1965) 3826.
- 7 C.J. Werkhoven, Thesis, University of Amsterdam, Amsterdam, The Netherlands (1974).
- 8 J. Koziol, *Photochem. Photobiol.* 5 (1966) 41.
- 9 J. Koziol and A. Koziolowa, in: *Flavins and Flavoproteins, Physicochemical Properties and Function*, Proc. Int. Meeting, ed. W. Ostrowsky (Polish Scientific Publishers, Warsaw and Cracow (1977) 81).
- 10 W.J. Moore, *Physical Chemistry* (Prentice-Hall, London, 1962).
- 11 M. Wang and C.J. Fritchie Jr., *Acta Cryst.* B29 (1973) 2040.
- 12 M. Leijonmarck, Thesis, University of Stockholm, Sweden, *Chem. Commun.* VIII (1977).
- 13 P. Brown, L.C. Hornbeck and J.R. Cronin, *Org. Mass Spectrom.* 6 (1972) 1383.
- 14 R. Tümmler, K. Steinfelder, E.C. Owen, D.W. West and M. von Ardenne, *Org. Mass Spectrom.* 5 (1971) 41.

- 5 B. Tyrakowska and J. Koziol, in: *Flavins and Flavoproteins, Physicochemical Properties and Function*, Proc. Int. Meeting, ed. W. Ostrowsky (Polish Scientific Publishers, Warsaw and Cracow (1977) 109).
- 6 R.D. Fugate and P.S. Song, *Photochem. Photobiol.* 24 (1976) 479.
- 7 J.B. Birks, *Photophysics of Aromatic Molecules* (Wiley, London, 1970).
- 8 N.G. Bakhshiev, *Opt. Spectrosc.* 12 (1962) 309.
- 9 J. Olmsted, *Chem. Phys. Letters* 38 (1976) 287.
- 0 P.S. Song and D.E. Metzler, *Photochem. Photobiol.* 6 (1967) 691.
- 1 P.S. Song, in: *Flavins and Flavoproteins, Proc. 3rd. Int. Conf.*, ed. H. Kamin (University Park Press, Baltimore, 1971).
- 2 K. Yagi, N. Ohnishi, A. Takai, K. Kawano and Y. Kyogoku, *Biochemistry* 15 (1976) 2877.
- 3 M. Bixon and J. Jortner, *J. Chem. Phys.* 48 (1968) 715.
- 4 B.R. Henry and W. Siebrand, in: *Organic Molecular Photophysics, Vol. 1*, ed. J.B. Birks (Wiley, London, 1973).

5 HE(I) AND HE(II) PHOTOELECTRON SPECTRA OF ALLOXAZINES AND ISOALLOXAZINES

5.1. INTRODUCTION

The electronic structure of isoalloxazines and alloxazines has been the subject of extensive theoretical study and quantum mechanical calculations. Such research efforts are motivated by the fact that 7,8-dimethyl-10-ribityl-isoalloxazine derivatives, commonly referred to as flavins, form the prosthetic group of flavoproteins and participate in reduction-oxidation reactions and electron transport in living organisms. A brief summary of the relevant literature was given in previous work¹. The main reason to start comparative studies on alloxazines and isoalloxazines is that the former compounds are decomposition product of riboflavin and show a very interesting ground and electronically excited state tautomerism, which relates them to isoalloxazines^{2,3}.

Quantum mechanical calculations, irrespective of their degree of approximation, need rigorous experimental support, especially in the case of molecules like (iso)alloxazines. This was recognized to a greater or less extent in the various publications which appeared in the last two decades describing the results from Hückel^{4,5}, Extended Hückel^{6,7}, SCF-PPP^{3,8-15}, CNDO/2^{7,16} and MINDO/3¹⁷ calculations. The experimental data used thus far to support the theoretical work were 1) molecular structure and geometry^{6,8,9,13}, 2) excited state energies and optical spectra^{3,8-15,17}, 3) correlation with ESR and NMR spectra^{7,8,16,17} and 4) chemical properties derived from the application of Fukui's Frontier Molecular Orbital Theory¹⁸ by some authors^{17,19}. All these experimentally observable properties used to test the theoretical models, however, generally depend in a very complex way on the orbital structure. For this reason, correlation between theory and the experiments mentioned before give only rough indication of the reliability of the theoretical method under consideration. Especially when electronic transitions are calculated, incorporation of configuration interaction into the computation is needed to obtain results which reasonably agree with the experiment. This has already been recognized^{8,10-12,14} but the methods employed have the disadvantage that a limited number of singly and doubly excited configurations of only $\pi\pi^*$ character was allowed to interact. Moreover, these configurations arise from an orbital level scheme which is with-

out experimental verification. Fox partially solved this problem by performing a direct calculation on the first excited singlet and triplet states of an isoalloxazine derivative in its oxidized form¹⁷, but this method also left some of the essential features of the electronic structure unverified.

Song⁷ has expressed the need to obtain more information about the electronic structure of isoalloxazines by measurements of the ionization potentials. Our discovery that (iso)alloxazines can be sublimed under appropriate conditions, which makes them accessible to vapour phase emission and absorption spectrometry²⁰, prompted us to measure also He(I) and He(II) photoelectron spectra. Such spectra, which were not available up till now, allow for a verification of the orbital energies by experiment.

It was already noted by Visser and Müller²¹ that CNDO/S calculations were never applied to these molecules, although they can be very useful for the experimentalist. It is now firmly established that the CNDO/S method gives a reliable interpretation and assignment of the bands in ultraviolet photoelectron spectra²²⁻²⁶ using Koopmans theorem²⁷. The experiment, therefore, enables us to test the CNDO/S and the other theoretical methods by new experimental data.

5.2. EXPERIMENTAL

The compounds studied here were synthesized according to the methods published elsewhere^{1,20,21}. The compound 3,7,8,10-tetramethyl-5-deaza-isoalloxazine was a generous gift of Professor Dr. P. Hemmerich, University of Konstanz, FRG.

Determination of the sublimation temperatures of the compounds under investigation was done by means of a Mettler Thermoanalyzer type 1. Analysis was done under conditions as closely comparable as possible to those which exist in the target chamber of the photoelectron spectrometer. The spectra were measured on a Perkin-Elmer PS 18 photoelectron spectrometer modified with a Helectros He(I) - He(II) source and calibrated using Xe and Ar lines as an internal calibrant.

The He(I) and He(II) photoelectron spectra of (iso)alloxazines can be measured rather easily on a PS 18 photoelectron spectrometer at temperatures about 40 to 60 K above the approximate sublimation temperatures as determined by thermogravimetric analysis. In spite of the low count rate (200-800 counts/second), higher temperatures should be avoided because of decomposition of the samples and condensation of (iso)alloxazine vapour on vital parts in the interior of the spectrometer, causing loss of sensitivity and bad reproducibility in the experiments.

5.3. CALCULATION PROCEDURES

The MO-calculations were performed according to the CNDO/S method of Del Bene and Jaffé²⁸ (cf. Chapter 2, section 2.5). The parameterization, however, was taken from more recent work by Kuehnlenz and Jaffé²⁹ (cf. Chapter 2, Table 2.2.2, p. 18), in which mainly the one-center two-electron integrals γ_{AA} were ad-

justed to obtain better agreement between the calculated and observed spectral properties of a larger variety of molecules than was calculated in the earlier CNDO/S work. The two-center two-electron integrals γ_{AB} were approximated utilizing the Nishimoto-Mataga formula³⁰ (eq.(2.26), p.18), originally introduced into the CNDO/S framework by Ellis *et al.*³¹.

The spectrum of eigenvalues was shifted by means of the expression derived by Bigelow²² to fit the calculated eigenvalues of benzene in the CNDO/S2 parameterization of Lipari and Duke³² to the experimental photoelectron spectrum:

$$\epsilon_i^{\text{corr}} = 11.364 \ln (\epsilon_i^{\text{calc}}/4.400) \quad (5.1)$$

Although this purely empirical expression was intended for the interpretation of benzene only, it appears to be able to give a reasonable agreement between CNDO/S eigenvalues and experimentally observed ionization potentials, even in other molecules than benzene²⁴.

Photoionization cross sections were calculated by means of Ellison's method³³, modified by Beerlage and Feil³⁴. The modification consists of adjustment of the photoelectron wavenumber k to account for the electrostatic interaction between the free electron and the remaining molecular cation according to

$$k' = (k^2 + \beta)^{1/2} \quad (5.2)$$

in which:

$$\frac{\hbar^2 k'^2}{2m} = \hbar\omega - \text{IP}_n \quad (5.3)$$

where $\hbar\omega$ represents the incident photon energy, IP_n the ionization potential for the n^{th} MO and m the electron mass.

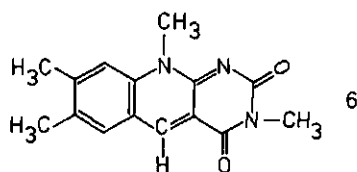
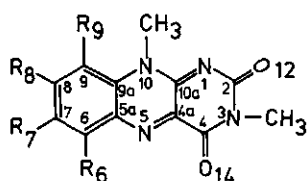
Structural data for isoalloxazines were taken from the crystallographic work performed on both the oxidized^{13,35-37} and the reduced forms^{36,38,39}. Since no structural data are known for alloxazines and 5-deaza-isoalloxazine derivatives, the geometry of these compounds was assumed to be the same as that of the oxidized isoalloxazines.

5.4. EXPERIMENTAL RESULTS AND SPECTRAL ASSIGNMENTS

5.4.1. Isoalloxazine derivatives in the oxidized form

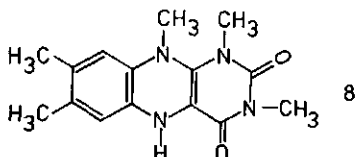
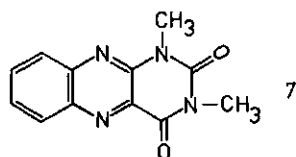
The oxidized isoalloxazine derivatives (compounds 1 to 5; cf. Scheme 5.1) show very similar photoelectron spectra. The full He(I) and He(II) spectra of compound 1 are presented in Fig. 5.1 as representative examples. None of these compounds shows any considerable difference between its He(I) and He(II) spectra. This indicates large orbital delocalization and it rules out the possibility to use He(I) - He(II) intensity differences as an assignment criterion in these molecules. Large molecules like isoalloxazines evidently do not show any vibrational structure in their photoelectron spectra, so for assignment of spectral bands we are forced to rely on substituent effects and comparison with theoretical data.

At first glance, the corrected²² CNDO/S eigenvalues agree surprisingly well



Isoalloxazine derivatives :

- 1: $R_6=R_7=R_8=R_9=H$
- 2: $R_6=R_9=H; R_7=R_8=CH_3$
- 3: $R_7=R_8=R_9=H; R_6=CH_3$
- 4: $R_6=R_7=R_8=H; R_9=CH_3$
- 5: $R_6=R_8=R_9=H; R_7=F$



Scheme 5.1. Structures of (iso)alloxazines investigated by photoelectron spectroscopy.

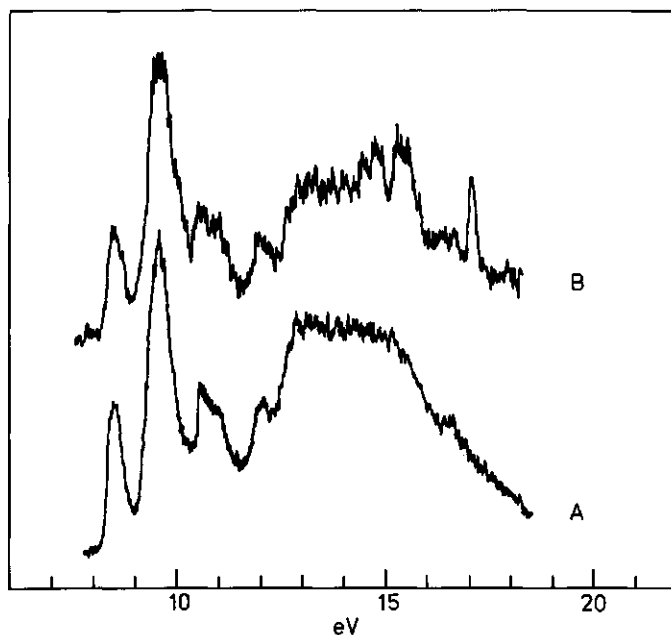


Figure 5.1. He(I) (A) and He(II) (B) photoelectron spectra of 3,10-dimethylisoalloxazine (1) at 508 K.

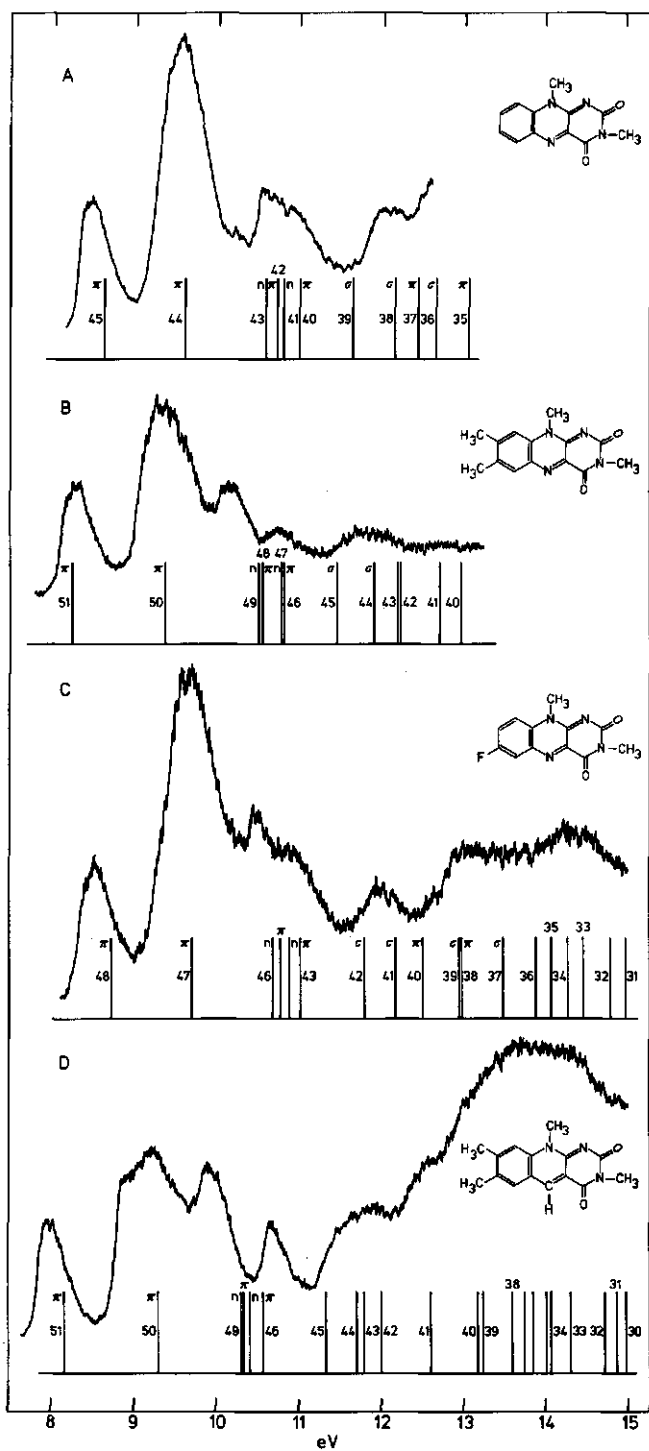
with the observed spectra (Fig. 5.2). However, intensity considerations⁴⁰ indicate that it is highly improbable that the intense band, observed between 9 and 10 eV in all spectra can be assigned to a single π orbital, although this is suggested by the calculation. If this were true, the photoionization cross-section of the two highest occupied π orbitals would differ by a factor of 3.5 as deduced from the relative band areas.

For verification, a modified plane wave cross-section calculation³⁴ was performed, using the corrected eigenvalues and eigenvectors of the "ideal" all-proton isoalloxazine model as defined in section 5.5. The dependence of the cross-sections on the β parameter (eq. 5.2) is shown in Fig. 5.3 ($0.0 \leq \beta \leq 4.0$). Although the first ionization potential (~ 8 eV) is reasonably far off-threshold, a rather large β -value is required to obtain theoretical results which do not imply appreciable intensity differences between the He(I) and He(II) spectra. However, full agreement with the experimentally observed differences cannot be achieved by calculation. On the other hand, there is no β -value giving a cross-section ratio of 3.5 for the highest occupied orbitals π_8 and π_9 . So, according to the tentative rule by Schweig and Thiel⁴⁰ (in first approximation the intensity of a photoelectron band is proportional to the orbital degeneracy), the intense band in the photoelectron spectra of oxidized isoalloxazines should be due to a threefold degeneracy in the orbital level scheme at ~ 9.5 eV.

This feature was further explored by a study of substituent effects. It is known that π orbitals are destabilized upon methylation whereas introduction of a fluoro substituent stabilizes σ orbitals⁴¹. Additionally, methyl groups hardly affect σ orbitals and fluoro substituents hardly affect π orbitals. Therefore, it should be possible to lift the above-mentioned degeneracy by introducing substituents in appropriate positions in the molecule. In this respect, the CNDO/S calculations may offer guidance in what particular position a substituent should be placed to obtain an experimentally observable effect.

Inspection of the CNDO/S results frequently shows quasi-degeneracy in the orbital level scheme ($\Delta E < 0.02$ eV). Whenever this occurs, the orbitals involved therein are of *different type* (π and σ) and localized in different parts of the

Figure 5.2. He(I) spectra and corrected²² CNDO/S eigenvalues (cf. eq. 5.1) of some oxidized isoalloxazine derivatives. A: 3,10-dimethyl-isoalloxazine (1) at 542 K; B: 3,7,8,10-tetramethyl-isoalloxazine (2; 3-methyl-lumiflavin) at 529 K; C: 3,10-dimethyl-7-fluoro-isoalloxazine (5) at 490 K; D: 3,7,8,10-tetramethyl-5-deaza-isoalloxazine (6) at 513 K. The orbital numbers are counted up from the lowest occupied CNDO/S orbital.



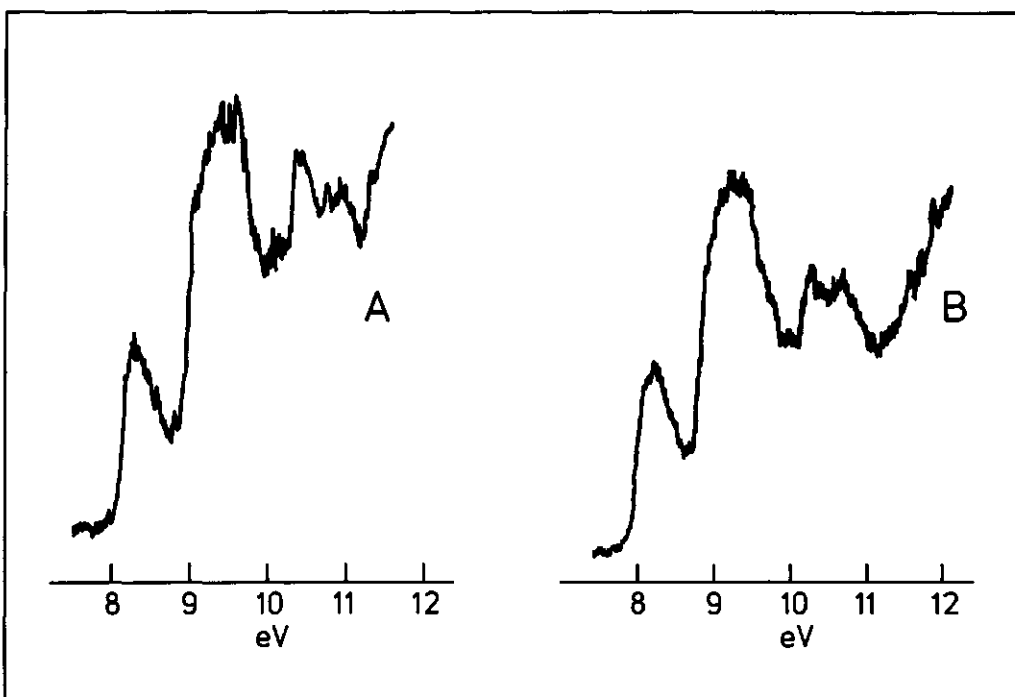


Figure 5.4. Details of the He(I) photoelectron spectra of 3,9,10-trimethyl-isoalloxazine (4) at 462 K (A) and of 3,6,10-trimethyl-isoalloxazine (3) at 497 K (B).

in π_8 . Comparison with benzene itself⁴² shows a striking resemblance of π_8 and π_9 with the benzene e_{1g} orbitals. The nodal plane of π_8 intersects the $C_7 - C_8$ and $C_{5a} - C_{9a}$ bonds whereas the nodal plane of π_9 passes almost exactly through the centers C_6 and C_9 . This is in agreement with the pronounced methyl group effect on the highest occupied orbital as deduced from the first ionization potentials of compounds 1 and 2 (Fig. 5.2 and Table 5.1). Because of the high density on C_6 and C_9 calculated for π_8 ($c \approx 0.6$), we do expect a similar methyl group effect on this orbital upon methylation of these centers. For this reason, we also studied compounds 3 and 4 although they were found to be thermally less stable than the other compounds, both by thermoanalysis and in the photoelectron spectrometer. Photoelectron spectra of these compounds, however, proved to be measurable without serious interference from decomposition, as long as the temperature was not raised more than 20 K above the sublimation temperature (cf. caption to Fig. 5.4). The low-energy parts of their He(I) spectra are given in Fig. 5.4, showing considerable broadening of the intense second band in the spec-

trum of compound 3 (Fig. 5.4B) and a distinct shoulder in the corresponding band of compound 4 (Fig. 5.4A). This clearly points towards degeneracy.

For reasons given before, it is most likely that degeneracy occurs between σ and π orbitals. Inspection of the two highest occupied orbitals of σ character (σ_{30} and σ_{29} in the all-proton model), shows them to be linear combinations of oxygen and imine-like nitrogen lone pairs. This implicates large through-bond interactions^{43,44}. The σ orbitals involved herein are localized in the pyrimidin subnucleus of the molecule. This is supported to some extent by the absence of a fluoro substituent effect upon introducing this atom at position C₇ in the benzene subnucleus (Fig. 5.2C). In order to investigate this prediction more thoroughly, the photoelectron spectra of a 5-deaza-isoalloxazine derivative were measured (Fig. 5.2D). Formal replacement of N₅ by a C - H fragment causes the intense second band in the spectrum to split and produces an additional shoulder on its high energy edge at ~ 9.5 eV. The remaining spectral characteristics, including the absence of He(I) - He(II) intensity differences, do not differ considerably from those observed in the spectra of compounds 1 to 5. This result definitely provides strong evidence for a three-fold degeneracy in the orbital level-scheme of an oxidized isoalloxazine at about 9.5 eV.

Comparison of the CNDO/S results (corrected by Bigelows formula²², eq.(5.1) p. 54) with Song's SCF-PPP calculations¹⁰, shows excellent agreement for both the π eigenvalues (cf. Fig. 5.7) and the π eigenvectors⁴⁵. Especially the benzenoid E_{1g} character of the two highest occupied orbitals is predicted independently by both methods. This supports the spectral assignments. The relevant data are summarized in Table 5.1.

5.4.2. 1,3-dimethyl-alloxazine

The measurements on alloxazine were confined to the simplest derivative which was found to be stable in the vapour phase. The lack of X-ray crystallographic data on alloxazines makes a theoretical calculation less accurate than for isoalloxazine. This obstructs unambiguous assignment of the spectral bands. Full He(I) and He(II) spectra of 1,3-dimethyl-alloxazine and an expanded He(I) spectrum combined with the corrected CNDO/S eigenvalues are given in Fig. 5.5. Notwithstanding a large overall difference with the isoalloxazine spectrum, similarities are clearly present. Comparison with the spectra of compound 1 shows the first ionization potential to be only 0.16 eV higher in the case of alloxazine. The intense band observed in the isoalloxazine spectrum is split into two

TABLE 5.1.

EXPERIMENTAL AND CALCULATED^{a)} IONIZATION POTENTIALS OF VARIOUS ALLOXAZINES AND ISOMALLOXAZINES.

Ideal Isoalloxazine ^{b)}		1		2		3		4	
No.	Calc. Ass.	Exp.	No. d)	Calc.	Ass. E)	Exp.	No.	Calc.	Ass.
39	8.66 σ_9	8.47	45	8.62	π	8.22	51	8.21	π
	9.81 σ_8	9.54	44	9.58	π	9.33	50	9.33	π
	10.89 σ_{30}	10.54	43	10.58	π	9.33	49	10.47	π
	10.92 σ_7	10.54	41	10.79	π	9.33	47	10.76	π
35	11.00 σ_{29}	10.55	42	10.71	π	10.09	48	10.51	π
	11.43 σ_6	10.88	40	11.00	π	10.87	46	10.77	π
	11.88 σ_{28}	11.98	39	11.63	σ	11.84	45	11.42	σ
	12.47 σ_{27}	12.74	38	12.14	σ	11.84	44	11.87	σ
	12.77 σ_5	12.74	37	12.42	π	12.17	43	12.17	σ
30	12.83 σ_{26}	12.74	37	12.42	π	12.17	43	12.17	σ
	13.47 σ_4	13.47	36	12.64	σ	12.21	42	12.21	π
	13.57 σ_{25}	13.57	35	13.03	σ	12.67	41	12.67	π
	14.24 σ_3	14.24	34	13.27	σ	12.94	40	12.94	σ
	14.33 σ_{24}	14.33	34	13.27	σ	13.53	39	13.53	σ
25	14.62 σ_{23}	14.62	34	13.27	σ	13.53	39	13.53	σ
	15.19 σ_{22}	15.19	34	13.27	σ	13.53	39	13.53	σ
	15.27 σ_2	15.27	34	13.27	σ	13.53	39	13.53	σ
	15.28 σ_{21}	15.28	34	13.27	σ	13.53	39	13.53	σ
20	15.72 σ_{20}	15.72	34	13.27	σ	13.53	39	13.53	σ
	15.94 σ_{19}	15.94	34	13.27	σ	13.53	39	13.53	σ
	16.30 σ_1	16.30	34	13.27	σ	13.53	39	13.53	σ
	16.51 σ_{18}	16.51	34	13.27	σ	13.53	39	13.53	σ
	16.91 σ_{17}	16.91	34	13.27	σ	13.53	39	13.53	σ
15	17.70 σ_{16}	17.70	34	13.27	σ	13.53	39	13.53	σ
	18.75 σ_{15}	18.75	34	13.27	σ	13.53	39	13.53	σ
	19.15 σ_{14}	19.15	34	13.27	σ	13.53	39	13.53	σ
	19.27 σ_{13}	19.27	34	13.27	σ	13.53	39	13.53	σ
	20.34 σ_{12}	20.34	34	13.27	σ	13.53	39	13.53	σ
	20.85 σ_{11}	20.85	34	13.27	σ	13.53	39	13.53	σ
10	21.38 σ_{10}	21.38	34	13.27	σ	13.53	39	13.53	σ
	22.47 σ_9	22.47	34	13.27	σ	13.53	39	13.53	σ

a) Calculated ionization potentials corrected according to Bigelow²² (cf. Eq. 1); b) According to the geometry given by Wang and Fritchie³⁵;

c) Experimental value (eV); d) Number of calculated orbital counted up from the lowest occupied orbital = 1; e) Calculated value (eV);

f) Assignment; g) No calculation performed; h) Planar molecular conformation assumed; j) Mixed: ~ 50% π , ~ 50% σ .

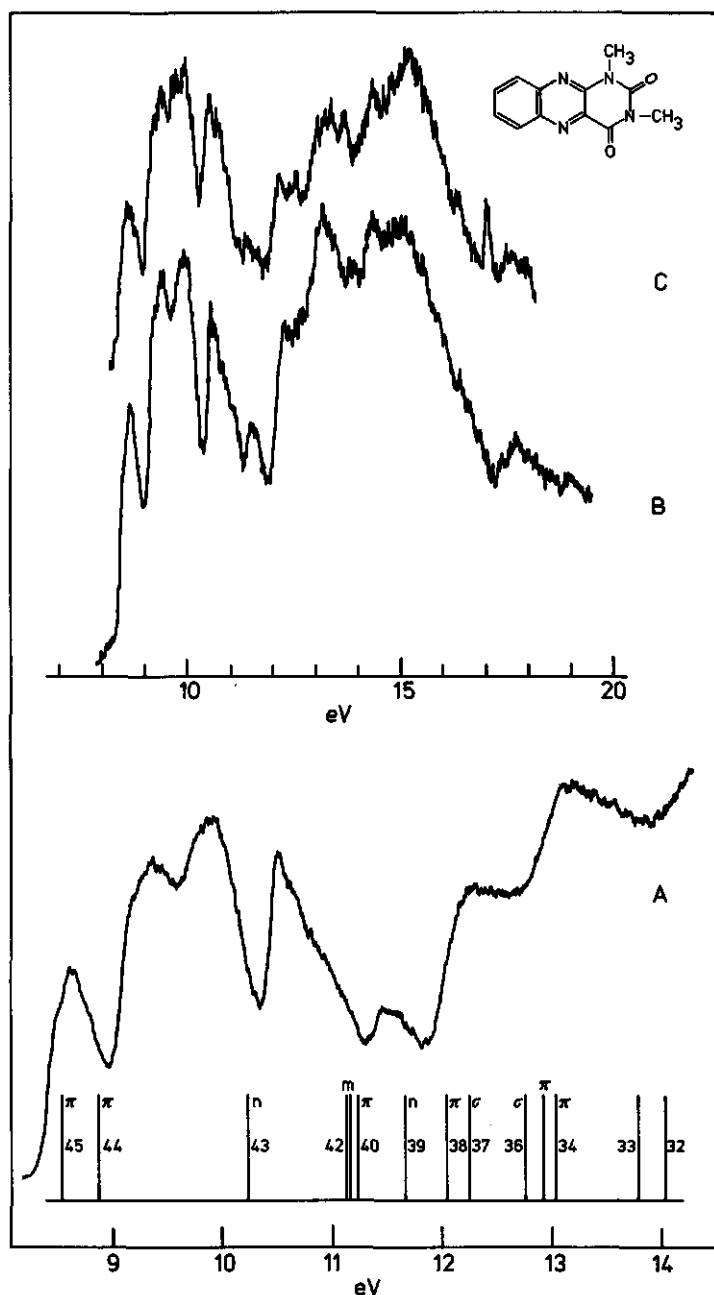


Figure 5.5. Photoelectron spectra and corrected²² CNDO/S eigenvalues (cf. eq. 5.1) of 1,3-dimethyl-alloxazine (7) at 443 K. A: He(I) spectrum compared with the CNDO/S eigenvalues. The orbital numbers are counted up from the lowest occupied orbital. Orbitals 41 and 42 show considerable $\sigma - \pi$ mixing as denoted by "m"; B: Full He(I) spectrum; C: Full He(II) spectrum.

distinct bands in the spectrum of alloxazine. The strongly asymmetric band in the alloxazine spectrum with an origin at 10.54 eV is apparently due to more than one orbital.

The agreement between the calculated and the observed spectrum of alloxazine is not as good as in the case of isoalloxazine. This may be due to an error in the molecular conformation used in the calculation. Because of the lack of X-ray data, the calculations on alloxazine were performed using the molecular geometry of isoalloxazine, except for the position of the N_{10} methyl group. In alloxazine, N_1 was assumed to be methylated instead of N_{10} . The $C_{\text{methyl}} - N_1$ bond distance was taken to be equal to the $C_{\text{methyl}} - N_{10}$ bond distance in isoalloxazine and the bond angle towards C_2 was taken as 120° . Both the eigenvalues and the eigenvectors are affected considerably by this operation. The benzenoid character and approximate E_{1g} symmetry of the two highest occupied π orbitals as was calculated for isoalloxazine is broken down completely in alloxazine. The highest occupied σ orbital is still of non-bonding character, but now contains mainly the N_5 , N_{10} and O_{14} lone pairs. It also extends more into the benzene subnucleus than in isoalloxazine. The orbitals labelled 41 and 42 in Fig. 5.5 are found to be almost perfect linear combinations of a π and a σ orbital which are both localized mainly on the carbonyl groups and N_3 . Orbital 42 contains 41% π and orbital 41 contains 54% π character. Calculation of the scalar products between all eigenvectors of compound 1 and those of compound 7 also shows strong mixing of orbitals. Consequently, alloxazine has to be regarded as a totally different molecule. This obstructs unequivocal assignment of photoelectron bands. A tentative assignment of a few orbitals is proposed in Table 5.1, based on the following considerations: The orbitals labelled 44 (π) and 43 (n) are both destabilized with respect to the corresponding orbitals calculated for isoalloxazine (compound 1), the destabilization being the largest for the π orbital. This apparently lifts the degeneracy discussed before and yields the order π , π , n for the highest occupied orbitals as is predicted by the calculation. However, quantitatively the agreement between the theory and the experiment is not very good. In the 10.0 - 12.0 eV energy region a marked He(I) - He(II) intensity difference is observed, but owing to the strong overlap of spectral bands it is impossible to use this observation as an assignment criterion. Any attempt to draw more conclusions from these data appears to be speculative. More experimental information, particularly crystallographic data, will be necessary for definitive assignment of the alloxazine photoelectron spectrum.

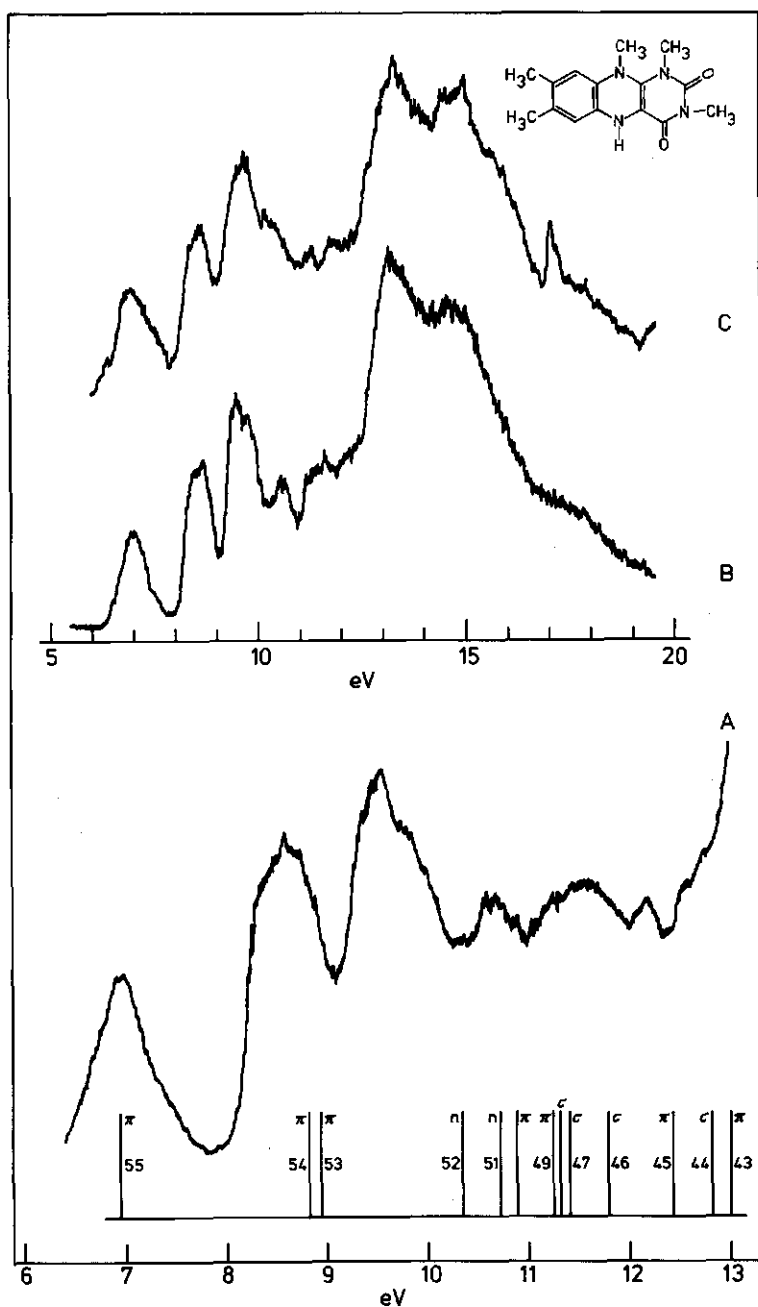


Figure 5.6. Photoelectron spectra and corrected²² CNDO/S eigenvalues (cf. eq. 5.1) of 1,3,7,8,10-pentamethyl-1,5-dihydro-isoalloxazine (8) at 451 K. The molecular geometry was assumed to be planar in the calculation. See caption to Fig. 5.5 for further details.

4.3. 1,3,7,8,10-pentamethyl-1,5-dihydro-isoalloxazine

This compound (cf. Scheme 5.1) was studied as a model for a fully reduced isoalloxazine. Its photoelectron spectra and corrected CNDO/S eigenvalues, assuming a planar molecular structure, are given in Fig. 5.6. We made this assumption after an apparent failure of the theoretical method, to predict the lower energy part of the spectrum correctly when the structure, as determined by x-ray crystallography^{38,39}, was employed. Such a failure was not encountered in the study of the other compounds: when the molecular structure was known, at least the π orbitals were predicted satisfactorily by the theory (*vide infra*).

The overall features of the photoelectron spectrum of compound 8 are very similar to those of an oxidized isoalloxazine, with one additional band at 6.99 eV, due to the presence of the two extra electrons. The CNDO/S calculation on the other hand does not give such a resemblance. Although the coefficients in the highest occupied orbital of compound 8 do not differ considerably from those in the lowest virtual orbital of the all-proton model, distinct differences are present. The lower occupied orbitals of compound 8 show considerable reorganization compared to the all-proton model. Regarding the distinct shoulders in the photoelectron bands observed at 8.7 eV and 9.6 eV, it is clear that both bands contain transitions from two different orbitals. This also follows from the band areas relative to that of the band at 6.99 eV and from the application of the tentative rule by Schweig and Thiel⁴⁰ (*vide supra*). The orbitals labelled 54 and 55 in Fig. 5.6 formally originate from the highest occupied orbitals π_9 and π_8 of the all-proton model. Their reorganization, however, causes complete loss of the benzenoid E_{1g} character and a concomitant destabilization of π_8 by 0.87 eV. This is confirmed by the shape of the photoelectron band observed from compound 8 at 8.7 eV. Like in the oxidized compounds, the non-bonding orbitals 52 and 51 are calculated about 1 eV too low in energy. Their energy difference has increased with respect to the oxidized compounds, which is confirmed by the shape of the band at 9.6 eV. The next band in the photoelectron spectrum likely can be assigned to a π orbital. It is impossible to assign more bands due to the severe crowding of orbitals below -11 eV in the level scheme and the absence of other assignment criteria.

These results support our preceding conclusion that the intense second band in the spectra of the oxidized derivatives is due to a three-fold degeneracy. Reduction lifts this degeneracy and destabilizes the π orbital involved considerably. Ionization potentials and calculated data are collected in Table 5.1.

5.5. CALCULATED RESULTS

The first CNDO/S calculations were performed on an oxidized isoalloxazine skeleton carrying only hydrogen atoms as substituents. Although this is a molecule which does not exist in nature (it would tautomerize to alloxazine), it was very useful as a theoretical model (for symmetry reasons). From crystallographic data^{13,35-37} it is known that oxidized isoalloxazines have a planar ring system. A planar "all-proton model" is thus a reasonable, simplified, model which contains the molecular plane as only symmetry element. Such a model will at least give unambiguous $\sigma - \pi$ separation.

In the methylated derivatives, $\sigma - \pi$ separability is highly dependent on the rotation of methyl groups. For methylated isoalloxazines in the solid state, the angle of rotation of the methyl groups is determined to be such that the molecular plane is not retained as a symmetry element³⁷. This may be different in the vapour phase, but there are also C - H bond length differences within one particular methyl group³⁷. Additionally, the all-proton model was required in the calculation of cross-sections because of the fact that the modified plane wave computer program was limited to planar molecules.

First, the all-proton model was used to test if the small differences in molecular geometry derived from the various crystallographic experiments^{13,35-37} affect the results of the CNDO/S calculations. It was established that the eigenvalues did not change by any experimentally observable amount. Moreover, the sets of eigenvectors obtained on different molecular conformations did not show a deviation from orthonormality greater than 1.5 percent when compared to each other. This was established by the calculation of scalar products between eigenvectors. Consequently, these geometry-differences are negligible.

Secondly, the influence of substitution and rotation of methyl substituents was investigated. When the coordinates of the hydrogen atoms were not given explicitly in the literature, we used standard bond distances and bond angles⁴⁶ in the calculations. Small variations in these also proved to be of no importance. The degree of $\sigma - \pi$ mixing was explored primarily by verification to what extent the calculated linear combinations of the methyl group hydrogen 1s functions (denoted by a, b and c) satisfy the group orbital approximation⁴⁷:

$$\begin{aligned}\phi_1 &= 3^{-\frac{1}{2}}(a + b + c) \\ \phi_2 &= 2^{-\frac{1}{2}}(b - c) \\ \phi_3 &= 6^{-\frac{1}{2}}(2a - b - c)\end{aligned}\tag{5.4}$$

When the conformation is such that the (iso)alloxazine molecular plane contains a proton of each methyl group ("eclipsed" conformation) the molecule has perfect C_s symmetry, like the all-proton model. In this case ϕ_1 and ϕ_3 have A' symmetry and ϕ_2 has A'' symmetry which makes ϕ_2 the only group orbital which can be part of a π orbital. Rotation of methyl groups around the central C - C or C - N bonds over an angle of 90° with respect to the previous situation ("staggered" conformation) breaks down C_s symmetry and, consequently, $\sigma - \pi$ separation. Nevertheless, now ϕ_3 approximately has the proper symmetry to be part of a π orbital. This behaviour is found to a good degree of approximation in the CNDO/S results. Rotation of methyl groups causes formal interchange of ϕ_2 and ϕ_3 in the eigenvectors, whose corresponding eigenvalues remain constant within 1%. This finding supports the group orbital approximation made by Song in his SCF-PPP-CI calculations^{10,45}. Whenever $\sigma - \pi$ mixing is introduced by rotation of methyl groups, it is found to occur primarily on the centers carrying the largest negative charges, i.e. O_{12} ; O_{14} ; N_1 and N_3 .

This analysis was pursued by the calculation of correlations between the CNDO/S eigenvectors. Because of symmetry determined $\sigma - \pi$ separation in the all-proton model, the scalar products between the eigenvectors of this model and those of compounds 1 to 8 were calculated to examine the character-changes of the eigenvectors upon substitution and reduction. By inspection of the CNDO/S eigenvectors it was found that the highest occupied orbitals and the lowest virtual orbitals of (iso)alloxazine do not acquire appreciable density on the methyl or proton substituents. The majority of the eigenvectors can be expressed in an AO basis consisting of the 64 2s and 2p functions corresponding to the 14 ring atoms and the two oxygen atoms in the molecular frame. Scalar products between σ eigenvectors of the all-proton model and vectors derived therefrom by neglecting all hydrogen 1s AO coefficients, show one-to-one correlations within an error of 5% for the eigenvectors corresponding to eigenvalues greater than -18.47 eV (-16.30 eV after Bigelow correction). Similar results were obtained with the structure of compound 1. Therefore, in the calculation of the scalar products between the eigenvectors of two derivatives carrying different substituents in the same ring position (e.g. methyl group versus proton), the AO contributions of both substituents were simply omitted to obtain contracted eigenvectors on the same AO basis. The scalar product between eigenvector j of molecule "a", denoted by $\langle^a\psi_j|$ and eigenvector k of molecule "b", denoted by $^b\psi_k\rangle$, was thus approximated by:

$$\langle a_{\Psi_j} | b_{\Psi_k} \rangle = \left[\sum_{\mu} a_{c_{\mu j}}^2 \right]^{-\frac{1}{2}} \left[\sum_{\nu} b_{c_{\nu k}}^2 \right]^{-\frac{1}{2}} \left[\sum_{\lambda} a_{c_{\lambda j}} \cdot b_{c_{\lambda k}} \right] \quad (5.5)$$

in which $a_{c_{\mu j}}$ denotes the coefficient of the μ -th AO in the j -th MO of molecule "a". Summation runs over all the retained basic functions.

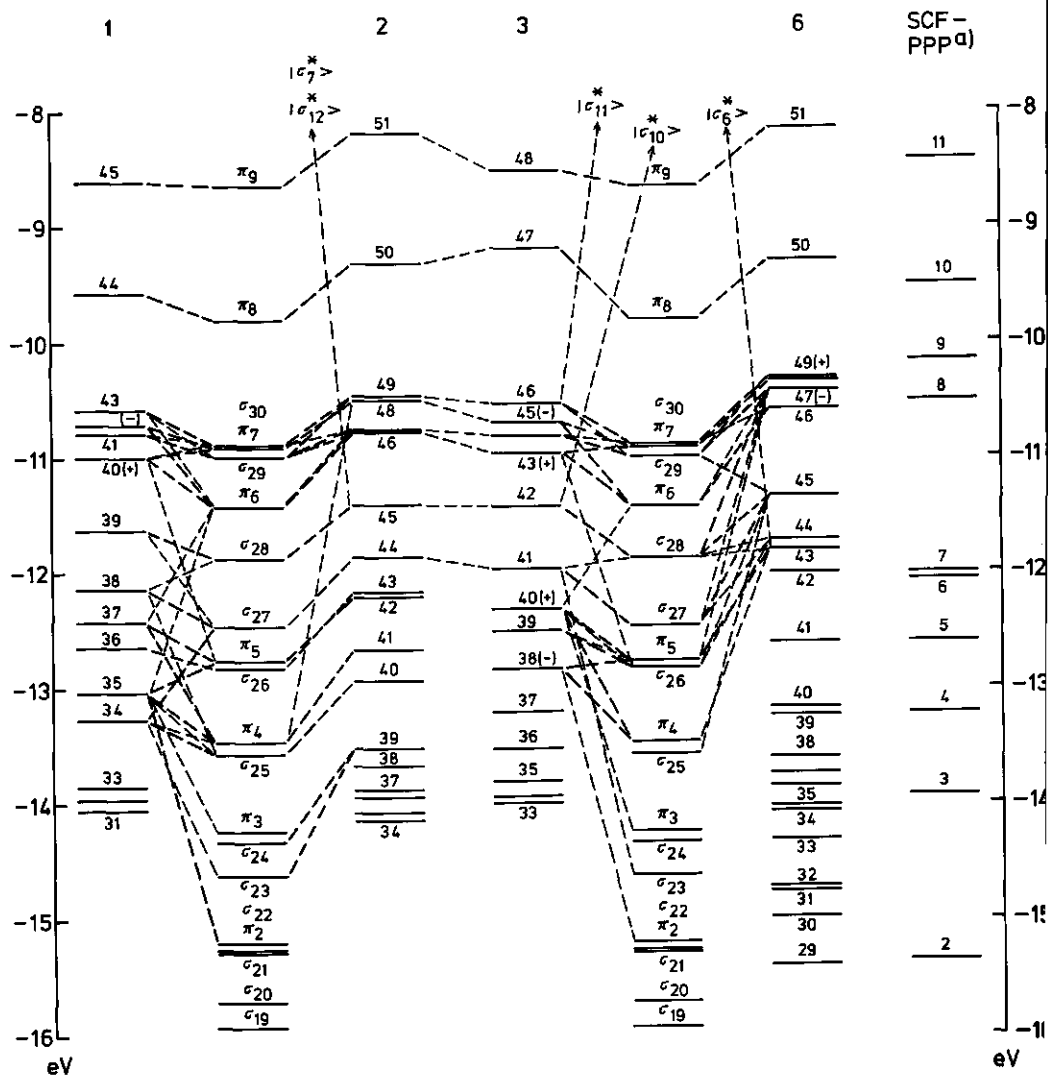


Figure 5.7. Correlation diagram of the CNDO/S eigenvectors of some substituted isoalloxazines with those of the unsubstituted "ideal isoalloxazine" nucleus³⁵. The numbers refer to the compounds given in Scheme 5.1. The scalar products > 0. are indicated by heavy dotted lines. The orbital energies (calculated values) are given in Table 5.1; the scalar products are given in Table 5.2; a) = SCF-PPP eigenvectors obtained by Song^{10,45}.

5.5.1. The influence of substitution

Representative data on the calculated correlations between the orbitals of the all-proton model and those of some oxidized derivatives are given in Fig. 5.7 and Table 5.2. Throughout all calculations, a "staggered" conformation was adopted for the methyl groups. Admixture of other orbitals into the two highest occupied orbitals upon substitution is fully negligible. Even the formal replacement of N_5 by a C - H fragment in compound 6 does not have an appreciable influence on these orbitals which, consequently, retain their benzenoid E_{1g} character. At lower orbital energies, mixing primarily occurs within the π and σ systems separately. Only in case of almost degenerate π and σ orbitals mutual admixture is found, ranging from 5% (compounds 1; 3 - 5) to 14% (compound 2) and 21% (compound 6). Remarkably, compound 3 shows small admixture of the antibonding orbital σ_{11}^* of the all-proton model into its highest non-bonding orbital, labelled 46. The orbital σ_{11}^* is calculated to be localized for 88% on the centers N_1 ; C_2 ; N_3 ; O_{12} and the proton substituent on N_3 , about the same molecular region where orbital 46 is localized.

The results obtained on alloxazine (compound 7) are omitted here for two reasons. First, the calculation yields a large number of small scalar products and, secondly, there is bad agreement of the CNDO/S eigenvalues with the photoelectron spectrum. A correlation diagram cannot be given with these data. Only the two highest occupied alloxazine orbitals can be expressed approximately as linear combinations of π_8 and π_9 of the all-proton model, the minus combination having the highest energy. Both alloxazine orbitals, however, suffer from serious admixture of a large number of other orbitals, both real and virtual. So, also in a theoretical description, alloxazine turns out to be totally different from isoalloxazine.

5.5.2. The influence of reduction

Mutual correlations between orbitals of isoalloxazine in its oxidized and reduced forms, respectively, are of particular interest in connection with the function of the molecule in living organisms, as was denoted before. In first approximation, one expects the two additional electrons, taken up by the molecule upon full reduction to a hypothetical divalent anion, to enter into the lowest unoccupied orbital (LUMO) of the oxidized form. Assuming no conformational change, the only consequence for a SCF-LCAO-MO description within this picture is a change of the Fock matrix elements due to an alteration of the density

TABLE 5.2.

CORRELATIONS BETWEEN THE CMO/S EIGENVECTORS OF OXIDIZED ISOALLOXAZINES.

Compound	Orbital	39 π_9	38 π_8	37 σ_{30}	36 π_7	35 σ_{29}	34 π_6	33 σ_{28}	32 σ_{27}	31 π_5	30 σ_{26}	29 π_4	28 σ_{25}	Other Orbitals	Main Character
1	HOMO-45	.9979													π
	44		-.9987												π
	43			.9613	-.1037	-.1786	.1482								π
	42			.1719	.8608		-.4679								π
	41			-.1959		-.9787									π
	40			-.1049	.5293		.8215			.1273					π
	39						-.9870	.1150							σ
	38						.1342	.9725					.1130		σ
	37						-.1834			.9451		.2215			π
	36						-.1374				-.9902				σ
	35									.2766		-.8732	.1334	.1690 $ \pi_3\rangle + .2788 \pi_2\rangle$	π
	34								.2464			-.1592	-.9231	-.1493 $ \sigma_{23}\rangle$	σ
2	HOMO-51	-.9945													π
	50		-.9957												π
	49			-.9485	.1726	.2201									π
	48			-.1711	-.9677							-.1136			π
	47			-.1860		-.9049	-.3781								π
	46			-.2053		-.3790	.8915								π
	45							.9852							σ
	44							.9742						.1488 $ \sigma_{23}\rangle + .1584 \sigma_7^*\rangle$ +.1047 $ \sigma_{12}^*\rangle$	σ

matrix (cf. eq. (2.14), p. 16) only. Subsequent protonation giving the neutral hydroquinone will be of greater influence, because of the addition of two functions to the AO basis set. Both processes will cause reorganisation but, still a high scalar product between the LUMO of the oxidized form and the HOMO of the reduced form is expectable.

Severe breakdown of a correlation diagram will likely originate from geometry-differences existing between the oxidized and reduced forms of isoalloxazine³⁵⁻³⁹. Contrary to the quinoid form, all 1,5-dihydro-isoalloxazines have a non-planar structure, consisting to a good degree of approximation of two planar parts, bent along the $N_5 - N_{10}$ axis^{38,39}. Two geometries were tested in the calculations on compound 8. The first one (structure A), was based on a derivative³⁸ carrying a bromine atom in position 9 and an acetyl group in position 5, whereas in the second one (structure B), the acetyl group was changed into a hydrogen atom³⁹. Stereo-view computer drawings of these structures, as derived from the published fractional coordinates of the atoms^{38,39}, are given in Fig. 5.8. For structure A, hydrogen atoms were generated at standard bond distances and bond angles⁴⁶ and the bromine atom and acetyl group were replaced by hydrogen atoms at appropriate bond distances without altering the bond angles. In structure B, all hydrogen atoms were determined by X-ray crystallography, restricting alteration to replacement of the bromine atom. Nevertheless, both structures give rise to CNDO/S eigenvalues which do not agree with the photoelectron spectrum, the agreement being particularly bad in case of structure A. After application of the Bigelow correction, the first ionization potentials are found to be too high by 0.94 eV and 0.61 eV for structures A and B, respectively. The difference can be ascribed to a stereochemical difference of the proton at N_5 in structures A and B. Due to bending, the pyrazine ring in the molecule acquires the boat conformation with the N_5 acetyl group in axial position due to steric effects³⁸. Formal replacement of this acetyl group by a hydrogen atom causes large overlap between the hydrogen 1s and the N_5 nitrogen $2p_z$ functions, leading to a bonding orbital and a concomitant decrease of the orbital energy. This creates a protonated π orbital, however, which is a physically unrealistic situation, as confirmed by the real position of the N_5 proton as determined in structure B³⁹. Contrary to the discussion given by Norrestam and Von Glehn³⁹, direct conversion of their fractional into cartesian coordinates undoubtedly shows the N_5 proton to be in equatorial position (Fig. 5.8). The general features of the CNDO/S results, therefore, agree better with the experiment for structure B than for structure A. Moreover, an INDO calculation⁴⁸ on structure A fails to converge,

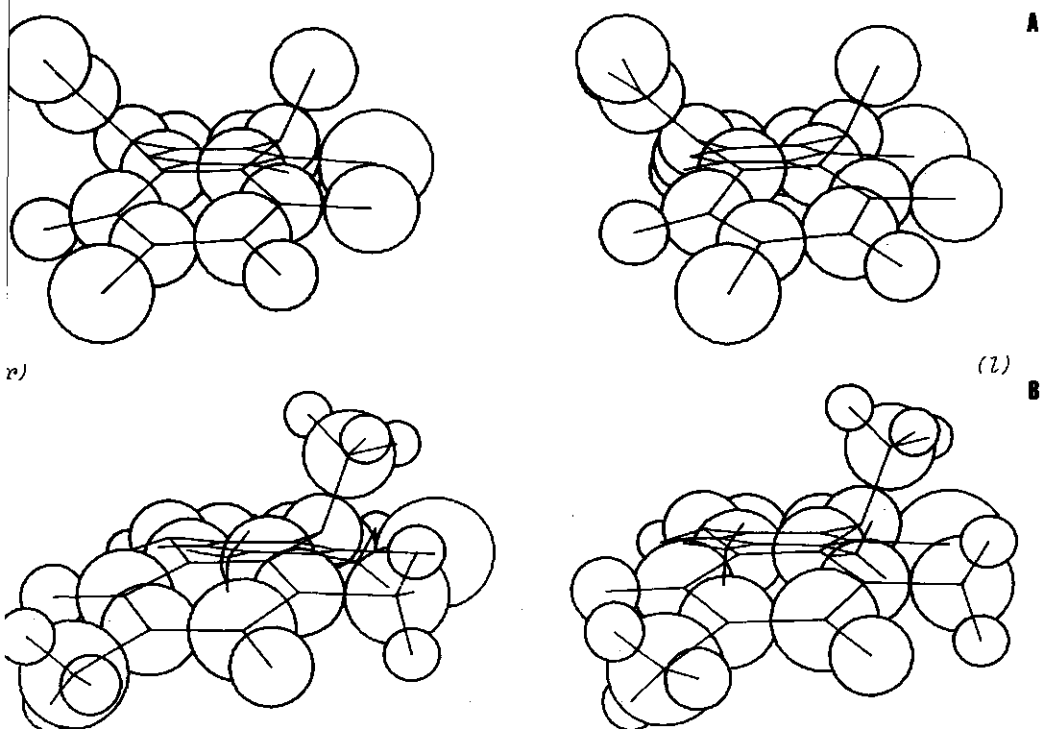


Figure 5.8. Molecular structures of two reduced isoalloxazine derivatives as determined by X-ray crystallography^{38,39}. A: 9-Bromo-5-acetyl-1,3,7,8,10-pentamethyl-1,5-dihydro-isoalloxazine³⁸ (without hydrogen atoms); B: 9-Bromo-1,3,7,8,10-pentamethyl-1,5-dihydro-isoalloxazine³⁹. Reference to these structures in the text is made by A and B, respectively. A stereo view showing the stereochemical difference of the N₅ substituent⁵⁴.

whereas such a calculation on structure B converges normally. However, only a planar system of three condensed rings, as derived from structure B by adjustment of the (4a-5-5a) and (9a-10-10a) bond angles, has a set of eigenvalues which agree as satisfactorily with the experiment as those of the oxidized compounds.

Consequently, the calculations of scalar products gave reasonable correlation diagrams for structure B and a planar geometry only. The results are given in Fig. 5.9 and Table 5.3. Considerable reorganization of the orbitals is found to occur upon reduction, even in case of a planar structure. Presumably, reorganization will also be due to differences in bond distances existing between the oxidized and reduced forms of isoalloxazines³⁶. The highest three occupied orbitals of the reduced form, however, can be assigned to π orbitals, regarding the main character as estimated from the correlation diagram. The HOMO (55) of the reduced form is predominantly a minus linear combination of the HOMO (π_9)

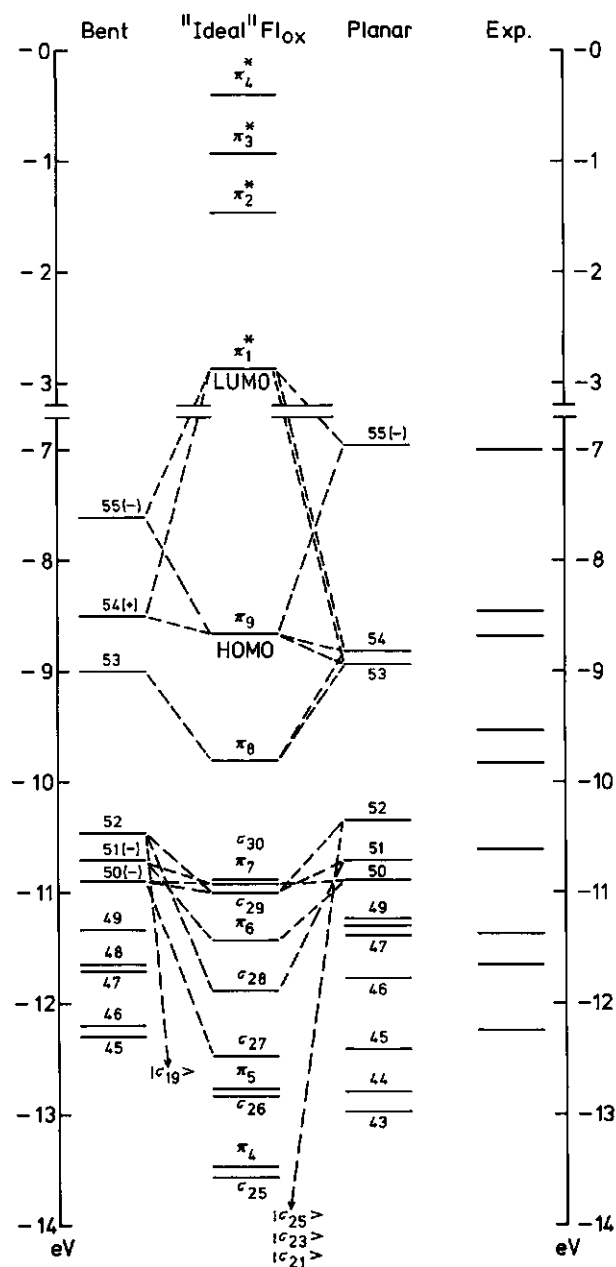


Figure 5.9. Correlation diagram of the CNDO/S eigenvectors of 1,3,7,8,10-pentamethyl-1,5-dihydro-isoalloxazine (8) with those of the unsubstituted "ideal isoalloxazine" nucleus³⁵, denoted by "Fl_{ox}" to indicate the oxidized form. Comparison is made for the bent and planar structures³⁹ and the experimental values (Exp.). Only the scalar products > 0.3 are indicated, the values are given in Table 5.3. The orbital energies (calculated values) are given in Table 5.1.

TABLE 5.3.

CORRELATIONS BETWEEN THE CMO/S EIGENVECTORS OF AN OXIDIZED AND A REDUCED ISOALLOXAZINE.

Orbital	44 π_5	42 π_3	41 π_2	40 π_1	39 π_9	38 π_8	37 σ_{30}	36 π_7	35 σ_{29}	34 π_6	33 σ_{28}	Other Orbitals	Main Character
HOMO=55	-.1450	.1843	.1581	-.7577	.3661			.1815		.1533		Dot product with 3 orbitals >.1	π
54		.1391	.1414	-.4117	-.7277	.1481		-.2687		-.1014		Dot product with 7 orbitals >.1	π
53					.1624	.8868						Dot product with 5 orbitals >.1	π
52								-.1751	-.3853		.5997	[-.3072 $ \sigma_{19}>$; Dot product with 18 other orbitals >.1	π
BENT								.4479		.8209		Dot product with 2 orbitals >.1	π
51							.3559	.2051	-.5067			[-.3077 $ \sigma_{27}>$ - .2223 $ \sigma_{14}>$ +.3058 $ \sigma_4>$; Dot product with 12 other orbitals >.1	π
50													
HOMO=55	.1425	-.1563	-.1525	.8383	-.3770	.1043		-.1100				.1939 $ \pi_5>$	π
54			.1681	-.3446	-.6574	.5438		-.2743				-.1243 $ \pi_4>$	π
53				.1560	.4856	.8256		.1496					π
PLANAR													
52					.1050	.1632		-.1632	.7595	-.1063	-.1981	Dot product with 10 orbitals >.1	π
51								-.1412	.8910	.1706	-.2999	Dot product with 3 orbitals >.1	π
50								.4873	.1631	-.8419			π

Row numbers: Eigenvectors of compound 8 in the bent and planar molecular conformations³⁹. For further details: see annotations to Table 5.2.

and LUMO (π_1^*) of the (oxidized) all-proton model, for both the non-planar (B) and planar structures. The orbitals π_8 and π_9 mix heavily upon reduction to give the orbitals labelled 53 and 54. Especially in case of a planar structure, these orbitals differ only by 0.12 eV in energy, giving strong mixture and, consequently, complete breakdown of benzenoid E_{1g} character. Due to admixture of π_1^* , the orbitals 53 and 54 also acquire higher density outside the benzene subnucleus as compared to the oxidized form. Admixture of other orbitals into 53, 54 and 55 is limited to 29% in case of the bent structure and to 15% for the planar conformation. The redox properties of the molecule, therefore, are governed mainly by π_8 , π_9 and π_1^* .

Similar results were obtained in a calculation of the correlation diagram with respect to the eigenvectors of compound 2.

5.6. DISCUSSION

Comparison of the isoalloxazine photoelectron spectra with the results of the applied theoretical methods⁴⁻¹⁷, shows that none of these methods, including the present CNDO/S calculation, is capable of predicting the orbital energies accurately. Reviewing the available data⁴⁻¹⁷, we will skirt the Extended Hückel method because of its extremely poor agreement with the experiment⁴⁻⁷.

The SCF-PPP method predicts the experimental π ionization potentials surprisingly well for both the oxidized and reduced forms of isoalloxazine. There is some dependence on the particular parameterization chosen, due to which Song's results^{10,45} agree better with the experiment than those of Grabe⁸, who predicts the π ionization energies systematically too low. Regarding the complexity of the photoelectron spectra caused by (near) degeneracy of π , n and σ orbitals, however, a π electron calculation like SCF-PPP cannot serve as a guide to spectral assignment unless at least comparison with all-valence electron calculations is made.

The power of the CNDO/2 method^{7,16} to predict photoelectron spectra is extremely poor. For this reason we omitted our own CNDO/2 results, which agree with those of Song⁷ as far as the eigenvalues are concerned. The eigenvectors were found to be different, presumably due to geometry differences (Song had to assume a molecular geometry by the lack of crystallographic data).

Before the application of corrections, the results from CNDO/S and INDO calculations are rather similar, except for random differences in energy up to ± 2 eV for resembling eigenvectors. This leads to differences in level ordering

between the two methods. Both methods, however, predict ionization potentials which are systematically too high and orbital energy differences which are systematically too large. The Bigelow formulas^{22,23} partly compensate this error.

The MINDO/3 calculation, which was only applied to oxidized isoalloxazine derivatives¹⁷, yields π orbital energies which agree perfectly with the experiment, the SCF-PPP method and the corrected CNDO/S π orbital energies. Differences are as small as a few tenth's of an eV. Conversely, the calculated n and σ orbital energies are systematically too high. The highest n orbital is even predicted to be quasi-degenerate with the highest occupied π orbital. According to the MINDO/3 method, crowding of orbitals in the -8 to -12 eV energy region is that large that the corresponding photoelectron spectrum should be completely structureless. This is in contrast with the experiment.

Thus, only π orbitals are predicted satisfactorily by the SCF-PPP, the (corrected²², eq. (5.1), p. 54) CNDO/S and the MINDO/3 methods, the only reservation being our lack of knowledge of the MINDO/3 eigenvectors. Apart from the necessity to correct the CNDO/S eigenvalues, Del Bene and Jaffé²⁸ state correctly that their CNDO/S method includes the simpler π electron theory as a special case. However, it would be an exaggeration to say that for economic reasons one should confine oneself to π electron calculations. Firstly, this analysis is restricted to orbital energies exclusively and, secondly, awareness of the intrinsic errors of the NDO methods may preclude wrong interpretations.

Even when the Bigelow formula²² (eq. (5.1), p. 54) is applied, the CNDO/S calculations on isoalloxazines invariably predict the n orbital energies about 1 eV too low. Conversely, the correction method²² adjusts the π orbital energies satisfactorily. This can be ascribed to the fact that the n orbitals are spatially more localized than the π orbitals, due to which calculational errors may accumulate in the former orbitals. Apart from the intrinsic errors in any particular SCF-calculation, the neglect of the electronic correlation and reorganization cause such errors⁴¹. The correlation error originates from the multiplication of probability distributions of electrons in any SCF-calculation, i.e. the probability of finding two electrons in the same region of space is given equal statistical weight as finding them largely separated⁴⁹. The major contribution to this error originates from two electrons of different spin occupying the same spatial orbital⁴⁹. Because the electronic repulsion will tend to keep such electrons apart, it is found that the repulsion integrals are generally taken too large in an *ab initio* SCF-calculation⁴⁹. In a semi-empirical calculation like CNDO/S, the parameterization only may compensate this error in an average way⁴⁹,

so certain orbitals still may contain residual errors. However, neglect of correlation destabilizes the orbitals due to an over-estimation of the electronic repulsion. Therefore, the error in the isoalloxazine n orbital calculations must be due to the neglect of reorganization and/or intrinsic shortcomings of the calculation. Obviously, the reorganization will be important because a localized hole is created by ionizing an electron from the n orbitals. De Bruijn⁵⁰ has pointed out that an important intrinsic error of all NDO-theories arises from incorrect resonance integrals. The one-center integrals $H_{\mu\mu}^C$ and the two-center integrals $H_{\mu\nu}^C$ (μ and ν nearest neighbours, cf. eq. (2.21), p. 17) were shown to be too negative, which is partly compensated by an opposite error in $H_{\mu\nu}^C$ for second neighbours. So the diagonal elements of the core hamiltonian⁵¹:

$$H_{ii}^C = \sum_{\mu,\nu} c_{\mu i} c_{\nu i} H_{\mu\nu}^C \quad (5.6)$$

are too negative. Because $\sum_{\mu,\nu} c_{\mu i} c_{\nu i}$ is increasingly positive towards lower bonding MO's, the error in H_{ii}^C increases in that direction, causing a spurious divergence in the orbital level scheme. This explains the success of the correction methods by Bigelow^{22,23} which compress the divergence. In case of a deviation from an uniform charge distribution, these errors increase appreciably⁵⁰. This situation is encountered in case of isoalloxazine. The calculations predict a large dipole moment due to charge differences on the carbonyl groups and, particularly, in the n orbitals localized thereon. Typical values range from 6.1 D (compound 8) to 10.7 D (compound 6).

Probably the three-fold degeneracy in the isoalloxazine orbital level scheme in the oxidized state at -9.6 eV is responsible for some of the molecule's peculiar properties such as the pronounced solvent influence on the $S_0 \rightarrow S_2$ electronic transition^{1,52}. Based on its red shift observed on going to polar solvents assignment to an intramolecular charge transfer transition is made⁵², whereas the theory predicts a $\pi\pi^*$ transition at the corresponding wavelength¹⁰. It should be realized, however, that singly excited configurations which most likely contribute considerably to the S_2 state in a configuration interaction scheme, will arise from the concerned set of degenerate n and π orbitals. Such configurations may be almost degenerate too, depending on the values of Coulomb and Exchange integrals. One of these configurations surely will be a $\pi\pi^*$ transition carrying large oscillator strength, but due to the admixture of $n\pi^*$ character and intramolecular charge transfer character (owing to the spatial separation of n and π orbitals), a strange composite S_2 state is expected. In this respect strong perturbations like H-bond formation cannot be described properly

in a π electron theoretical framework as was done recently^{14,15}.

The small admixture of antibonding character into the highest non-bonding MO of compound 3 (cf. Fig. 5.7 and Table 5.2) provides another example of the considerable influence of small perturbations. In this respect, we do not expect the thermal instability of compounds 3 and 4 to be a fortuity, but to originate from electronic properties.

Comparison of the theory (of which the intrinsic errors are known) and experiment, shows the reduced isalloxazine derivative (compound 8) to have a planar structure with sp^2 -hybridization on N_5 and N_{10} . This is at variance with the bent structure found by X-ray crystallography^{38,39} (cf. Fig. 5.8) and by 1H -NMR coalescence spectroscopy carried out in solution^{48,53}. Crystallography shows the presence of two enantiomers being each others mirror image, which occur in a 1 : 1 molar ratio in the solid state^{36,38,39}. So, if the bent structure is the most stable one, a plot of the total energy of the molecule versus the dihedral bending angle gives a double minimum potential energy curve. This curve will be perfectly symmetrical with respect to a dihedral angle of 180° at which a maximum occurs, constituting a "transition state" of energy ΔU^\ddagger relative to the minima. Suppose the minima to be localized at dihedral angles of $180^\circ \pm \alpha$. Typical values³⁶ range from $\alpha = 36^\circ$ to $\alpha = 9^\circ$ (the latter value refers to a protein-bound isalloxazine). According to Tauscher *et al.*⁵³, ΔU^\ddagger should be about 45 kJ mole^{-1} . Due to mirror symmetry, both enantiomers will have the same orbital energies, hence they will have the same photoelectron spectrum and any change in their thermal equilibrium, therefore, will be unobservable. So, except for two details, we adopt the interconversion scheme for the enantiomers as proposed by Tauscher *et al.*⁵³ where both ring-inversion and N-inversion in the pyrazine ring occurs. First, we reject the proposal that only N_5 should undergo inversion. The absence of N_{10} -inversion would cause interchange between axial and equatorial positions for the N_{10} methyl substituent, giving appreciably different photoelectron spectra for both enantiomers. If this were the case, the spectral bands would have been broadened considerably and the spectrum would have been temperature dependent, contrary to the actual measurements. The second exception is the high probability of an all-coplanar transition state, regarding the agreement between the experiment and the calculation on such a conformation. Consequently, if α and ΔU^\ddagger are of the order of magnitude as quoted before, the population of the transition state is negligible under our experimental conditions (Boltzmann factor of 1.4×10^{-5} at 450 K). In that case the photoelectron spectrum should correspond to an averaged bent structure, which is highly improbable by virtue

of the foregoing discussion. If α is assumed to be the same and ΔU^\ddagger is such that the transition state is appreciably populated (i.e. at least one order of magnitude smaller), the potential energy curve will allow such a large root mean square deviation $\delta\alpha$ in α , that only broad structureless photoelectron bands would be observed, contrary to the measurements.

Therefore, the actual potential energy curve must contain one single minimum at 180° . The CNDO/S calculations give total energies which are in agreement with this due to a decrease in nuclear-nuclear repulsion, which exceeds the increase of the electronic energy on going to a planar conformation. However, the latter argument cannot be used as evidence for a planar structure regarding the failures of the CNDO/S method⁵⁰. On the other hand, we reject also the argument referring to an oversimplified π electron concept that, due to "anti-aromaticity" the reduced form of isoalloxazine should be bent⁵³.

Now it should be realized that, *under the present experimental conditions only, we are dealing with truly isolated molecules*. It is, therefore, very likely that environmental forces govern the molecular conformation of the reduced isoalloxazine molecule. This is supported by the presence of hydrogen bonded dimers in the solid state³⁹ and it may explain the variety of values³⁶ found for the dihedral angle α . The high values of ΔU^\ddagger , obtained by application of the absolute rate theory⁵³, refer to a solvated molecule carrying large substituents. Ascribing these properties to isolated molecules is erroneous.

The dependence of the energy of the highest occupied orbital of a reduced isoalloxazine on the molecular conformation, which in turn is governed by external forces, deserves special attention. It is this "valence-orbital" which has to acquire and to lose electrons in the redox reactions, in which the isoalloxazine nucleus participates in biochemical processes. Thus, the apoprotein may influence the "valence-orbital" energy by interaction and, concomitantly, the redox potential of an isoalloxazine prosthetic group associated with it⁵³. In addition to protonation, such interactions may explain the large variety of redox potentials of flavoproteins and their further quantification may provide insight into the structure-function relationships in these proteins.

REFERENCES AND NOTES

- 1 Cf. Chapter 3 or: J.K. Eweg, F. Müller, A.J.W.G. Visser, C. Veeger, D. Bebe-laar and J.D.W. van Voorst, *Photochem. Photobiol.* 30 (1979) 463.
- 2 P.S. Song, M. Sun, A. Koziolowa and J. Koziol, *J. Amer. Chem. Soc.* 96 (1974) 4319.
- 3 J. Koziol and A. Koziolowa, in: *Flavins and Flavoproteins*, Physicochemical

- Properties and Function, Proc. Int. Meeting, ed. W. Ostrowsky (Polish Scientific Publishers, Warsaw and Cracow (1977) 81).
- 4 B. Pullman and A. Pullman, Proc. Natl. Acad. Sci. USA. 45 (1959) 136.
- 5 G. Karreman, Bull. Math. Biophys. 23 (1961) 55.
- 6 R. Norrestam, P. Kierkegaard, B. Stensland and L. Torbjörnsson, Chem. Comm. (1969) 1250.
- 7 P.S. Song, J. Phys. Chem. 72 (1969) 536.
- 8 B. Grabe, Biopolym. Symp. 1 (1964) 283, *ibid.*, Acta Chem. Scand. 26 (1972) 4084.
- 9 J.L. Fox, K. Nishimoto, L.S. Forster and S.P. Laberge, Biochim. Biophys. Acta 109 (1965) 626, *ibid.* 136 (1967) 544.
- 10 P.S. Song, Int. J. Quantum Chem. 2 (1968) 463, *ibid.* 3 (1969) 303.
- 11 M. Sun, T.A. Moore and P.S. Song, J. Amer. Chem. Soc. 94 (1972) 1730.
- 12 P.S. Song, T.A. Moore and W.E. Kurtin, Z. für Naturf. 27b (1972) 1011.
- 13 M. von Glehn, Thesis, University of Stockholm, Sweden, Chem. Commun. XI (1971).
- 14 K. Nakano, T. Sugimoto and H. Suzuki, J. Phys. Soc. Japan 45 (1978) 236.
- 15 K. Nishimoto, Y. Wanatabe and K. Yagi, Biochim. Biophys. Acta 526 (1978) 34.
- 16 B. Grabe, Acta Chem. Scand. A28 (1974) 363.
- 17 M.F. Teitell, S.-H. Suck and J.L. Fox, Theoret. Chim. Acta (Berlin) 60 (1981) 127, J.L. Fox, Personal Communication.
- 18 K. Fukui: Theory of Orientation and Stereoselection (Springer, Heidelberg, 1970).
- 19 M. Sun and P.S. Song, Biochemistry 12 (1973) 4663, *ibid.*, Jerusalem Symp. Quantum Chem. Biochem. 6 (1974) 407.
- 20 Cf. Chapter 4 or: J.K. Eweg, F. Müller, D. Bebelaar and J.D.W. van Voorst, Photochem. Photobiol. (1980) in press.
- 21 A.J.W.G. Visser and F. Müller, Helv. Chim. Acta 62 (1979) 593.
- 22 R.W. Bigelow, J. Chem. Phys. 66 (1977) 4241.
- 23 R.W. Bigelow and G.E. Johnson, J. Chem. Phys. 66 (1977) 4861.
- 24 H. van Dam and A. Oskam, J. Electron Spectrosc. Relat. Phenom. 13 (1978) 273.
- 25 B.J.M. Neijzen, Thesis, Free University of Amsterdam, Amsterdam, The Netherlands (1978).
- 26 W.A. Mellink, Thesis, University of Groningen, Groningen, The Netherlands (1978).
- 27 T. Koopmans, Physica (Utrecht) 1 (1934) 104.
- 28 J. Del Bene and H.H. Jaffé, J. Chem. Phys. 48 (1968) 1807.
- 29 G. Kuehnlenz and H.H. Jaffé, J. Chem. Phys. 58 (1973) 2238.
- 30 K. Nishimoto and N. Mataga, Z. Phys. Chem. (Frankfurt am Main) 12 (1957) 335.
- 31 R.L. Ellis, G. Kuehnlenz and H.H. Jaffé, Theoret. Chim. Acta (Berlin) 26 (1972) 131.
- 32 N.O. Lipari and C.B. Duke, J. Chem. Phys. 63 (1975) 1748.
- 33 F.O. Ellison, J. Chem. Phys. 61 (1974) 507.
- 34 M.J.M. Beerlage and D. Feil, J. Electron Spectrosc. Relat. Phenom. 12 (1977) 161.
- 35 M. Wang and C.J. Fritchie Jr., Acta Cryst. B29 (1973) 2040.
- 36 M. Leijonmarck, Thesis, University of Stockholm, Sweden, Chem. Commun. VIII (1977).
- 37 R. Norrestam and B. Stensland, Acta Cryst. B28 (1972) 440.
- 38 P.E. Werner and O. Rönquist, Acta Chem. Scand., 24 (1970) 997.
- 39 R. Norrestam and M. von Glehn, Acta Cryst. B28 (1972) 434.
- 40 A. Schweig and W. Thiel, J. Electron Spectrosc. Relat. Phenom. 3 (1974) 27, *ibid.*, J. Chem. Phys. 60 (1974) 951.
- 41 J.W. Rabalais: Principles of Ultraviolet Photoelectron Spectroscopy (Wiley, London, 1977).
- 42 F.A. Cotton: Chemical Applications of Group Theory (Wiley, London, 1971).
- 43 R. Hoffmann, A. Imamura and W. Hehre, J. Amer. Chem. Soc. 90 (1968) 1499.

- 44 R. Hoffmann, Acc. Chem. Res. 4 (1971) 1.
- 45 P.S. Song, Personal Communication.
- 46 L.E. Sutton: Tables of Interatomic Distances (The Chemical Society, London, 1958).
- 47 A. Carrington and A.D. McLachlan: Introduction to Magnetic Resonance (Harper and Row, London, 1967).
- 48 C.G. van Schagen and F. Müller, Helv. Chim. Acta 63 (1980) 2187, *ibid.* Eur. J. Biochem. 120 (1981) 33.
- 49 R.G. Parr: The Quantum Theory of Molecular Electronic Structure (Benjamin, Reading, Massachusetts, USA, 1972).
- 50 S. de Bruijn, Chem. Phys. Letters 54 (1978) 399, *ibid.*, Personal Communication.
- 51 J.A. Pople and D.L. Beveridge: Approximate Molecular Orbital Theory (McGraw-Hill, New York, N.Y., USA, 1970).
- 52 G.R. Penzer and G.K. Radda, Quart. Rev. Biophys. 21 (1967) 43.
- 53 L. Tauscher, S. Ghisla and P. Hemmerich, Helv. Chim. Acta 56 (1973) 630.
- 54 Stereo picture can be observed skew-eyed with some exercise. For observation with a viewer, photocopy and reverse left and right pictures.

ANOMALOUS INTRAMOLECULAR HYDROGEN BOND IN 10-HYDROXYALKYL ISOALLOXAZINES AS REVEALED BY PHOTOELECTRON SPECTROSCOPY, AND THE IMPLICATIONS FOR OPTICAL SPECTRA

1. INTRODUCTION

In our current research on the isoalloxazine electronic structure¹⁻³, two important aspects were not elaborated. First, the discovery of an anomalous long fluorescence lifetime of 3-methyl-10-(γ -hydroxypropyl)-isoalloxazine in the vapour phase². This phenomenon was explained assuming the formation of an intramolecular complex in the vapour phase in which the hydroxyl group of the N₁₀ side-chain should be hydrogen-bonded towards the N₁ atom² (cf. Scheme 6.1, below). Since the N₁ lone pair contributes considerably to a MO, which can be identified in the isoalloxazine photoelectron spectrum, it should be possible to verify the foregoing proposal by photoelectron spectroscopy. Additionally, it may be investigated whether CNDO/S, which gives a fairly good description of the isoalloxazine orbital structure³, can be extended to this more complicated system.

The second aspect is the extension of the CNDO/S method to the calculation of excited states in order to correlate the available optical spectra^{1,2} and photoelectron spectra³ of a variety of isoalloxazines. Regarding a CNDO/S-CI procedure as a two-stage process, photoelectron spectroscopy constitutes a powerful experimental check on the first stage, the ground state orbital calculation. This check should preferably be made before proceeding with the second stage, the calculation of excited states by CI between configurations arising from that orbital structure. Previously, such an approach proved to be very useful in the interpretation of the glyoxal optical spectrum⁴.

The combination of both aspects is of particular interest. If photoelectron spectroscopy confirms the existence of the intramolecularly H-bonded complex, the experimental data on its electronic transitions in the isolated (vapour phase!) state² can be supplemented with those on its orbital structure. Closer resemblance between experimental conditions and those tacitly assumed in MO calculations cannot be achieved, an excellent opportunity to apply the stepwise

procedure outlined above to both complexed and uncomplexed isoalloxazines. Thus the relatively volatile⁵ 10-hydroxyalkyl-isoalloxazines may serve as a model to examine solvent influences on the isoalloxazine optical spectrum^{1,2}. At the same time, they allow for a photoelectron spectroscopic study of a H-bond in an isolated molecule in the vapour phase which, up till now, was only performed on smaller molecules^{6,7}. Particularly, the solvatochromy of the isoalloxazine $S_0 \rightarrow S_2$ electronic transition is not satisfactorily explained, as we discussed before³. It may be anticipated that the MO which is involved in H-bond formation, also gives rise to singly excited singlet configurations which contribute significantly to the S_2 state³. Therefore, the combination of photoelectron and optical spectral data is of value for a better understanding of the latter, and it may reveal the reliability of CNDO/S. This should be analyzed before applying the method to models of protein-bound isoalloxazine in flavoproteins, the molecule's natural environment which, obviously, is not accessible to photoelectron spectroscopy. In this environment the molecule is known to be hydrogen-bonded⁸⁻¹ to the apoprotein.

6.2. EXPERIMENTAL AND THEORETICAL SECTION

The 10-(hydroxyalkyl)-isoalloxazine derivatives were synthesized according to the methods published elsewhere^{1,2,5}. Photoelectron spectra were measured using equipment and procedures as described previously³. Orbital energies and correlation diagrams were calculated by the CNDO/S method, including the appropriate approximations and corrections used before^{3,13}. The inclusion of CI for the calculation of spectral properties was done in two different ways with respect to the approximations used in the determination of the two-electron integrals (cf. eq.(2.7) and (2.8), p. 15 and Table 2.3, p. 19):

$$(ij|kl) = \sum_{\mu\nu\lambda\sigma} c_{\mu i} c_{\nu j} c_{\lambda k} c_{\sigma l} (\mu\nu|\lambda\sigma) \quad (6.1)$$

and the transition moments:

$$m_{ij} = e \sum_{\mu\nu} c_{\mu i} c_{\nu j} (\mu | \mathbf{r}_p | \nu) \quad (6.2)$$

In (6.1) we adopted the notation of Pariser¹⁴, $c_{\mu i}$ represents the coefficient of AO μ in MO i and in (6.2) e represents the electronic charge and \mathbf{r}_p the position vector of the p -th electron.

In the first approach, we followed exactly the CNDO/S-CI scheme of Del Bene and Jaffé¹⁵, i.e. we applied the strict ZDO approximation (cf. eq. (2.19), p. 17 to all valence electrons in the evaluation of (6.1). The only surviving integral on the right hand side of (6.1) are those of the type $(\mu\mu|\lambda\lambda)$, being approximate in turn by the Nishimoto-Mataga formula¹⁶. Similarly, the only terms to be retained in (6.2) are those of the type¹⁴ $(\mu|\mathbf{r}_p|\mu)$.

In the second approach, we relaxed the ZDO approximation in the evaluation of (6.1) and (6.2) in view of its inadequacy noted by several investiga-

ors^{15,17-19}. In abandoning the ZDO approximation, we achieve a situation in which the singlet and triplet arising from the same $n\pi^*$ configuration are no longer degenerate and the m_{ij} for $i=n$ and $j=\pi^*$, or *vice versa*, are no longer zero¹⁷. Hence, we retained in the evaluation of (6.1) the two-electron one-center integrals which are also retained in the INDO approximation²⁰. In this way, our method becomes similar to that of Ridley and Zerner¹⁹. In (6.2) we similarly included the one-center terms analogous to Ellis *et al.*¹⁷.

Hence, the integrals in (6.1) were extended with the one-center terms of the type:

$$\begin{aligned}(ss|ss) &= (ss|xx) = F^0 = \gamma_{AA} \\(sx|sx) &= G^1/3 \\(xy|xy) &= 3F^2/25 \\(xx|xx) &= F^0 + 4F^2/25 \\(xx|yy) &= F^0 - 2F^2/25\end{aligned}\tag{6.3}$$

and similar expressions for $(ss|yy)$, etc.

The values of the Slater-Condon parameters F^2 and G^1 are given by²⁰:

$$\begin{aligned}\text{C: } F^2 &= 4.73 \text{ eV; } G^1 = 7.28 \text{ eV} \\ \text{N: } F^2 &= 5.96 \text{ eV; } G^1 = 9.42 \text{ eV} \\ \text{O: } F^2 &= 7.25 \text{ eV; } G^1 = 11.82 \text{ eV} \\ \text{F: } F^2 &= 8.59 \text{ eV; } G^1 = 14.48 \text{ eV}\end{aligned}\tag{6.4}$$

The integrals in (6.2) were extended with the one-center terms¹⁷ of the type:

$$(2s|ex|2p_x) = 5ea_0/2\zeta\sqrt{3}\tag{6.5}$$

in which e represents the electronic charge, a_0 the Bohr radius and ζ the Slater-exponent (p. 27 of ref. 20).

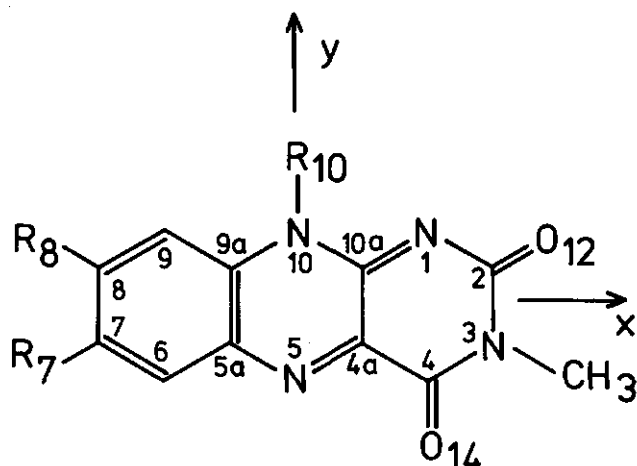
Since the agreement between the photoelectron spectra and CNDO/S orbitals was reasonably good³, we did no further reparameterization like Ridley and Zerner¹⁹. For the same reason, we performed the INDO/S-CI calculations directly on configurations arising from the CNDO/S orbitals without a recalculation of the ground state and MO structure within the new approximations made. This was done using Pople's formulas²¹ (Table 2.3, p.19) bearing in mind that the Fock matrix F is no longer diagonal due to the change in the level of approximation. Therefore, the CI-matrix elements 2^2F_{ki} which connect the ground state Ψ_0 with the excited configurations $\Psi_{i \rightarrow k}$ become non-vanishing, leading to a breakdown of Brillouin's theorem²¹ (cf. Section 2.5.3, p.19). However, for the isoalloxazines calculated, the admixture of excited configurations into the ground state resulted in changes in total energy of ~ 1 eV (~ 300 ppm of the total energy), ultimately, a negligible amount. The effect was only important for the transition energies. Only singly excited configurations were used in the CI-procedures.

6.3. RESULTS

6.3.1. Photoelectron spectra and orbital structure

The theoretical model used to account for hydrogen bond formation towards

N_1 of the isoalloxazine molecule (cf. Scheme 6.1) consisted of a super-molecule description of a complex of 3,10-dimethyl-isoalloxazine (Compound 4, Scheme 6.1)



Scheme 6.1. Isoalloxazine derivatives used:

- 1: $R_7 = R_8 = H$; $R_{10} = n-C_4H_9$; 3-methyl-10-(*n*-butyl)isoalloxazine.
- 2: $R_7 = R_8 = H$; $R_{10} = n-C_3H_6OH$; 3-methyl-10-(γ -hydroxypropyl)isoalloxazine.
- 3: $R_7 = R_8 = H$; $R_{10} = n-C_2H_4OH$; 3-methyl-10-(β -hydroxyethyl)isoalloxazine.
- 4: $R_7 = R_8 = H$; $R_{10} = CH_3$; 3,10-dimethylisoalloxazine.
- 5: $R_7 = R_8 = R_{10} = CH_3$; 3,7,8,10-tetramethylisoalloxazine (3-methyl-lumiflavin).
- 6: $R_7 = R_8 = CH_3$; $R_{10} = n-C_{18}H_{37}$; 3,7,8-trimethyl-10-*n*-octadecylisoalloxazine.

and methanol. The isoalloxazine part of the complex was identical to that used in previous calculations³ and the methanol molecular structure was taken from standard tables²². The $C_m-O_m-H_m$ plane of the methanol moiety was taken to be coincident with the isoalloxazine molecular plane, the atoms N_1 (isoalloxazine)- H_m-O_m were put on a straight line in that plane having an angle of 120° with the $C_{10a}-N_1$ bond of isoalloxazine, and the methanol methyl group was bent away from the isoalloxazine N_{10} methyl group (i.e. the $(C_m-O_m-H_m; H_m-N_1-C_2)$ dihedral angle was zero). The hydrogen bond length H_m-N_1 was varied from 10 Å (1 nm) to 1 Å (0.1 nm). At 10 Å (1 nm) distance no mutual interactions were found either in the orbital energies or in the orbital correlations. At ~ 3.5 Å (0.35 nm) distance mutual interactions in the complex became apparent and at 1 Å (0.1 nm) we ended up with the correlation diagram given in Fig. 6.1 (calculated). The short distance was deliberately chosen to obtain appreciable effects. Values of ion-

TABLE 6.1.
EXPERIMENTAL AND CALCULATED^{a)} IONIZATION POTENTIALS OF N₁₀-SUBSTITUTED ISOALLOXAZINES.

COMPOUND 1				COMPOUND 2				COMPOUND 3			
Exp. ^{b)}	No. ^{c)}	Calc. ^{d)}	Ass. ^{e)}	Exp.	No.	Calc.	Ass.	Exp.	No.	Calc.	Ass.
8.28	45	8.62	π	6.75	52	6.60	σ^*	7.00	f)	f)	σ^*
	44	9.58	π	8.48	51	8.86	π	9.01			π
9.42	43	10.58	n		50	9.37	g)				
	41	10.79	n		49	9.70	π				
10.34	42	10.71	π	9.50	48	10.50	n+ π	9.55			π
10.83	40	11.00	π		46	11.10	m ^{h)}				m ^{h)}
11.91	39	11.63	σ	10.50	47	10.89	π +n	10.21			π
	38	12.14	σ	10.85	45	11.24	π +n	10.92			π
12.67				11.92				12.01			
13.10											

a) Calculated ionization potentials corrected according to Bigelow as previously^{3,13}; b) Experimental value (eV); c) Number of calculated orbital counted up from the lowest occupied orbital = 1; d) Calculated value (eV); e) Assignment; f) Calculation as for compound 2; g) Artefact in the calculation (cf. text for explanation); h) Mixed.

Two remarkable features were found. First, the calculated ionization potentials of methanol deviate from their experimental values^{23,24} by a few eV and, secondly, the super-molecule orbitals labelled 50 and 52 (Fig. 6.1) behave very strangely. Regarding the character calculated for the methanol orbitals 6 and 7 (Fig. 6.1), however, their order and AO parentage was found to agree with earlier experimental²³ and theoretical²⁴ data. Accordingly, orbital 7 can be assigned to the 2a" (n_o) orbital²³. It consists mainly of the O_m ($2p_z$) and C_m ($2p_z$) AO's in the same ratio as calculated by Dewar and Worley²⁴. CNDO/S calculates it (after appropriate corrections for photoelectron spectroscopy^{3,13}) only 1.87 eV too low (experimental value^{23,24}: -10.85 eV). It is a π orbital in our super-molecule. Similarly, orbital 6 can be identified with the 7a' orbital²³ of σ_{C-H} character, calculated 1.38 eV too low (experimental value^{23,24}: -12.37 eV).

We initially considered the behaviour of the super-molecule orbitals 50 and 52 (Fig. 6.1) to be typical CNDO/S errors as described by De Bruijn²⁵. Both arise from strong anti-bonding interactions. Orbital 50 is produced by perturbation of the isoalloxazine orbital 32 which is localized on the N₁₀ methyl group, N₁₀ itself and the C₂-O₁₂ carbonyl group. When the methanol OH group approaches the N₁₀ methyl group too closely, spurious "steric" interactions cause calculational errors which is a well-known property of the CNDO meth-

TABLE 6.2.
CORRELATIONS BETWEEN THE CNDO/S EIGENVECTORS OF A 3,10-DIMETHYL-ISOALLOXAZINE - METHANOL COMPLEX AND THOSE OF THE PARENT MOLECULES.

Super- molecule orbital	45	44	43	42	41	40	39	38	37	36	35	Methanol orbital 7	6	Other isalloxazine orbitals	Other methanol orbitals
52			.5220	.1111			-.1839	.3916		.1398		.3150		Dot product with 6 orbitals >.1 and with 3 other orbitals >.1	-.1032 3> -.2381 2> -.2477 5*>
51	-.9638														
50 [†]	-.2056	.5579						.1077			-.1162	-.1433		+ .3230 32> and with 5 other orbitals >.1	Dot product with 7 orbitals >.1
49	.8258													Dot product with 4 orbitals >.1	Dot product with 4 orbitals >.1
48			-.3939	.2952	.6705	-.1064	-.1540	.1390				.2042	.1969		
47			.2915	-.7727	.5193	.1946									
46			-.4545	-.4491	-.4709	-.3301	-.2670	.2876		.1103		.1245	.1263		
45			.2944	.2683		-.8439		-.1048				.1246			
44			-.1486				.8640	.4595							+ .1142 4>
43			-.1818	.1354		-.3119	-.1459		-.2781			-.4440		-.1516 32>	-.1085 1> -.3881 4> -.3812 2*> +.3530 3*> +.1063 4>
42								-.1577	-.9252	.1376	-.1265	.1284			
41							.1124	-.4031	.1860	.8527			.1057		
40								.1774	-.1319	.2459	.8885			-.1741 34> +.1359 32>	
39			.1005					-.1262	.3011	.2460	-.3276			-.7916 34> +.2237 33> -.1038 31>	

Column numbers: Eigenvectors of 3,10-dimethyl-isoalloxazine (4) and methanol; Row numbers: Eigenvectors of the complex; Numbers are counted up from the lowest occupied CNDO/S orbital; †: orbital 50 is an artefact in the calculation (cf. text for explanation).

od^{25,26}. Since orbital 32 of the isoalloxazine moiety is heavily mixed, supermolecule orbital 50 also acquires a large amount of π character. Orbital 52 originates from the breakdown of the through-bond linear plus combination of the N_1 and O_{12} lone pairs³ upon complex formation and is made up for 81% by an antibonding linear combination of the $N_1(2s)$, $N_1(2p_y)$ and $O_m(2p_y)$ AO's. The net interaction between the isoalloxazine and methanol moieties in the complex, however, is calculated to be bonding. The complex gains 594 kJ mole^{-1} with respect to the separated molecules (an unrealistically large *calculated* value owing to the short H-bond length) and the dipole moment is reduced from a total of 10.2 D to 7.2 D upon complexation ("free" isoalloxazine yields 9.1 D). A large positive bond order is calculated between H_m and N_1 (0.26 between $N_1(2s)$ and $H_m(1s)$ and 0.36 between $N_1(2p_y)$ and $H_m(1s)$ at 1 Å (0.1 nm) distance). Also the net bond order between O_m and N_1 was found to be positive whereas the bond orders between the methanol OH group and other atoms in the isoalloxazine moiety are predominantly negative. Clearly, the calculation yields the picture one would expect by simple chemical intuition, except for the behaviour of orbitals 50 and 52.

In an attempt to eliminate the spurious steric interactions, we replaced the N_{10} methyl substituent by a proton, i.e. the calculations were repeated using the "ideal" all-proton isoalloxazine model from previous calculations³. This leads to the disappearance of orbital 50, so it clearly is an artefact in the calculation. Orbital 52, however, proved to be persistent, no matter how we varied the relative orientation of the methanol moiety with respect to isoalloxazine, keeping the hydrogen bond in the isoalloxazine molecular plane. Its energy was found to depend approximately only on the N_1-H_m distance which, in turn, had no appreciable effect on the character of the orbital. To our great surprise, this finding was confirmed by photoelectron spectroscopy. When the spectrum of an isoalloxazine derivative is recorded carrying a *n*-butyl substituent in position 10 (compound 1, Scheme 6.1), which is unable to form a hydrogen bond towards the isoalloxazine ring system, the normal isoalloxazine characteristics are observed³ (Fig. 6.2). Introduction of a hydroxyl group into the N_{10} side-chain (compounds 2,3) enables intramolecular hydrogen bond formation towards N_1 , as we proposed before to explain the long fluorescence lifetime of these compounds in the vapour phase². Indeed both compounds have an additional band in their photoelectron spectrum around 7 eV (Figs. 6.3 and 6.4), the same energy region where orbital 52 was calculated. Compound 1 does not show this band, neither could it be produced in the spectrum of compound 1 by admittance of methanol vapour into the photoelectron spectrometer target chamber during the measurements. The band is too intense to

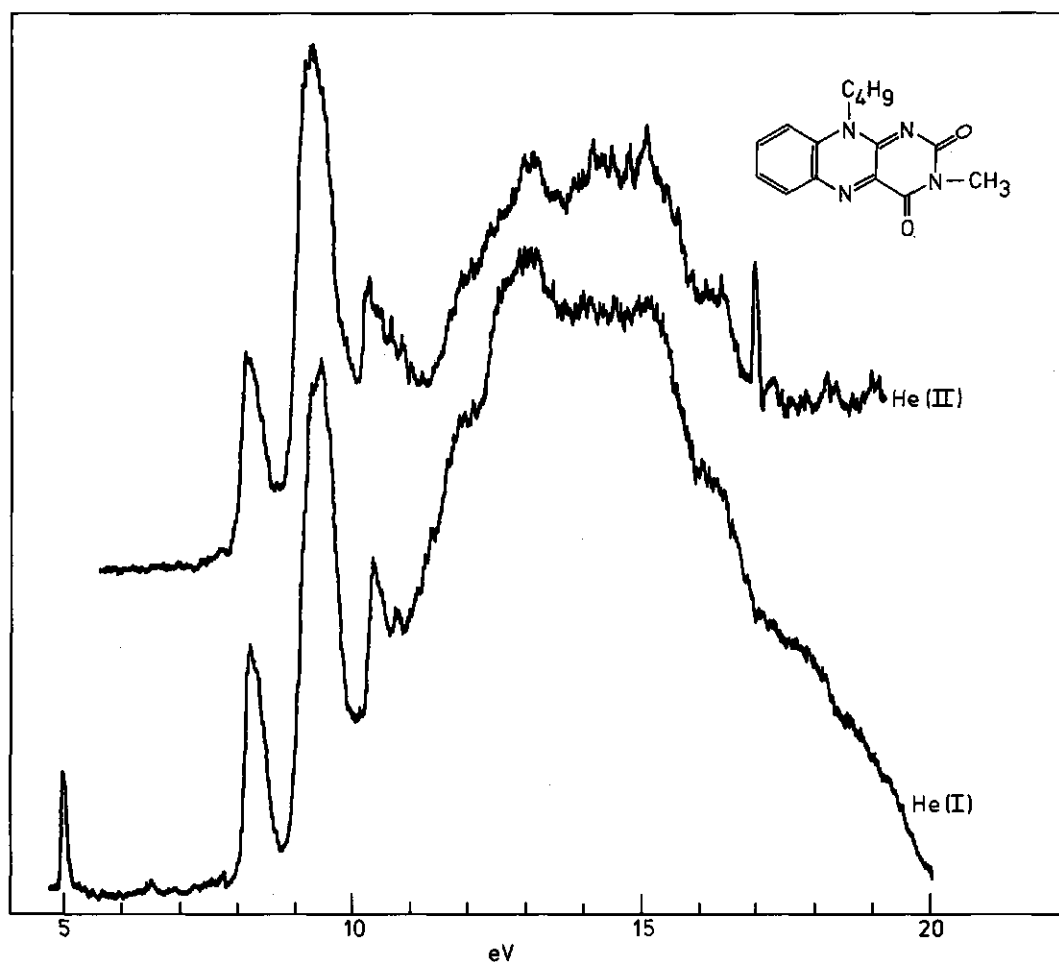


Figure 6.2. Photoelectron spectra of 3-methyl-10-(*n*-butyl)-isoalloxazine (1) at 510 K.

be produced by photoionization from unperturbed isoalloxazine orbitals by He(I)- β radiation since the He(I)- β /He(I)- α intensity ratio²⁷ is less than 0.02. Similarly, the possibility that the band is a He(II)- β ghost can be excluded since in that case the band would appear at another ionization energy²⁷. A real He(I)- β ghost is visible in the spectrum of compound 1 (Fig. 6.2) as a very weak band around 6.5 eV, disappearing in the He(II) spectrum. Conversely, the bands at ~ 7 eV of compounds 2 and 3 remain in the He(II) spectra, excluding the possibility that they could be ghosts.

The stabilization of the highest occupied isoalloxazine π orbital as calculated for the complex (orbital 51 in Fig. 6.1 and Tables 6.1, 6.2) is also con-

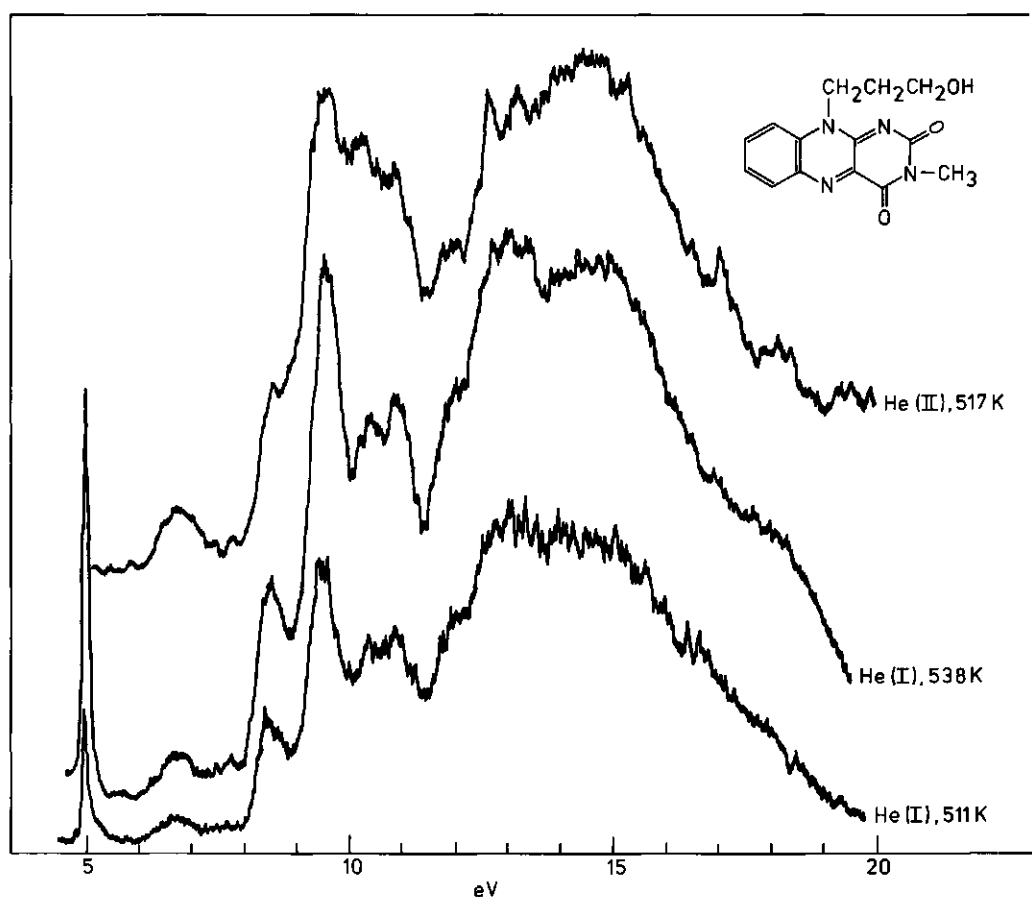


Figure 6.3. Photoelectron spectra of 3-methyl-10-(γ-hydroxypropyl)-isoalloxazine (2).

firmed by the photoelectron spectra. For compound 3, the apparent stabilization is even larger than the calculated one (Figs. 6.1, 6.2, 6.4), so that the corresponding band almost merges with the adjacent band in the photoelectron spectrum. The highest occupied isoalloxazine orbital was previously found to have a large amount of benzenoid E_{1g} character³ and to be localized for 56% in the benzene subnucleus of the molecule³. The remaining part of this orbital is calculated to be localized on N_1 (16%), C_{4a} (13%) and N_{10} (7%). Upon complexation, the calculation predicts a charge redistribution in which the methanol proton H_m loses 0.12 and N_1 and N_{10} both lose 0.02 electron to the gain of the O_m . Other atoms show random charge density changes of at least one order of magnitude less than 0.02 electron. Since the character of orbital 51 is hardly affected in the complex (Table 6.2),

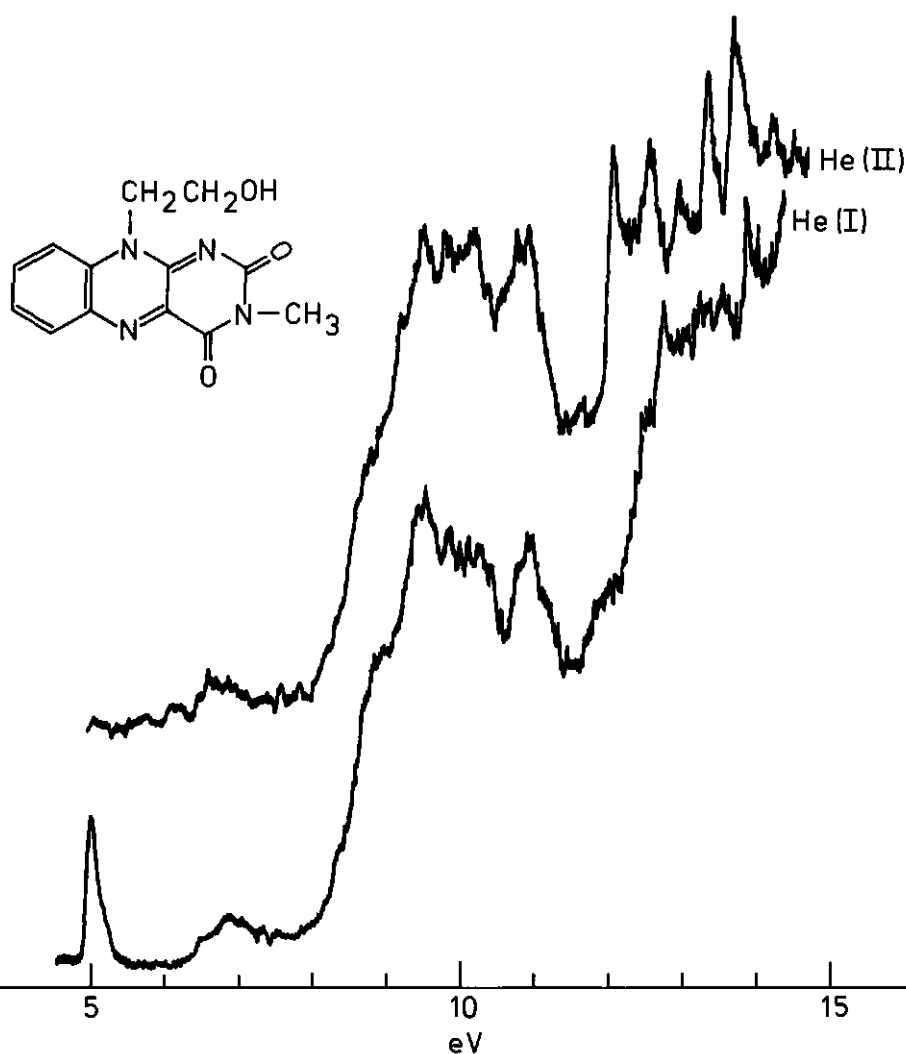


Figure 6.4. Photoelectron spectra of 3-methyl-10-(β-hydroxyethyl)-isoalloxazine (3) at 517 K.

its stabilization is easily explained by the charge redistribution process. A similar argument was used tentatively by Nishimoto *et al.*¹¹ for the reparameterization used in their theoretical work.

The intense second band at 9.42 eV in the spectrum of compound 1 (Fig. 6.2 and Table 6.1) can be assigned to a degenerate set of orbitals, one of which is

another benzenoid e_{1g} orbital (π) and the other two are through-bond linear combinations of oxygen and imine-like nitrogen lone pairs³. Since this second e_{1g} orbital is localized for 85% in the benzene subnucleus of the molecule, its energy is hardly affected upon complexation towards N_1 . This is reflected in the photoelectron spectra, each of which shows a distinct band at ~ 9.5 eV (Figs. 6.2-6.4). The orbital also retains its character upon complexation (Fig. 6.1 and Table 6.2). As a consequence of the breakdown of the N_1-O_{12} lone pair through-bond interaction in the complex, the calculation produces new through-bond interactions between the O_{12} and O_{14} lone pairs. This gives rise to two orbitals with a relatively small energy difference (~ 0.5 eV) depending slightly on the strength of the hydrogen bond (interaction distance). Both suffer from serious additional π admixture and are calculated around -11 eV (orbitals 46 and 48 of the supermolecule, after appropriate correction¹³; Tables 6.1, 6.2 and Fig. 6.1). If the calculational error for these orbitals is of the same order of magnitude as was found previously for n orbitals³, they really should be located somewhere around -9.5 to -10.0 eV.

Also based on previous experience³, the bands in the photoelectron spectrum of compound 1 at 10.34 and 10.83 eV are most likely to be assigned to π orbitals. They remain present in the spectra of compounds 2 and 3, apart from small shifts and a considerable admixture of σ character predicted by the calculation (Fig. 6.1 and Table 6.2). Since their energy is of the same order as that of the methanol oxygen lone pair (cf. the $2a''$ orbital of methanol at -10.85 eV^{23,24}), the latter is expected to admix as well. Probably, this admixture is underestimated by the CNDO/S calculation owing to the large error in the calculated energy of the $2a''$ orbital (*vide supra*). The photoelectron spectra, however, neither deny nor confirm this. The crowding of bands in the 10-12 eV energy region is so large that the band corresponding to $2a''$ ionization, which is expected to be located in this energy region, cannot be distinguished clearly. Conversely, compounds 2 and 3 do not show a pronounced He(I)-He(II) intensity-difference between 10 and 12 eV, a behaviour which could be anticipated from basic cross-section considerations^{28,29} if a $2a''$ oxygen lone pair were present.

These considerations finally give the correlation diagram proposed in Fig. 6.1 (Experimental). The relative intensities in different parts of the photoelectron spectra reasonably agree with this picture as deduced from rough estimates of band areas, bearing in mind the basic cross-section rules^{28,29}. Only the band at ~ 7 eV has an exceptionally low cross-section which cannot be ascribed to hydrogen $1s$ character since in that case the band should have a relatively lower

intensity in the He(II) spectrum²⁸, contrary to the measurements. The total amount of s character calculated for the ~ 7 eV orbital is only 20%, lower than one would expect by intuition, but higher than in an average isoalloxazine orbital.

Another explanation for the low intensity could be the existence of a thermal equilibrium between complexed and uncomplexed molecules in the vapour phase. The temperature range in which photoelectron spectra could be measured reliably is too small, however, to establish this firmly. In this respect the present compounds behave similarly as those measured previously³. The He(I) spectra of compound 2 at the maximum and minimum accessible temperature are given in Fig. 6.3. Lower temperatures resulted in count rates which were too low (< 100 counts/second) and higher temperatures caused noticeable decomposition. The temperature range for compound 3 (Fig. 6.4) was even smaller. The present data, however, clearly demonstrate the internal complexation of compounds 2 and 3 in the vapour phase, the interaction being dependent on the length of the N_{10} side-chain.

6.3.2. The isoalloxazine optical spectrum

The CI calculations were performed on the "ideal" isoalloxazine molecule carrying only proton substituents³, compounds 4 and 5 (Scheme 6.1) and the isoalloxazine-methanol complex described above. Molecular geometries were identical to those used before³. The "all-proton model", although non-existent in nature, was used again for approximate symmetry classification³. The results are compared with optical spectra measured in non-protic solvents of lowest possible polarity¹. Vapour phase spectra are less suitable for comparison purposes since they suffer from serious broadening due to sequence congestion². It was established that the radiative properties of compounds 5 and 6 (position and shape of spectral bands, radiative lifetimes) are the same in 2-methyl-tetrahydrofuran (2-MTHF). Only their non-radiative properties differ slightly as could be judged from the fluorescence lifetimes (compound 5: 7.4 ns at 300 K, 9.0 ns at 77 K; compound 6: 6.5 ns at 300 K, 9.2 ns at 77 K; solvent 2-MTHF, carefully degassed¹). We, therefore, compared the calculated spectrum of compound 5 to the experimental spectrum of compound 6 in 3-methyl-pentane (3-MP) at 300 K. Thus, advantage could be taken from the solubility of compound 6 in 3-MP, a solvent of the lowest possible polarity which does not obscure the isoalloxazine far UV band at 45000 cm^{-1} (222 nm).

All isoalloxazines calculated give rise to basically the same CI pattern. Comparison between calculated and experimental transition energies and band intensities is made in Figs. 6.5 and 6.6. Detailed information on the contribution of the various configurations to the excited states is given in Appendix 1. The

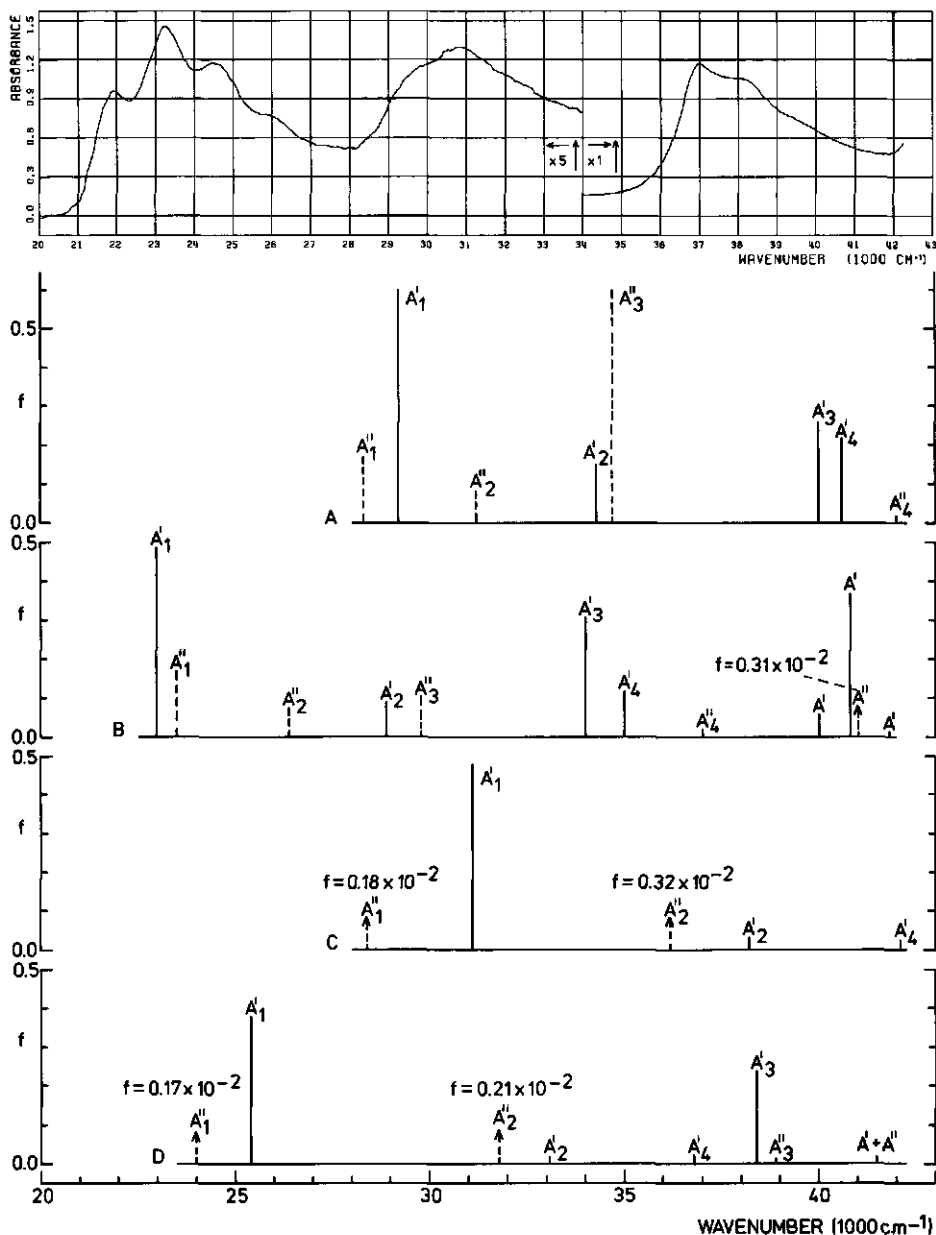


Figure 6.5. Absorption spectrum of 3,10-dimethyl-isoalloxazine (4) in 2-methyl-tetrahydrofuran¹, 77 K, $c = 29 \mu\text{M}$. Calculated spectra: A: CNDO/S-CI, 100 singly excited singlet configurations; B: as A, occupied orbitals Bigelow-corrected³; C: INDO/S-CI, 81 singly excited singlet configurations and D: as C using Bigelow corrected^{3,13} CNDO/S orbitals as starting orbitals (f = oscillator strength). The absorbance scale in the experimental spectrum is expanded in the long-wavelength region ($20000 - 34000 \text{ cm}^{-1}$). Dotted stick-bars indicate f -values multiplied by 1000 prior to plotting.

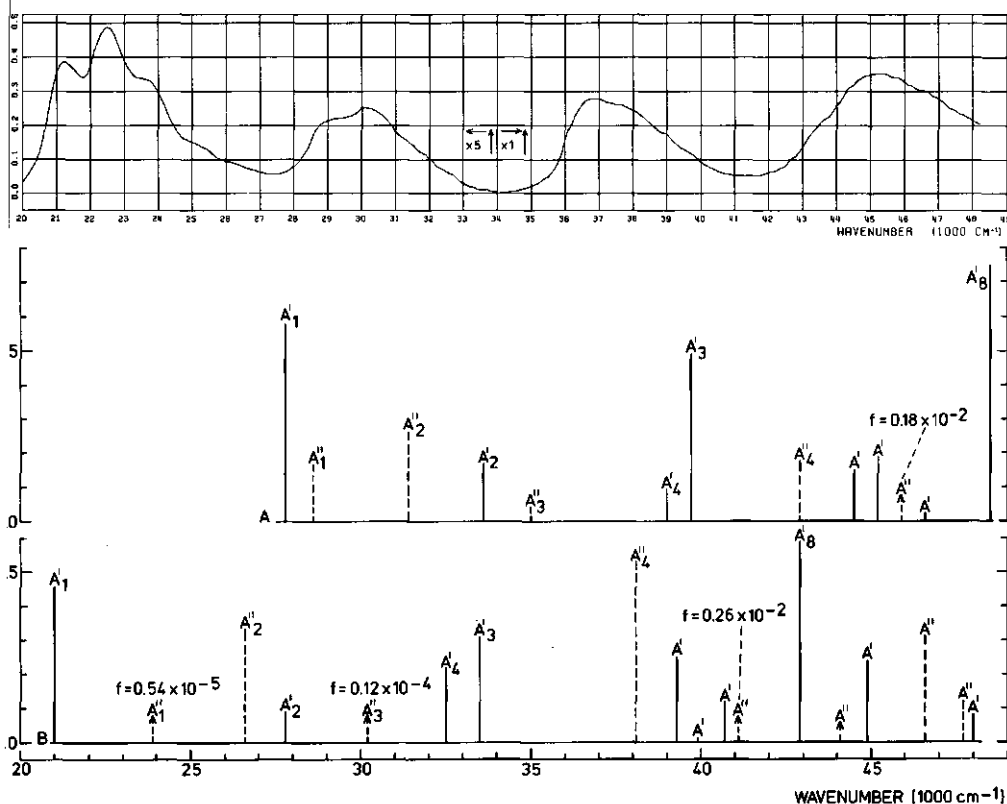


Figure 6.6. Absorption spectrum of 3,7,8-trimethyl-10-(*n*-octadecyl)-isoalloxazine 6) in 3-methyl-pentane¹, 300 K, $c = 6.6 \mu\text{M}$. Calculated: 3,7,8,10-tetramethyl-isoalloxazine (3-methyl-lumiflavin; 5), cf. legend to Fig. 6.5 for further explanation.

calculated excited states are labelled by their main symmetry, A' for $\pi\pi^*$ and A'' or $n\pi^*$ (or $\sigma\pi^*$) states (the admixture of A'' ($\pi\sigma^*$) and A' ($\sigma\sigma^*$) states was found to be negligible). As in the previous orbital calculations³, the all-proton model was used as a reference in the labelling process since it has the property of unambiguous σ - π separation³. Consequently, there is no admixture of A' states into A'' states and *vice versa*. The approximate symmetry of the states calculated for derivatives 4 and 5 (Scheme 6.1) was determined from the approximate symmetry of the most contributing configurations. The calculation of scalar products as previously³, extended to the eigenvectors of the CI matrices as well, was employed as an objective criterion in the symmetry determination. A second assignment

criterion was the absence of a singlet-triplet splitting for the A' states in the CNDO approximation¹⁵. This property was found to be retained almost exactly (deviations <5%) when the symmetry was lowered by rotating the methyl groups into the "staggered" position as defined earlier³. The third, but least objective, assignment criterion was, of course, the very small oscillator strength of the ${}^1A'_0 \rightarrow {}^1A''_n$ transitions. The states belonging to each symmetry species were numbered consecutively in the all-proton model. The labels thus obtained were transferred to the methylated derivatives as far as the above-mentioned criteria permitted. In this way the reversal of states in the different compounds became immediately apparent in the figures.

The CI results do not depend very much on the number of configurations used. It was varied between 50 and 200. In the straightforward CNDO/S-CI method^{15,17,30} the ${}^1A'_0 \rightarrow {}^1A''_n$ transition energies are calculated systematically too high by ~ 1 eV (Figs. 6.5A and 6.6A). Conversely, the first excited ${}^3A'_1$ state is calculated very well (Compound 4: calc. 16500 cm^{-1} , exp.¹ 17400 cm^{-1} ; compounds 5/6: calc. 15700 cm^{-1} , exp.¹ 16800 cm^{-1}). The error in the ${}^1A'$ states is of the same order of magnitude as the error in the calculated orbital energies before correction with the Bigelow formula^{3,13}. Application of this correction or, equivalently, adjusting the energy of the higher occupied π orbitals to their experimental values³, improves the agreement between theory and experiment for the ${}^1A'$ states, but impairs it for the ${}^3A'_1$ state. Evidently, the calculated singlet-triplet splitting of the A'_1 state is much too large ("ideal" isoalloxazine: before CI 9900 cm^{-1} , after CI 13900 cm^{-1} ; compound 4: calc. after CI 12700 cm^{-1} , exp.¹ 4000 cm^{-1} ; compound 5: calc. after CI 12100 cm^{-1} , exp.¹ 4000 cm^{-1}).

The first excited ${}^1A''$ state is calculated in the vicinity of ${}^1A'_1$ (Figs. 6.5, 6.6). Sometimes it is even calculated as the lowest excited singlet state, contrary to all available spectral data^{1,2,9,12,31-39} and to the experimental radiative lifetimes of ~ 12 ns in solution¹ and 22 ns in the vapour phase². Such values cannot correspond to an oscillator strength of $\sim 10^{-3}$ which is calculated for the ${}^1A'_0 \rightarrow {}^1A''_1$ transition using the method of Ellis *et al.*¹⁷ (cf. Experimental Section). The ${}^1A''_1$ state is predominantly a linear combination of the configurations⁴⁰ $|\sigma_{29}\pi_1^*|$ and $|\sigma_{30}\pi_1^*|$ arising from the orbitals of the all-proton model. The occupied orbitals σ_{29} and σ_{30} are the well-known through-bond linear combinations³ of the N_1 , O_{12} and N_5 , O_{14} lone pairs, respectively, whereas π_1^* is the LUMO. The ${}^1A''_1$ state approximately stabilizes by 12000 cm^{-1} after CI, much more than the average stabilization of the ${}^1A'$ states. Adjustment of the energy of σ_{29} and σ_{30} to either the Bigelow corrected^{3,13} or experimental³ value makes the

agreement of the $^1A''$ states with the experiment even worse. Thus the error in the orbital energies³ of σ_{29} and σ_{30} is opposite to the error in the excited states arising from σ_{29} and σ_{30} : The calculations yielded orbital energies for σ_{29} and σ_{30} which are too negative³, hence one expects the energy of the configurations⁴⁰ $|\sigma_{29}\pi_1^*|$ and $|\sigma_{30}\pi_1^*|$ to be too large, but the latter mix to produce an excited $^1A''$ state with an energy which is too low. In order to raise the energy of all $^1A''$ configurations we abandoned the strict ZDO approximation to obtain non-vanishing exchange integrals between σ and π orbitals^{15,18,19}. This was done since symmetry-breaking by rotation of methyl groups did not change the results significantly within the CNDO/S approximations. The relaxation of the ZDO approximation to the INDO/S level¹⁹ (cf. Experimental Section), however, did not alter the calculated spectrum appreciably (Fig. 6.5). This was mainly due to an increased amount of configuration interaction, which compensated the increase of the diagonal $^1A''$ elements of the CI matrix in going to INDO/S. Only a slight improvement of the singlet-triplet splitting was obtained in this way, i.e. that of the $^1A''$ states was no longer zero and that of the A' states was reduced by 1500 cm^{-1} for "ideal isoalloxazine" and by 1100 cm^{-1} for compound 4.

The calculated oscillator strengths generally agree with those obtained from other theoretical methods^{11,33,34,41-44}, but deviate from the experiment at first sight (Figs. 6.5, 6.6). Since none of the theorists^{11,33,34,41-44} bothered about accurate experimental values of the oscillator strengths, we estimated them from the band areas in our previously measured absorption spectra¹ using Birks' formula⁴⁵ and known values of the molar extinction coefficients^{1,31,39}. The results, corrected similarly for the medium refractive index as in the calculation of radiative lifetimes^{1,2}, are surprising (Table 6.3). Apparently, it has been over-

TABLE 6.3.
EXPERIMENTAL ELECTRONIC SINGLET TRANSITION ENERGIES^{a)} (1000 cm^{-1}) AND OSCILLATOR STRENGTHS^{b)} OF SOME ISOALLOXAZINES.

Compound	Solvent	$S_0 \rightarrow S_1$		$S_0 \rightarrow S_2$		$S_0 \rightarrow S_3$		$S_0 \rightarrow S_4$	
		ΔE	f	ΔE	f	ΔE	f	ΔE	f
4	2MTHF ^{c)}	21.9	0.12	29.9	0.13	37.0	0.45	-	-
6	2MTHF ^{c)}	21.5	0.14	28.5	0.11	36.9	0.43	-	-
6	3MP ^{d)}	21.3	0.14	29.0	0.065	36.8	0.42	45.1	0.73

a) 0 - 0 Transitions as measured previously¹; b) Calculated from the integrated absorption spectra¹ according to Birks' formula⁴⁵; c) 2-methyl-tetrahydrofuran¹, 7 K; d) 3-methylpentane¹, 300 K.

looked in the literature^{11,33,34,41-44} that all theories predict oscillator strengths which reasonably agree with experimental values, *except for that of the isoaalloxazine* $S_0 \rightarrow S_1$ (${}^1A'_0 \rightarrow {}^1A'_1$) transition. This latter value is calculated by a factor of ~ 5 times too large! Since this transition invariably consists of more than 90% of the HOMO \rightarrow LUMO configuration in which the (calculated) character of the HOMO is well-established by experiment³, the calculations apparently give rise to an erroneous LUMO. In this respect it is also noteworthy that the calculations were unable to reproduce the decrease of the oscillator strength of the ${}^1A'_0 \rightarrow {}^1A'_1$ transition in a 6-methyl derivative as established experimentally³⁹.

The oscillator strength of the ${}^1A'_0 \rightarrow {}^1A'_2$ transition was found to be highly sensitive to the degree of approximation used in the calculations and the degree of methylation of the molecule. Generally, its value is small due to an effective cancellation of the one-electron transition moments of the configurations involved. In this respect the transition resembles the Pariser¹⁴ sign-forbidden transitions in the polyacenes. To what extent the cancellation occurs depends on the CI eigenvectors. In a recent calculation on the "ideal" all-proton model, Jaffé obtained an ${}^1A'_0 \rightarrow {}^1A'_2$ oscillator strength of the same order of magnitude as for an average ${}^1A'_0 \rightarrow {}^1A'_n$ transition²⁶ by using Pariser¹⁴ instead of Nishimoto-Mataga integrals. These findings may explain the difficulty in observing the $S_0 \rightarrow S_2$ transition in vapour phase excitation spectra².

In the S_3 region, the calculations invariably predict two ${}^1A'$ states (${}^1A'_3$ and ${}^1A'_4$). Their composition and relative intensity is highly dependent on the degree and site of methylation in the molecule. The sum of the calculated oscillator strengths of the ${}^1A'_0 \rightarrow {}^1A'_3$ and ${}^1A'_0 \rightarrow {}^1A'_4$ transitions, however, is roughly constant and agrees reasonably with the experimental $S_0 \rightarrow S_3$ value. Regarding the partially resolved vibrational structure of the experimentally observed $S_0 \rightarrow S_3$ band, it is not very likely that the band should consist of two overlapping transitions of about equal intensity (Fig. 6.5). Hence, starting from excitation energies above $\sim 38000 \text{ cm}^{-1}$ the calculations no longer offer any guidance in the interpretation of the optical spectra. This applies especially to the $S_0 \rightarrow S_4$ region (Fig. 6.6).

CI calculations performed on the isoaalloxazine-methanol complex, generally give rise to the same spectral characteristics as in the isolated compounds except for considerable shifts owing to the change in energy for some of the occupied orbitals. Upon complexation, the virtual orbitals retain their energy and character within 0.1 eV and 5%, respectively, contrary to earlier SCF-PPP results¹¹. The spurious orbital 50 (*vide supra*) gives rise to a one-electron transition to the LUMO which does not significantly mix with other configurations.

it occurs in one of the CI-eigenvectors with a coefficient of 0.91 and thus leads to a spurious excited state which is easily recognizable. The latter state disappears when "ideal isoalloxazine" is taken as the parent compound in the complex. The energies of the calculated ${}^1A'_0 \rightarrow {}^1A'_1$ and ${}^1A'_0 \rightarrow {}^1A'_2$ transitions are not greatly affected upon complexation. Only those excited ${}^1A''$ states, in which configurations arising from the antibonding orbital 52 participate significantly, are considerably stabilized.

The calculated directions of transition moments agree reasonably with experimental values⁴⁶. The angles with the positive x-axis (perpendicular to the line joining the N_{10} and N_5 atoms in the direction of the C_2-N_3 bond, cf. Scheme 6.1) are: ${}^1A'_0 \rightarrow {}^1A'_1$: exp.⁴⁶ -32° , calc. -8° ; ${}^1A'_0 \rightarrow {}^1A'_2$: exp.⁴⁶ $+7^\circ$, calc. $+1^\circ$ to -13° .

4. DISCUSSION

The present results clearly demonstrate the serious difficulties the applied MO calculations have in coping with the isoalloxazine molecule. Since both NDO/S^{15,17,30} and INDO/S¹⁹ give much better descriptions of simpler heteroaromatic molecules containing either oxygen or nitrogen atoms, it probably is the combination of both which produces the errors. The errors in the one-electron integrals discussed previously^{3,25} partly account for this, but the two-electron integrals must contain appreciable errors, too. This follows from the erroneous excited state pattern which is calculated after extensive CI from quite a reasonable orbital structure³. Based on the calculated and observed singlet-triplet splittings and the experimental fact that both S_1 and T_1 are A' states, we arrive at the conclusion that the applied methods overestimate the exchange integrals between π orbitals and underestimate those between σ (or n) and π orbitals. The comparable off-diagonal exchange-like terms in the CI matrix, i.e. those of the type $(ik|jk)$, behave similarly. This gives rise to a large amount of CI of the ${}^1A''$ relative to the ${}^1A'$ configurations, owing to an inadequate balance of the $(ik|jk)$ with the corresponding Coulomb-like terms $-(ij|kk)$ in the ${}^1A''$ CI matrix elements. The final result is the error in the relative locations of ${}^1A'$ and ${}^1A''$ states, especially in case of hydrogen bond formation towards N_1 . In the latter situation, i.e. protic solvents^{12,31}, there is no experimental evidence whatsoever that the S_1 should be an ${}^1A''$ state in spite of the considerable destabilization of the N_1 lone pair established by photoelectron spectroscopy (Figs. 6.3, 6.4).

On the other hand, erroneous exchange integrals cannot fully account for the error in the ${}^1A''$ states. As shown in the previous section, the latter arise from orbitals which contain an opposite error in energy of about the same order of

magnitude³ (~ 1 eV). Straightforward correction would require a physically unrealistic adjustment of exchange integrals between σ and π orbitals, hence Koopmans defects (electronic relaxation upon photoionization) largely must be held responsible for the difference between the calculated³ and experimental³ orbital energies of the (localized!) n orbitals. Similar Koopmans defects were found for uracil⁴⁷, a molecule which strongly resembles the part of the isoalloxazine ring containing the carbonyl groups. This discussion equally applies to the hydrogen-bonded case since, in spite of the n orbital destabilization, the first excited singlet state of isoalloxazine remains an $^1A'$.

Further support for this interpretation arises from the frequently discussed solvatochromy of the $S_0 \rightarrow S_2$ transition^{1-3,12,31,39}. The available spectral data^{1-3,12,31,39} show the solvent influence on this transition to be twofold. First, in non-protic solvents, the $S_0 \rightarrow S_2$ oscillator strength increases with increasing solvent polarity, without an appreciable spectral shift^{1-3,12,31,39} (Figs. 6.5, 6.6; Table 6.3). Secondly, as soon as the solvent becomes protic, the $S_0 \rightarrow S_2$ transition displays the well-known red shift^{31,39} up to ~ 3000 cm^{-1} . The first property is easily explained by the "sign-forbidden" character of the calculated $^1A'_0 \rightarrow ^1A'_2$ transition, whereas the second property is in accordance with the N_1 lone pair destabilization upon H-bond formation. We, therefore, assign the S_2 to a mixed state of both $^1A'$ and $^1A''$ character of which the latter causes the solvatochromy of the $S_0 \rightarrow S_2$ transition. Also the red shift of this transition upon methylation of the molecule in the 6-position³⁹ (cf. Scheme 6.1) supports this assignment. This shift is brought about by the corresponding destabilization of the second highest occupied π orbital of benzenoid E_{1g} character which is degenerate with two n orbitals³. All three orbitals give rise to configurations which appreciably contribute to the S_2 state. Compared to compound 4, the second highest occupied π orbital of 3,6,10-trimethyl-isoalloxazine is destabilized³ by ~ 0.6 eV. Methylation in the 9-position produces a similar spectral shift owing to the equivalency of the 6- and 9-positions in the relevant π orbital. The calculated (CNDO/S) spectral shift of ~ 2000 cm^{-1} corresponds reasonably to the experimental value³⁹ of ~ 1500 cm^{-1} .

Thus the $S_0 \rightarrow S_2$ solvatochromy of isoalloxazines can be regarded as an accidental "by-product" of a peculiar electronic structure. In this respect, the spectral changes observed upon addition of CCl_3COOH to isoalloxazine solutions in CCl_4 are interpreted correctly in terms of H-bond formation¹², but the theoretical backup¹¹ of these experiments by SCF-PPP calculations cannot be sufficient since this theory does not treat the σ framework of the molecule. This particularly applies to the very complex cases of multiple H-bond formation¹¹. Also the

SCF-PPP perturbational treatment of isoalloxazine-solvent interactions by Takano *et al.*⁴⁴ must be regarded as incomplete. On the other hand, it seems to be out of the question to observe ever a pure $n \rightarrow \pi^*$ ($^1A'_0 \rightarrow ^1A''_n$) transition in isoalloxazine as suggested in the past³³. The effect of rotation of methyl groups in our calculations shows that even very small vibronic interactions allow for sufficient admixture of π character into n orbitals and of A' character into A'' states to produce an in-plane polarized transition moment for an $^1A'_0 \rightarrow ^1A''_n$ transition, which largely exceeds the out-of-plane transition moment calculated by relaxing the ZDO approximation. Nevertheless, for the π orbital system and the A' states, the initial SCF-PPP calculations^{33,34,41-43} show the best agreement with the experiments¹⁻³ of all theories applied to isoalloxazines. This includes a recent *ab initio* calculation by Palmer *et al.*⁴⁸ which agrees poorly with the photoelectron spectra of the compounds investigated here and previously³.

The applicability of calculational methods to isoalloxazines clearly is limited to trend-analysis in a series of related experiments. CNDO/S appears to be remarkably successful in describing the peculiar behaviour of the molecule upon H-bond formation. Assuming similar calculational errors for the (destabilized) n orbital in both free³ and hydrogen-bonded isoalloxazine (likely due to Koopmans defects³), the most reasonable agreement between experiment and calculation occurs at a H-bond distance somewhere between 1.2 Å (0.12 nm) and 1.8 Å (0.18 nm), quite a realistic value considering the rather strong intramolecular interaction. The reason why the hydrogen bond behaves anomalously is the breakdown of the existing N_1 -O₁₂ through-bond interaction in the isolated isoalloxazine molecule. As a consequence, all other through-bond interactions rearrange, too. This "domino-effect" enables a hydrogen bond at N_1 to extend its influence *via* the σ framework towards N_5 , which is known to be a catalytical site in biochemical processes^{8,49,50}. At the same time, H-bond formation towards N_1 also affects the π electronic system. Thus, in addition to the conformational flexibility of the molecule in the reduced form³, H-bond formation can be regarded as a tuning mechanism of the electronic and redox properties of flavins. N_1 , already known from crystallographic studies⁵¹ to be a good hydrogen acceptor for the oxidized molecule, thus turns out to be a "tuning-site" and N_5 turns out to be a "reaction-site", in conformity with previous proposals based on adduct formation with phosphines at the N_5 center⁸. In this model, the N_{10} side-chain and the N_3 proton (present in the molecule's biologically active form) can be regarded as binding sites to the apo(flavo)protein.

REFERENCES AND NOTES

- 1 Cf. Chapter 3 or: J.K. Eweg, F. Müller, A.J.W.G. Visser, C. Veeger, D. Bebelaar and J.D.W. van Voorst, Photochem. Photobiol. 30 (1979) 463.
- 2 Cf. Chapter 4 or: J.K. Eweg, F. Müller, D. Bebelaar and J.D.W. van Voorst, Photochem. Photobiol. 31 (1980) 435.
- 3 Cf. Chapter 5 or: J.K. Eweg, F. Müller, H. van Dam, A. Terpstra and A. Oskam, J. Amer. Chem. Soc. 102 (1980) 51.
- 4 J. Kelder, H. Cerfontain, J.K. Eweg and R.P.H. Rettschnick, Chem. Phys. Letters 26 (1974) 491.
- 5 W.R. Knappe, Chem. Ber. 108 (1975) 2422.
- 6 S. Leavell, J. Steichen and J.L. Franklin, J. Chem. Phys. 59 (1973) 4343.
- 7 F. Carnovale, M.K. Livett and J.B. Peel, J. Amer. Chem. Soc. 102 (1980) 569.
- 8 F. Müller, Z. Naturf. 27b (1972) 1023.
- 9 P.K. Dutta, J.R. Nestor and T.G. Spiro, Proc. Natl. Acad. Sci. USA 74 (1977) 4146, *ibid.* Biochem. Biophys. Res. Commun. 83 (1978) 209.
- 10 M. Benecky, T.Y. Li, J. Schmidt, F. Frerman, K.L. Watters and J. McFarland, Biochemistry 16 (1979) 3471.
- 11 K. Nishimoto, Y. Watanabe and K. Yagi, Biochim. Biophys. Acta 526 (1978) 34, *ibid.* in: Flavins and Flavoproteins, Proc. 6th Int. Conf., eds. K. Yagi and T. Yamano (Japanese Scientific Soc. Press, Tokyo (1980) 493).
- 12 K. Yagi, N. Ohishi, K. Nishimoto, J.D. Choi and P.S. Song, Biochemistry 19 (1980) 1553.
- 13 R.W. Bigelow, J. Chem. Phys. 66 (1977) 4241.
- 14 R. Pariser, J. Chem. Phys. 24 (1956) 250.
- 15 J. Del Bene and H.H. Jaffé, J. Chem. Phys. 48 (1968) 1807.
- 16 K. Nishimoto and N. Mataga, Z. Phys. Chem. (Frankfurt am Main) 12 (1957) 335.
- 17 R.L. Ellis, G. Kuehnlenz and H.H. Jaffé, Theoret. Chim. Acta 26 (1972) 131.
- 18 C. Giessner-Pretre and A. Pullman, Theoret. Chim. Acta 13 (1969) 265.
- 19 J. Ridley and M. Zerner, Theoret. Chim. Acta 32 (1973) 111.
- 20 J.A. Pople and D.L. Beveridge: Approximate Molecular Orbital Theory (McGraw-Hill, New York, N.Y., USA, (1970) 80-83).
- 21 J.A. Pople, Proc. Phys. Soc. A, 68 (1955) 81.
- 22 CRC Handbook of Chemistry and Physics, 55th ed. (CRC-press, Cleveland, Ohio, USA (1975) F203).
- 23 J.H.D. Eland: Photoelectron Spectroscopy (Butterworths, London (1974) 22-23).
- 24 M.J.S. Dewar and S.D. Worley, J. Chem. Phys. 50 (1969) 654.
- 25 S. de Bruijn, Chem. Phys. Letters 54 (1978) 399, *ibid.*, Personal Communication.
- 26 H.H. Jaffé, Personal Communication.
- 27 J.W. Rabalais: Principles of Ultraviolet Photoelectron Spectroscopy (Wiley, New York, N.Y., USA (1977) 22-23).
- 28 A. Schweig and W. Thiel, J. Electron Spectrosc. Relat. Phenom. 3 (1974) 27, *ibid.*, J. Chem. Phys. 60 (1974) 951.
- 29 H. van Dam and A. Oskam, J. Electron Spectrosc. Relat. Phenom. 13 (1978) 273.
- 30 G. Kuehnlenz and H.H. Jaffé, J. Chem. Phys. 58 (1973) 2238.
- 31 J. Koziol, Photochem. Photobiol. 5 (1966) 41, *ibid.*, 5 (1966) 55, *ibid.*, 9 (1969) 45.
- 32 P.S. Song, T.A. Moore, W.H. Gordon III, M. Sun and C.N. Ou, in: Organic Scintillators and Liquid Scintillation Counting (Academic Press, New York, N.Y., USA (1971) 521).
- 33 M. Sun, T.A. Moore and P.S. Song, J. Amer. Chem. Soc. 94 (1972) 1730.
- 34 P.S. Song, T.A. Moore and W.E. Kurtin, Z. Naturf. 27b (1972) 1011.
- 35 N.Y.C. Chu and K. Weiss, Chem. Phys. Letters 27 (1974) 567.
- 36 W.A. Eaton, J. Hofrichter, M.W. Makinen, R.D. Andersen and M.L. Ludwig, Biochemistry 14 (1975) 2146.

- 7 K. Yagi, in: Biochemical Fluorescence Concepts, eds. R.F. Chen and H. Edelhoch, vol. 2 (Marcel Dekker, New York, N.Y., USA (1976) 639).
- 8 P.K. Dutta and T.G. Spiro, J. Chem. Phys. 69 (1978) 3119.
- 9 A.J.W.G. Visser and F. Müller, Helv. Chim. Acta 62 (1979) 593.
- 0 The notation $|ab|$ or $|a,b|$ is an abbreviation for either the normalized singlet $2^{-\frac{1}{2}}(|a\bar{b}| - |\bar{a}b|)$ or the normalized triplet $2^{-\frac{1}{2}}(|a\bar{b}| + |\bar{a}b|)$ configuration in which an electron is promoted from orbital a to orbital b.
- 1 J.L. Fox, K. Nishimoto, L.S. Forster and S.P. Laberge, Biochim. Biophys. Acta 109 (1965) 626, *ibid.*, 136 (1967) 544.
- 2 P.S. Song, Int. J. Quantum Chem. 3 (1969) 303.
- 3 B. Grabe, Acta Chem Scand. 26 (1972) 4084, *ibid.*, A28 (1974) 363.
- 4 K. Nakano, T. Sugimoto and H. Suzuki, J. Phys. Soc. Japan 45 (1978) 236.
- 5 J.B. Birks: Photophysics of Aromatic Molecules (Wiley, London (1970) 44-52).
- 6 L.B.Å. Johansson, Å. Davidsson, G. Lindblom and K. Razi Naqvi, Biochemistry 18 (1979) 4249.
- 7 G. Lauer, W. Schäfer and A. Schweig, Tetrahedron Letters 45 (1975) 3939.
- 8 M.H. Palmer, I. Simpson and R.J. Platenkamp, J. Mol. Struct. 66 (1980) 243.
- 9 P. Hemmerich, G. Nagelschneider and C. Veeger, FEBS Letters 8 (1970) 69.
- 0 T.C. Bruice, Acc. Chem. Res. 13 (1980) 256.
- 1 N. Tanaka, T. Ashida, Y. Sasada and M. Kakudo, Bull. Chem. Soc. Japan 42 (1969) 1546.

7 ON THE ENIGMA OF OLD YELLOW ENZYME'S SPECTRAL PROPERTIES

7.1. INTRODUCTION

The spectral changes induced by the binding of a low molecular weight compound to Old Yellow Enzyme (OYE) were initially regarded to be sufficiently mysterious to refer to this unknown compound as "regreening factor"¹. After the identification of this "regreening factor" as 4-hydroxybenzaldehyde², Abramovitz and Massey³ showed that OYE has a strong affinity for a large variety of phenolic compounds. *Para*-substituted phenolate anions all bind strongly to OYE a FMN containing macromolecule, and all cause similar spectral changes upon binding³. These changes are: 1) an appreciable decrease of the FMN absorbance over the entire absorption spectrum and 2) a concomitant appearance of a new broad absorption band centered at long wavelength (500-600 nm, dependent on the particular phenolate anion bound to OYE³). The latter band was assigned to a charge transfer (CT) transition from phenolate (donor) to enzyme-bound FMN (acceptor), an assignment entirely based on the existence of a positive correlation between the energy of the CT transition ($h\nu_{CT}$) and the Hammett σ_p constant of the phenolic compound used to induce the transition³.

However, this concept, presented as physical evidence for a charge transfer transition³, can be criticized. The references cited by Abramovitz and Massey³ in support of the $h\nu_{CT}-\sigma_p$ correlation^{4,5} provide experimental evidence for such a correlation only with the σ_p of the *acceptor* instead of the donor molecule. The possibility of a correlation with the donor σ_p is only mentioned in the original paper⁵ without rigorous experimental support. Additionally, part of the correlation is regarded as "certainly accidental"⁴, since the Hammett constant, being a typical ground state parameter⁶ is not always the proper quantity to correlate to excited state properties.

Instead of the foregoing procedure, the energy of a CT transition is usually correlated with the ionization potential (I_D) of the donor⁷⁻¹². Within a first approximation, $\bar{\nu}_{CT}$ (in cm^{-1}) should obey the relation⁷⁻¹²:

$$hc\bar{\nu}_{CT} = I_D - E_A - W \quad (7.1)$$

in which h denotes Planck's constant, c the velocity of light in vacuum, E_A the electron affinity of the acceptor and W an appropriate correction term for the

difference in interaction between donor (D) and acceptor (A) in the ground and (excited) CT states, respectively. In fact eq. (7.1) was used to estimate ionization potentials from CT absorptions before photoelectron spectroscopy became widely available. In the case of OYE, E_A is constant as long as no artificial flavins are recombined with the apoenzyme. Hence, a necessary condition for a linear relationship between the Hammett constant of the phenolate ion bound to OYE and $\bar{\nu}_{CT}$ is the requirement that $I_D - W$ should be proportional to σ_p . Since I_D itself does not satisfy this condition¹³ it is unlikely that $I_D - W$ should do so. On the contrary, W is expected to be nearly a constant in the case of OYE, because it is the protein and not the FMN prosthetic group which is responsible for the phenolate binding³. This is confirmed by binding constants of complexes between free phenols and free flavins in solution^{14,15} which are several orders of magnitude less than for OYE-phenol complexes³. Moreover, the former complexes behave spectrally completely different from OYE^{14,15}. This leaves only one possible correlation, i.e. the proportionality of $\bar{\nu}_{CT}$ and I_D which is normally found for CT complexes⁷⁻¹².

Ionization potentials of *para*-substituted phenols have been measured by photoelectron spectroscopy^{13,16-20}. There is no ambiguity whatsoever in the assignment of the observed first and second ionization potentials to the phenolic $5b_2$ and $1a_2$ (π) orbitals, respectively²¹. These orbitals originate from the splitting of the symmetry-degenerate benzene e_{1g} orbitals upon lowering the benzenoid D_{6h} symmetry to the phenolate C_{2v} symmetry^{13,16-20}. Subsequent lowering of the symmetry to C_s (neutral phenol), does not appreciably affect the character of these orbitals, it only decreases their energies^{13,16-20}. Accordingly, the $3b_2$ (originally benzene e_{1gS}) orbital has its nodal plane through the bonds between the *ortho* and *meta* positions and the $1a_2$ (originally benzene e_{1gA}) orbital has a nodal plane which contains the C-O group and the *para* position. The $3b_2$ orbital thus has a large density on the C-O group and the *para* position and is, therefore, very sensitive to *para*-substitution, both through inductive and mesomeric effects, whereas the $1a_2$ orbital is relatively insensitive to *para*-substitution^{13,16-20}. In neutral phenols, the oxygen lone pair ($6b_1$) is located at least 3 eV below $3b_2$. Removal of the OH proton to form the phenolate anion will, of course, raise $6b_1$ considerably but, regarding the fact that in the ion all orbitals will be raised and that the phenolate lowest excited singlet state is a π^* state²², a reversal of $6b_1$ and $3b_2$ apparently does not occur.

Photoelectron spectroscopy^{13,16-20} revealed an increasing first ionization potential ($3b_2$ orbital) in the series *p*-cresol, *p*-bromophenol, phenol, *p*-chlorophenol, *p*-fluorophenol. If this trend is not greatly affected in the cor-

responding phenolate anions (as suggested by preliminary unpublished calculated data, not surprising since $3b_2$ is a π orbital), the first ionization potential of the phenolate anions does not correlate at all with the observed $\bar{\nu}_{CT}$ of OYE in the sense of eq. (7.1).

Thus the assignment of the long-wavelength absorption band of OYE-phenol complexes to a CT transition, although at first sight reasonable, can be questioned. Resonance Raman spectra of OYE published recently^{23,24} were also interpreted more or less on the prejudice of CT interaction. Additionally, the strong perturbation of the flavin absorption spectrum upon the binding of phenols to OYE seems to be at variance with CT interactions rather than to support it, as claimed by Abramovitz and Massey³. This follows from experiments by McConnell *et al.*⁸ who demonstrated that the acceptor singlet \rightarrow singlet transitions "are not greatly affected" in CT complexes.

Despite these questions, there remains a wealth of experimental data^{1-3,23,24} which must fit into some unambiguous interpretation. This consideration and our previous experience with isoalloxazine spectroscopy²⁵⁻²⁸ prompted us to a further examination of this highly intriguing flavoprotein by a variety of spectroscopic techniques. The importance of such an investigation goes beyond a characterization of OYE alone since the protein was regarded as a model system for other flavoproteins³ which, under certain conditions, exhibit long-wavelength absorptions, too. We consider this a hazardous concept, however. Although OYE marked the start of flavin chemistry, 50 years ago, it still appears to be the least understood flavoprotein known nowadays. This will be demonstrated by the present results, providing clear evidence for the inadequacy of the model of simple CT interaction and the existence of a highly intricate FMN-apoenzyme complex. Despite interesting observations, due to the complexity of the system the results allow only for a few firm conclusions.

7.2. MATERIALS AND METHODS

Old Yellow Enzyme and 4-hydroxy-N-*n*-butylbenzamide (4-HNBBA) were prepared and purified as described by Abramovitz and Massey³. Low-temperature glasses (77-153 K) were freshly prepared by freezing mixtures of 0.45 volume of a solution of OYE in 50 mM sodium pyrophosphate buffer (pH 8.5) and 0.55 volume of glycerol (Merck, fluorescence microscopy grade). The glycerol used was free from luminescence under irradiation with a 1600 W Xe-arc source, as far as could be established with our detection system capable of determining quantum yields^{25,26} as low as 10^{-6} . 4-Methoxybenzaldehyde was purchased from Fluka and distilled prior to use.

Spectra and lifetimes were measured on the same equipment as used previously^{25,26}. In the fluorescence lifetime measurements, the extension to longer wave-

lengths than those available from the CR-5 model argon ion laser was made by the method of synchronous pumping^{29,30} as described in Chapter 2 (pp. 10-13). Pumping of the dye laser at 514.5 nm (19436 cm^{-1}) with 2.1 W average mode-locked power yielded 300 mW average mode-locked power at 590 nm (16950 cm^{-1}).

Circular dichroic absorption was measured on a Jouan dichrograph, described in detail in the literature³¹. Electron paramagnetic resonance spectra were measured on a Bruker 200-tt-esr spectrometer equipped with a liquid helium cooling system.

CNDO/S-CI calculations on isoalloxazine phenol-complexes were performed using parameterization and isoalloxazine molecular geometry from previous work^{27,28}. The phenol molecular structure was taken from the literature^{32,33}.

7.3. RESULTS AND DISCUSSION

7.3.1. Absorption and CD spectra

Absorption and CD spectral data on native (free) Old Yellow Enzyme and its 4-hydroxy-N-n-butylbenzamide (4-HNBBA) complex are collected in Fig. 7.1. At room temperature, the well-known spectral properties³ are observed (Fig. 7.1A). Although native OYE has flavin-like absorption characteristics, there are distinct differences with free FMN under identical conditions, the most important being the considerably red-shifted long-wavelength absorption band: maximum at 21700 cm^{-1} (461 nm) as compared to 22500 cm^{-1} (444 nm) in free FMN³⁴. This red shift is considerably larger than usually observed for the isoalloxazine $S_0 \rightarrow S_1$ transition upon changing the solvent polarity^{25,26}. Also the maximum of the near UV transition is slightly red-shifted as compared to free FMN, but this behaviour is usual for the isoalloxazine $S_0 \rightarrow S_2$ transition²⁸. Apart from the appearance of the new absorption band centered at 16750 cm^{-1} (597 nm), the most marked change induced by the binding of 4-HNBBA to OYE is a decrease of the absorbance over the entire flavin spectrum and a blue-shift of the 21700 cm^{-1} (461 nm) band maximum, returning to the position of free FMN. From this observation the questions arise whether the shoulder in the spectrum of native OYE at 20500 cm^{-1} (488 nm) is the electronic $S_0 \rightarrow S_1$ 0-0 transition or not and whether the shift observed is real or apparent, i.e. implies a change in electronic excitation energy or a change in Franck-Condon envelope as observed previously²⁵.

To answer these questions, CD and low-temperature absorption spectra were measured (low-temperature CD spectra could not be measured reliably due to instrumental limitations). Our CD spectra agree closely with those measured by Otani *et al.*³⁵. In the native enzyme, only the $S_0 \rightarrow S_2$ transition displays circular dichroic absorption (Fig. 7.1B). This is a remarkable observation since optical activity of *all* transitions in flavins, carrying a ribityl side chain or

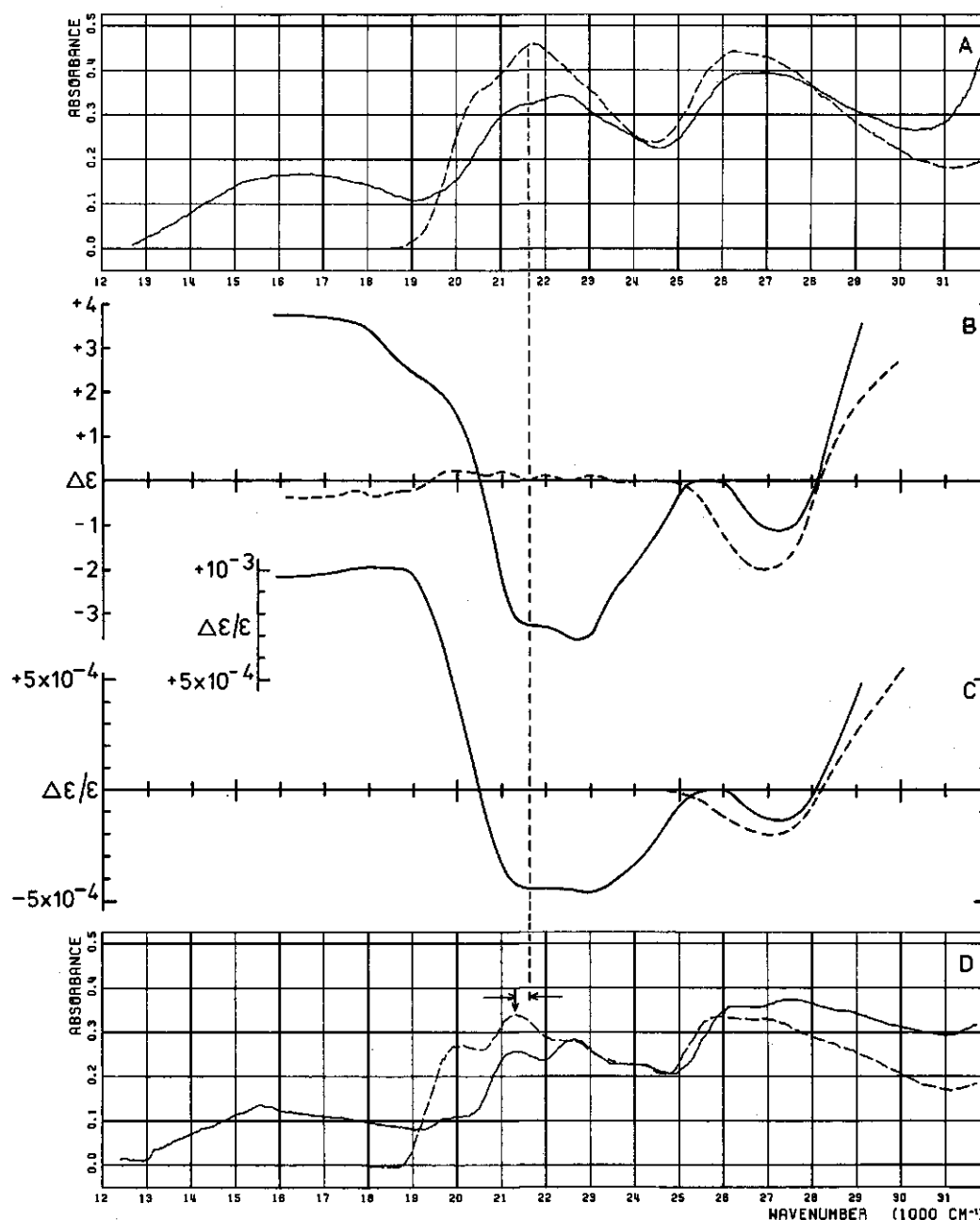


Figure 7.1. Absorption and CD spectra of Old Yellow Enzyme in 50 mM sodium pyrophosphate buffer (pH 8.5). ----- native enzyme; — OYE - 4-hydroxy-N-n-butylbenzamide complex, molar ratio 1:1. OYE concentrations³ based on $\epsilon(21645\text{ cm}^{-1} = 462\text{ nm}) = 10600\text{ M}^{-1}\text{cm}^{-1}$. A: Absorption spectra at 293 K, $c = 43.3\text{ }\mu\text{M}$. B: CD spectra at 293 K, $c = 84.9\text{ }\mu\text{M}$. C: Kuhn's anisotropy factor³¹ $g = \Delta\epsilon/\epsilon$ calculated from A and B. D: Absorption spectra at 143 K, $c = 32.1\text{ }\mu\text{M}$ (details in Section 7.2).

a derivative of it, is a rule rather than an exception, a fact well-established by experiment³⁶⁻⁴⁰ and theory. From the thorough quantum mechanical treatment of optical activity by Caldwell and Eyring⁴¹, it is known that CD occurs in case of a non-zero value of the rotational strength R_{On} , containing the scalar product of the electric and magnetic transition dipole moments of a particular transition $S_0 \rightarrow S_n$:

$$R_{On} = \text{Im}(\langle S_0 | \boldsymbol{\mu} | S_n \rangle \cdot \langle S_n | \mathbf{m} | S_0 \rangle) \quad (7.2)$$

$$\boldsymbol{\mu} = e \sum_i \mathbf{r}_i \quad ; \quad \mathbf{m} = (e/2mc) \sum_i [\mathbf{r}_i \times \mathbf{p}_i]$$

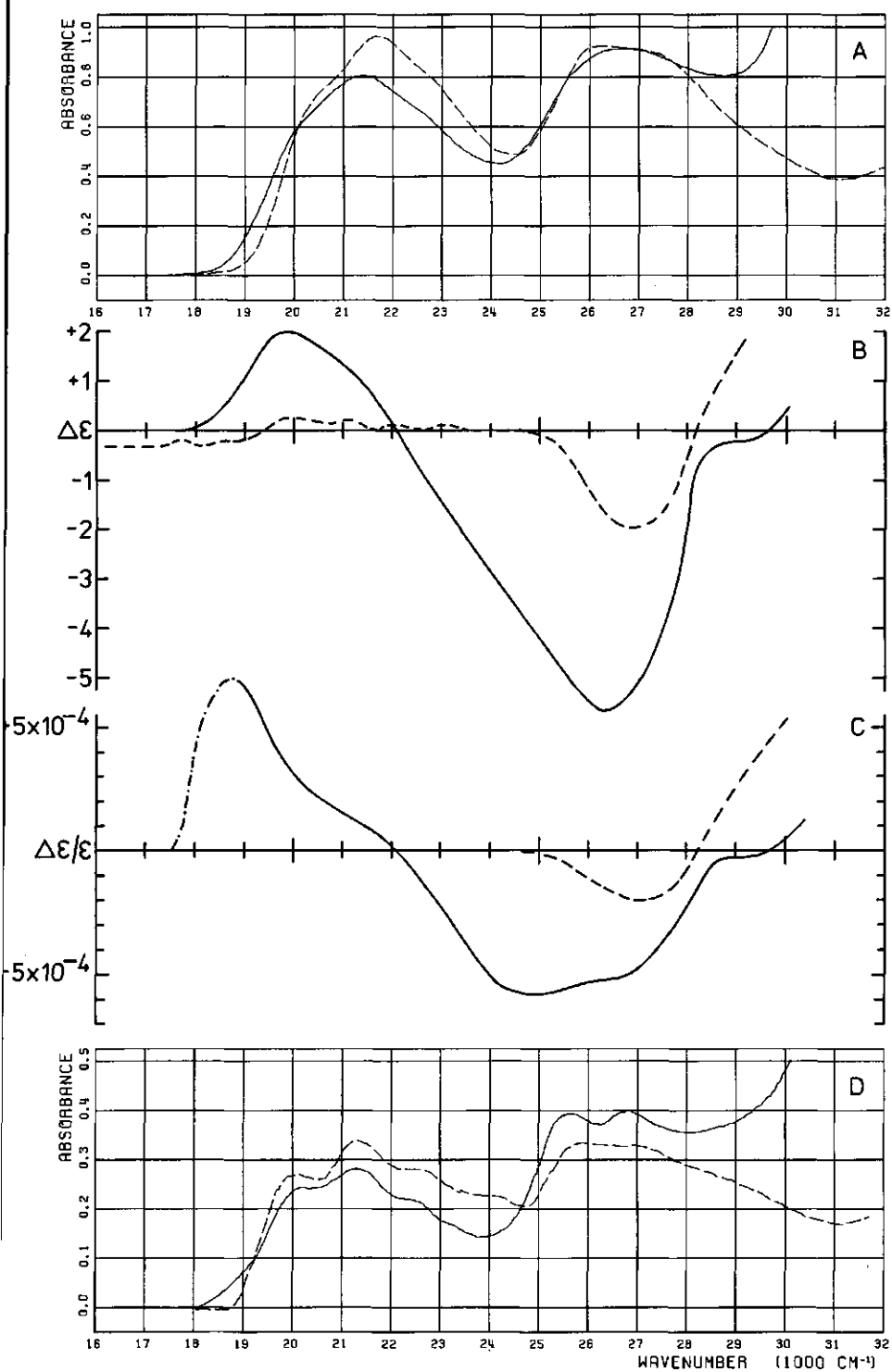
in which e and m represent the electronic charge and mass, respectively, c the velocity of light and \mathbf{r}_i the position vector of electron i with conjugate momentum \mathbf{p}_i . The summation runs over all electrons in the molecule.

The optical transitions of the isoalloxazine ring system, belonging to the molecular point group C_s , fall into the category of both electrically and magnetically dipole-allowed, but possessing perpendicular moments⁴¹ $\boldsymbol{\mu}$ and \mathbf{m} . Hence, R_{On} vanishes intrinsically. However, the slightest perturbation is sufficient to produce a non-zero value, requiring only the generation of a component of $\boldsymbol{\mu}$ in the direction of \mathbf{m} , and *vice versa*. Possible perturbations are: 1^o the presence of chiral centers in substituents like the ribityl side chain-and 2^o hindered rotation of the methyl substituents of protein-bound flavins (distortion of the isoalloxazine ring from planarity is energetically less favourable in the oxidized form⁴²). In principle, these perturbations, both present in OYE, induce optical activity in every electronic transition. Nevertheless, in native OYE, dichroism is completely absent in the flavin $S_0 \rightarrow S_1$ region and weak in the $S_0 \rightarrow S_2$ region (Fig. 7.1B). For the $S_0 \rightarrow S_1$ transition, having a large moment^{25,26,28} $\boldsymbol{\mu}$, it would be fortuitous that hindered rotation of methyl groups alone should be capable of compensating the effect of chirality of the FMN D-ribose side-chain. An attractive alternative explanation would be a complex of FMN with a L-amino acid in the apoprotein, presumably L-tyrosine, which has been indicated to be involved in the binding of FMN to the apoprotein^{34,43}. The substantial difference in character between the isoalloxazine S_1 and S_2 electronically excited states²⁸ is likely the reason why the dichroism of the $S_0 \rightarrow S_2$ transition is not fully compensated in the complex of FMN with the apoprotein. In previous work²⁸, we showed this transition to contain both $n\pi^*$ and $\pi\pi^*$ character and it was found that rotation of methyl substituents considerably affects $\sigma-\pi$ separation in orbitals localized on the isoalloxazine carbonyl groups²⁷. It is well-known that carbonyl $n\pi^*$ transitions have large intrinsic magnetic transition moments⁴¹, hence for the isoal-

loxazine $S_0 \rightarrow S_2$ we encounter the situation of a relatively small μ ($\pi\pi^*$ component more or less sign-forbidden²⁸) and a relatively large m . This situation is particularly sensitive to external perturbation, which may explain the difference in circular dichroic absorption observed for the two long-wavelength bands in native OYE (Fig. 7.1B).

Upon binding to OYE, 4-HNBBA apparently interferes strongly with the existing FMN-apoenzyme complex, regarding the dichroism induced over the entire spectrum. An overall positive $\Delta\epsilon$ is measured for the new absorption band at 16750 cm^{-1} (597 nm). There is, however, a distinct shoulder in the CD spectrum around 19000 cm^{-1} (526 nm) whereas the FMN $S_0 \rightarrow S_1$ region displays a strong negative $\Delta\epsilon$ with a band shape resembling the molecule's ordinary absorption under similar conditions. To establish the FMN $S_0 \rightarrow S_1$ 0-0 location in the spectrum (*vide supra*), we made use of the general property of an electric dipole-allowed transition that Kuhn's anisotropy factor ($g = \Delta\epsilon/\epsilon$) is constant over the vibrational progression belonging to that transition^{31,41}. In Fig. 7.1C this factor is plotted versus the wavenumber, a graph which clearly shows the presence of an electronic origin at 21300 cm^{-1} (469 nm) and a vibrational progression of $\sim 1250 \text{ cm}^{-1}$ in the spectrum of the complex. The low-temperature absorption spectra (Fig. 7.1D) confirm this conclusion. It was established that the addition of glycerol to OYE solutions did not affect the spectral properties at room temperature. At 143 K native OYE shows four subbands in its $S_0 \rightarrow S_1$ region, suggesting the origin to be located at 20150 cm^{-1} (496 nm). However, this apparent origin has no counterpart in the CD spectra and it almost vanishes upon complexation with 4-HNBBA. The loss of intensity upon complexation ($\sim 80\%$ as estimated by rough deconvolution) is far too much to ascribe to a change in Franck-Condon factors as observed for free isoalloxazines²⁵. Moreover, if the 20150 cm^{-1} (496 nm) subband were the origin of the band extending to $\sim 25000 \text{ cm}^{-1}$ (400 nm), the Franck-Condon envelope of this band in the OYE - 4-HNBBA complex would strongly deviate from that of a common electric dipole-allowed electronic transition⁴⁴. Thus it may be concluded that the 20150 cm^{-1} (496 nm) and 21300 cm^{-1} (469 nm) bands represent different electronic origins and, presumably, even belong to different species. This conclusion is further supported by the low temperature absorption spectrum of free FMN under the same conditions, in which the $S_0^0 \rightarrow S_1^0$ band origin is located at 21300 cm^{-1}

Figure 7.2. Absorption and CD spectra of Old Yellow Enzyme and its 4-methoxybenzaldehyde complex, molar ratio 1:1. For details cf. legend to Fig. 7.1. Deviating conditions: A and B: $c = 90.8 \text{ }\mu\text{M}$. C: ----- part of the g-curve which can only be estimated owing to extremely small numerical values of $\Delta\epsilon$ and ϵ .



(469 nm) and in which the $S_0 \rightarrow S_1$ band displays a vibrational progression of 1250 cm^{-1} , identical to the spectra of alkylated isoalloxazines in apolar solvents²⁵. The formation of the glycerol-water glass only shifts the whole vibrational pattern between 19000 cm^{-1} (526 nm) and 25000 cm^{-1} (400 nm) by 400 cm^{-1} to the red (Fig. 7.1D). It is thus immediately clear that, in the *flavin spectral region*, the absorption spectra of the OYE-phenolate complex and free FMN have a closer resemblance than the absorption spectra of the native enzyme and free FMN. The only influence exerted by the complexing agent is a change in the relative intensities of the spectral bands without any observable energy shift.

In support for CT complex formation, Abramovitz and Massey³ suggested identical intermolecular interactions between OYE and 4-methoxy-benzaldehyde (4-MBA) and between OYE and 4-HNBBA, except for the inability of 4-MBA to produce the long-wavelength band. When the foregoing experiments were repeated with 4-MBA (Fig. 7.2), it turned out that the interaction of the latter molecule with OYE is totally different. Instead of a decrease of the intensity of the 20150 cm^{-1} (496 nm) absorption band, a relative increase was observed. The intensity-changes are moderate, however, and can be sufficiently explained in terms of changes of Franck-Condon factors²⁵. Also the CD spectrum of the complex with 4-MBA was completely different from that with 4-HNBBA. Although the former CD spectrum is less well-defined than the latter one, it still indicates the presence of an electronic transition around 20000 cm^{-1} (500 nm). Clearly, the differences between the effects induced by 4-HNBBA and 4-MBA must be ascribed to the presence of a charged group in the former, but there cannot be a direct influence of the charge on the observed CD spectrum in the sense of a Stark-effect, since this effect is, contrary to the Zeeman-effect, not accompanied by circular polarization phenomena⁴⁵. Thus the properties observed, including the long-wavelength absorption in the OYE-phenol complexes, must be due to an indirect mechanism, i.e. changes induced in the existing FMN-apoenzyme complex depending on the molecule bound to it.

7.3.2. Luminescence spectra

In order to establish a useful standard to which the OYE luminescence experiments could be referred to, we first investigated purified free FMN under identical conditions. Following the same procedures as previously in the measurements on alkylated isoalloxazines^{25,26}, the following data were obtained:

293 K: fluorescence quantum yield $\phi_f = 0.48$, radiative lifetime $\tau_0 = 13.8$ ns, fluorescence actual lifetime $\tau_f = 5.7$ ns, $\tau_f/\tau_0 = 0.41$; **143 K:** $\phi_f = 0.70$, $\tau_0 = 2.5$ ns, $\tau_f = 9.3$ ns, $\tau_f/\tau_0 = 0.74$, phosphorescence quantum yield $\phi_p = 5.0 \times 10^{-3}$, phosphorescence actual lifetime $\tau_p = 224$ ms. The difference in τ_0 between 293 and 143 K is due to the change in the medium refractive index²⁶ upon glycerol addition. The FMN excitation spectra were independent of the detection wavelength and all fully matched the absorption spectra measured under the same conditions. Decay curves were all singly exponential. Thus, the behaviour of FMN is identical to that of the alkylated isoalloxazines measured previously^{25,26}, including the influence of the rigidity of the medium on the Franck-Condon factors governing the intensity of vibronic subbands^{25,26} and the good agreement between ϕ_f and the ratio τ_f/τ_0 . The addition of phenols in *stoichiometric* amounts did not measurably alter these FMN data, in conformity with earlier results by Yagi and Matsuoka¹⁴, who showed that a considerable excess of phenol is needed to give a measurable riboflavin fluorescence quenching. For FMN the situation is even less favourable owing to the negatively charged groups in both FMN and phenolate under our experimental conditions (pH 8.5).

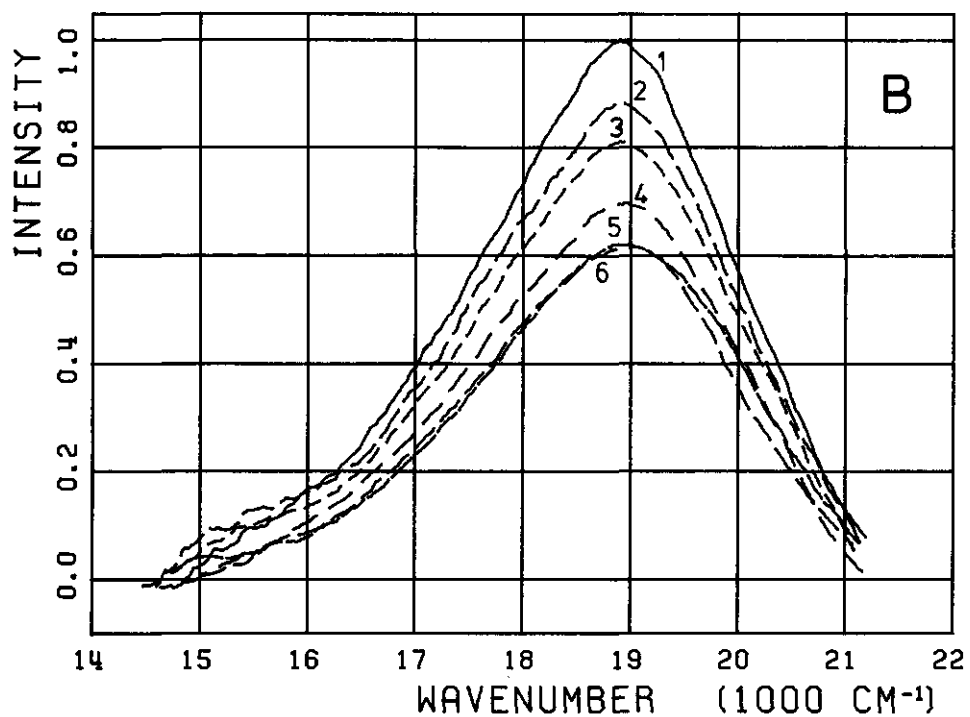
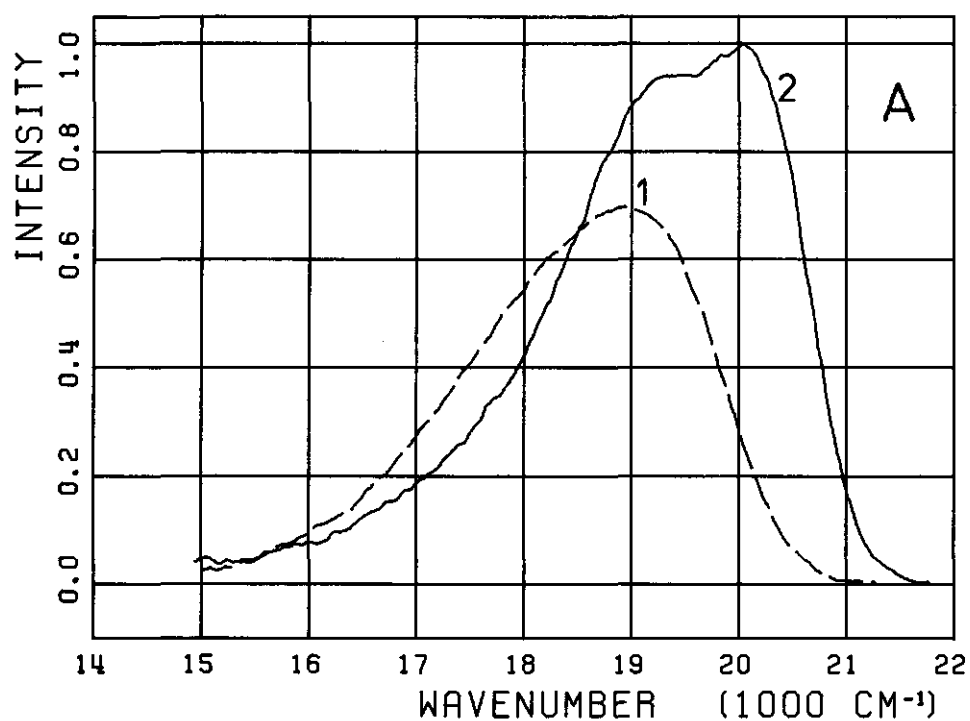
The most striking result of the luminescence experiments on OYE is the complete absence of any difference in the shapes of the spectral bands and decay curves between the native enzyme and its complexes with phenols or 4-MBA, except for one measurement: the emission spectrum observed with 30000 cm^{-1} (333 nm) excitation (*vide infra*). The only effect of the addition of complexing agents is an overall decrease of the luminescence quantum yields (Figs. 7.3 and 7.4). Upon 21300 cm^{-1} (469 nm) or 22500 cm^{-1} (444 nm) excitation, the OYE prompt and delayed emission spectra resemble those of free FMN under identical conditions. At room temperature, OYE has a $\phi_f = 1.4 \times 10^{-3}$ upon 21300 cm^{-1} (469 nm) or 22500 cm^{-1} (444 nm) excitation. An estimate of the free FMN concentration under our experimental conditions, using the known binding constants of flavins to the apoenzyme of OYE³, yields the same order of magnitude as ϕ_f . Thus the emission of OYE in fluid solution originates predominantly from free FMN, confirmed by identical fluorescence lifetimes of OYE and FMN (Table 7.1) and a very low degree of polarization (p) of the OYE luminescence. By the same method as previously²⁵, we determined a value of $p = 0.04$ at 293 K, for both the native and complexed enzyme. Since τ_f is not affected by phenolate binding (Table 7.1), the apparent quenching of the fluorescence upon phenol addition (Fig. 7.3B) must be ascribed to an increased binding of FMN to apo-OYE as observed by Abramowitz and Massey³ for the OYE-phenol complexes. At 143 K, the quantum yield of native OYE increases to $\phi_f = 7.5 \times 10^{-3}$, a larger increase than in case of free

FMN. Also the vibronic structure in the emission spectrum of OYE is more manifest than in that of FMN. Apparently, also protein-bound FMN contributes slightly to the luminescence in solid solution. For the native enzyme $\phi_p = 3.6 \times 10^{-5}$ at 143 K. Both ϕ_f and ϕ_p reduced by ~60% in the phenolate complexed enzyme, similar to the data obtained at room temperature. The value of ϕ_p was too low to allow for an accurate measurement of phosphorescence excitation spectra.

Upon excitation at higher wavenumber ($30000 \text{ cm}^{-1} = 333 \text{ nm}$), we discovered a second emission in OYE (Figs. 7.4A,B). Also this emission is partly quenched when the OYE-phenolate complex is formed. It is centered at 22500 cm^{-1} (444 nm) in fluid solution (both in buffer and in buffer-glycerol mixtures) and at 25500 cm^{-1} (392 nm) in solid solution, a blue shift of 3000 cm^{-1} on going to glassy solution. Such a shift is too large to be explained by changes in Franck-Condon factors. Only the change in the shape of the $19000 - 20000 \text{ cm}^{-1}$ (526 - 500 nm) band upon complex formation (Fig. 7.4A) might be explained in this way because this phenomenon was not observed in glassy solution. It possibly indicates some protein-bound FMN emission, sensitized by high-energy excitation, since isoalloxazines in an apolar environment show a tendency to an increased $S_0 + S_1$ 0-0 emission intensity²⁵. A third band observed upon UV-excitation (Fig. 7.4A), had a constant energy-difference with the exciting light and can be assigned, therefore, to Raman scatter from the fundamental $\nu_1 = 3654.5 \text{ cm}^{-1}$ (A_1) of the water molecule⁴⁶.

The low-temperature fluorescence spectra (Fig. 7.4B) have roughly similar phosphorescence counterparts (Fig. 7.4C). Phosphorescence lifetime measurements indicated the presence of two triplet states. The first one, corresponding to the band at 16700 cm^{-1} (599 nm) with a lifetime of 206 ms, can clearly be assigned to FMN regarding the fact that the lifetime corresponds to that of free FMN. Moreover, alkylated isoalloxazines generally have a first excited triplet state²⁵ at 16700 cm^{-1} (599 nm). The second one, corresponding to the 20500 cm^{-1} (488 nm) band with a lifetime of 800 ms, has still to be assigned. The location and life-

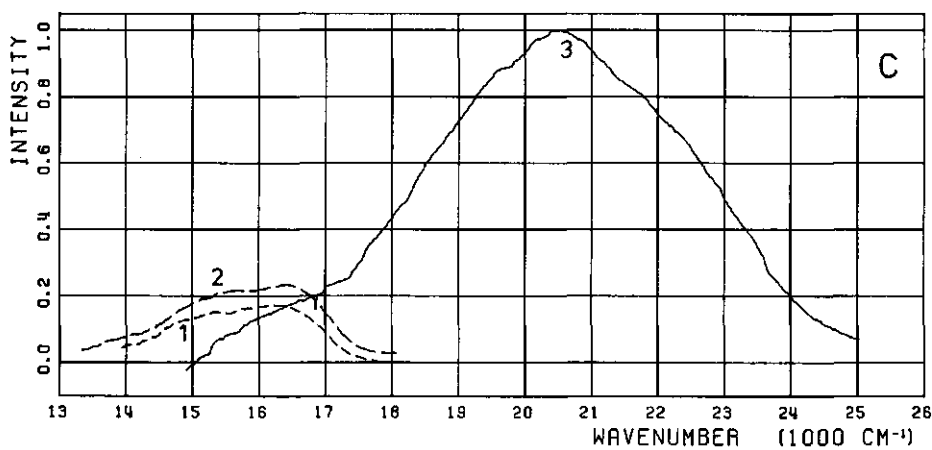
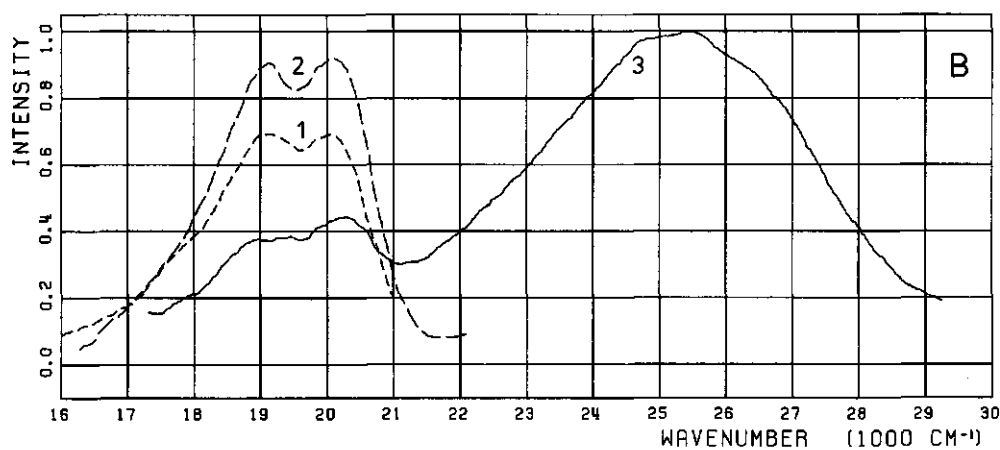
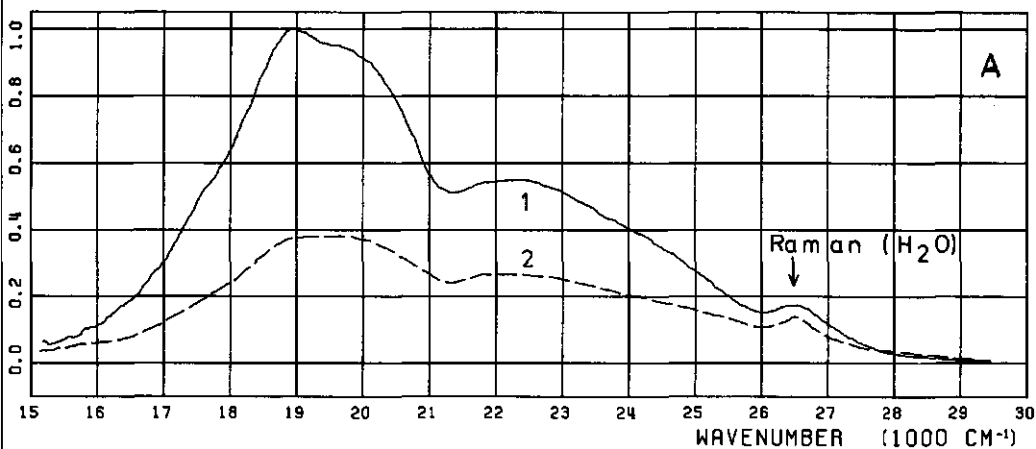
Figure 7.3. Prompt emission of flavin mononucleotide (FMN) and Old Yellow Enzyme in 50 mM sodium pyrophosphate buffer (pH 8.5), excitation at 21300 cm^{-1} (469 nm). A: FMN, $c = 56.1 \text{ } \mu\text{M}$, excitation bandwidth $\Delta\nu_{\text{ex}} = 88 \text{ cm}^{-1}$, detection bandwidth $\Delta\nu_{\text{em}} = 32 \text{ cm}^{-1}$; curve 1: 293 K; curve 2: 143 K (glycerol-water glass as described in Section 7.2, spectra corrected for wavelength-dependence of lamp intensity and detector sensitivity). B: OYE, $c = 24.1 \text{ } \mu\text{M}$ (cf. legend to Fig. 7.1), $\Delta\nu_{\text{ex}} = 132 \text{ cm}^{-1}$, $\Delta\nu_{\text{em}} = 86 \text{ cm}^{-1}$, $T = 293 \text{ K}$, samples contain 4-hydroxy-N-n-butylbenzamide in a molar ratio with respect to OYE of 0.00 (curve 1), 0.25 (2), 0.50 (3), 0.75 (4), 1.00 (5) and 1.25 (6).



times of the delayed emissions were not affected by the presence of phenols within the experimental uncertainty of $\sim 8\%$. In the spectral overlap region ($15000 - 18000 \text{ cm}^{-1} = 667 - 556 \text{ nm}$), a double exponential decay was observed which contained both above-mentioned lifetimes in a ratio proportional to the (estimated) overlap of the spectral bands. Outside this region, the phosphorescence decay was a single exponential.

The excitation spectra (Fig. 7.5) confirm our foregoing conclusion that the 20150 and 21300 cm^{-1} bands (496 and 469 nm) in the absorption spectrum of the native enzyme belong to different electronic transitions. Below 29000 cm^{-1} (345 nm), the excitation spectra of the $\sim 19000 \text{ cm}^{-1}$ (526 nm) prompt emission band are identical to those of free FMN. They only have a tendency to tail far into the red, even in the native enzyme, but there is no distinct band or shoulder at 20150 cm^{-1} (496 nm) like in the absorption spectrum. Apparently, the species excited at the latter wavenumber is non-fluorescent. In the near ultraviolet, the excitation spectra have bands which are hidden in the absorption spectra and cannot be assigned to FMN since they appear between the FMN $S_0 \rightarrow S_2$ and $S_0 \rightarrow S_3$ transitions at 26500 cm^{-1} (377 nm) and 37000 cm^{-1} (270 nm). The former bands appear at 30000 cm^{-1} (333 nm) and 35400 cm^{-1} (282 nm). At room temperature, the excitation spectrum of the 22500 cm^{-1} (444 nm) emission has only the well-defined peak at 35400 cm^{-1} (282 nm). In the 143 K spectra, the intensity gradually dropped upon scanning the exciting light towards the UV (Fig. 7.5B), owing to an increased absorbance and scatter at the cuvette wall as the wavenumber increased. This reduced the depth of penetration of the exciting light into the sample and moved the fluorescent spot out of the detection system focus. This

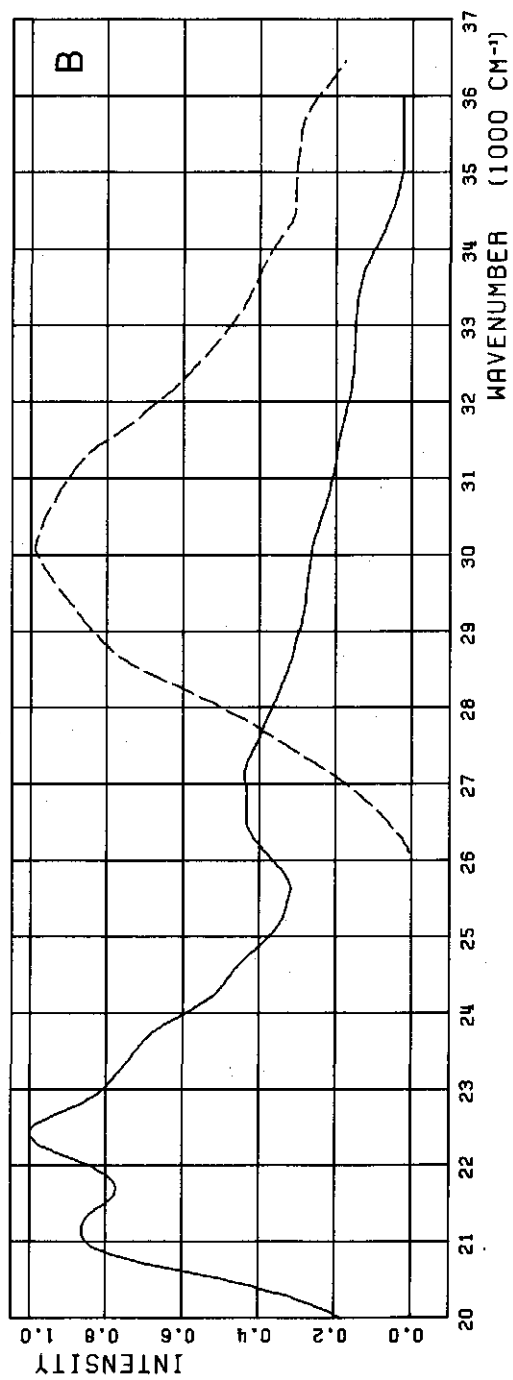
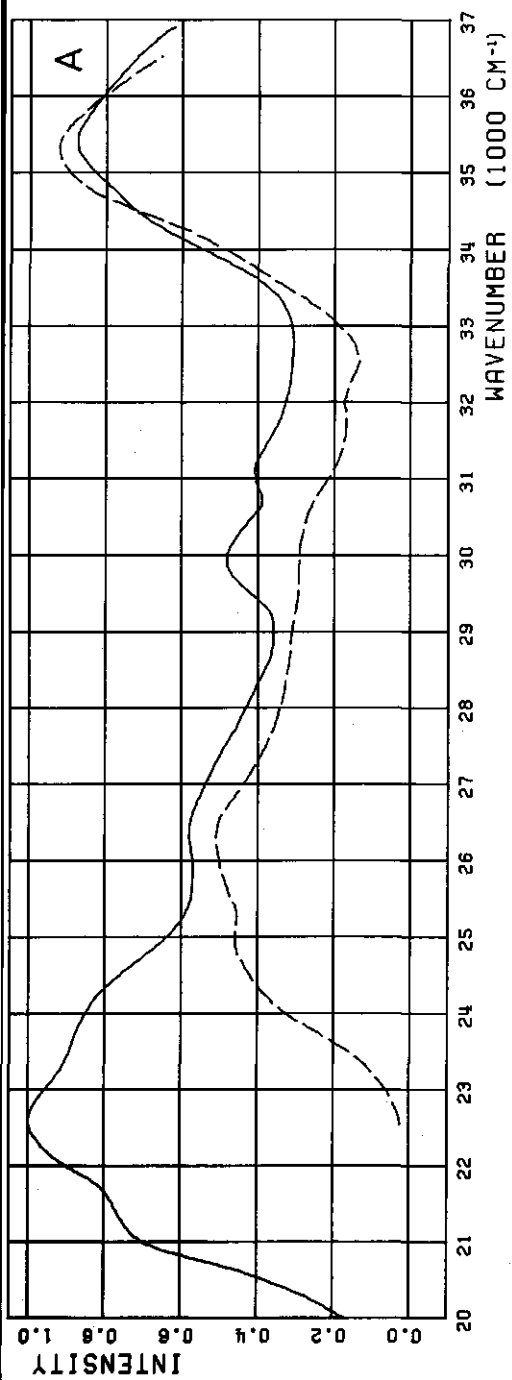
Figure 7.4. Emission spectra of Old Yellow Enzyme (cf. legend to Fig. 7.3 for details). A: Prompt emission, 293 K , $c = 24.1 \text{ }\mu\text{M}$, excitation at 30000 cm^{-1} (333 nm), $\Delta\bar{\nu}_{\text{ex}} = 90 \text{ cm}^{-1}$; curve 1: native enzyme, $\Delta\bar{\nu}_{\text{em}} = 121 \text{ cm}^{-1}$; curve 2: OYE - 4-hydroxy-N-n-butylbenzamide complex (molar ratio 1:1), $\Delta\bar{\nu}_{\text{em}} = 194 \text{ cm}^{-1}$. The Raman band of H_2O originates from the A_1 mode⁴⁶ $\nu_1 = 3654.5 \text{ cm}^{-1}$. B: Prompt emission of the native enzyme at 143 K (emission bands of the OYE-phenol and OYE - 4-MBA complexes are similarly shaped, cf. text), $c = 12.5 \text{ }\mu\text{M}$; curve 1: excitation wavenumber $\bar{\nu}_{\text{ex}} = 21300 \text{ cm}^{-1}$ (469 nm), $\Delta\bar{\nu}_{\text{ex}} = 220 \text{ cm}^{-1}$, $\Delta\bar{\nu}_{\text{em}} = 103 \text{ cm}^{-1}$; curve 2: $\bar{\nu}_{\text{ex}} = 22800 \text{ cm}^{-1}$ (439 nm), $\Delta\bar{\nu}_{\text{ex}} = 205 \text{ cm}^{-1}$, $\Delta\bar{\nu}_{\text{em}} = 114 \text{ cm}^{-1}$; curve 3: $\bar{\nu}_{\text{ex}} = 30000 \text{ cm}^{-1}$ (333 nm), $\Delta\bar{\nu}_{\text{ex}} = 300 \text{ cm}^{-1}$, $\Delta\bar{\nu}_{\text{em}} = 212 \text{ cm}^{-1}$. C: Delayed emission corresponding to B; curve 1: $\bar{\nu}_{\text{ex}} = 21300 \text{ cm}^{-1}$ (469 nm), $\Delta\bar{\nu}_{\text{ex}} = 880 \text{ cm}^{-1}$, $\Delta\bar{\nu}_{\text{em}} = 180 \text{ cm}^{-1}$; curve 2: $\bar{\nu}_{\text{ex}} = 22800 \text{ cm}^{-1}$ (439 nm), $\Delta\bar{\nu}_{\text{ex}} = 820 \text{ cm}^{-1}$, $\Delta\bar{\nu}_{\text{em}} = 180 \text{ cm}^{-1}$; curve 3: $\bar{\nu}_{\text{ex}} = 30000 \text{ cm}^{-1}$ (333 nm), $\Delta\bar{\nu}_{\text{ex}} = 600 \text{ cm}^{-1}$, $\Delta\bar{\nu}_{\text{em}} = 315 \text{ cm}^{-1}$.



problem could not be overcome: lower concentrations gave an unacceptable signal-to-noise ratio and the cryostat did not allow for front-face measurements. The recordable part of the low-temperature excitation spectrum, however, clearly shows two well-defined band systems, one identical to that of free FMN and the other related to the 25500 cm^{-1} (392 nm) emission (Figs. 7.4B and 7.5B). The emission and excitation bands observed at low temperature at 25500 cm^{-1} (392 nm) and 30120 cm^{-1} (332 nm), respectively, even have a rough mirror-image relationship (Figs. 7.4B and 7.5B).

Definitive assignment of the OYE blue emission is, of course, impossible. It must originate from a chromophore which is firmly bound to the protein and not released upon reduction, since it survives both the affinity chromatography purification and the consecutive dialysis in the presence of dithionite³. The emission occurs at a wavenumber which is too low to ascribe it to aromatic amino acids in the apoprotein⁴⁷⁻⁵⁰ or to their excimers⁴⁷. Control experiments with these amino acids confirmed this. Considering alternative assignments, we reject the possibility of reduced nicotinamides⁵¹ because OYE samples did not change their luminescent properties after several days of air exposure. Pyridoxal phosphate⁵² also seems rather unlikely. This would imply the presence of two different prosthetic groups which was never found in preparations of the apoenzyme. A reasonable tentative explanation left is the presence of nucleic acids, which are known to emit in the concerned wavelength region^{47,53,54}, an emission ascribable to excimers⁴⁷. The 3000 cm^{-1} blue shift observed on going to glassy solution, which restricts the mobility of chromophores, would fit into an excimer picture. On the other hand, unless energy transfer processes take place, an excimer picture seems to be at variance with the fact that the 30000 cm^{-1} (333 nm) band in the excitation spectrum at 293 K appears to be predominantly associated with the FMN emission (Fig. 7.5A). Unfortunately, instrumental limitations did not allow for a thorough investigation of the OYE blue emission by time-resolved measurements.

Figure 7.5. Excitation spectra of Old Yellow Enzyme's prompt emission (cf. legend to Fig. 7.3 for details). A: $c = 11.3\text{ }\mu\text{M}$, $T = 293\text{ K}$; solid line: detection wavenumber 19000 cm^{-1} (526 nm), $\Delta\bar{\nu}_{\text{em}} = 361\text{ cm}^{-1}$, $\Delta\bar{\nu}_{\text{ex}} = 200\text{ cm}^{-1}$; dotted line: detection wavenumber 22500 cm^{-1} (444 nm), $\Delta\bar{\nu}_{\text{em}} = 507\text{ cm}^{-1}$, $\Delta\bar{\nu}_{\text{ex}} = 150\text{ cm}^{-1}$. B: $c = 12.5\text{ }\mu\text{M}$, $T = 143\text{ K}$; solid line: detection wavenumber 19000 cm^{-1} (526 nm), $\Delta\bar{\nu}_{\text{em}} = 271\text{ cm}^{-1}$, $\Delta\bar{\nu}_{\text{ex}} = 102\text{ cm}^{-1}$; dotted line: detection wavenumber 25800 cm^{-1} (388 nm), $\Delta\bar{\nu}_{\text{em}} = 499\text{ cm}^{-1}$, $\Delta\bar{\nu}_{\text{ex}} = 60\text{ cm}^{-1}$. Spectra of OYE-phenol and OYE - 4-MBA complexes were identically shaped (cf. text).



The observed fluorescence lifetimes are collected in Table 7.1. Clearly, the decay curves are dominated by the emission of free FMN, which is immediately apparent in the single exponential decay observed at room temperature. At 143 K, the fluorescence decay upon 20987 cm^{-1} (476.5 nm) laser excitation is not a single exponential. Analysis of the decay curves (Table 7.1) revealed two components. The longer lifetime of $\sim 9\text{ ns}$ corresponds to free FMN as confirmed by control experiments. This value is approximately the same as observed from alkylated isoalloxazines²⁵. The shorter lifetime, contributing the most to the decay on the long-wavelength edge of the emission spectrum, remains at long-wavelength excitation with the Rhodamine 6G dye laser. It was the tailing of the excitation spectra into the red which prompted us to perform the latter measurements, although they only gave rise to a clearcut decay curve at 143 K. It is impossible to conclude whether the $\sim 3\text{ ns}$ component has something to do with the long-wavelength absorbance in the OYE-phenol complex or not. It is observed in both native OYE and its complex. Only the overall count rate in the single photon counting experiments on the complex seems to be slightly larger than that on the native enzyme, at a constant power from the dye laser. On the other hand, we would expect to observe at least a change in the contribution of both lifetimes to the total decay in case of 20987 cm^{-1} (476.5 nm) excitation, if the addition of phenol to OYE leads to a CT complex. This is not observed (Table 7.1).

7.3.3. Theoretical data

We attempted to obtain a qualitative picture of possible isoalloxazine-phenolate intermolecular interactions from CNDO/S calculations. From minute comparison of this calculational method with a large variety of experimental data, we already had a good impression of its reliability^{27,28}. Considering alternatives for the charge transfer explanation of Old Yellow Enzyme's spectral behaviour³, the idea of tautomerization arose, i.e. the phenolate anion may interfere with an existing hydrogen-bonded structure between FMN and the apoprotein. As discussed in the section on CD spectra, such a structure, involving a L-tyrosine residue in the apoprotein, was proposed by Theorell^{34,43}. In this structure, tyrosine donates a proton for a H-bond with a flavin carbonyl group and flavin donates its N_3 proton to a H-bond with the apoprotein. This may lead to a flavin tautomeric form (cf. Fig. 7.6). Earlier theoretical⁵⁵ and experimental⁵⁶ work showed that flavin tautomers possess a red-shifted $\text{S}_0 \rightarrow \text{S}_1$ transition. This might explain the 20150 cm^{-1} (496 nm) absorption band of OYE, losing most of its intensity in the phenolate but not in the 4-methoxy-benz-

TABLE 7.1.

LIFETIMES OF THE PROMPT EMISSION OF OLD YELLOW ENZYME (OYE) AND FMN UNDER VARIOUS CONDITIONS a).

Excitation ^{b)}		Detection ^{c)}		Temp. d)		Native OYE				OYE + 4-HNBBA ^{e)} (1:1)				FMN ^{f)}
$\bar{\nu}$ (cm^{-1})	P (mW)	$\bar{\nu}$ (cm^{-1})	$\Delta\bar{\nu}$ (cm^{-1})	Temp. (K)		τ_1 (ns)	τ_2 (ns)	α_1	α_2	τ_1 (ns)	τ_2 (ns)	α_1	α_2	τ (ns)
20,987	50	19,000	245	278		5.7	-	-	-	5.8	-	-	-	5.7
20,987	50	20,400	138	143		3.0	9.3	0.59	0.41	3.3	9.4	0.58	0.42	9.3
20,987	50	19,000	147	143		3.1	9.1	0.66	0.34	3.0	9.4	0.71	0.29	9.2
20,987	50	18,000	175	143		3.4	9.2	0.74	0.26	3.5	9.1	0.75	0.25	9.0
20,987	50	17,500	300	143		3.0	9.3	0.72	0.28	3.2	9.2	0.74	0.26	9.4
20,987	50	17,000	310	143		3.4	9.2	0.77	0.23	3.3	9.5	0.77	0.23	9.1
20,987	50	15,500	1140	143		2.9	9.0	0.75	0.25	3.2	9.3	0.79	0.21	9.3
17,544	300	15,500	1140	278		-	-	-	-	-	-	-	-	-
17,544	300	15,500	400	143		3.2	-	-	-	3.3	-	-	-	-
16,667	18	15,500	400	143		3.4	-	-	-	3.0	-	-	-	-
17,544	300	16,200	1000	143		3.3	-	-	-	3.2	-	-	-	-

a) Decay curves were analyzed in two components according to: $I(t)/I(0) = \alpha_1 \cdot \exp(-t/\tau_1) + \alpha_2 \cdot \exp(-t/\tau_2)$, in which $I(0)$ and $I(t)$ represent the luminescence intensity at times $t = 0$ and t , respectively; b) Using an Ar ion laser or a Rhodamine 6G dye laser (cf. Materials and Methods), P = Average Mode-locked Power; c) Using a Zeiss MM12Q monochromator and a Philips XP2020 photomultiplier; d) 278 K samples in 0.05 M pyrophosphate buffer without glycerol (pH 8.5), 143 K samples as described in Materials and Methods in a glycerol-water glass; e) 4-HNBBA = 4-Hydroxy-N-n-butylbenzamide; f) FMN = Flavin mononucleotide measured under the same conditions as the Old Yellow Enzyme samples.

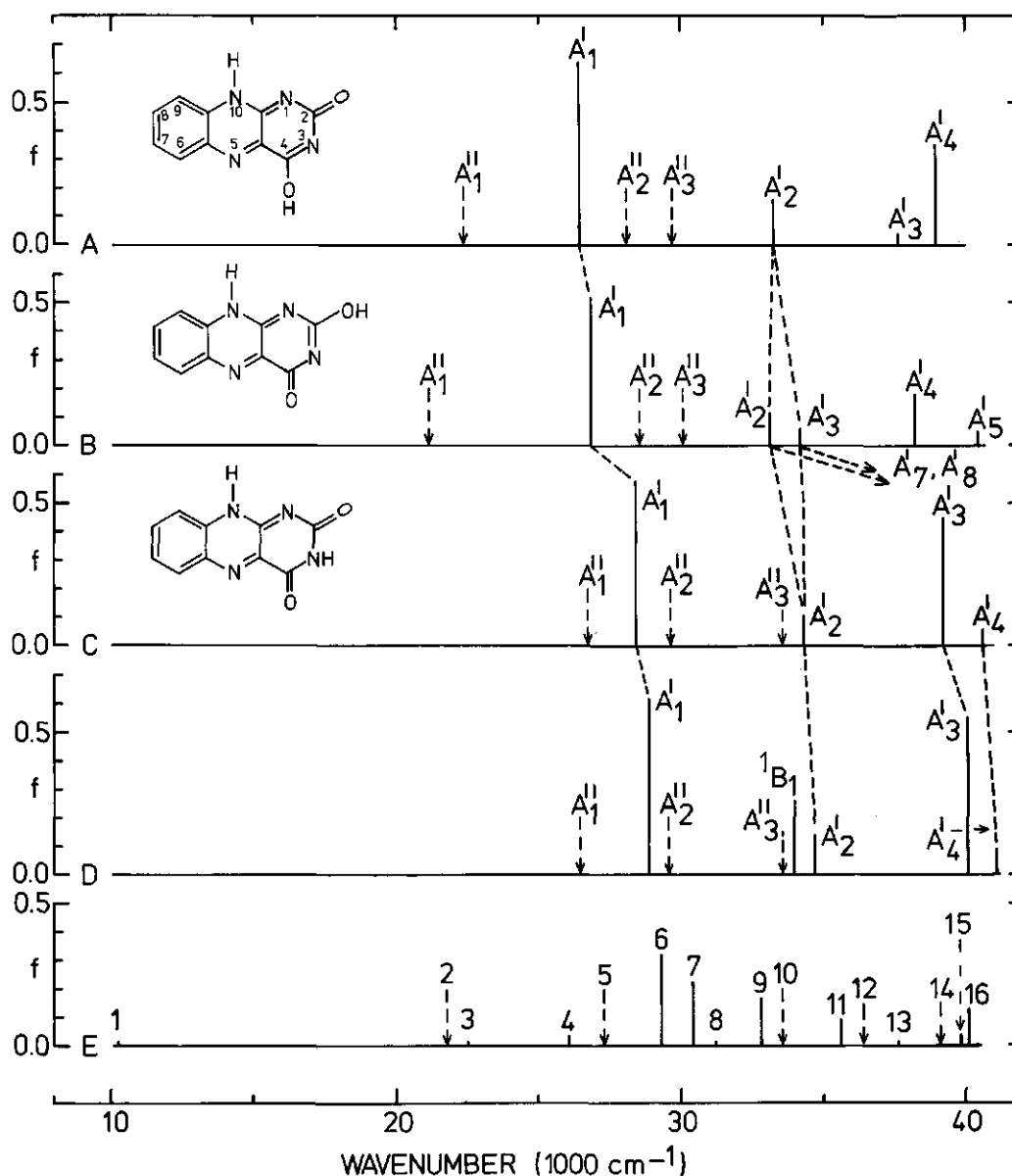


Figure 7.6. Calculated singlet \rightarrow singlet transition energies and oscillator strengths (f) of "ideal" isoalloxazine analogues, CNDO/S-CI method, 100 singly excited singlet configurations^{27,28,61}. Solid stick bars: electric dipole-allowed transitions, dotted arrows: electric dipole-forbidden transitions, main correlations indicated by dotted lines. A and B: isoalloxazine tautomeric forms as indicated; C: "ideal"^{27,28} isoalloxazine; D: stacked complex of C and the phenolate anion, parallel molecular planes (cf. text), interplanar distance 20 Å (2 nm); E: as D, interplanar distance⁶⁰ 3.18 Å (0.318 nm).

aldehyde complex (Figs. 7.1 and 7.2).

Apart from the usual error²⁸ in absolute excitation energies, CNDO/S indeed predicts a stabilization of both the $^1A_1'$ and $^1A_1''$ states in tautomers of "ideal" isoalloxazine^{28,57} (Figs. 7.6A,B). The $^1A_1'$ state retains its character upon tautomerization whereas the $^1A_1''$, obviously, loses it completely. To obtain the tautomers given in Figs. 7.6A,B from "ideal" isoalloxazine (Fig. 7.6C), an energy of the order of 100 kJ mole^{-1} was required (theoretically!), not an insuperable threshold for protein-bound FMN^{34,43}. The protein may also sufficiently compensate the calculated increase of the dipole moment from $\sim 9 \text{ D}$ in "ideal" isoalloxazine to $\sim 13 \text{ D}$ in its tautomers. Within this model, binding of the phenolate anion disrupts the existing FMN-apoprotein hydrogen-bonded structure, leading to the disappearance of the 20150 cm^{-1} (496 nm) absorption band and the formation of a new species absorbing at longer wavelength. The 4-methoxybenzaldehyde molecule, having no proton-withdrawing capability, binds to OYE but does not affect the spectral properties beyond the level of Franck-Condon factor changes. The recurrence of the protein-bound FMN to its keto form restores its circular dichroic absorption for the $S_0 \rightarrow S_1$ transition. Nuclear magnetic resonance experiments with ^{13}C enriched FMN, recombined with the OYE-apoenzyme⁵⁸, support this model. The ^{13}C resonance of C_4 of FMN⁵⁹ (cf. Fig. 7.6) is appreciably downfield shifted upon binding to apo-OYE and this resonance shifts back towards the value of free FMN upon subsequent phenol addition⁵⁸. Thus, provided the model outlined above is correct, the $\text{CO}(4)$ rather than the $\text{CO}(2)$ would be involved in the tautomerization.

Additionally, complexes of "ideal" isoalloxazine^{27,28} and the phenolate anion in stacked conformations with parallel molecular planes (cf. Section 7.2) were calculated. Deviations from this conformation did not significantly alter the calculated quantities when the molecules were separated by a distance of 3.4 \AA (0.34 nm , Van der Waals contact distance). Two different relative orientations, *viz.* one with antiparallel isoalloxazine and phenolate dipole moments (calculated) and another derived from crystallographic data on an isoalloxazine-tyramine complex⁶⁰ with approximately perpendicular dipole moments, yielded almost identical results. It was only the distance between the molecules in the complex which appeared to be critical. The results obtained on the geometry determined crystallographically are summarized⁶¹ in Figs. 7.6D,E and Fig. 7.7. At 20 \AA (2 nm) distance, the phenolate anion already manifests its presence by raising the energy of all isoalloxazine orbitals by an amount which deviates at most by 8% from the classical coulombic repulsion energy of two electrons at the

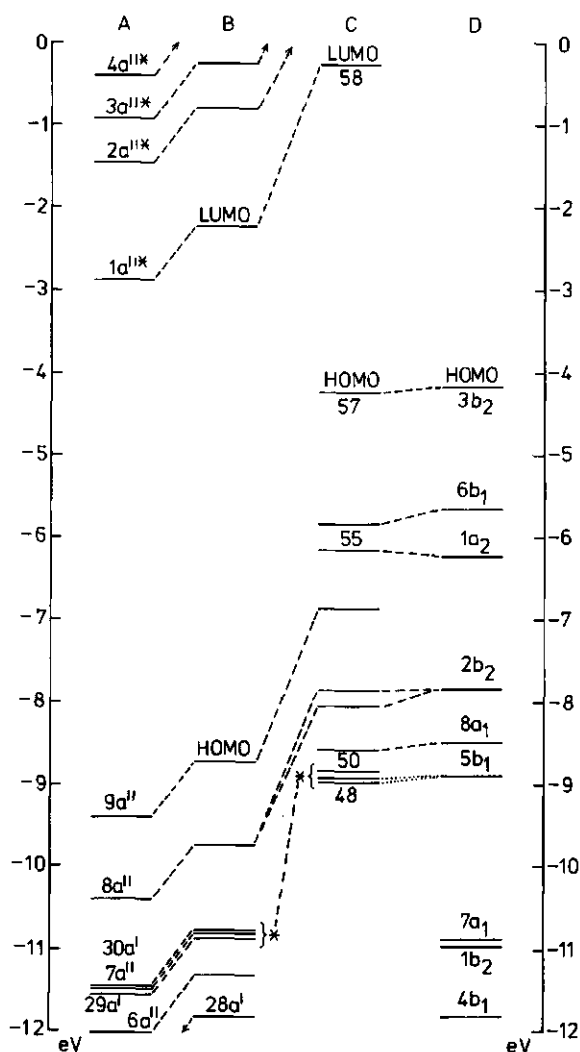
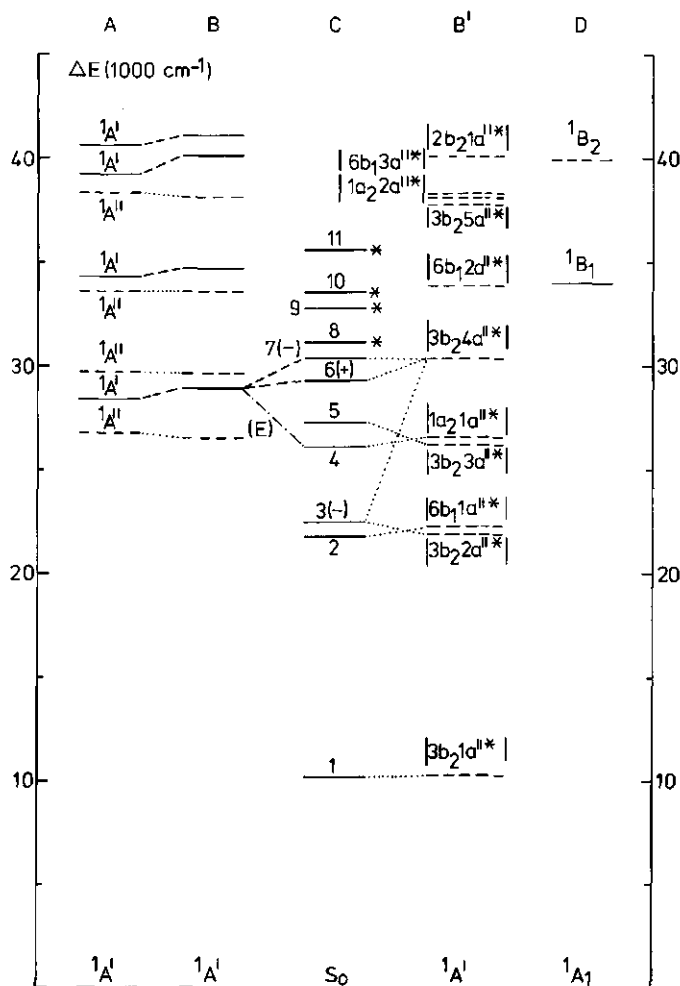


Figure 7.7. Calculated (CNDO/S-CI) orbital (left) and excited singlet state (right) correlation diagrams of "ideal" isoalloxazine-phenolate complexes, 100 singly excited singlet configurations^{27,28,61}. A: "ideal" isoalloxazine in the absence of phenolate (cf. Fig. 7.6C), no corrections applied⁶¹; B: "ideal" isoalloxazine-phenolate complex, intermolecular distance 20 Å (2 nm) as in Fig. 7.6D, excited state correlation diagram subdivided in isoalloxazine states (B) and phenolate → isoalloxazine charge transfer states (B'), the latter of which



ive no zero-order configuration interaction and are, consequently, denoted by heir singly excited singlet configuration label⁶¹; C: As Fig. 7.6E; D: phenolate orbitals and singlet states denoted by the appropriate²¹ symmetry labels (molecular point group C_{2v}); E: ----- indicates a ~4% correlation by which CT state 4 of the complex $^{21}C_{2v}$ borrows over 90% of its transition probability to the ground state. HOMO = highest occupied molecular orbital, LUMO = lowest unoccupied molecular orbital. Dotted excited level bars represent states to which electronic ransitions from the ground state are electrically dipole-forbidden.

same distance. It produces a slight blue shift of the isoalloxazine $^1A_0' \rightarrow ^1A_1'$ transition (Fig. 7.6D). The calculated phenolate $^1A_1 + ^1B_1 (S_0 \rightarrow S_1)$ transition reasonably agrees with that measured for 4-HNBBA at 28000 cm^{-1} (357 nm) in a control experiment. In the long-distance complex, a large number of zero-order CT states is calculated having no transition probability to the ground state, as expected. At shorter ($3.18 \text{ \AA} = 0.318 \text{ nm}$) distance⁶⁰, they acquire some oscillator strength to the ground state owing to an increased orbital overlap (Figs. 7.6E and 7.7), but not enough to explain a molar extinction of $3000\text{--}4000 \text{ M}^{-1}\text{cm}^{-1}$ as observed for the long-wavelength absorbance of the OYE-phenolate complexes³. Perhaps state 4 (Figs. 7.6E and 7.7C) is an exception since it borrows transition probability from the electric dipole-allowed isoalloxazine $^1A_0' \rightarrow ^1A_1'$ transition. It should be realized, however, that the calculated oscillator strength of the latter transition is too large²⁸ by a factor of ~ 5 and that calculations using the dipole operator have a tendency to overestimate the transition moments of CT states⁶². Thus, this "outer complex" in Mulliken's terminology⁷ does not sufficiently explain the actual observations.

When the intermolecular distance was shortened to 2 \AA (0.2 nm), an attempt to explore the physical consequences of "inner complex" formation⁷, the calculations predicted a migration of electronic charge in the ground state from phenolate to isoalloxazine. This process is accompanied by the creation of a highest occupied orbital, delocalized over the whole complex, containing a significant (>40%) amount of isoalloxazine lowest unoccupied molecular orbital (LUMO) character. Consequently, this "inner complex" has low excited states which have a large amount of isoalloxazine semiquinone character and appreciable oscillator strength to the ground state ($f > 0.4$). Obviously, the complex as a whole remains a closed-shell electronic system and all excited configurations mix heavily due to the large perturbations. The "inner complexes" should stabilize (theoretically!) by $4\text{--}6 \text{ MJ mole}^{-1}$ owing to the charge migration, the actual quantity being critically dependent on the relative orientation of the molecules. So, if this were true, we should be able to observe the OYE phenomena just by mixing isoalloxazines with phenols at the right pH. This has never been observed^{14,15,60} and our own control experiments were also negative, even in the presence of a thousandfold excess of 4-HNBBA with respect to lumiflavin, riboflavin or FMN. Changing the buffer solution to an anionic micellar solution of the same pH, which was shown to enhance donor-acceptor complex formation⁶³, had no effect whatsoever: the results remained negative. On the contrary, when paraquat in micellar solution was used as a CT acceptor⁶³, both neutral and anionic 4-HNBBA (and other phenols as well) gave pronounced CT absorptions. These

experiments also deny the mixing of the isoalloxazine 1A_1 state with the $3b_{2g}4a''_{g1}$ (CT) configuration in the "outer complex" (Fig. 7.7).

The calculations do not give conclusive support for the existence of the "inner" or "outer" complex, although they predict the existence of low lying excited states of different character, depending on the intermolecular distance. The term charge transfer transition, however, usually refers to a transition in which the charge is transferred in the *excited* and not in the electronic ground state⁴⁻¹², i.e. the situation encountered in the "outer complex". Thus the theoretical framework only suggests the hydrogen-bond rearrangement to be more likely than a CT complex to explain the OYE spectral properties.

3.4. Electron paramagnetic resonance (ESR) spectra

For all "inner" isoalloxazine-phenolate complexes, the CI calculations yielded a triplet state of extremely low energy (0.4-0.6 eV above the ground state) having a varying amount of CT character (10-50%), the actual quantities being critically dependent on the mutual orientation of the constituents of the complex. A varying degree of admixture of a phenolate configuration having an extremely large singlet-triplet splitting, appeared to be responsible for this result. Since the triplet energy values were sufficiently smaller than the usual errors in energy calculated by the CNDO/S-CI method^{27,28}, the possibility of a triplet ground state leading to the occurrence of the long-wavelength absorption and in the OYE-phenolate complexes was investigated by ESR experiments. Instead of a triplet, a doublet signal was discovered, both in free OYE and its complexes. The signal showed the following properties: $g = 2$, linewidth 11.2 gauss (1.12 mT) at 9.4 GHz microwave frequency, extremely easily saturatable, only observable at temperatures below 15 K and of equal intensity in the free and complexed enzyme. Comparison with a standard copper solution yielded, after double integration and correction for the temperature, a spin concentration varying between 0.1 and 10% of the concentration of protein-bound FMN. The actual percentage seemed to vary with various batches of independent isolations of the enzyme. No doubt, the detected unpaired spin was associated with the protein since the buffer against which OYE was dialysed in the last purification step³ appeared to be spinfree when measured under identical conditions as the OYE samples.

Nevertheless, two important questions remain entirely open. The first concerns the localization of the spin within the protein and how it was formed. The second question is whether or not the spin is related to the long-wavelength absorption band of the OYE-phenolate complexes. Regarding the first question, it

is unlikely that the spin belongs to a metal ion. The observed ESR line is rather broad for an unpaired spin residing on a metal ion and searches for metal in OYE were negative³⁴. Hence, the unpaired spin must reside on an organic molecule. Regarding the second question, a possible relation as suggested cannot be rejected in advance since it should be remembered that OYE is a dimeric system³. This may lead to spin-spin interaction within a biradical of yet unknown nature, resulting in a spuriously low apparent spin concentration. This may also be the reason why the ESR signal is only observed at very low temperature, contrary to the usual relaxational behaviour of organic radicals. Regrettably, we had no equipment at our disposal to verify this by measurements of the magnetic susceptibility.

While conducting the ESR experiments, another remarkable observation was made. When quickly frozen samples of the OYE-phenolate complexes were removed from the liquid nitrogen container, used to store them prior to the 7-15 K measurements, and were subsequently allowed to stand overnight at 253 K, their colour reverted to that of the free enzyme, even in the presence of a thousandfold excess of phenol! Subsequent thawing to fluid solution restored the usual green colour of the complex. An already frozen *solid* solution of the OYE-phenolate complex exhibited a similar colour-change when slowly cooled from ~273 to 253 K. These processes were fully reversible. They did not occur in the glassy buffer/glycerol solutions used for optical spectroscopy. Apparently, a phase transition occurs in the *solid* polycrystalline mixture of water, buffer salts and protein. the colour-reversion were due to the disappearance of a CT band, this would imply the dissociation of the complex, which is unlikely in the solid state. It is however, well-documented that pyrophosphate buffers may change their pH appreciably upon cooling⁶⁴. Hence, changes in state of protonation of several groups in the complex upon cooling are likely to occur. Consequently, these observations are also in favour of a proton-transfer mechanism, a change in state of protonation of some chromophore(s) leading to the appearance or disappearance of the long-wavelength absorption band. In this respect, it should be realized that only the phenolate anion is able to induce this band³ (cf. Section 7.3.1). Apparently melting of the polycrystalline solid, being a second phase transition, is again accompanied by proton-transfer.

7.4. CONCLUSIONS

The present results clearly show the insufficiency of the simple charge transfer explanation³ of the spectral properties of Old Yellow Enzyme. These

properties are apparently governed by more than two chromophores, one of which undoubtedly is FMN. The others still have to be identified firmly, whereas the whole network of interactions between them, a network which apparently is strongly perturbed by phenolate, is still completely enigmatic. By favouring a proton-transfer mechanism for this network, we merely wish to emphasize that it is the only mechanism from which contradictions do not emerge immediately. Also the existing Resonance Raman studies on OYE^{23,24} fit into this model. These studies only allow for the firm conclusion that Raman lines corresponding to mainly in-plane vibrations of phenolate and, possibly, FMN are resonance-enhanced by the long-wavelength electronic transition of the OYE-phenolate complex. Comparison of the Raman spectra of OYE^{23,24} with published work on the vibrational analysis of *para*-substituted phenols⁶⁵⁻⁶⁸, shows the Resonance Raman spectrum of the OYE-phenolate complex to be dominated by totally symmetric phenolate modes. According to the standard second order perturbational quantum mechanical treatment of the resonance Raman effect⁶⁹, this implies that we are dealing with Condon scatter in which the transition probability is governed by a dyadic product of zero-order electronic transition moments. Admittedly, within this framework, a CT transition in a sandwich complex of flavin and phenolate can give rise to Condon scatter through the z^2 diagonal element of the scattering tensor⁶⁹, owing to the fact that such a transition is perpendicularly polarized to the molecular planes of the two moieties in the complex. But, since x^2 and y^2 have exactly the same symmetry as z^2 , in-plane polarized electronic transitions may equally contribute to Condon scatter and there is no way to establish the CT character of the long-wavelength transition in the OYE-phenolate complex in this respect.

The most prominent Resonance Raman line in the spectra of the OYE-phenolate complexes investigated^{23,24} corresponds to the phenolate A_1 mode ν_{6a} . This mode was previously assigned to a substituent (oxygen atom!) sensitive mode⁶⁵⁻⁶⁸. In the OYE measurements^{23,24} the frequency of ν_{6a} is slightly ($10-20\text{ cm}^{-1}$) higher than in neutral phenols⁶⁵⁻⁶⁸, a shift which can be sufficiently accounted for by (again) a hydrogen-bonded structure. Since phenols in such structures show a tendency to proton-transfer upon electronic excitation²², large Franck-Condon factors favouring Condon scatter are very probable for ν_{6a} because the C-O bond-order will not remain unaffected upon proton-transfer. Consequently, the approximate matching of the ν_{6a} excitation profile with the long-wavelength absorption band of the OYE-phenolate complex²⁴ solely proves the excitation likely to be associated with the phenolate electronic system. About the excited state character one can only guess. Of more interest is the fact that the ν_{6a} excitation profile²⁴ suggests the presence of a second transition around 500 nm

(20000 cm^{-1}), nearly coincident with the 20150 cm^{-1} (496 nm) band in the native enzyme which we ascribed to a separate electronic transition (cf. Sections 7.3.1 and 7.3.3). Apparently, the bands at 20150 cm^{-1} (496 nm) and 16750 cm^{-1} (597 nm) are related to each other. The simultaneous decrease and increase of their intensities upon the addition of phenols to OYE thus may reflect no more than a change in the state of protonation of two, possibly different, chromophores.

Accordingly, the spectral behaviour of OYE is actually identical to that encountered in an ordinary titration experiment, *viz.* a colour-change due to changes in state of protonation of chromophores *in their electronic ground state*. This obviously leads to an isosbestic point and one single value of the binding constant of a phenol to OYE, irrespective from which spectral region the constant is determined³. As shown, the exact mechanism underlying the observed phenomena is highly complicated. We believe to have reached the boundaries of what reasonably can be concluded from spectroscopy alone. Possibly X-ray crystallographic structure determination may induce further progress in the characterization of this remarkable flavoprotein.

REFERENCES AND NOTES

- 1 R.G. Matthews and V. Massey, *J. Biol. Chem.* 244 (1969) 1779.
- 2 R.G. Matthews, V. Massey and C.C. Sweeley, *J. Biol. Chem.* 250 (1975) 9294.
- 3 A.S. Abramovitz and V. Massey, *J. Biol. Chem.* 251 (1976) 5321; *ibid.* 5327.
- 4 P.R. Hammond, *J. Chem. Soc.* (1964) 471.
- 5 E.M. Kosower, D. Hofmann and K. Wallenfels, *J. Amer. Chem. Soc.* 84 (1962) 275.
- 6 H.H. Jaffé, *Chem. Rev.* 53 (1953) 191.
- 7 R.S. Mulliken, *J. Phys. Chem.* 56 (1952) 801.
- 8 H. McConnell, J.S. Ham and J.R. Platt, *J. Chem. Phys.* 21 (1953) 66.
- 9 R. Foster, *Nature* 181 (1958) 337.
- 10 G. Briegleb and J. Czekalla, *Z. Elektrochem.* 63 (1959) 6.
- 11 M.J.S. Dewar and A. Leply, *J. Amer. Chem. Soc.* 83 (1961) 4560.
- 12 R.S. Mulliken and W.B. Person, *Ann. Rev. Phys. Chem.* 13 (1962) 107 and references therein.
- 13 D.W. Turner, C. Baker, A.D. Baker and C.R. Brundle: *Molecular Photoelectron Spectroscopy* (Wiley, London, 1970), pp. 279-322.
- 14 K. Yagi and Y. Matsuoka, *Biochem. Z.* 328 (1956) 138.
- 15 K. Yagi, T. Ozawa and K. Okada, *Biochim. Biophys. Acta* 35 (1959) 102.
- 16 T.P. Debies and J.W. Rabalais, *J. Electron Spectrosc. Relat. Phenom.* 1 (1972) 355.
- 17 J.P. Maier and D.W. Turner, *J. Chem. Soc. (Faraday)* 69 (1973) 521.
- 18 T. Kobayashi and S. Nagakura, *J. Electron Spectrosc. Relat. Phenom.* 6 (1975) 421.
- 19 J.W. Rabalais: *Principles of Photoelectron Spectroscopy* (Wiley, London, 1977) pp. 303-308.
- 20 M.H. Palmer, W. Moyes, M. Speirs and J.N.A. Ridyard, *J. Mol. Struct.* 52 (1979) 293.
- 21 Some authors label these orbitals as b_1 and a_2 , respectively. This apparent

- ambiguity is caused by the choice of the symmetry label (σ_v or σ'_v) for the molecular plane. Throughout this Chapter we adopt the convention, that vectorial properties (like p_z orbitals) which are anti-symmetric with respect to the phenolate molecular plane, transform according to either the A_2 or B_2 irreducible representations of the point group C_{2v} .
- 2 H. Baba, J. Chem. Phys. 49 (1968) 1763.
 - 3 T. Kitagawa, Y. Nishina, K. Shiga, H. Watari, Y. Matsumura and T. Yamano, J. Amer. Chem. Soc. 101 (1979) 3376.
 - 4 Y. Nishina, T. Kitagawa, K. Shiga, H. Watari and T. Yamano, J. Biochem. (Tokyo) 87 (1980) 831.
 - 5 Cf. Chapter 3 or: J.K. Eweg, F. Müller, A.J.W.G. Visser, C. Veeger, D. Bebelaar and J.D.W. van Voorst, Photochem. Photobiol. 30 (1979) 463.
 - 6 Cf. Chapter 4 or: J.K. Eweg, F. Müller, D. Bebelaar and J.D.W. van Voorst, Photochem. Photobiol. 31 (1980) 435.
 - 7 Cf. Chapter 5 or: J.K. Eweg, F. Müller, H. van Dam, A. Terpstra and A. Oskam, J. Amer. Chem. Soc. 102 (1980) 51.
 - 8 Cf. Chapter 6 or: J.K. Eweg, F. Müller, H. van Dam, A. Terpstra and A. Oskam, J. Phys. Chem. 86 (1982) 1642.
 - 9 B.B. Snively, in: Organic Molecular Photophysics, Vol. 1, ed. J.B. Birks (Wiley, London, 1973).
 - 10 J. de Vries, D. Bebelaar and J. Langelaar, Opt. Commun. 18 (1976) 24.
 - 11 L. Velluz, M. Legrand and M. Grosjean: Optical Circular Dichroism, principles, measurements and applications (Academic Press, New York, 1965), pp. 57-77.
 - 12 H. Forest and B.P. Dailey, J. Chem. Phys. 45 (1966) 1736.
 - 13 T. Pedersen, N.W. Larsen and L. Nygaard, J. Mol. Struct. 4 (1969) 59.
 - 14 Å. Åkeson, A. Ehrenberg and H. Theorell, in: The Enzymes, 2nd. Ed., Vol. 7, eds. P.D. Boyer, H. Lardy and K. Myrbäck (Academic Press, New York, 1963).
 - 15 S. Otani, Y. Note, Y. Nishina and Y. Matsumura, in: Flavins and Flavoproteins, Proc. 6th. Int. Conf., eds. K. Yagi and T. Yamano (Japanese Scientific Soc. Press, Tokyo, 1980).
 - 16 G. Tollin, Biochemistry 7 (1968) 1720.
 - 17 D.E. Edmondson and G. Tollin, Biochemistry 10 (1971) 113; *ibid.* 133.
 - 18 G. Scola-Nagelschneider and P. Hemmerich, Z. Naturf. 27b (1972) 1044.
 - 19 H.A. Harbury, K.F. La Nove, P.A. Loach and R.M. Amick, Proc. Natl. Acad. Sci. USA. 45 (1959) 1708.
 - 20 H.E. Auer and F.E. Frerman, J. Biol. Chem. 255 (1980) 8157.
 - 21 D.J. Caldwell and H. Eyring: The Theory of Optical Activity (Wiley, London, 1971), pp. 51-95.
 - 22 M. Leijonmarck, Thesis, University of Stockholm, Sweden, Chem. Commun. VIII (1977).
 - 23 H. Theorell and A.P. Nygaard, Acta Chem. Scand. 8 (1954) 877; *ibid.* 1489, *ibid.* 1649.
 - 24 B.R. Henry and W. Siebrand, in: Organic Molecular Photophysics, Vol. 1, ed. J.B. Birks (Wiley, London, 1973).
 - 25 H.E. White: Introduction to Atomic Spectra (McGraw-Hill-Kogakusha, New York-Tokyo, 1934), pp. 401-417.
 - 26 G. Herzberg: Molecular Spectra and Molecular Structure, II: Infrared and Raman Spectra of Polyatomic Molecules, 12th ed. (D. van Nostrand, New York, 1966), pp. 280-281.
 - 27 W. Klöpfer, in: Organic Molecular Photophysics, Vol. 1, ed. J.B. Birks (Wiley, London, 1973).
 - 28 I. Tatischeff and R. Klein, in: Excited States of Biological Molecules, ed. J.B. Birks (Wiley, London, 1976).
 - 29 C.F. Beyer, L.C. Craig, W.A. Gibbons and J.W. Longworth, in: Excited States of Biological Molecules, ed. J.B. Birks (Wiley, London, 1976).
 - 30 O. Shimizu and K. Imakubo, Photochem. Photobiol. 26 (1977) 541.

- 51 A.J.W.G. Visser and A. van Hoek, *Photochem. Photobiol.* 33 (1981) 35.
- 52 J. Krüse, B.J.M. Verduin and A.J.W.G. Visser, *Eur. J. Biochem.* 105 (1980) 395.
- 53 D. Labuda, Z. Janowicz, T. Haertlé and J. Augustyniak, *Nucleic Acid Res.* 1 (1974) 1703.
- 54 P. Vigny and M. Duquesne, in: *Excited States of Biological Molecules*, ed. J.B. Birks (Wiley, London, 1976).
- 55 P.S. Song, *Int. J. Quantum Chem.* 2 (1968) 463.
- 56 K.H. Dudley, A. Ehrenberg, P. Hemmerich and F. Müller, *Helv. Chim. Acta* 47 (1964) 1354.
- 57 For the labels used to denote the excited states cf. Chapter 6; A' refers to $\pi\pi^*$, A'' to a $n\pi^*$ state.
- 58 F. Müller, C.G. van Schagen and R. Kaptein, *Methods in Enzymology* 66 (1980) 385.
- 59 C.G. van Schagen and F. Müller, *Eur. J. Biochem.* 120 (1981) 33.
- 60 M. Inoue, M. Shibata, Y. Kondo and T. Ishida, *Biochem. Biophys. Res. Commun.* 93 (1980) 415; *ibid.* *Biochemistry* 20 (1981) 2936.
- 61 The conventions adopted to label the singly excited electronic configurations and excited states arising therefrom are the same as used previously²⁸. Orbitals are labelled by lower-case symmetry labels, i.e. na'' represents the n -th π (a'') orbital of the isoalloxazine molecule, ma' represents the m -th σ (a') or n (a') orbital, phenolate orbitals are labelled according to the literature¹⁶⁻²⁰ and the convention adopted in the introduction²¹ (Section 7.1). The notation $|pq|$ is an abbreviation for the normalized singly excited singlet configuration $2^{-\frac{1}{2}}(|p\bar{q}| - |\bar{p}q|)$ in which an electron is promoted from orbital p to orbital q . The corrections according to Bigelow^{27,28} were not applied since we are dealing with anionic closed shell systems.
- 62 S. de Bruijn, Personal Communication.
- 63 F.M. Martens and J.W. Verhoeven, *J. Phys. Chem.* 85 (1981) 1773.
- 64 A.G. Porras and G. Palmer, in: *Flavins and Flavoproteins*, Proc. 7th. Int. Conf., eds. V. Massey and C.H. Williams Jr. (Elsevier North Holland, Inc., New York, 1982).
- 65 J.H.S. Green, *J. Chem. Soc.* (1961) 2236.
- 66 J.H.S. Green, D.J. Harrison and W. Kynaston, *Spectrochim. Acta* 27A (1971) 219.
- 67 J.H.S. Green and D.J. Harrison, *J. Chem. Thermodyn.* 8 (1976) 529.
- 68 J.H.S. Green, D.J. Harrison and C.P. Stockley, *J. Mol. Struct.* 33 (1976) 307.
- 69 R.J.H. Clark and B. Stewart, *Struct. and Bonding* 36 (1979) 1.

ON THE ELECTRONIC STRUCTURE OF FREE AND PROTEIN-BOUND ISOALLOXAZINES, A POSTSCRIPT¹

In the time elapsed between the preparation of the first and last chapters of this thesis, a number of papers have appeared which need to be mentioned or deserve a comment. First, the proceedings of the seventh international symposium on flavins and flavoproteins were published recently² (cf. p. 3). Furthermore, besides general review articles³⁻⁸ (cf. p. 3), the literature on covalently-bound flavin prosthetic groups (cf. p. 4) augmented considerably⁹⁻¹⁹. The latter subject was reviewed recently²⁰ and even a flavoprotein containing both covalently and non-covalently bound flavins (*Corynebacterium Sarcosine Oxydase*) was discovered²¹. Improved methods of fluorescence-rejection in (Resonance) Raman spectroscopy made isoalloxazines, flavins and flavoproteins also accessible to this spectroscopic technique (cf. pp. 4-5). Consequently, the literature cited on p. 5 needs to be supplemented²²⁻⁴¹. On the other hand, the present "state of the art" of isoalloxazine vibrational spectroscopy is still far removed from definitive assignment of the observed frequencies to isoalloxazine vibrational modes^{42,43}. The best tentative assignments currently available are those based on the spectra obtained from ¹³C and ¹⁵N labelled compounds²⁶. Also the assignment of a vibrational mode involving the isoalloxazine N₃ atom seems to be rather sound, since it behaves similar as a corresponding mode in uracil upon N₃ deuteration^{42,43}. Complex formation of flavins with Ag⁺ and Ru²⁺ cations was also studied by Resonance Raman spectroscopy⁴⁴. Additionally, the literature on the phototautomerism of alloxazines cited in Section 5.1 (p. 52) increased^{45,46}. However, the phototautomeric explanation of the dual luminescence of alloxazines was also questioned⁴⁷.

The idea of using isoalloxazines substituted with long alkyl side-chains (amphiphilic flavins) to improve their solubility in an apolar environment (Chapter 3, pp. 22-36) was further explored by other investigators⁴⁸⁻⁵⁷. It even proved to be feasible to obtain highly resolved optical site selection spectra from *n*-undecyl-7,8,10-trimethyl-isoalloxazine^{49,57} (cf. Table 3.1, p. 27, Compound I) and the corresponding alloxazine derivative⁵⁷ in *n*-decane Spolshkii matrices at 4.2 K. On the basis of these experiments, the conclusions concerning the conformational change of (iso)alloxazine upon electronic excitation (Chapters 3 and 4, pp. 34 and 48) were criticized. The main argument for this criticism was

the near equality of the isoalloxazine vibrational frequencies in the ground and electronically first excited singlet states, as deduced from the site selected spectra, a property indeed observed for most *but not all* frequencies^{49,57}. Furthermore, it was observed that at 4.2 K, a "substantial fraction" of the total spectral intensity goes into the 0-0 transition^{49,57}, contrary to the observation made in glassy (77 K) or fluid (300 K) solution and the vapour phase (Chapters 3, 4, pp. 22-51), which show the relative intensity of the 0-0 transition to be highly dependent on the solvent polarity and state of aggregation. The vibrational frequencies observed in the site selection experiments^{49,57} are the same as those discernible in Resonance Raman (RR) spectra²²⁻⁴² (*vide supra*), i.e. frequencies corresponding to in-plane or "totally symmetric" vibrational modes. This is not surprising: only such modes give rise to a vibrational progression in relaxed fluorescence or absorption (excitation) spectra⁵⁸ and for RR it implies that the scattering tensor is dominated by the Albrecht A-term⁵⁹. Thus, for isoalloxazine one deals with the Condon scattering mechanism (cf. p. 131), in accordance with the electric dipole-allowed character of the $S_0 \rightarrow S_1$ transition (Chapters 3, 4, 6 pp. 22, 37, 83). Hence, neither the optical site selection nor the RR spectra provide any information on the non-totally symmetric modes. Many of these are presumably of low frequency owing to small force constants (e.g. out-of-plane bending, wagging or torsional modes) and, for that reason, sensitive to external forces. These are also likely internal molecular coordinates along which the discussed conformational change may occur so, the discrepancy between the conclusion drawn from the doped crystal spectra^{49,57} and from the spectra measured in solution (p. 34) and the vapour phase (p. 48) is only apparent: At 4.2 K, the rigid crystal lattice generates a potential which does not allow for the concerned geometry change. Moreover, apart from criticizing a possible conformational change⁴⁹, a "possible reorientation of the guest (molecule) in the host" is claimed at the same time⁵⁷ and peculiar photochemical phenomena are observed^{49,57}, which are hard to explain without assuming small conformational changes, even at 4.2 K. Thus the occurrence of geometry changes is merely a question whether or not and to what extent the molecule's environment permits such changes.

The molecular geometry of reduced isoalloxazine as discussed in Chapter 5 (pp. 65, 69-76, 79, 80) was also criticized by the same group of authors^{60,61} as those cited above. They suggested^{60,61} that the intrinsically planar conformation of reduced isoalloxazine was proposed (pp. 65, 69-76, 79, 80) solely on the basis of total molecular energies obtained from CNDO/S calculations. On the contrary, it was the combination of calculated and experimental orbital energies which led to the proposal of a planar structure. Additionally, the theo-

retical method was firmly checked against the *experimental* photoelectron spectroscopic technique (Chapter 5, pp. 52-82) before making the concerned proposal of a planar structure *in the vapour phase but not in condensed media!* Under the latter circumstances, there is conclusive evidence for a folded structure (pp. 73 and 79). Thus, reduced and electronically excited isoalloxazine apparently possesses such a conformational flexibility, that the molecular structure in any actual situation depends on the molecule's environment. This is further supported by X-ray crystallographic data⁶², which demonstrate that even the oxidized isoalloxazine ring system has a tendency to deviate from planarity when it becomes involved in a molecular complex. Consequently, calculations *alone*, no matter their degree of sophistication (ranging from CNDO/S *via* the advanced PRDDO method applied recently to isoalloxazine⁶³ to the *ab initio* level^{60,61,64-66}), cannot serve as a basis to make predictions about the isoalloxazine molecular conformation.

Regarding the *ab initio* calculations^{60,61,64-66}, one may wonder if the results merit the enormous increase of computational labour compared to semi-empirical methods. The poor agreement between the *ab initio* calculations and the photoelectron spectra of isoalloxazines was already noticed (Chapter 6, p. 103). Thus, disagreement between theory and experiment already exists on the level of simple scalar observables like orbital energies. Excitation energies were not calculated by the *ab initio* method^{60,61,64-66}. Apparently, this disagreement is a consequence of the constraints put on the AO basis set by the size of the isoalloxazine molecule, a basis set whose dimensions should be in accordance with the space and time limits of the computer on which the calculation is performed. On the contrary, Palmer *et al.*^{60,61} claimed a good agreement between their calculations and the photoelectron spectrum they measured from only one, N₃ protonated, isoalloxazine. This spectrum is of extremely poor quality, however. It displays a He(I)-He(II) intensity-difference which is unlikely for a molecule of the size and atomic composition of isoalloxazine and it was reported not to be recordable in one single run⁶¹. We had the same difficulty with N₃ protonated isoalloxazines. These compounds, among which the derivative measured by Palmer *et al.*^{60,61}, were found to sublime under decomposition, both in the preparation procedure of samples for vapour phase spectrometry (Chapter 4, p. 38) and in thermoanalysis experiments (Chapter 5, p. 53). In the latter, the differential thermal analysis (DTA) curves, obtained by registration of the temperature-difference between the isoalloxazine sample and the reference compound (Al₂O₃) while both were slowly heated in vacuum (1 μ Torr = 0.13 mPa), had a distinct inflection or peak prior to noticeable loss of weight of the sample owing to evaporation. This clearly indicates a heat-effect caused by a chemical reaction. We, therefore,

confined the photoelectron spectrometry to the N_3 methylated compounds whose spectra are given in Chapters 5 and 6 (pp. 52-95). Moreover, the differences between the spectra published by Palmer *et al.*^{60,61} and those presented in Chapter 5 and 6 (pp. 52-95) are too large to be explained by the difference in N_3 substituent (methyl group vs. proton). Hence, the former spectra likely suffer from interference by decomposition products of isoalloxazine.

In connection with the UV photoelectron spectra, the X-ray photoelectron spectrum (XPS) of one isoalloxazine derivative was also measured on a VG-ESCA 3 instrument. The information content of the XPS spectrum is low, however, and interesting features like shake-up or shake-off satellites^{67,68} were not observed (Fig. 8.1). The only satellites are the well-known trivial ones owing to Al -

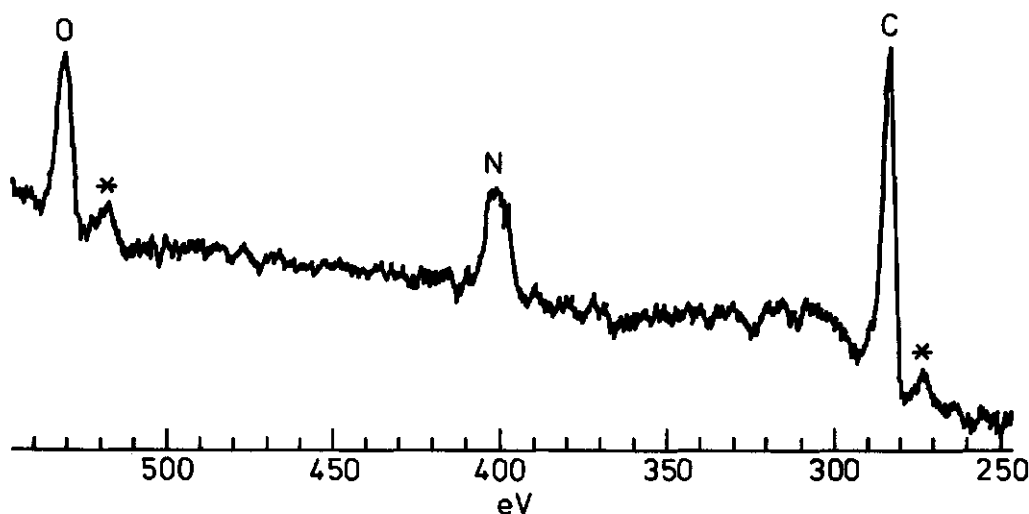


Figure 8.1. The ESCA (XPS photoelectron) spectrum of 3,7,8,10-tetramethyl-isoalloxazine (3-methyl-lumiflavin, cf. Compound 5, Scheme 6.1, p. 86) excited with Al - K_{α} radiation (1486.6 eV). The abscissa is calibrated in ionization energy. Carbon, Nitrogen and Oxygen peaks are indicated. The asterisks mark satellite lines owing to Al - $K_{\alpha-3,4}$ radiation⁶⁸.

$K_{\alpha-3,4}$ radiation⁶⁸ (cf. legend to Fig. 8.1). The carbon, nitrogen and oxygen core ionizations appear at 283, 401 and 530 eV, respectively (bandmaxima!), close to the free atomic values⁶⁷ of $C(1s_{\frac{1}{2}}) = 285$ eV, $N(1s_{\frac{1}{2}}) = 399$ eV and $O(1s_{\frac{1}{2}}) = 532$ eV. The nitrogen peak is significantly broader than the other peaks, presumably because of the presence of both imine-like and pyrrole-like nitrogen atoms in isoalloxazine. The relative intensity of the $O(1s_{\frac{1}{2}})$ peak is too large, indicative of enclosed solvent molecules with a relatively high oxygen abundance in the iso-

alloxazine crystalline powder used (XPS is measured in the solid state!). This was also noticed in other experiments (Chapter 4, p. 38). It is hazardous to draw further conclusions from XPS on isoalloxazine, although it was attempted to do so in a comparative study of isoalloxazines and lumazines⁶⁶. This study, however, relies heavily on deconvolution procedures, e.g. to extract the four individual N(1s_i) core levels from the corresponding XPS peak. Hence, UPS is a more powerful tool to study the isoalloxazine electronic structure than XPS.

REFERENCES AND NOTES

- 1 The reference listing to this chapter collects relevant literature on *optical spectroscopy* of (iso)alloxazines (flavins) not referred to in the preceding chapters. Papers on flash-photolysis work are not included. The last up-date of this listing was made upon the appearance of Vol. 96 of Chemical Abstracts, Columbus, Ohio, 1982 and of Vol. 1982-2 of Science Citation Index, Institute for Scientific Information, Philadelphia, Pennsylvania, 1982.
- 2 V. Massey and C.H. Williams Jr. (eds.): *Flavins and Flavoproteins*, Proc. 7th. Int. Conf. (Elsevier North Holland Inc., New York, 1982).
- 3 D.E. Edmondson, W.C. Kenney and T.P. Singer, *Methods Enzymol.* 53 (1978) 449.
- 4 T.P. Singer and D.E. Edmondson, *Methods Enzymol.* 53 (1978) 397.
- 5 M. Husain and V. Massey, *Methods Enzymol.* 53 (1978) 429.
- 6 T.C. Bruice, *Acc. Chem. Res.* 13 (1980) 256.
- 7 C. Walsh, *Acc. Chem. Res.* 13 (1980) 148.
- 8 F. Müller, *Photochem. Photobiol.* 34 (1981) 753.
- 9 W.C. Kenney, D.E. Edmondson, T.P. Singer, M. Nishikimi, E. Noguchi and K. Yagi, *FEBS Letters* 97 (1979) 40.
- 10 N. Ohishi and K. Yagi, *Biochem. Biophys. Res. Commun.* 86 (1979) 1084; *ibid.* 88 (1979) 335.
- 11 M. Sato, N. Ohishi and K. Yagi, *Biochem. Biophys. Res. Commun.* 87 (1979) 706.
- 12 M. Fukuyama and M. Yoshihiro, *J. Biochem. (Tokyo)* 85 (1979) 1183.
- 13 W.C. Kenney, T.P. Singer, M. Fukuyama and M. Yoshihiro, *J. Biol. Chem.* 254 (1979) 4689.
- 14 K. Wanatabe, N. Minamiura and K.T. Yasunobu, *Biochem. Biophys. Res. Commun.* 94 (1980) 579.
- 15 M. Ohta-Fukuyama, Y. Miyake, K. Shiga, Y. Nishina, H. Watari and T. Yamano, *J. Biochem. (Tokyo)* 88 (1980) 205.
- 16 W. McIntire, D.E. Edmondson, T.P. Singer and D.J. Hopper, *J. Biol. Chem.* 255 (1980) 6553.
- 17 G. Oestreicher, S. Grossman, J. Goldenberg, E.B. Kearney, D.E. Edmondson, T.P. Singer and J.P. Lambooy, *Comp. Biochem. Physiol.* 67B (1980) 395.
- 18 N. Mori, Y. Tani, H. Yamada and R. Hayashi, *Agric. Biol. Chem.* 45 (1981) 539.
- 19 Section "Covalently-bound Flavins" in ref. 2.
- 20 T.P. Singer and D.E. Edmondson, *Methods Enzymol.* 66 (1980) 253.
- 21 S. Hayashi, S. Nakamura and M. Suzuki, *Biochem. Biophys. Res. Commun.* 96 (1980) 924.
- 22 P.K. Dutta and T.G. Spiro, *J. Chem. Phys.* 69 (1978) 3119.
- 23 Y. Nishina, T. Kitagawa, K. Shiga, K. Horike, Y. Matsumura, H. Watari and T. Yamano, *J. Biochem. (Tokyo)* 84 (1978) 925.
- 24 T. Kitagawa, Y. Nishina, K. Shiga, Y. Matsumura and T. Yamano, in: *Flavins and Flavoproteins*, Proc. 6th. Int. Conf., eds. K. Yagi and T. Yamano (Japanese Scientific Soc. Press, Tokyo, 1980).

- 25 Y. Nishimura and M. Tsuboi, Chem. Phys. Letters 59 (1978) 210.
- 26 T. Kitagawa, Y. Nishina, Y. Kyogoku, T. Yamano, N. Ohishi, A. Takai-Suzuki and K. Yagi, Biochemistry 18 (1979) 1804.
- 27 M. Benecky, T.Y. Li, J. Schmidt, F. Frerman, K.L. Watters and J. McFarland, Biochemistry 18 (1979) 3471.
- 28 T. Kitagawa, Y. Nishina, K. Shiga, H. Watari, Y. Matsumura and T. Yamano, J. Amer. Chem. Soc. 101 (1979) 3376.
- 29 P.K. Dutta, R. Spencer, C. Walsh and T.G. Spiro, Biochim. Biophys. Acta 623 (1980) 77.
- 30 P.K. Dutta and T.G. Spiro, Biochemistry 19 (1980) 1590.
- 31 Y. Nishina, T. Kitagawa, K. Shiga, H. Watari and T. Yamano, J. Biochem. (Tokyo) 87 (1980) 831.
- 32 Y. Nishina, K. Shiga, K. Horiike, H. Tojo, S. Kasai, K. Yanase, K. Matsui, H. Watari and T. Yamano, J. Biochem. (Tokyo) 88 (1980) 403; *ibid.* 88 (1980) 411.
- 33 R.M. Irwin, A.J.W.G. Visser, J. Lee and L.A. Carreira, Biochemistry 19 (1980) 4639.
- 34 L.M. Schopfer and M.D. Morris, Biochemistry 19 (1980) 4932.
- 35 A.J.W.G. Visser, L.A. Carreira, J. Le Gall and J. Lee, J. Phys. Chem. 84 (1980) 3344.
- 36 L.M. Schopfer, J.P. Haushalter, M. Smith, M. Milad and M.D. Morris. Biochemistry 20 (1981) 6734.
- 37 R. Miura, Y. Nishina, K. Shiga, H. Tojo, H. Watari, Y. Miyake and T. Yamano, in ref. 2.
- 38 L.M. Schopfer and M.D. Morris, in ref. 2.
- 39 Y. Nishina, K. Shiga, H. Tojo, R. Miura, T. Yamano and H. Watari, in ref. 2.
- 40 J. Schmidt and J.T. McFarland, in ref. 2.
- 41 H. Sakamoto, T. Kitagawa, T. Sugiyama, Y. Miyake and T. Yamano, in ref. 2.
- 42 W.D. Bowman and T.G. Spiro, J. Chem. Phys. 73 (1980) 5482; *ibid.* Biochemistry 20 (1981) 3313.
- 43 T.G. Spiro, W.D. Bowman, P.K. Dutta and M.J. Benecky, in ref. 2.
- 44 M. Benecky, T.J. Yu, K.L. Watters and J.T. McFarland, in: Proc. 7th. C.R. Conf. Int. Spectrosc. Raman, ed. W.F. Murphy (NRCC, Ottawa, 1980).
- 45 A. Koziolowa, Zesz. Nauk. Acad. Ekon. Poznaniu, Ser. 1, 80 (1978) 104; *ibid.*, Photochem. Photobiol. 29 (1979) 459.
- 46 J.D. Choi, R.D. Fugate and P.S. Song, J. Amer. Chem. Soc. 102 (1980) 5293.
- 47 S. Bergström and B. Holmström, Pro. IUPAC Symp. Photochem. 7th. (1978) 40.
- 48 W. Schmidt, J. Membrane Biol. 47 (1979) 1; *ibid.*, in: Blue Light Syndr., Proc. Int. Conf. Eff. Blue Light Plants Microorg., ed. H. Senger (Springer, Berlin, 1980); *ibid.*, J. Membrane Biol. 60 (1981) 164.
- 49 R.J. Platenkamp, H.D. van Osnabrugge and A.J.W.G. Visser, Chem. Phys. Letters 72 (1980) 104.
- 50 S. Shinkai, A. Harada, Y. Ishikawa, O. Manabe and F. Yoneda, Chemistry Letters (Tokyo) 4 (1981) 479.
- 51 W. Schmidt and P. Hemmerich, J. Membrane Biol. 60 (1981) 129.
- 52 H. Michel and P. Hemmerich, J. Membrane Biol. 60 (1981) 143.
- 53 M. Fragata, J. Membrane Biol. 60 (1981) 163.
- 54 W. Schmidt, Photochem. Photobiol. 34 (1981) 7.
- 55 S. Shinkai, A. Harada, Y. Ishikawa, O. Manabe and F. Yoneda, J. Chem. Soc. Perkin Trans. II (1982) 125.
- 56 S. Shinkai, A. Harada, O. Manabe and F. Yoneda, Bull. Chem. Soc. Japan 55 (1982) 928.
- 57 R.J. Platenkamp, A.J.W.G. Visser and J. Koziol, in ref. 2.
- 58 M. Stockburger, in: Organic Molecular Photophysics, Vol. 1, ed. J.B. Birks (Wiley, London, 1973).
- 59 R.J.H. Clark and B. Stewart, Struct. and Bonding 36 (1979) 1.
- 60 M.H. Palmer and R.J. Platenkamp, Jerusalem Symp. Quantum Chem. Biochem. 12

- (1979) 147.
- 61 M.H. Palmer, I. Simpson and R.J. Platenkamp, *J. Mol. Struct.* 66 (1980) 243.
- 62 M. Inoue, M. Shibata, Y. Kondo and T. Ishida, *Biochemistry* 20 (1981) 2936 and references therein.
- 63 D.A. Dixon, D.L. Lindner, B. Branchaud and W.N. Lipscomb, *Biochemistry* 18 (1979) 5770.
- 64 Y. Watanabe, K. Nishimoto and H. Kashiwagi, in ref. 2.
- 65 Y. Watanabe, K. Nishimoto, H. Kashiwagi and K. Yagi, in ref. 2.
- 66 M.H. Palmer, J.R. Wheeler, R.J. Platenkamp and A.J.W.G. Visser, in ref. 2.
- 67 A.D. Baker and D. Betteridge, *Photoelectron Spectroscopy* (Pergamon, Oxford, 1972).
- 68 D. Briggs, in: *Handbook of X-ray and Photoelectron Spectroscopy*, ed. D. Briggs (Heyden and Son, London, 1977).

APPENDIX 1 CONFIGURATION INTERACTION DATA ON OXIDIZED ISOALLOXAZINE DERIVATIVES*

A1.1. GENERAL INFORMATION

Lower electronically excited states of various isoalloxazine derivatives calculated by configuration interaction between singly excited singlet (or triplet) configurations⁴⁰. For each derivative, the relevant data on singlet states obtained from the methods described in Chapter 6 (Experimental and Theoretical Section, p. 84), are summarized in two tables and one figure.

The first of these tables collects configurations which contribute significantly to the lower excited states. A quick-reference label is assigned to each configuration, its energy (cf. Table 2.3, p. 19, diagonal element of the CI matrix) and its transition moment to the ground state is given in units of 1000 cm^{-1} and atomic units (cf. p. 14), respectively. Uncorrected (uncorr.) configuration energy values are obtained by application of the strict CNDO/S³⁰ or INDO/S¹⁹ approximations. Corrected (corr.) energy values are obtained after correction of the energy of the occupied orbital involved in the configuration according to Bigelow¹³ (eq. 5.1, p. 54), prior to the calculation of the configuration energy (Table 2.3, p. 19). The INDO/S-CI calculations were performed directly on configurations arising from CNDO/S orbitals as described on p. 85. The components of the transition moment are calculated with respect to the cartesian coordinate system pictured in Scheme 6.1 (p. 86).

The second of these tables collects the excited singlet states calculated after CI. For each excited state, the approximate symmetry in terms of "ideal isoalloxazine" (cf. pp. 97, 98), the energy relative to the ground state (in units of 1000 cm^{-1}), the oscillator strength (f) for a radiative transition from the ground state to the concerned excited state, and the most contributing configurations (indicated by the quick-reference configuration labels and the CI eigenvector components), are given. In case of "ideal isoalloxazine"³, also the transition moment to the ground state is given, similarly to the table which lists the configuration data.

In the figure, the calculated singlet \rightarrow singlet transition energies relative

* Compound numbers refer to scheme 6.1, p. 86; Reference numbers refer to the reference listing to Chapter 6 (p. 104).

to the ground state are compared with the experimental spectrum, when available. Excited configurations are plotted as stick-bars with a length proportional to the total transition moment to the ground state (M) in atomic units (a.u., cf. p. 14). Excited states are plotted as stick-bars with a length proportional to the oscillator strength (f) of the transition from the ground state to the concerned excited state. Dotted excited state stick-bars indicate f -values multiplied by 1000 prior to plotting.

The relevant calculated data on the triplet states of the various isoalloxazines are collected in a separate table (Table A1.9). Experimental triplet energies can be found in Chapter 3, p. 22.

TABLE A1.1.
SINGLY EXCITED SINGLET CONFIGURATIONS OF THE "IDEAL"^{a)} ISOALLOXAZINE^{b)} MOLECULE.

Configuration ^{b)} Symm. c)	Energy (1000 cm ⁻¹) d)		Transition Moments (a.u.)				
	uncorr.	corr. INDO/S	x	y	z	total	
a: $\pi_9\pi_1^*$ A'	29.5	23.3	29.9	2.97	-0.41	0.00	3.00
b: $\sigma_{30}\pi_1^*$ A''	39.1	-	40.0	0.00	0.00	-0.03	0.03
c: $\pi_8\pi_1^*$ A'	37.5	32.5	37.8	1.26	0.87	0.00	1.53
d: $\sigma_{29}\pi_1^*$ A''	38.4	-	39.5	0.00	0.00	0.07	0.07
e: $\pi_9\pi_2^*$ A'	40.7	34.5	41.3	-1.24	-1.82	0.00	2.21
f: $\sigma_{28}\pi_1^*$ A''	43.5	-	44.9	0.00	0.00	0.08	0.08
g: $\pi_9\pi_3^*$ A'	44.0	37.8	44.3	0.78	-0.14	0.00	0.79
h: $\pi_7\pi_1^*$ A'	47.0	42.3	47.3	-0.33	-1.18	0.00	1.23
j: $\pi_6\pi_1^*$ A'	49.2	44.4	49.5	0.13	0.10	0.00	0.16
k: $\pi_8\pi_2^*$ A'	46.7	41.7	47.1	1.94	-0.43	0.00	1.98
l: $\pi_9\pi_4^*$ A'	48.2	42.0	48.5	0.15	-0.11	0.00	0.19
m: $\pi_8\pi_3^*$ A'	52.3	47.3	53.4	-0.08	1.36	0.00	1.36
n: $\sigma_{29}\pi_4^*$ A''	55.3	-	56.7	0.00	0.00	-0.11	0.11

a) Idealized isoalloxazine model carrying only proton substituents³; b) Notation according to footnote 40, orbitals given in Table 5.1, p. 61; c) Symmetry; d) cf. General Information for explanation.

TABLE A1.2.

CONFIGURATION INTERACTION ON THE "IDEAL" ISOALLOXAZINE" MOLECULE (SINGLET STATES).

State Opt.	Energy b) (1000 cm ⁻¹)	Transition Moments (a.u.) f ^{c)}			Composition ^{d)}	Other configurations										
		x	y	total		a	c	e	g	h	j	k	l	m		
a	28.4	2.56	-0.36	2.59	0.58	.97										
b	22.2	2.60	-0.35	2.63	0.47	.98										
A ₁ c	33.3	2.39	-0.32	2.41	0.44	.89			.29	.18						
a	34.3	1.04	0.02	1.04	0.11		.78	.35	-.39			.24				
b	28.9	0.83	-0.08	0.84	0.06		.74	.41	-.42			.24				
c	41.9	0.43	-0.10	0.45	0.02		.74	.34	-.46			.17				
a	39.2	-1.54	-1.17	1.93	0.45			.85	.34			-.24	-.17		-.18 $\pi_7\pi_3^*$	
b	33.1	-1.51	-1.19	1.92	0.37				.83	.38		-.23	-.17			
c	46.6	-0.80	-1.45	1.66	0.32			-.41	.78			-.30				
a	40.6	0.45	0.56	0.72	0.06		.58	-.24	.54	.18		-.44			-.20 $\pi_8\pi_4^*$ +.25 $\pi_7\pi_3^*$	
b	35.2	0.65	0.58	0.87	0.08		.63	-.21	.56			-.38				
c	45.4	0.37	-0.23	0.43	0.02		.41	.26	.62			-.44				
a	45.5	-1.40	-0.67	1.55	0.33			-.37	.83	.24	-.24					
b	40.4	-1.50	-0.54	1.60	0.31			-.36	.77	.27	-.32	-.21				
c	50.1	-1.39	-0.22	1.40	0.25		-.33		.60	.60						
a	46.7	-0.41	-0.09	0.42	0.03			.18		-.18		.89	.22			
b	40.6	-0.62	-0.21	0.65	0.05			.18			.20	.90	.18			
a	47.9	-0.79	0.77	1.10	0.18				-.27	-.44	.74	-.36				
b	42.9	-0.92	0.86	1.26	0.21				-.26	-.54	.63	-.43				
a	49.0	1.79	-0.24	1.81	0.49				.37	.21	.54	.61				
b	43.8	1.56	-0.16	1.57	0.33				.29	.18	.67	.55				
a	46.6	-0.19	1.20	1.21	0.21							-.19	.93		.90 $\pi_9\pi_5^*$ +.19 $\pi_8\pi_4^*$	
b	49.1	-0.29	0.64	0.71	0.07											
z f ^{c)}						d	b	f	n							
a	26.8	0.000	0.00			.62	-.54	.22	-.32							Completely mixed
A ₁ c	29.7	0.173	0.20 × 10 ⁻²			.58	-.62	.29	-.22							
a	29.7	0.000	0.00									Completely mixed				
A ₂ c	39.8	0.002	0.55 × 10 ⁻⁶									Completely mixed				
a	33.6	0.000	0.00									Completely mixed				
A ₃ c	45.1	0.023	0.59 × 10 ⁻⁴									Completely mixed				

a) Cf. Table A1.1; b) Options: a = CNDO/S uncorrected, b = CNDO/S corrected, c = INDO/S uncorrected; c) Oscillator strength; d) Configuration labels refer to Table A1.1.

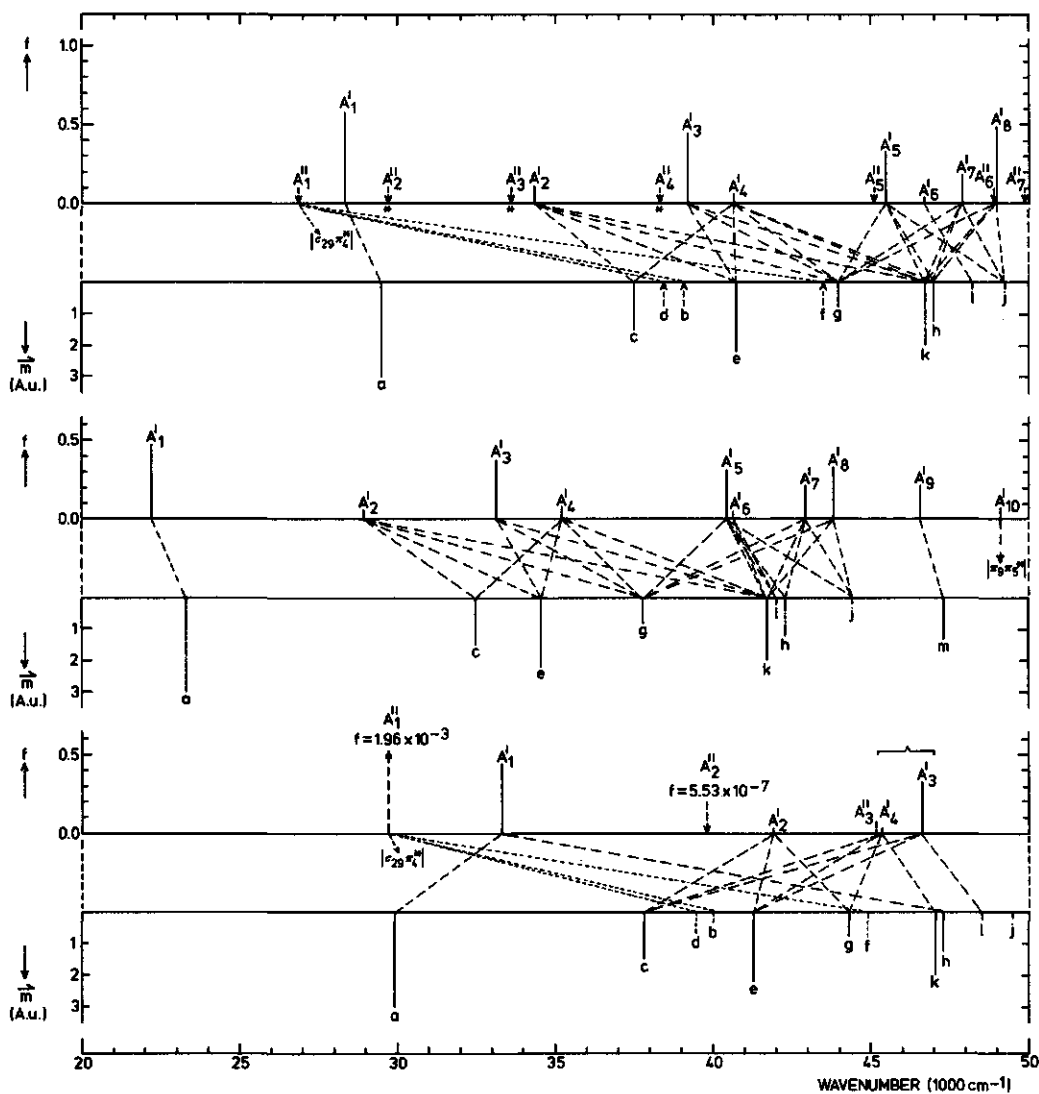


Figure A1.1. CI on "ideal" (all-proton) isoalloxazine³, lower excited singlet \rightarrow singlet transitions, 97 $^1A'$ and 98 $^1A''$ singly excited configurations. A: CNDO/S-CI transition energies and oscillator strengths (uncorr.); B: CI pattern (cf. Table A1.2); C: corresponding singly excited singlet configurations (cf. Table A1.1); D: as A, occupied orbitals Bigelow-corrected^{3,13} (cf. General Information E: INDO/S-CI transition energies and oscillator strengths (uncorr.). The apparent destabilization of the excited states in E is due to a slight admixture (2%) of singly excited configurations into the ground state, owing to a breakdown of Brillouin's Theorem connected with the calculational procedure used (cf. Section 6.2, p. 85). INDO/S-CI ground state stabilization: 8290 cm^{-1} .

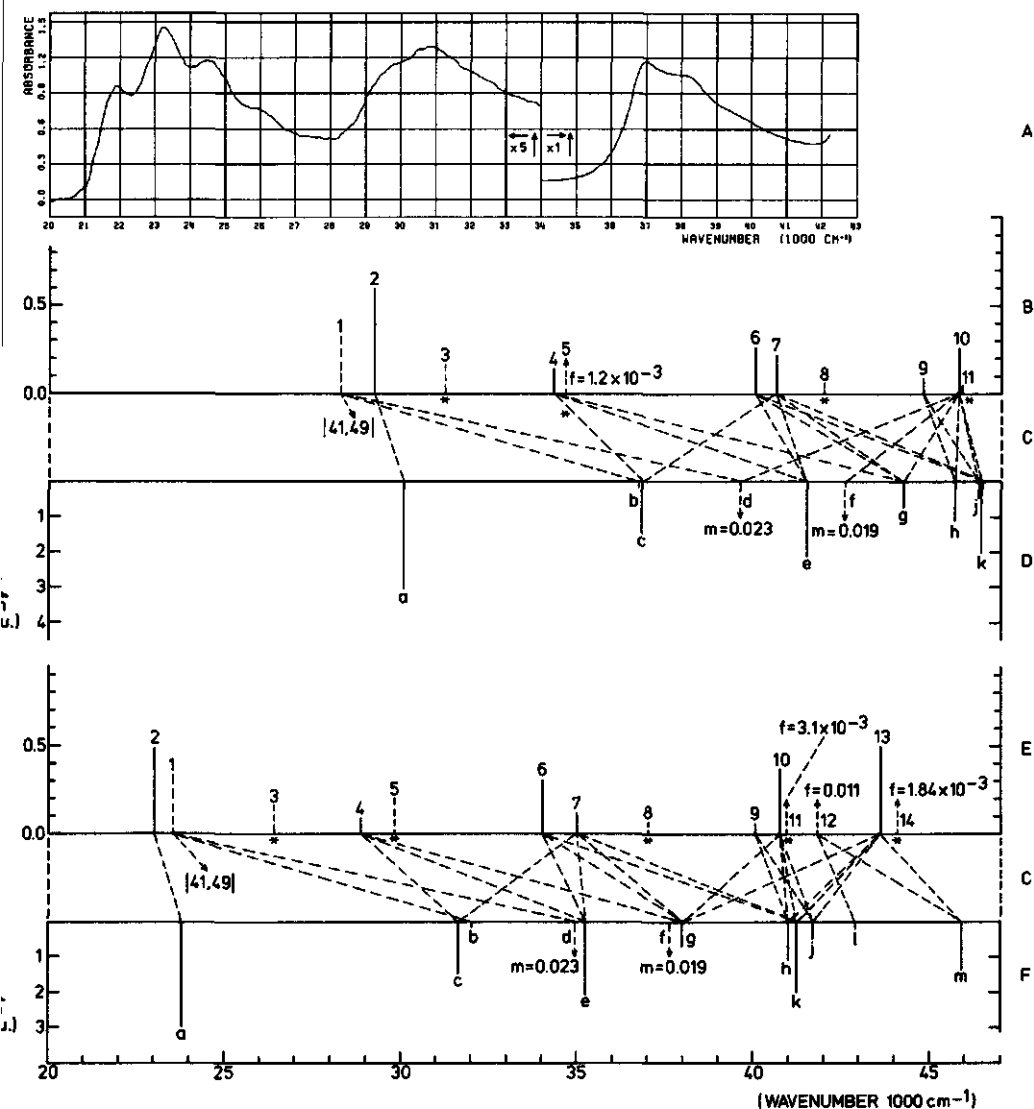


Figure A1.2. Experimental and calculated singlet \rightarrow singlet transitions in 3,10-dimethyl-isalloxazine (4), CNDO/S-CI method, 100 singly excited singlet configurations. A: Absorption spectrum in 2-methyl-tetrahydrofuran¹, 77 K, $c = 29 \mu\text{M}$; B: Calculated transition energies and oscillator strengths (uncorr.) after CI; C: CI pattern (cf. Table A1.4); D: Corresponding singly excited singlet configurations (cf. Table A1.3); E: as B, occupied orbitals Bigelow-corrected^{3,13}; F: as D, occupied orbitals Bigelow-corrected^{3,13}.

TABLE A1.3.

SINGLY EXCITED SINGLET CONFIGURATIONS OF 3,10-DIMETHYL-ISOALLOXAZINE (4) IN THE CNDO/S APPROXIMATION.

Configuration	Energy (1000 cm^{-1})		Transition Moments (a.u.)			
	uncorr.	corr.	x	y	z	total
a: 45,46	30.1	23.8	-3.05	0.27	0.00	3.06
b: 43,46	36.7	32.0	-0.06	-0.13	0.00	0.15
c: 44,46	36.8	31.6	1.12	0.94	0.00	1.47
d: 41,46	39.6	34.9	0.01	-0.02	0.00	0.02
e: 45,47	41.5	35.3	1.13	1.78	0.00	2.11
f: 39,46	42.6	37.7	0.00	0.02	0.00	0.02
g: 45,48	44.2	38.0	-0.68	0.09	0.00	0.69
h: 42,46	45.7	41.0	0.33	1.05	0.00	1.10
j: 40,46	46.4	41.7	-0.06	0.46	0.00	0.47
k: 44,47	46.4	41.3	1.99	-0.42	0.00	2.03
l: 45,49	49.1	42.9	-0.13	0.15	0.00	0.20
m: 44,48	51.1	45.9	-0.06	1.36	0.00	1.36

Cf. General Information and annotations to Table A1.1 for explanation.

TABLE A1.4.

CONFIGURATION INTERACTION ON 3,10-DIMETHYL-ISOALLOXAZINE (4) IN THE CNDO/S APPROXIMATION (SINGLET STATES).

State Ass.		Energy (1000 cm ⁻¹)	f	Composition													Other configurations contributing*
a)	b)			a	b	c	d	e	f	g	h	i	j	k	l	m	
1a	A ₁ ^u	28.3	0.33 × 10 ⁻³		.63		.56										-.34 41,49
1b	A ₁ ^u	23.5	0.34 × 10 ⁻³		.63		.56										-.34 41,49
2a	A ₁ ^u	29.2	0.60	.97													
2b	A ₁ ^u	23.0	0.49	.98													
3a	A ₂ ^u	31.2	0.16 × 10 ⁻³		.51		-.41	.29									-.32 43,47 +.35 41,50
3b	A ₂ ^u	26.4	0.15 × 10 ⁻³		.51		-.40	.30									5 more configurations
4a	A ₂ ^u	34.3	0.15		.82		-.30	.36						.21			
4b	A ₂ ^u	28.9	0.09		.79		-.34	.39						.22			
5a	A ₃ ^u	34.7	0.12 × 10 ⁻²														Completely mixed
5b	A ₃ ^u	29.8	0.21 × 10 ⁻³														Completely mixed
6a	A ₃ ^u	40.0	0.26					.66		.51				.42			
6b	A ₃ ^u	34.0	0.31					.79		.43				.31			
7a	A ₄ ^u	40.6	0.22		.52			.60		-.36				-.31			
7b	A ₄ ^u	35.0	0.12		.58			.39		-.50				-.37			
8a	A ₄ ^u	42.0	0.32 × 10 ⁻⁴														Completely mixed
8b	A ₄ ^u	37.0	0.37 × 10 ⁻⁴								.74	-.59					Completely mixed
9a	A ^u	44.8	0.97 × 10 ⁻¹								.69	-.63					
9b	A ^u	40.0	0.58 × 10 ⁻¹	-.19													
10a	A ^u	45.8	0.26				-.21	.19	-.39	.51	.58	.22					
10b	A ^u	40.8	0.37						-.42	.57	.54	.37					
11a	A ^u	45.9	0.46 × 10 ⁻¹				.39	-.48		.21	.26						
11b	A ^u	41.0	0.31 × 10 ⁻²				.41	-.52									
12b	A ^u	41.8	0.11 × 10 ⁻¹												.88	-.35	
13b	A ^u	43.6	0.50						.38	.30	.43	-.66					
14b	A ^u	44.1	0.18 × 10 ⁻²													-.22	Completely mixed

a) Affixes indicate option: a = uncorr., b = corr. (cf. General Information and annotations to Table A1.1);

b) Assignment; further explanation in General Information and annotations to Table A1.2. *contributions >5% only.

TABLE A1.5.

SINGLY EXCITED SINGLET CONFIGURATIONS OF 3,10-DIMETHYL-ISOALLOXAZINE (4) IN THE INDO/S APPROXIMATION.

Configuration	Energy (1000 cm^{-1})		Transition Moments (a.u.)			
	uncorr.	corr.	x	y	z	total
a: 45,46	30.5	24.2	-3.05	0.27	0.00	3.06
b: 43,46	37.7	33.0	-0.06	-0.13	0.05	0.15
c: 44,46	37.1	32.0	1.12	0.94	0.00	1.47
d: 41,46	40.5	35.8	0.01	-0.02	0.06	0.07
e: 45,47	42.1	35.8	1.13	1.78	0.00	2.11
f: 39,46	43.9	39.0	0.00	0.02	0.08	0.08
g: 45,48	44.6	38.3	-0.68	0.09	0.00	0.69
h: 42,46	45.9	41.2	0.33	1.05	0.01	1.11
j: 40,46	46.7	42.0	-0.06	0.46	0.00	0.47
k: 44,47	46.8	41.6	1.99	-0.42	0.00	2.03
l: 45,49	49.5	43.2	-0.13	0.15	0.00	0.20

The only configuration which admixes significantly ($c \approx 0.11$) into the ground state is $|42,49| \approx |\pi_7\pi_4^*|$ (60870 cm^{-1} corr. and 65561 cm^{-1} uncorr.). Cf. General Information and annotations to Table A1.1 for further explanation.

TABLE A1.6.

CONFIGURATION INTERACTION ON 3,10-DIMETHYL-ISOALLOXAZINE (4) IN THE INDO/S APPROXIMATION (SINGLET STATES).

State Ass.	Energy (1000 cm ⁻¹)	f	Composition												Other configurations contributing >5%
			a	b	c	d	e	f	g	h	i	j	k	l	
1a A ₁ ⁺	28.4	0.18 × 10 ⁻²		.69		.49		.31							-.23 41,49 -.18 43,48
1b A ₁ ⁺	24.0	0.17 × 10 ⁻²		.68		.49		.32							-.23 41,49 -.18 43,48
2a A ₁ ⁺	31.1	0.48	.90							.20		.25			
2b A ₁ ⁺	25.4	0.38	.91							.18		.24			
3a A ₂ ⁺	36.2	0.32 × 10 ⁻²													Completely mixed
3b A ₂ ⁺	31.8	0.21 × 10 ⁻²													Completely mixed
4a A ₂ ⁺	38.2	0.32 × 10 ⁻¹			.81		-.29		.38						
4b A ₂ ⁺	33.1	0.16 × 10 ⁻¹			.77		-.32		.43						
5a A ₄ ⁺	42.1	0.26 × 10 ⁻¹		-.39					.64				.47		+.22 44,49 +.22 40,48 +.20 42,48
5b A ₄ ⁺	36.8	0.21 × 10 ⁻¹		-.43					.64				.45		+.22 44,49 +.20 40,48 +.19 42,48
6a A ₃ ⁺	43.4	0.66 × 10 ⁻²													Completely mixed
6b A ₃ ⁺	38.9	0.68 × 10 ⁻²													Completely mixed
7a A ₃ ⁺	44.1	0.24		.25			.82							-.30	
7b A ₃ ⁺	38.4	0.24		.31			.81							-.31	

Cf. General Information and annotations to Table A1.4 for explanation.

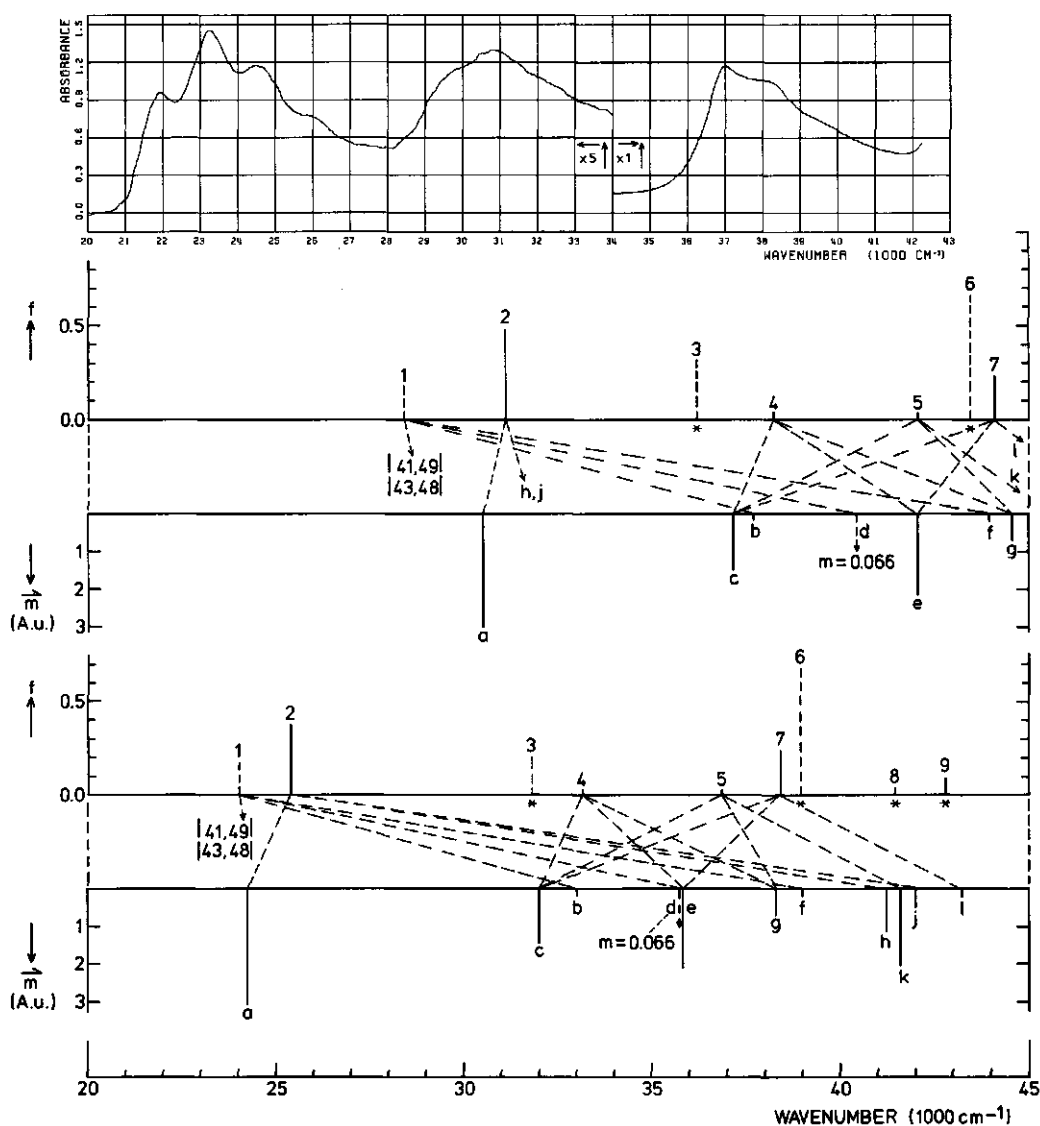


Figure A1.3. Experimental and calculated singlet \rightarrow singlet transitions in 3,10-dimethyl-isoalloxazine (4), INDO/S-CI method (cf. General Information), 81 singl excited singlet configurations. Labels as in Fig. A1.2, CI pattern and configuration data in Tables A1.5 and A1.6. The apparent destabilization of excited states in B and E is due to breakdown of Brillouin's Theorem (cf. Caption to Fig A1.1). Corresponding ground state stabilizations: 4670 cm^{-1} in B (3% admixture) and 5035 cm^{-1} in E (6% admixture).

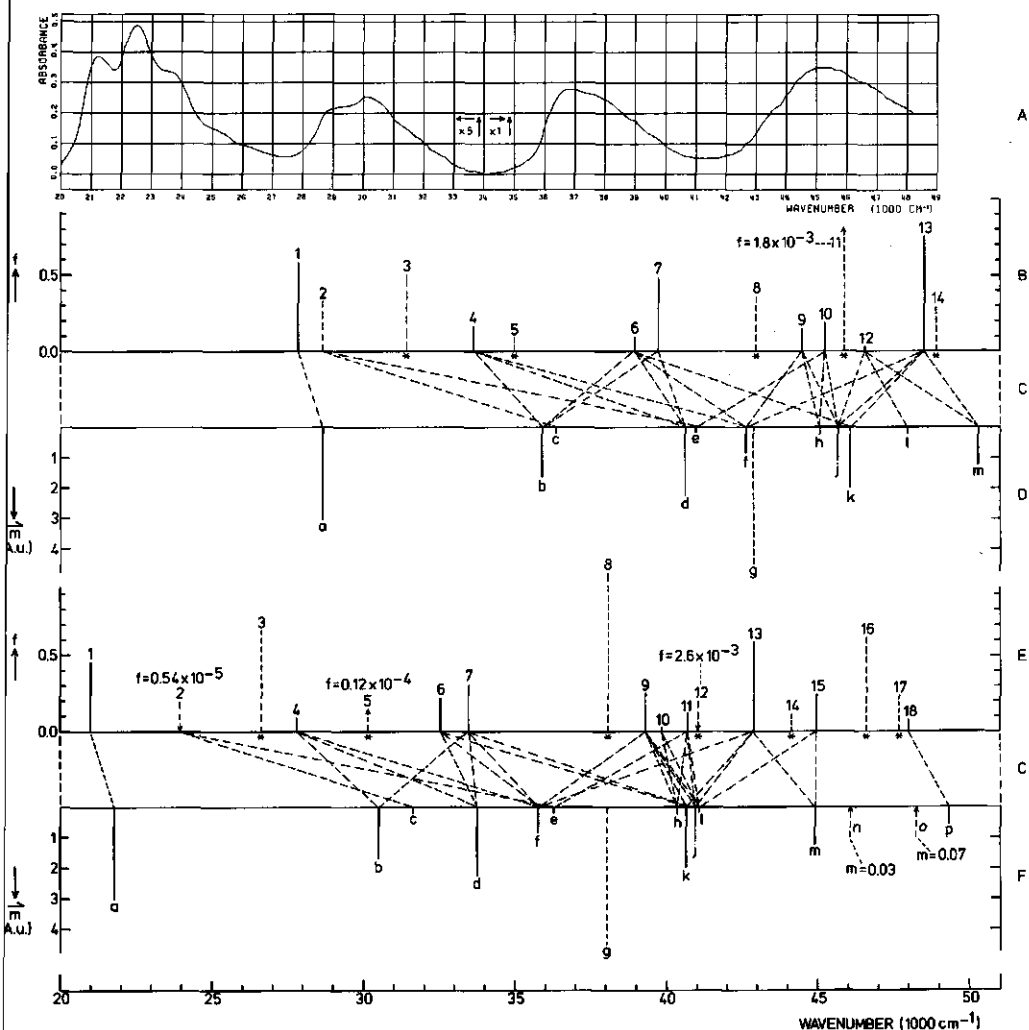


Figure A1.4. Experimental and calculated singlet \rightarrow singlet transitions in 7,8-dimethylated isoalloxazines (flavins), CNDO/S-CI method, 100 singly excited singlet configurations. A: Absorption spectrum of 3,7,8-trimethyl-10-(n-octadecyl)-isoalloxazine (6) in 3-methyl-pentane¹, 300 K, c = 6.6 μM; further labels refer to a calculation on 3,7,8,10-tetramethyl-isoalloxazine (3-methyl-lumiflavin; 5) as in Fig. A1.2, CI pattern and configuration data in Tables A1.7 and A1.8.

TABLE A1.7.

SINGLY EXCITED SINGLET CONFIGURATIONS OF 3,7,8,10-TETRAMETHYL-ISOALLOXAZINE (5) IN THE CNDO/S APPROXIMATION.

Configuration	Energy (1000 cm ⁻¹)		Transition Moments (a.u.)				
	uncorr.	corr.	x	y	z	total	
a: 51,52	28.7	21.8	-3.00	0.44	-0.01	3.03	
b: 50,52	35.9	30.5	-1.38	-0.89	0.00	1.64	
c: 49,52	36.3	31.6	-0.07	-0.19	0.00	0.20	
d: 51,53	40.6	33.8	1.32	1.82	0.01	2.25	
e: 47,52	41.0	36.3	-0.08	-0.12	0.00	0.14	
f: 51,54	42.6	35.8	-0.79	0.35	-0.01	0.86	
g: 45,52	42.9	38.0	0.00	0.00	0.00	0.00	
h: 46,52	45.0	40.4	0.14	0.19	0.00	0.24	
j: 48,52	45.7	40.9	0.35	1.07	-0.01	1.13	
k: 50,53	46.1	40.7	-1.91	0.61	-0.02	2.01	
l: 51,55	47.9	41.1	-0.09	0.19	0.00	0.21	
m: 50,54	50.3	44.9	-0.09	-1.23	0.00	1.23	
n: 44,52	51.2	46.1	0.02	0.02	-0.01	0.03	
o: 49,53	53.0	48.3	0.06	-0.03	0.00	0.07	
p: 51,56	56.2	49.3	-0.44	0.40	0.00	0.60	

Cf. General Information and annotations to Table A1.1 for explanation.

TABLE A1.8.

CONFIGURATION INTERACTION ON 3,7,8,10-TETRAMETHYL-ISOALLOXAZINE (5) IN THE CNDO/S APPROXIMATION (SINGLET STATES).

State Ass.	Energy (1000 cm ⁻¹)	f	Composition													Other configurations contributing >5%
			a	b	c	d	e	f	g	h	j	k	l	m		
1a A ₁ ¹	27.8	0.58	.97													+ .30 47,55
1b A ₁ ¹	21.0	0.46	.98													+ .30 47,55
2a A ₁ ¹	28.6	0.33 × 10 ⁻³			.69		-.48									5 more configurations
2b A ₁ ¹	23.9	0.54 × 10 ⁻⁵			.69		-.48									5 more configurations
3a A ₂ ¹	31.4	0.51 × 10 ⁻³			.45		.39		.31	.25						
3b A ₂ ¹	26.6	0.66 × 10 ⁻³			.45		.39		.32	.25						
4a A ₂ ¹	33.6	0.17		.82	.32		-.35					.21				
4b A ₂ ¹	27.8	0.90 × 10 ⁻¹		.77	.38		-.40					.22				
5a A ₃ ¹	35.0	0.81 × 10 ⁻⁴														Completely mixed
5b A ₃ ¹	30.2	0.12 × 10 ⁻⁴														Completely mixed
6a A ₄ ¹	39.0	0.96 × 10 ⁻¹		.30	.40		.66					-.46				
6b A ₄ ¹	32.5	0.22			.66		.60					-.34				
7a A ₃ ¹	39.7	0.49		-.44	.79		-.16						-.19			
7b A ₃ ¹	33.5	0.31		-.59	.57		-.39		.41			.25	-.17			
8a A ₄ ¹	42.9	0.36 × 10 ⁻³														8 more configurations
8b A ₄ ¹	38.1	0.10 × 10 ⁻²							.41							8 more configurations
9a A ¹	44.5	0.15					.21	-.34		-.47	.71	-.23				
9b A ¹	39.3	0.25					.33			.27	-.63	.38	-.44			
10a A ¹	45.2	0.19					-.33			.72	.46		.20			3 more configurations
10b A ¹	39.9	0.70 × 10 ⁻²			.15	-.24				.50	-.24	.71	.20			
11a A ¹	45.9	0.18 × 10 ⁻²														Completely mixed
11b A ¹	40.7	0.12		-.17			-.29			.66	.52	-.35				
12a A ¹	46.6	0.23 × 10 ⁻¹														-.17 50,53
12b A ¹	41.1	0.26 × 10 ⁻²			.18	-.38		-.55	-.14	-.28	.84	.30				6 more configurations
13a A ₆ ¹	48.5	0.75					.46			.31	.70	.27				
13b A ₆ ¹	42.9	0.59					.39			.42	.70	.24				
14a A ¹	48.9	0.29 × 10 ⁻³			.37	.42		-.39	.24							-.28 49,55 + .43 49,53
14b A ¹	44.1	0.11 × 10 ⁻³			.36	.42		-.37	.24							-.28 49,55 + .43 49,53
15b A ¹	44.9	0.24										-.20	-.27	.89		Completely mixed
16b A ¹	46.6	0.62 × 10 ⁻³														Completely mixed
17b A ¹	47.7	0.23 × 10 ⁻³														
18b A ¹	48.0	0.82 × 10 ⁻¹														+ .89 51,56 -.23 50,55

Cf. General Information and annotations to Table A1.4 for explanation.

TABLE A1.9.

CONFIGURATION INTERACTION ON VARIOUS ISOALLOXAZINE DERIVATIVES (TRIPLET STATES).

Compound			Option	State	Energy (1000 cm ⁻¹) calc. exp. ^{b)}									
"ideal"	CNDO/S	(a)	$^3A_1'$ $^3A_2'$	14.5 21.9		Configuration ^{c)}	:	a	c	e	g	h	l	m
						E _{conf.} ^{d)} (1000 cm ⁻¹):	:	19.6	30.7	29.6	36.1	40.6	42.1	35.4
						Composition	:	.87	.23	.17				.17
						Composition	:	-.23	.21	.68		.26		.38
"ideal"	INDO/S	(a)	$^3A_1'$ $^3A_2'$	20.9 26.5		Configuration ^{c)}	:	a	c	e	g	h	l	m
						E _{conf.} ^{d)} (1000 cm ⁻¹):	:	19.1	30.4	29.0	35.8	40.3	41.8	34.3
						Composition	:	.84	.21	.21				.18
						Composition	:	-.30		.67			.25	.36
"ideal"	INDO/S	(a)	$^3A_1''$	27.0		Configuration ^{c)}	:	b	d	f	σ ₂₉ π ₄ [*]			
						E _{conf.} ^{d)} (1000 cm ⁻¹):	:	39.9	38.7	43.8	55.6			
						Composition	:	-.60	.56	.32	-.23			
4	CNDO/S		$^3A_1'$ $^3A_2'$	16.5 23.9	17.4	Configuration ^{c)}	:	a	c	e	g	h	j	m
						E _{conf.} ^{d)} (1000 cm ⁻¹):	:	20.1	30.0	31.3	36.7	41.8	40.9	34.0
						Composition	:	.91	-.21					
						Composition	:	.21	.55	-.52	-.20		-.22	-.41
4	INDO/S		$^3A_1'$ $^3A_2'$	20.1 26.5	17.4	Configuration ^{c)}	:	a	c	e	g	h	j	m
						E _{conf.} ^{d)} (1000 cm ⁻¹):	:	19.7	29.6	30.8	36.4	41.6	40.6	32.9
						Composition	:	.90	-.20					
						Composition	:	-.21	-.20	.70	.19			-.42
4	INDO/S		$^3A_1''$	26.5		Configuration ^{c)}	:	b	d	f	41,49		43,48	
						E _{conf.} ^{d)} (1000 cm ⁻¹):	:	36.8	39.8	42.8	57.3		60.7	
						Composition	:	.67	.49	.31	-.24		-.18	
5	CNDO/S		$^3A_1'$ $^3A_2'$	15.7 23.0	16.8	Configuration ^{c)}	:	a	b	d	h	j	k	m
						E _{conf.} ^{d)} (1000 cm ⁻¹):	:	19.5	29.3	29.8	42.3	39.1	38.6	34.2
						Composition	:	.90	.24					
						Composition	:	-.23	.46	.58		.21		.47

a) Idealized all-proton model as calculated previously³; b) Experimental value¹
c) Configuration labels identical to those used to identify the singlet configurations; d) Energy of the triplet configuration.

SUMMARY

The subject of this thesis, as apparent from its title, is a detailed study of the isoalloxazine molecule by a variety of techniques belonging to the field of optical spectroscopy. After a brief introduction to the subject in general terms, together with some historical background and citation of relevant review papers which appeared before 1979 (Chapter 1), a general outline of experimental techniques and theoretical methods used is given (Chapter 2). More detailed information about specific experiments or calculations is provided in the experimental sections of the individual chapters.

Chapters 3 and 4 describe the continuous wave and time-resolved spectral properties of (iso)alloxazines determined under experimental conditions, in which external perturbation of the molecules of interest is minimized as much as possible. This could be achieved by measurements in apolar solvents (Chapter 3) and in the vapour phase (Chapter 4), a state of aggregation in which the molecule could be brought with some experimental skill. Thus, a large temperature range (77 to 520 K) could be employed. In solution at 77 and 300 K (Chapter 3), the spectra revealed a 1250 cm^{-1} vibrational progression in all isoalloxazines investigated (probably a stretching mode); actual lifetimes of 5 - 10 ns for fluorescence and $\sim 300\text{ ms}$ for phosphorescence (77 K, no phosphorescence could be detected in fluid solution) were observed; the ratio of the actual and radiative lifetimes of the electronically first excited singlet state agreed very well with an independent quantum yield determination and solvent interactions were found to affect primarily the Franck-Condon envelopes of the spectra and not the electronic transition energies. The non-radiative decay of isoalloxazine, on the other hand, is strongly dependent on the molecule's environment. An anomalously large Stokes-loss in fluid and glassy solution is indicative of a conformational change of the molecule occurring upon electronic excitation. In alkane solution at 77 K, isoalloxazines form clusters exhibiting P-type (triplet-triplet annihilation process) delayed fluorescence. Vapour phase spectra (Chapter 4), although less structured than solution spectra owing to sequence congestion, provided primary information on *isolated* (iso)alloxazines when comparison with spectra obtained in condensed media was made. Fluorescence lifetimes range from $< 0.5\text{ ns}$ for alloxazine to 1-18 ns for isoalloxazine vapour. The data indicate possible intramolecular complex formation

between the isoalloxazine ring system and its own aliphatic side-chain carrying a (polar) hydroxyl group. Direct photodissociation of isoalloxazine in the electronically first excited singlet state is not a probable process in the vapour phase.

Chapter 5 describes the continuation of (iso)alloxazine vapour phase experiments by the application of ultraviolet photoelectron spectroscopy. Both He(I) and He(II) excitation was used. The spectra are interpreted using various methyl substituted isoalloxazines and by comparison with the results obtained from CNDO/S calculations and photoionization cross-sections derived therefrom. The dependence of the electronic properties of isoalloxazines on the redox state and the degree of substitution is analyzed. A critical review of the data obtained from semiempirical MO calculations by various other authors and the CNDO/S results shows that a few methods give a fairly good prediction of the π orbital energies only. Without exception, the calculated σ orbital energies contain considerable error. Particularly, all theoretical methods fail to predict a threefold degeneracy in the orbital level scheme at ~ 9.6 eV, in which both π and σ orbitals are involved. Possible reasons for the failures are discussed. Analysis of the experimental and theoretical results reveals a planar molecular conformation to be the most probable one for an *isolated reduced* isoalloxazine molecule in the vapour phase, contrary to the bent conformation which is encountered in solution or the solid state. Bending is, therefore, most likely caused by interaction of the molecule with its environment. Such interactions, leading to changes in orbital energies, may in part be responsible for the ability of the protein-bound flavocoenzyme to be involved in a broad diversity of biological reactions.

In chapter 6, all foregoing data are put together in a combined analysis to establish relationships between the photoelectron and ordinary optical spectra. First, additional photoelectron spectra of 10-hydroxyalkyl-isoalloxazines confirmed the existence of the intramolecular complex proposed on the basis of vapour phase fluorescence lifetimes (*vide supra*). The hydrogen-bond between the side-chain OH group and the N_1 imine-like nitrogen atom (cf. Scheme 1.1, p. 1) leads to a destabilization of the lone pair on the latter atom, contrary to common experience. This anomalous behaviour can be ascribed to rearrangement of existing through-bond interactions in the free isoalloxazine molecule. Results from CNDO/S and INDO/S calculations agree reasonably with the observations. Secondly these findings have considerable impact on the interpretation of existing and in this thesis presented optical spectra. The new photoelectron spectroscopic data lead, in combination with optical spectra, to the assignment of the isoalloxazine

π_2 to a mixed state containing (anomalous) $n\pi^*$ character arising from the anomalous behaviour of the N_1 lone pair (cf. Scheme 1.1, p.1). The oscillator strength of the $S_0 \rightarrow S_2 \pi \rightarrow \pi^*$ component is very sensitive to external perturbation. Finally, the possible implications for biochemical catalysis by flavins are discussed.

Chapter 7 describes a thorough investigation of Old Yellow Enzyme (OYE), a (flavo)protein containing the isoalloxazine derivative flavin mononucleotide (FMN). It is attempted to interpret the spectral properties of this protein in terms of intermolecular interactions between its constituents, using the knowledge and experience acquired in the preceding research. The results demonstrate the inadequacy of the existing explanation of the phenomena occurring upon the addition of phenols to OYE, based on the formation of a simple phenolate-FMN donor-acceptor charge transfer complex. Instead, it was found that the phenolate anion interferes strongly with an existing tight complex between FMN and the protein, probably a H-bonded structure in which FMN is tautomerized and interacts with a L-chiral center. This is concluded from a separate electronic transition with an origin at 496 nm, thus far not recognized as such, and the circular dichroism observed. The emission of OYE is dominated by that of free FMN, although protein-bound FMN seems also to become luminescent in glassy solution at 143 K. A second fluorescence/phosphorescence emission appears upon UV-excitation of both native and complexed OYE. This emission is quenched by the addition of phenol to OYE, shows a large (3000 cm^{-1}) blue shift on going to a low temperature glass and is tentatively assigned to excimers of nucleic acids. Long-wavelength excitation with a synchronously pumped, mode-locked Rhodamine 6G dye laser revealed a third, extremely weak, emission in both native OYE and its complexes. It decays with ~ 3 ns lifetime at 143 K. ESR spectra revealed the presence of a low amount of an unpaired spin in OYE. Owing to an unusual relaxation behaviour it could only be observed below 15 K and the signal was measured in both the free enzyme and its complexes. Possible assignment and consequences of this observation are discussed. In frozen aqueous solutions of the OYE-phenolate complex, a phase transition was discovered at which the colour reverted to that of the native enzyme. Subsequent melting restored the original colour. The observed phenomena and existing literature data lead to the conclusion that the only model from which no apparent inconsistencies emerge, is that of a very complicated network of hydrogen-bonded structures in the protein. These involve several, partly unknown, chromophores. Phenols interfere with this network, leading to the formation of the long-wavelength absorption band in OYE.

Finally, a brief postscript (Chapter 8) is given, containing an overview of recent spectroscopic literature on isoalloxazines, a discussion in response to a

polemic in papers by other scientists and the ESCA (XPS) spectrum of 3,7,8,10-tetramethyl-isoalloxazine (3-methylumiflavin).

SAMENVATTING

Zoals reeds uit de titel blijkt, is het onderwerp van dit proefschrift een gedetailleerde studie van het isoalloxazine molecuul met behulp van optisch-spectroscopische technieken. Na een beknopte inleiding in algemene zin, waarin enige historische achtergronden en relevante overzichtsartikelen worden vermeld (Hoofdstuk 1), volgt een algemene beschrijving van gebruikte methoden, zowel experimenteel als theoretisch (Hoofdstuk 2). Meer gedetailleerde gegevens volgen in de betreffende hoofdstukken die zich met specifieke deelonderwerpen bezighouden.

In de hoofdstukken 3 en 4 wordt een overzicht gegeven van de spectrale eigenschappen van (iso)alloxazines, zowel continu als tijdsopgelost, onder omstandigheden waarin externe invloeden op het molecuul tot een minimum zijn gereduceerd. Dit kon worden bereikt via oplossingen in apolaire oplosmiddelen (Hoofdstuk 3), of door de metingen aan (iso)alloxazines in de gasfase uit te voeren. Dit laatste bleek, na het opdoen van de nodige ervaring, betrekkelijk eenvoudig uitvoerbaar. Aldus kon ook worden geprofiteerd van een groot temperatuurbereik (77 tot 520 K). In oplossing werd bij 77 en 300 K in alle isoalloxazines een vibratieprogressie van 1250 cm^{-1} gevonden. Dit is vermoedelijk een strekvibratie. Actuele fluorescentie levensduren varieerden van 5-10 ns in oplossing terwijl in glazen bij 77 K fosforescentielevensduren van $\sim 300\text{ ms}$ werden gemeten. In vloeibare oplossing werd geen fosforescentie waargenomen, ook niet na zorgvuldig ontgassen. De verhouding van de fluorescentielevensduur en de stralingslevensduur van de eerste elektronisch aangeslagen singuleettoestand kwam uitstekend overeen met onafhankelijke metingen van de quantumopbrengst. De invloed van het oplosmiddel op de excitatie-energieën was uiterst gering zolang niet-waterstofbrugvormende oplosmiddelen werden gebruikt. Wel zijn de relatieve intensiteiten van vibronische banden behorende bij één elektronenovergang (Franck-Condon factoren) en de stralingsloze processen sterk oplosmiddel-afhankelijk. Een ongewoon grote Stokes-loss in vloeibare en vaste (glas-achtige) oplossing duidt op een verandering in moleculaire conformatie wanneer isoalloxazine elektronisch wordt aangeslagen. In een 3-methyl-pentaan oplossing vormen zich conglomeraten van isoalloxazine-moleculen die, als gevolg van triplet - triplet annihilatie, aanleiding geven tot (z.g. P-type) uitgestelde fluorescentie. Gasfase spectra (Hoofdstuk 4), alhoewel nagenoeg structuurloos als gevolg van "sequence congestion", leveren toch belangrijke gegevens op

omtrent het *geïsoleerde* molecuul, wanneer vergelijkingen worden gemaakt met spectra die zijn verkregen in gecondenseerde media. De fluorescentielevensduren variëren in de gasfase van minder dan 0,5 ns voor alloxazines tot 1-18 ns voor isoalloxazines. Er zijn sterke aanwijzingen dat een isoalloxazine derivaat met een hydroxyl groep in zijn zijketen een intramoleculair complex vormt via een waterstofbrug tussen de OH groep en het heterocyclisch ringsysteem. Directe fotodissociatie van isoalloxazine in de eerste aangeslagen (singulet) electronentoestand is niet waarschijnlijk in de gasfase.

Hoofdstuk 5 beschrijft de uitbreiding van de gasfase-experimenten met de metingen van ultraviolet fotoelectronspectra, zowel met He(I) als He(II) excitatie. Deze spectra worden geïnterpreteerd aan de hand van (methyl) substituent effecten en door vergelijken met de resultaten van CNDO/S berekeningen en fotoionisatie waarschijnlijkheden (uitgedrukt in cross-sections), die daaruit kunnen worden afgeleid. De afhankelijkheid van de electronen-eigenschappen van de oxidatietoestand van het isoalloxazine molecuul en de mate waarin dit is gesubstitueerd, wordt diepgaand geanalyseerd. Een overzicht van de gegevens verkregen uit diverse semi-empirische berekeningen (inclusief CNDO/S) toont aan, dat slechts enkele methoden de gemeten orbital energieën redelijk voorspellen. Dit geldt bovendien slechts voor π orbitals, de fouten in de energie van σ orbitals zijn, zonder uitzondering, groot. Met name blijkt geen enkele theorie in staat te zijn een ontastoring in het energieschema bij ongeveer -9.6 eV, waarin zowel π als σ orbitals betrokken zijn, te voorspellen. Redenen hiervoor worden bediscussieerd. Het blijkt uit de verkregen gegevens dat een *geïsoleerd* isoalloxazine in gereduceerde toestand een vlakke structuur heeft, in tegenstelling tot de gebogen conformatie die wordt waargenomen in vloeibare of vaste fase. Derhalve kan de gebogen structuur worden toegeschreven aan wisselwerking van het molecuul met zijn omgeving. Dergelijke interacties geven aanleiding tot veranderingen in de orbital energieën en verklaren tenminste kwalitatief hoe isoalloxazine betrokken kan zijn in een breed scala van biochemische processen.

In Hoofdstuk 6 worden de verkregen gegevens verder uitgediept om de relatie tussen de optische en fotoelectron spectra verder vast te stellen. Allereerst bevestigden verdere fotoelectron spectroscopische metingen het bestaan van bovengenoemd intramoleculair complex in 10-hydroxyalkyl-isoalloxazines. De waterstofbrug tussen de OH groep in de zijketen en het N₁ imine-achtige stikstofatoom (zie Schema 1.1, p. 1) leidt tot een destabilisatie van het eenzame electronenpaar op dit atoom, precies het tegenovergestelde van wat men zou verwachten. Een en ander is een gevolg van ingrijpende wijzigingen in de bestaande through-bond interacties. CNDO/S en INDO/S berekeningen stemmen hiermee goed overeen. Ten

tweede blijkt nu de oplosmiddel-afhankelijkheid van de optische spectra van isoalloxazines in waterstofbrufvormende media goed verklaard te kunnen worden. De gecombineerde gegevens maken het mogelijk de isoalloxazine S_2 toestand toe te kennen aan een gemengde electronentoestand die zowel $n\pi^*$ als $\pi\pi^*$ karakter bevat. Tengevolge van het uitzonderlijk gedrag van het N_1 stikstof lone pair vertoont de $S_0 \rightarrow S_2$ een uitzonderlijke oplosmiddelverschuiving, ook al omdat de $\pi \rightarrow \pi^*$ component in de $S_0 \rightarrow S_2$ overgang uiterst gevoelig is voor externe storingen voor wat betreft zijn oscillatorsterkte. Tenslotte worden de implicaties van waterstofbrugvorming voor de biochemische werking besproken.

Hoofdstuk 7 bevat een beschrijving van een diepgaand onderzoek aan Old Yellow Enzyme (OYE), een (flavo)proteïne dat het isoalloxazine derivaat flavine-mononucleotide (FMN) als prosthetische groep bevat. Er is getracht een verklaring te geven van de spectrale eigenschappen van dit eiwit in termen van intermoleculaire wisselwerkingen tussen de erin aanwezige chromofore groepen. De resultaten tonen aan dat de bestaande verklaring van voornoemde eigenschappen, een verklaring die uitgaat van de vorming van een fenolaat-FMN donor-acceptor charge transfer complex als fenol aan OYE wordt toegevoegd, als onvolledig moet worden beschouwd. In plaats daarvan moet worden geconcludeerd dat het fenolaat anion drastisch ingrijpt in een bestaande structuur in het eiwit. In deze structuur vormt FMN een hecht complex met het apoproteïne, waarschijnlijk via een stelsel van waterstofbruggen, waardoor FMN in een tautomere vorm voorkomt en een wisselwerking heeft met een L-chiraal center. Dit volgt uit een, voorheen niet als zodanig onderkende, tweede electronenovergang in het flavine $S_0 \rightarrow S_1$ gebied en de gemeten CD spectra. De emissie van OYE kan hoofdzakelijk worden toegeschreven aan vrij FMN, alhoewel eiwit-gebonden FMN bij 143 K in vaste (glasachtige) oplossing ook tot de luminescentie lijkt bij te dragen. Een tweede fluorescentie/fosforescentie werd waargenomen bij UV excitatie, zowel in het vrije OYE als de gecomplexeerde vormen daarvan. Deze laatste emissie dooft partieel bij toevoegen van fenolen aan OYE, is in vaste oplossing 3000 cm^{-1} naar het blauw verschoven t.o.v. vloeibare oplossing en wordt toegeschreven aan excimeren van nucleinezuren. Excitatie bij lange golflengte m.b.v. een synchroon gepompte mode-locked Rhodamine 6G kleurstoflaser, geeft aanleiding tot een derde, zeer zwakke, emissie in OYE, zowel in vrije als gecomplexeerde vorm. Deze emissie heeft een levensduur van $\sim 3\text{ ns}$ bij 143 K. In een ESR meting werd een geringe hoeveelheid ongepaarde spin aangetroffen, zowel in vrij als gecomplexeed eiwit. Als gevolg van een ongebruikelijk relaxatiegedrag, werd het ESR signaal, dat zeer gemakkelijk te verzadigen is, alleen beneden 15 K waargenomen. Aan mogelijke gevolgen van deze waarneming wordt een korte discussie gewijd. In bevroren waterige oplossing werd een faseover-

gang gevonden waarbij de kleur van het OYE-fenolaat complex veranderde in die van het vrije enzym. Bij smelten keerde de kleur van het complex terug. Alle gegevens leiden tot de conclusie dat slechts een model van een netwerk van waterstofbruggen tussen verschillende, deels onbekende, chromofore groepen in het eiwit geen tegenstrijdigheden oplevert. Fenol grijpt klaarblijkelijk drastisch op dit netwerk in.

Tenslotte wordt in Hoofdstuk 8 een overzicht gegeven van recente spectroscopische literatuur over isoalloxazines, er wordt weerwoord gegeven op kritiek die de publikatie van de Hoofdstukken 3 en 5 oproept en er wordt een ESCA (XPS) spectrum van 3,7,8,10-tetramethyl-isoalloxazine (3-methylumiflavine) getoond.